Tailored ligands for zinc coordination

Christopher David Edlin

Tailored Ligands For Zinc Coordination

by

Christopher David Edlin B.Sc. (Hons)

Department of Chemistry
University of Durham

A Thesis submitted for the degree of Doctor of Philosophy September 1998

Abstract

Tailored Ligands For Zinc Coordination

Selective coordination to zinc over other members of the first row transition metal series is important for the commercial application of lipophilic ligands for the hydrometallurgic recovery of the metal. In order to achieve selectivity for zinc(II) over other ions, particularly copper(II) and iron(III), ligands have to be designed which take advantage of zinc's preferred tetrahedral coordination geometry and the borderline donor atom preference of the metal. With such ligands in mind, three new classes of ligand system have been designed and synthesised based on the benzimidazole, quinoline and pyridine ring systems with appended phosphinic and thiophosphinic acid anionic donor groups.

Benzimidazole ligands which bind zinc in a 2:1 manner in solution have been made and their complexation ability assessed by ESMS, ^{31}P NMR, liquid-liquid extraction, fluorescence and UV absorption spectroscopic methods. A bisbenzimidazole ligand with a C_3 spacer in the 2,2' position was synthesised and shown to bind zinc initially in a 2:1 manner, at low metal concentrations, and predominantly as a 1:1 species at higher metal concentrations. The formation constant for the ML complex was shown to be $\log K_{ML}=5$ by analysis of the NMR titration curve, which was in close agreement with the value obtained from liquid-liquid extraction studies. A directly linked 2,2'-bisbenzimidazole system was also synthesised as an extension to previous work, however isolation of the target ligand proved to be difficult due to the insolubility of the desired bis-acid.

8-(Quinolinyl)phenylphosphinic acid and 8-(2-methylquinolinyl)phenylphosphinic acid were also synthesised and their solution complexation behaviour studied in detail. The unsubstituted ligand appeared to form 1:1 complexes with zinc at all the metal concentrations studied, and the absence of the methyl substituent does not inhibit coordination to the ferric ion. In contrast the methyl substituted ligand initially forms a 2:1 L:M complex, and 1:1 complexes at higher metal concentrations. The initial ML_2 complex probably involves coordination of two of the phosphinic acid moieties.

Three pyridyl derived ligand systems were also synthesised varying the bulk of the C-6 substituent and the effect of the phosphinic versus the thiophosphinic acid moiety towards zinc coordination was examined. Both of the methyl appended ligands were shown to bind zinc in a 2:1 manner, with the thiophosphinic acid exhibiting a greater avidity for zinc. In contrast, the unsubstituted ligand predominantly forms 1:1 complexes at all metal concentrations.

Christopher David Edlin, 1998

Declaration

The content of this thesis represents the work of the author unless indicated to the contrary or acknowledged by reference. The thesis describes the results of research carried out in the Department of Chemistry at the University of Durham, and also at Zeneca Specialties, Blackley between October 1995 and September 1998. This work has not been submitted for a higher degree in any other academic institution.

Statement of Copyright

Acknowledgements

I would like to thank my supervisor, Professor David Parker, for his enthusiasm, help, encouragement and sometimes optimism throughout the time I have worked with him. For my short stay at Zeneca, I thank Dr. Dom Cupertino for looking after me.

I am also grateful to many staff in the department, without whom this work would not have been possible; Alan Kenwright, Ian McKeag, Julia Say and Ray Matthews for NMR; Mike Jones and Lara Turner for Mass Spectroscopy; Ritu Kataky for electrochemistry; Lenny Lauchlin for help with HPLC, ion analysis (and football!); and the remainder of the technical staff of the department for all their help over the years.

Special thanks are due to everbody who has passed through CG27 (the 'Wolfson' laboratory!) over the past three years, particularly Steve, for their support, friendship, laughs and a few beers!

Thanks to all the members of Grad. Soc football club for a great few years and the occaisonal sore head on a Saturday morning, and to all the members of SC Chemistry for a cup winning year!

Financial support from the EPSRC and Zeneca (under the CASE scheme) is gratefully acknowledged

To Mum and Dad

Contents

Chapter One

Chapter Two

Chapter Three

Abbreviations

Ac	acetyl
Ar	aromatic
aq	aqueous
bz	benzyl
Bu	butyl
°C	degrees celsius
CF	crystal field
CFT	crystal field theory
CFSE	crystal field stabilisation energy
Ch.	chapter
CHEF	chelation enhanched fluoresence
CHN	carbon, hydrogen, nitrogen combustion analysis
CI	chemical ionisation
cy	cyclohexyl
d	doublet
δ	chemical shift
2D	two dimensional
DCI	dicyclohexylcarbodiimide
DCM	dichloromethane
dd	doublet of doublets
D2EHPA	di(2-ethylhexyl)phosphoric acid
DIBAL-H	di-*iso*-Butyl Aluminium Hydride
DMF	N, N-dimethylformamide
DMSO	dimethylsulfoxide
e^-	electron
EDCI	1,1'-dimethylaminopropyl)-3-ethylcarbomide hydrochloride
EDTA	ethylene diamine diacetic acid
EI	electron impact ionisation
en	ethylenediamine
ESMS	electrospray mass spectrometry
Et	ethyl
EtOH	ethanol
Eqn.	Equation
eV	electron volt
Fig.	figure
FTIR	fourier transform infra red
h	hours
HDOP	di(n-octyl)phosphinic acid

HEH[EHP]	2-ethylhexylphosphonic acid mono 2-ethylhexyl ester
HOMO	highest occupied molecular orbital
HPLC	high performance liquid chromatography
HSAB	hard and soft, acid and base
Hz	hertz
I	ionic strength
ICT	internal charge transfer
IR	infra red
J	coupling constant
K	kelvin
L	ligand
LDA	lithium diisopropylamide
lit.	literature
LUMO	lowest unoccupied molecular orbital
m	multiplet
M	metal
Me	methyl
MeOH	methanol
mm	millimetre
M/L	metal:ligand ratio
min	minute
m. p.	melting point
MS	mass spectrometry
n	neutron
$12N_3$	1,5,9 triazacycldodecane
$12N_4$	1,4,7,10 tetra-aza cyclododecane
$14N_4$	1,5,8,12 tetra-aza cycloundecane
nm	nanometer
NMR	nuclear magnetic resonance
NOE	nuclear overhauser effect
p	pentet
PCC	pyridinium chloro chromate
Ph	phenyl
PhH	benzene
PhMe	toluene
PPA	polyphosphoric acid
q	quartet
r_i	ionic radius
R_f	retention time
s	singlet

$t_{1/2}$	half life
t	triplet
TBDMS	*tertiary*-butyldimethylsilyl
td	triplet of doublets
tt	triplet of triplets
TFA	trifluoroacetic acid
THF	tetrahydrofuran
tlc	thin layer chromatography
tren	tris(ethylenediamine)
Ts	toluene sulfonyl
UV	ultra violet
VT	variable temperature

Chapter One

Introduction

1 Introduction

A brief comparison is made between the more traditional methods of metal recovery (1.1) and hydrometallurgy, the industrial focus of this work (1.2). The set-up and factors influencing the design of the industrial extractants currently employed are surveyed in the second section. An introduction to coordination chemistry is presented (1.3) with an emphasis on the generation of tetrahedral arrays of donor atoms. The influence of this geometry on complex stability and selectivity is also examined. The criteria for ligand design (1.4) are discussed, followed by a brief discussion of the target compounds presented in this thesis (1.5). Finally, the content of subsequent chapters is outlined (1.6).

1.1 Metal Recovery

Man has sought to produce metals in their pure form since at least 5000 B.C., when the use of lead, (to glaze ceramics) and copper (in coinage) was first documented.[1] Today, the extraction of metals from their ores represents a considerable proportion of the chemical industry. Methods are constantly sought to improve methods of production, driven by economic and environmental pressures.

Historically the earliest metal to be refined was copper: by about 3500 B.C. it was obtained in the Middle East by charcoal reduction of its ores. Approximately 500 years later the addition of tin to the molten copper produced the much more durable bronze, this established the "Bronze Age". Copper continues to be one of the most important metals with production today at about 15 million tonnes per annum. By far the most important metal in current production is iron, with more than 700 million tonnes per annum being produced worldwide. The isolation and use of iron was initially hindered by the elevated temperatures required for its production, the technology only becoming widely available around 1200 B.C. leading to the "Iron Age". Pure iron is only produced on a small scale today, it is in the form of steels that iron finds its most widespread use. The blast furnace is the primary manufacturing process for steel.[2] The furnace is loaded with a mixture of iron ore, coke and limestone and a blast of hot air is blown in through the bottom. The coke burns producing temperatures around 2000°C around the base of the furnace and the carbon present reduces Fe_2O_3 to iron metal with the evolution of carbon dioxide. The impurities in the mixture combine with the added limestone to produce a slag which can easily be separated from the molten metal, which is tapped off the furnace to produce cast (or pig) iron. Cast iron is a brittle substance which is further processed to form steel using the Bessemer process, by which sulfur and phosphorus impurities are removed and the carbon content reduced to about 1.5% by blowing air through the molten cast iron.

Zinc, lead and nickel are produced worldwide on a large scale (6, 4.5 and 1 million tonnes per annum respectively). Their production is similar in principle to that of iron, with concentration of the ores followed by reduction in a blast furnace with added limestone. The isolation of each of these metals has its complications, but methods exist by which each of these metals can be purified.

Aluminium is produced using a different method to the preceding examples and is essentially a two stage process.[3] The first step involves the extraction, purification and dehydration of bauxite ($AlO_x(OH)_{3-2x}$). This is achieved by the Bayer process; which treats the bauxite with aqueous NaOH followed by filtration to remove the insoluble materials. Precipitation of the trihydrate followed by calcination at 1200°C gives pure Al_2O_3. The second step in aluminium production is the electrolysis of Al_2O_3 in molten cryolite (Na_3AlF_6) which is carried out at 940-980°C in a carbon lined steel cell (cathode) with carbon anodes. The operating conditions of a typical cell require 10^5A at 4.5V, production of one tonne of aluminium metal requires 1.9 tonnes Al_2O_3, 0.5 tonnes of C anode material, 0.07 tonnes of cryolite and 15, 000 kWh of electrical energy.

The major methods for the isolation of most of the world's important metals currently require extremely forcing conditions, such as elevated temperatures, strongly alkaline material and extremely high electrical currents. Associated with this is the threat to the environment; blast furnaces produce a significant amount of 'unfriendly' by-products, such as carbon monoxide, sulfur dioxide and nitrous oxides.

The traditional methods of metal production described above all have extremely high operating and start-up costs, and are only applicable to one metal. Clearly there is scope for a method of metal recovery which is economically and environmentally friendly and can be used for single or multiple selective metal recovery.

1.2 Hydrometallurgy

Traditionally the 'winning' of metals from their ores has been achieved by pyrometallurgy which has several disadvantages (*vide supra*). Hydrometallurgy is a relatively recent development in comparison, and is concerned with methods whereby metals, metal salts or other metal compounds are produced by means of chemical reactions involving aqueous and organic solutions.[4] It has definite advantages over the pyrometallurgic recovery of metals:[5]

1. Low-grade ores may be leached with complexing agents

2. Complex ores may be successfully treated and multiple metals separated under controlled conditions.
3. Reactions are generally carried out at room temperature.
4. No 'stack' gases are involved therefore air pollution does not represent a significant problem.
5. Can be used for small scale operations requiring a low capital expenditure.

However there are several disadvantages. The plant requires sophisticated control schemes to maintain efficient operation. There is no economic gain in substituting an existing pyrometallurgic plant, processing reasonably high grade ores, with a hydrometallurgy plant. Although there is little air pollution the process produces significant quantities of solid and liquid waste which need to be disposed of, creating a potential environmental problem.

1.2.1 Unit Processes in Hydrometallurgy

Hydrometallurgic processes can be divided into four main units of operation:[6]

1. Separation of the ore from inert material
2. Leaching to produce an aqueous solution of metal salts
3. Purification and concentration of the desired metal
4. Recovery of the pure metal

A typical plant for the recovery of metals by hydometallurgy is shown overleaf. In stage one the ore is prepared, this involves removal of insoluble materials by flotation, followed by mechanical crushing to reduce particle size. This removes silicate based material which may interfere with the leaching stage. Once the ore has been prepared the next stage is to dissolve the constituents of the ore to form a solution called the raffinate with a leaching reagent. Leaches fall into three categories, acids (sulfuric, hydrochloric or nitric), alkalis (ammonia, sodium hydroxide or sodium carbonate) and salts (cyanides, ferric and cupric). A reagent used as a leach must dissolve the minerals rapidly, be cheap, readily available and if possible be regenerated for use in subsequent leaches.

The raffinate is then transported to the solution purification tank (**3** overleaf), during this stage the metal is extracted into the organic phase. This can been achieved by a number of methodologies; ion exchange, carbon adsorption and solvent extraction are the common methods.

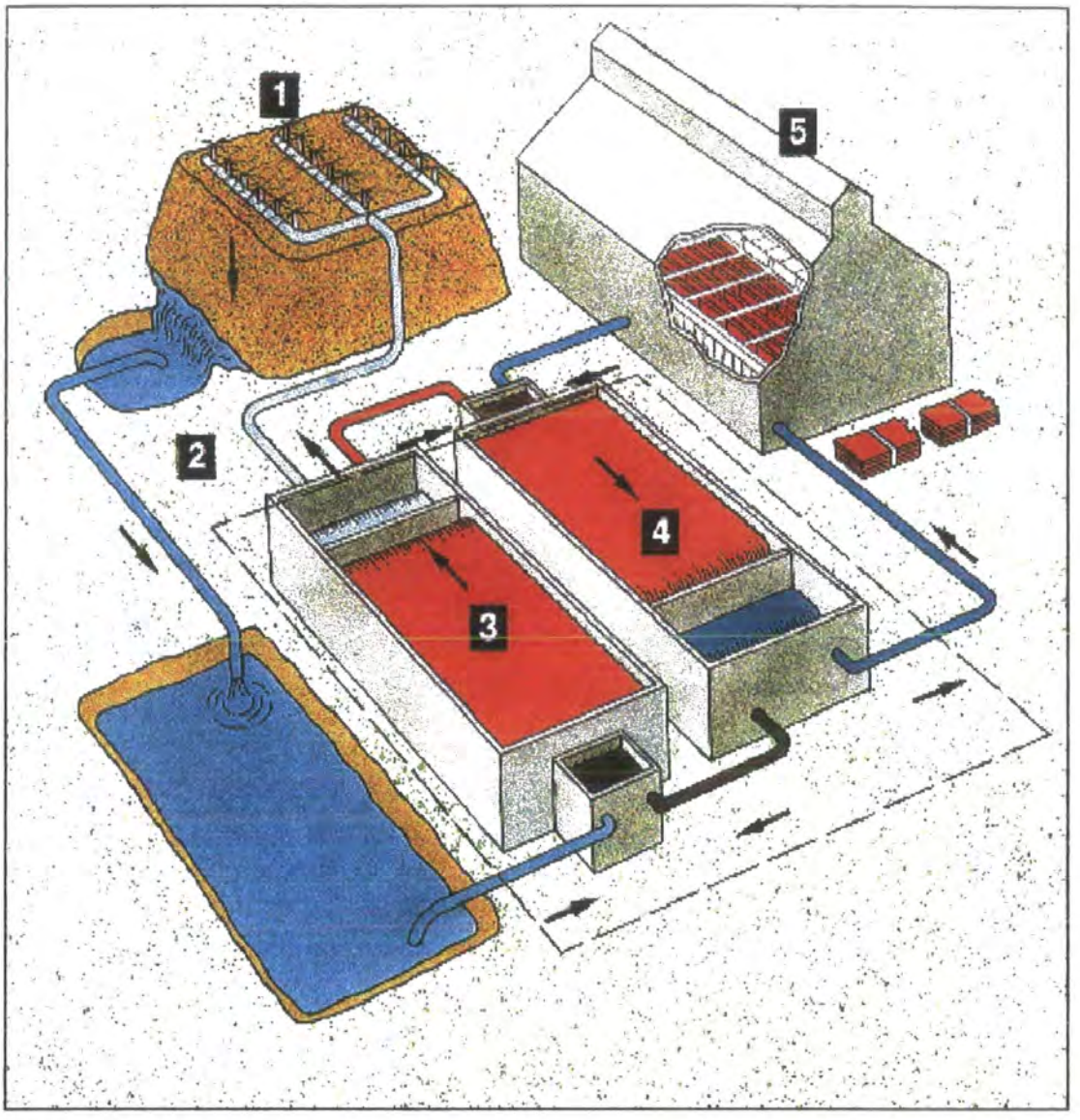

Figure 1.1 Diagrammatic representation of a typical solvent extraction plant

If the purification method is well designed, then an organic solution containing only the desired metal should result. In the final two units (**4** and **5** previous page) the metal is removed from the organic phase by contacting with a stronger acid solution to yield a pure metal aqueous stream. The aqueous stream is then electrolysed to deposit the pure metal, in a process called electrowinning.

In the case of zinc recovery, a mixture of ferric chloride and hydrochloric acid is used as the leach and the preferred method of purification is solvent extraction.[7] During the solvent extraction stage the pH is maintained below 2.5 to prevent precipitation of ferric hydroxide from the raffinate. The organic phase is then extracted with sulfuric acid to produce a pure zinc sulfate solution which is electrolysed to produce pure zinc (electrowinning). This solution should be free of other metals to prevent electrowinning of undesirable metals which are lower than zinc in the EMF series, as these would be reduced preferentially (Table 1.1).[8]

Metal ion	Sb(III)	Fe(III)	Cd(II)	Pb(IV)	Ag(II)	Bi(III)
Tolerance / ppm	< 0.01	< 0.1	< 0.5	< 1	< 1	< 25

Table 1.1 Tolerances of common contaminants in $ZnSO_4$ stream

There is a potential problem with the electrowinning of zinc from zinc sulfate solution. Zinc is relatively high in the EMF series, as such the reduction of zinc in aqueous media should produce hydrogen at the cathode and oxygen at the anode.

Decomposition of water	Decomposition of $ZnSO_4$
$H_2O \longrightarrow H_2 + 1/2\ O_2$	$Zn^{2+} + H_2O \longrightarrow Zn + 1/2\ O_2 + 2H^+$
$E^\circ = -1.23$ V	$E^\circ = -1.99$ V

However hydrogen evolution on zinc is not easy and a cell potential greater than 1.23 V is maintained to prevent hydrogen production. This is a phenomenon known as overpotential, and in this case called the hydrogen overvoltage.[9] At current densities of 100 A/m^2 the overpotential is 0.75V, allowing zinc deposition to occur in preference to hydrogen evolution.

1.2.2 Ligand Design Criteria for the Solvent Extraction of Zinc

For a ligand to be an efficient extractant for zinc it must fulfil several requirements.[10] Of primary importance is high selectivity over other metals, mainly iron (II and III), copper and cadmium. If iron finds its way into the final zinc stream then facile

reduction of iron (III) to iron (II) (E°/V Fe^{3+}/Fe^{2+} = +0.77) followed by aerial oxidation back to iron (III) will impede the efficiency of the electrowinning process. Copper and cadmium may also be competitively bound by the extractant and be transported into the electrolysis cell thus reducing the efficiency of metal recovery.

Complexation and decomplexation should also be pH dependent and occur over approximately one pH unit. The extractant must be able to complex zinc in acidic conditions (pH < 2.5) and de-complex when exposed to stronger acid. In order for the hydrometallurgic process to be viable, the kinetics of complexation must be rapid with equilibrium reached in approximately five minutes. The ligand should also be sufficiently robust to withstand many cycles of complexation and decomplexation in a continuous recovery process. It should also be sufficiently lipophilic to avoid loss of the ligand to the aqueous phase and to ensure solubility in the organic phase during solvent extraction.

The complexes formed with zinc should also be charge neutral to prevent transport of chloride ions from the raffinate to the pure zinc sulfate stream. If chloride is present in the electrolysis cell it will destroy the hydrogen overpotential generated and result in chlorine evolution at the anode.

1.2.3 Previous Ligands Employed for the Solvent Extraction of Zinc

The solvent extraction of zinc from aqueous metal salt solutions is a rapidly expanding technology with several plants currently recovering zinc by this process.[11] Several extractants are currently commercially available. The first product available was di(2-ethylhexyl)phosphoric acid D2HEPA (1) (figure 1.2).[12]

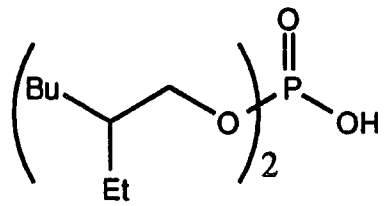

D2EHPA (1)

Figure 1.2 Structure of D2HEPA (1)

D2HEPA forms hydrogen bonded dimers in the organic phase and extraction can be represented by the general equation:

$$Zn^{2+}_{(aq)} + 1/2\,(H_2L_2)_{org} \rightarrow (ML_2)_{org} + 2H^+$$

Recently work has focussed on defining the exact nature of the zinc complex in the organic phase. At concentrations greater than 0.1M the species present in the organic phase is $[ZnL_2(HL)_2]$ whereas at concentrations of less than 0.1M, the major species present is $[ZnL_2(HL)]$. These studies were performed on a two phase system with an aqueous layer containg either zinc sulfate or perchlorate extracted into toluene or dodecane.[13]

Several other phosphorus acid based extractants are commercially available , 2-ethylhexyl phosphonic acid mono-2-ethylhexyl ester (2) from Daihachi Chemical Industries, Japan (HEH[EHP]) and di(n-octyl)phosphinic acid (3), HDOP (figure 1.3). These have both been shown to extract zinc in a similar manner to D2HEPA.[14]

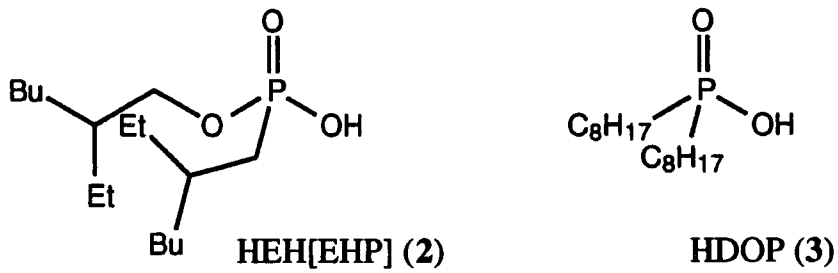

HEH[EHP] (**2**) HDOP (**3**)

Figure 1.3 Structures of HEH[EHP] (2) and HDOP (3)

The order of zinc extraction is in the sequence D2EHPA > HEH[EHP] > HDOP, which is the inverse order of the ligand's acidity. It can been postulated that branching of the alkyl chains alpha to the phosphorus atom accounts for this selectivity. If alpha branches are present then this imparts a degree of steric inhibition to the complexes which may favour the prefered coordination geometry of the zinc ion.

To increase the extraction of zinc at lower pH values, thio and dithiophosphinic acids have been studied as ligands. Cyanex 302, bis(2,4,4 -trimethylpentyl)mono thiophosphinic acid (4) is available commercially and has been used for the extraction of zinc from aqueous sulfate[15] and chloride raffinates (figure 1.4).[16]

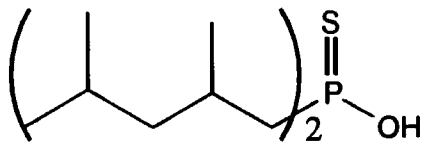

Cyanex 302 (**4**)

Figure 1.4 Structure of Cyanex 302 (4)

A useful measure of the ability of an extractant to transport a metal from the aqueous phase to an organic phase over a pH range is to examine the $pH_{1/2}$ values. The $pH_{1/2}$ is the acidity at which 50% of the maximium amount of metal is extracted and is a

valuable parameter for comparing different ligands propensity for extraction. For D2EHPA, HEH[EHP] and Cyanex 302 the $pH_{1/2}$ values are compared (table 1.2).

Ligand	Cyanex 302	D2EHPA	HEH[EHP]
$pH_{1/2}$	1.1	1.3	1.45

Table 1.2 $pH_{1/2}$ values for zinc extraction with phosphorus acids.

A disadvantage of these three ligands is that they also co-extract ferric and, to a lesser extent copper ions. Copper does not represent a significant problem as this can be removed hydrometallurgically by the Cuprex process.[17] Achieving selectivity over iron is more difficult to achieve, and can only be facilitated by careful control of the raffinate pH.

A commercially viable ligand has recently been developed by Zeneca Specialties based on the dithiophosphoramide moiety (5).[18] The ligand is structually analogous to the acetylacetonate ligand (6), and acts as a bidentate ligand forming ML_2 complexes with many first row transition elements (figure 1.5).

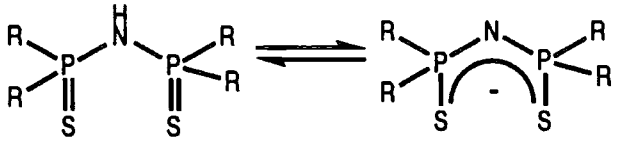

(5)

Dithiophosphoramide, R = isopropyl

cf.

(6)

Acetylacetonate

Figure 1.5 Dithiophosphoramide compared with acetylacetonate.

The nature of the R group in the ligand is critical in achieving selectivity for zinc over other first row transition metals. The alkyl group needs to be sufficiently lipophilic to ensure that the ligand and complex are extracted into the solvents used in the process. However, unless the R group contains an alpha substituent, there is little or no selectivity for zinc. Presumably this selectivity arises from a steric effect, in which alpha substitution provides sufficient steric bulk to prevent unwanted complex geometries from forming.

Other metals are still co-extracted with this ligand (table 1.3),[8] the major impurity is copper which can be effectively removed by the Cuprex process.

Metal ion	Zn	Cd	Cu	Hg, Ag	Pb	Sn, Ge	Fe	Ni, Co
Quantity mg/l	6400	110	105	100	12	4	1	< 1

Aqueous phase saturated with above metal salts and extracted into 'Escaid' with dithiophosphoramide ligand. 'Escaid' is an industrial solvent which consists of a mixture of aromatic fractions.

Table 1.3 Proportions of metals extracted by dithiophosphoramide ligand.

Bisbenzimidazole ligands for solvent extraction have also been studied. Systems based on 2,2'- and 1,3-bisbenzimidazole-2-oxopropane which have been functionalised at nitrogen to render them sufficiently lipophilic have been shown to extract zinc (figure 1.6).

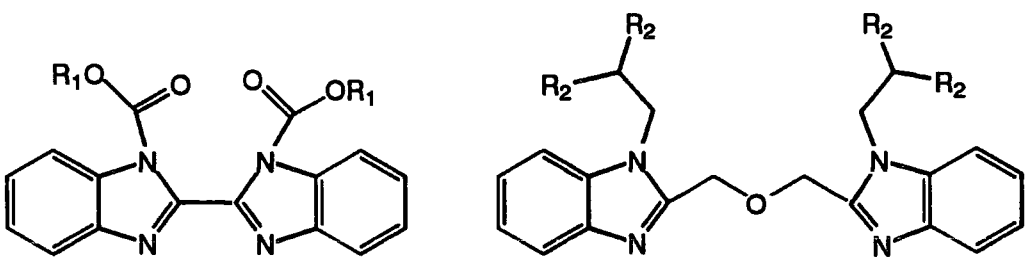

Bisbenzimidazole (7), R_1 = lipophilic

1, 3 bisbenzimidaole-2-oxopropane, (8)
R_2 = n-octyl

Figure 1.6 Structures of benzimidazole based extractants.

The 2,2' linked bisbenzimidazole (7) extracts zinc as a neutral dimeric species which has been shown to have the structure $[M_2L_2Cl_4]$ in the solid state.[19] The extraction of zinc from the raffinate shows a marked chloride concentration dependence. Maximal zinc extraction into the organic phase occurs at chloride concentrations greater than 5M. Kinetically the ligand performs well, with complexation and stripping equilibrium reached in two and five minutes respectively. Selectivity for zinc over iron has been demonstrated, but not over copper which is extracted in preference to zinc.

Metal ion	Cu^{2+}	Zn^{2+}	Cd^{2+}
Single ion[a]	92.8	131.1	23.8
Binary mixture[b]	99.8	27.8	
Tertiary mixture[c]	190.4	12.4	8.3

a. Feed solution, $[M^{2+}] = 0.1$ mol dm^{-3}. b. Feed solution, $[M^{2+}] = 0.2$ mol dm^{-3}. c. Feed solution, $[M^{2+}] = 0.3$ mol dm^{-3}.

Table 1.4 Extraction of copper, zinc and cadmium with (8)

The oxopropane spaced bisbenzimidazole (8) has been used to transport copper, zinc and cadmium ions across a liquid membrane from a buffered aqueous feed into a variety of organic solvents.[20] Transport across a chlorform/water interface with (8) shows a selectivity for zinc over both copper and cadmium when using single ion aqueous feeds. However in competitive extraction from binary and tertiary ion aqueous feeds, a selectivity in the order $Cu^{2+} > Zn^{2+} > Cd^{2+}$ was observed (table 1.4).

1.3 Coordination Chemistry

1.3.1 Introduction

The chemistry of the transition elements is largely concerned with the study of their coordination compounds. In the early days of inorganic chemistry, coordination compounds seemed unusual (hence the term 'complex' ions) as they seemed to defy the accepted rules of valency known at the time. Initially coordination compounds were regarded as only merely being of theoretical interest, but it is now realised that they are of vital importance in organic synthesis,[21] polymerisation processes,[22] and critical for the function of biological systems such as chlorophyll, haemaglobin and metallo-enzymes.[23]

1.3.2 Bonding Theories in Coordination Compounds

The field of coordination chemistry began as early as 1798 when Tassert observed that a solution of cobalt (II) in aqueous ammonia became brown upon exposure to air. This was later shown to be the oxidation of cobalt (II) to cobalt (III). It was not until the late 19th century when Werner proposed his theory on valency that our understanding of coordination became clear.[24] He proposed that metals have two types of valency. The first, primary or ionizable valency (i.e. the oxidation state) and the second which has fixed orientations in space (i.e. the coordination number).

The first succesful application of bonding theory to coordination compounds was made by Linus Pauling.[25] It is usually referred to as the valence bond theory of coordination compounds. It is closely related to the hydridization and geometry of non-complex compounds. From this point of view the formation of a complex ion is a reaction between a Lewis base (ligand) and a Lewis acid (metal) with the formation of a coordinate covalent (or dative) bond between the ligand and metal. Until the 1960s valence bond theory was the only one applied to coordination compounds. Since then, several more complete theories have been applied to the bonding of these systems: these will be briefly described below.

Crystal field theory (CFT) was developed by Bethe[26] and Van Vleck[27] and describes the symmetry and energetics of coordination compounds in a conceptually very simple manner. The CFT approach to bonding assumes solely an electrostatic interaction between a positively charged metal and a ligand. The electrostatic field created by the ligands splits the previously degenerate d orbitals (as described by valence bond theory) of the metal according to the coordination number and geometry of the complex. In order to understand how this degeneracy occurs it is neccesary to examine the angular dependancy of the 3d orbitals (figure 1.7).

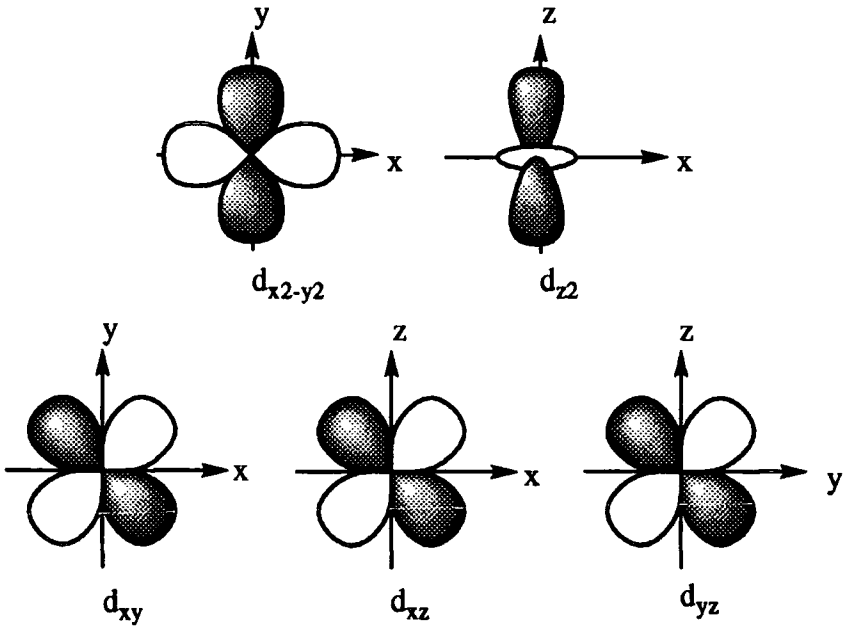

Figure 1.7 Angular dependance of d orbitals.

If we now consider a complex in an octahedral environment with the six ligands, represented as point charges, situated along the ±x, ±y and ±z axes at infinite distance from the metal. As the point charges approach the metal they will interact with the d orbitals as a function of their angular dependance. That is d orbitals oriented along the axes (dz^2 and dx^2-y^2) will be raised in energy relative to those orbitals oriented between the cartesian axes. Therefore in a simple octahedral field the five degenerate d orbitals in the free ion will be split into a higher energy e_g set containing the dz^2 and dx^2-y^2 orbitals and a lower t_{2g} set containing the remaining three orbitals (d_{xy}, d_{xz} and d_{yz}). In the case of a tetrahedral environment, the four ligands are aligned at the opposite vertices of a cube centered at the origin. Upon approach to the metal centre the d orbitals not aligned along the x, y or z axes are raised in energy relative to those orientated along the axes. In contrast to the octahedral case the e level is stabilised and the t_2 level raised in energy for tetrahedral complexes. The square planar stereochemical environment can be derived from the octahedral case by removing the axial ligands. This results in the e_g and t_{2g} levels being further split to raise the dx^2-y^2 and lower the dz^2 in energy from the e_g set. The d_{xz} and the d_{yz} remain degenerate while the d_{xy}

orbital is raised in energy (figure 1.8). The extent to which the e_g and t_{2g} orbitals are separated in the octahedral case is denoted by Δ_{oct}, this energy may be large or small depending on the magnitude of the ligand field. In the tetrahedral case it can be shown that for same metal, ligands and metal-ligand bond lengths $\Delta_{tet} = 4/9\ \Delta_{oct}$. The size of this energy is important in explaining trends in complex stability and will be used later.

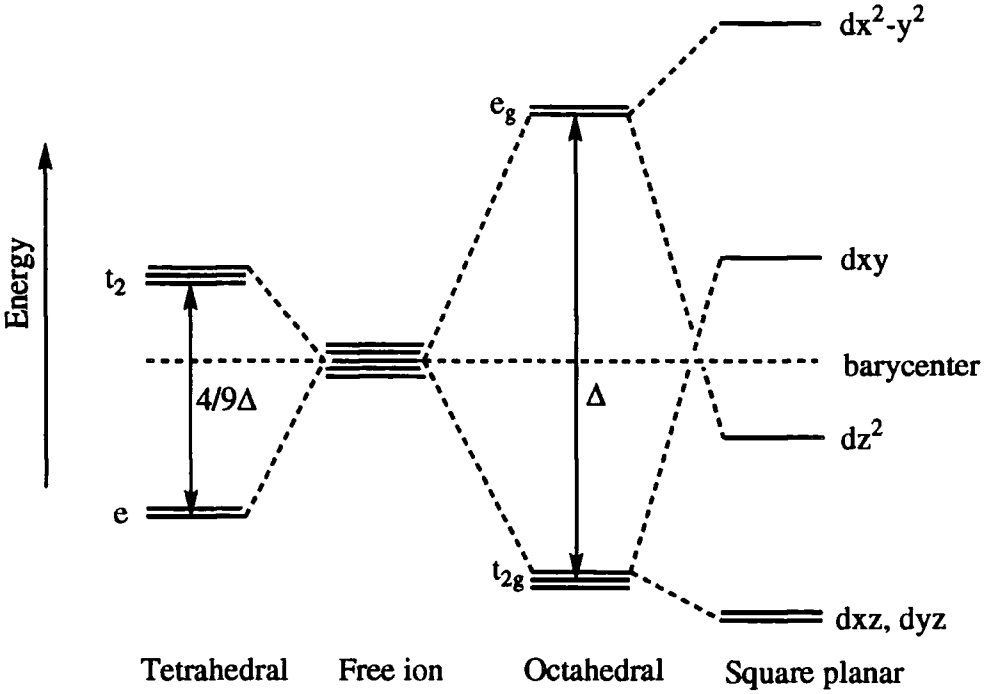

Figure 1.8 Relative energies of octahedral, tetrahedral and square planar coordination environments.

CFT accounts for a surprisingly large proportion of observed structures, but it suffers from several drawbacks. There is much evidence to suggest that there is a degree of covalent character in coordinate bonding, such as ESR and NMR which shows there is an appreciable amount of electron density between the ligand and metal. To account for these observations more complete theories of bonding have been proposed.

A molecular orbital approach has been used to accurately describe the bonding in complex ions. Using this approach linear combinations of atomic orbitals (LCAO) of the correct symmetry and energy are combined to produce molecular orbitals. Combination of metal and ligand atomic orbitals of vastly differing energies can be ignored, thus only the valence orbitals have been used in this theory. Using this approach the spectral and magnetic properties of coordination compounds can be more clearly understood. Although the molecular orbital description of bonding is theoretically more accurate than crystal field theory, the former theory desribes simply many of the properties described in the subsequent sections.

1.3.3 Types of Ligands and Coordination Number

Ligands are most conveniently classified according to the number of donor atoms, type of bonding interaction or number of electrons they donate to the metal centre.

The number of donor atoms a ligand contains are known as uni-, bi-, tri-, tetra- etc. according to the number of coordinating atoms in the ligand (figure 1.9). Unidentate ligands may be simple monoatomic ions or polyatomic systems which contain a single donor atom. Ligands with denticities higher than one are often chelating ligands and this has a profound effect on the complex stabilty (section 1.4).

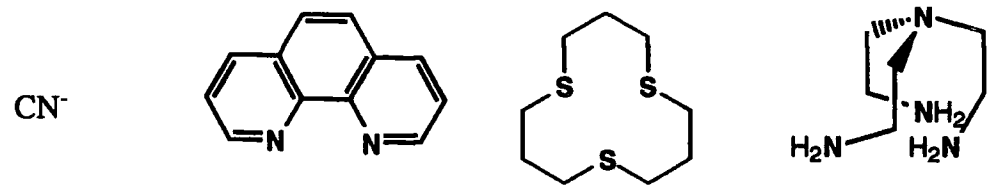

Unidentate Bidentate Tridentate Tetradentate

Figure 1.9 Classifiaction by number of donor atoms

Ligands can also be classified according to the type of bonding interaction between the donating atom and the metal acceptor or the number of electrons donated. There are three types of ligands in this classification. Firstly, Lewis bases which donate one electron to the metal (X type) examples of X-type ligands include halides, hydrides and alkyl groups. Secondly, Lewis bases which donate two electrons to the metal centre (L type) can be sub-divided into two classes; classical and π-bonding ligands. Classical ligands form adducts with all types of Lewis acicidic centres examples of theses include H_2O, H_2S, R_2O and pyridine. π-Bonding ligands donate electron density to the metal centre, generally by a sigma bond, but they have LUMOs which are capable of ovelap with orbitals of the correct symmetry on the metal centre. This overlap allows the metal to participate in a synergic π–bonding interaction and increases the stabilisation of the complex. Examples of π-bonding ligands include CO, PR_3 and ethene. A final classification is zero electron donors (Z type), examples of these are few and far between. Strongly Lewis acidic molecules such as BF_3, $AlMe_3$ and SiF_4 are capable of accepting a dative bond from the metal.

1.3.4 Transition Metal Complex Stability

For a given metal and ligand the stability is generally greater the larger the oxidation state of the metal. Also for a given oxidation state and ligand the stability of complexes across the first transition series varies according to the Irving-Williams series:[28]

$$Mn^{II} < Fe^{II} < Co^{II} < Ni^{II} < Cu^{II} > Zn^{II}$$

This trend is in the reverse of the order for the cation radii, and these observations are consistent with the view that the coordinate bond is largely electrostatic for metals in oxidation state +2. This order of stability is evident in the hydration energies of the divalent hexaquo ions (figure 1.10).[29]

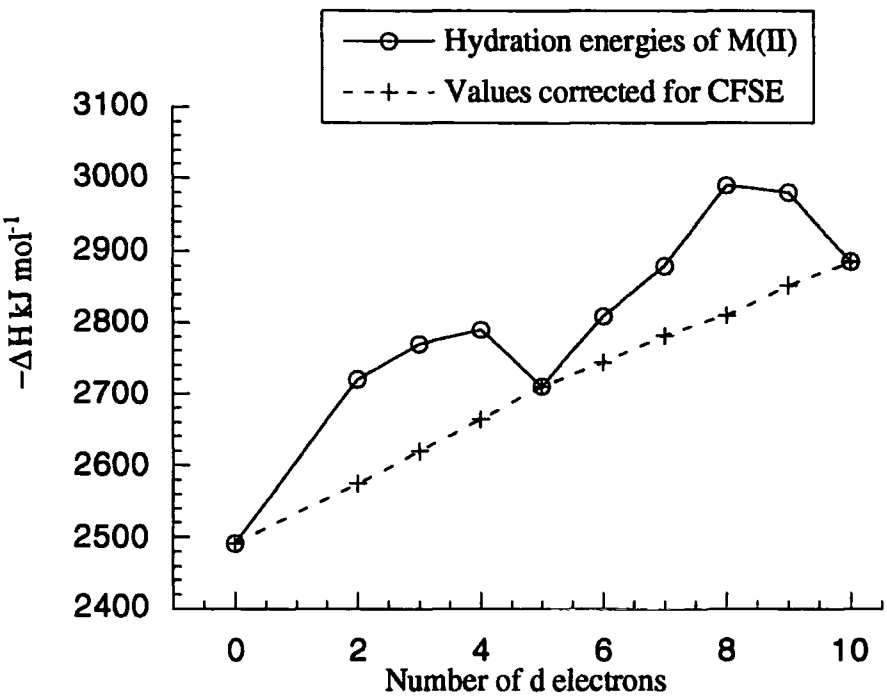

Figure 1.10 Hydration energies of divalent metal ions with values corrected for CFSE

However the trend is not a linear one and extra stabilty is seen across the series (figure 1.10, solid line). This effect can be explained using CFT, for an octahedral complex going across the transition the electrons fill the e_g and t_{2g} orbitals according to Hunds rule and the Aufbau principle. The t_{2g} level lies 2/5 Δ_{oct} below the arbitary barycentre, as such for the d^1, d^2 and d^3 electronic configurations the extra stabilisation will be 0.4Δ, 0.8Δ and1.4Δ respectively. The rest of the transition series follow the same trend (table 1.5).

Number of d electrons	d^1	d^2	d^3	d^4	d^5	d^6	d^7	d^8	d^9	d^{10}
Electronic Configuration	t_{2g}^1 e_g^0	t_{2g}^2 e_g^0	t_{2g}^3 e_g^0	t_{2g}^3 e_g^1	t_{2g}^3 e_g^2	t_{2g}^4 e_g^2	t_{2g}^5 e_g^2	t_{2g}^6 e_g^2	t_{2g}^6 e_g^3	t_{2g}^6 e_g^4
CFSE (Δ)	0.4	0.8	1.2	0.6	0.0	0.4	0.8	1.2	0.6	0.0

Table 1.5 CF stabilisation energies for high spin metal ions across the first transition series

1.3.5 Imposing Tetrahedral Geometry for Zinc

Zinc coordination compounds exist almost exclusively in the plus two oxidation state. There are few examples of zinc(I), with $[ZnL]^+$ (L=$14N_4$) being a rare example,[30] which was produced by pulse radiolysis of the zinc(II) complex. In general, zinc prefers to adopt a tetrahedral coordination geometry, indeed a survey of all known zinc containing crystal structures revealed 58% were four coordinate, with 13 and 27% being five and six coordinate respectively.[31] There is a vast amount of literature describing the solid state structures of zinc complexes, this has been described in detail elsewere.[32] Interest in the coordination chemistry of zinc has been driven by several factors. Firstly the interest in the solvent extraction of the metal has lead to the design of ligands which coordinate selectively to zinc in the presence of other metals (section 1.2.3). In the field of biological chemistry zinc is paramount to the function of many enzymes. Models have been sought to simulate the action of enzymes such as carbonic anhydrase[33] and carboxypeptidase A.[34] Also the use of zinc in asymmetric processes is well known.[35] Chiral catalysts based on amino-alcohols have been shown to add dialkyl zinc reagents enantioselectively to aldehydes, in the case of (9) chiral amplification was also observed.[36] Enantioselective modifications of the Simmons-Smith reaction have also employed chiral catalysts, use of the chiral boronic ester ligand (10) and CH_2I_2 with diethyl zinc gives effective cyclopropanation of allylic alcohols with high enantioselectivity.[37]

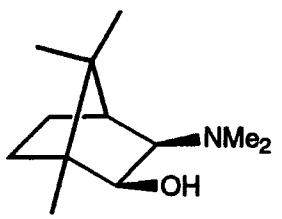

(9)

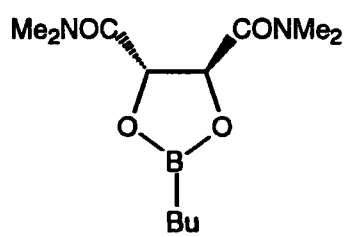

(10)

Figure 1.11 Chiral ligands used in zinc promoted asymmetric processes

Since zinc has an $[Ar]3d^{10}$ outer electronic structure it is not subject to crystal field stabilisation effects. Tetrahedral coordination to the zinc ion must be imposed on the metal by careful design of the ligand system. Ligands such as imidazole and ethylene diamine bind zinc in a tetrahedral manner. However these compounds bind to copper and nickel more avidly. It has been suggested that formation of four coordinate tetrahedral zinc (II) is driven by the Lewis basicity of the donors.[38] For strong donors this will result in a shortening of the metal-ligand bond lengths,[39] and to accommodate this shorter bond length the metal coordination number will be reduced. As the coordination number is reduced the ligands must arrange themselves in the coordination

sphere to minimise steric interactions. The least sterically demanding arrangement for the ligands will therefore be the tetrahedron.

Several other workers have attempted to synthesise ligand systems which engender a tetrahedral array of donor atoms for zinc. There are conceptually only five possible arrangements of donor atoms which achieve a tetrahedral environment, which are represented schematically below (figure 1.12).

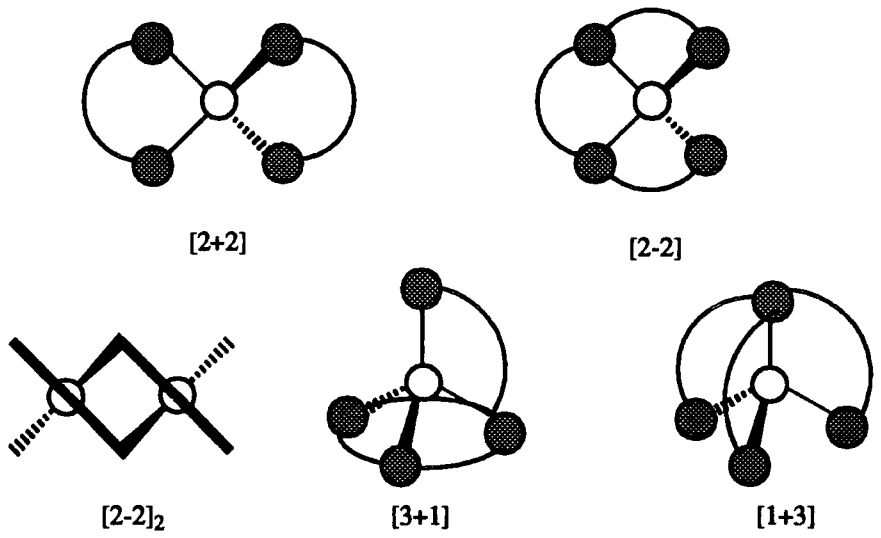

Figure 1.12 Schematic ligand geometries for tetrahedral coordination

[2 + 2] ligand arrangement

There are numerous examples of bidentate ligands which bind to zinc in a tetrahedral manner. These are generally non-specific and will also bind to other transition metals, adopting other coordination geometries, in accordance with the Irving-Williams series.[28] In order to favour tetrahedral geometries over octahedral, square planar or trigonal bypyramidal complexes it is necessary to impose stringent steric demands and choose the correct donor atoms.

Perhaps the best known bidentate ligand which enforces a tetrahedral geometry is neocuproine (1, 10-dimethylphenanthroline). The two methyl groups prevent the four nitrogen atoms participating in coordination in the same plane, which would produce square planar geometries. Selective tetrahedral coordination has been demonstrated with neocuproine in Cu(I) complexes (11) (figure 1.13).[40, 41] A further example of a bidentate ligand which has been predesigned to impose tetrahedral coordination is the dithiophosphoramide (5) based ligand, described previously (section 1.2.3).

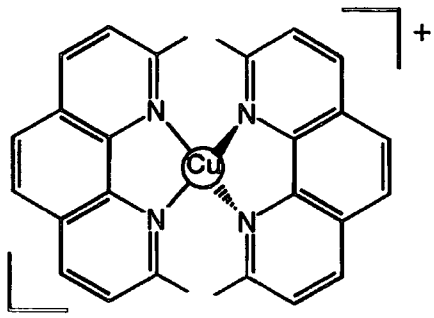

(11)

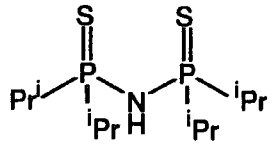

(5)

Figure 1.13 Neuocuproine and dithiophosphoramide ligands

Many zinc complexes with bidentate ligands have been characterised during the past five years , including 2:1 complexes with pyridyl-2-carboxylic acids (12),[42] bis phenols (13)[43] and amine substituted phenols (14) (figure 1.14).[44] However, although these complexes display a tetrahedral coordination geometry with zinc in the solid state, their synthesis was not rationally undertaken.

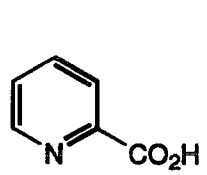

(12)

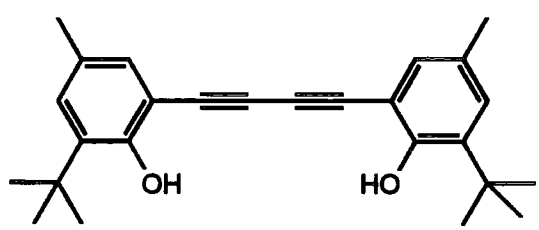

(13)

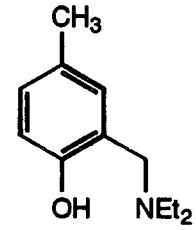

(14)

Figure 1.14 Previous examples of ligands forming 2:1 complexes with Zn(II)

[2 - 2] ligand arrangement

To define a tetrahedral array of donor atoms it is neccesary to limit the number of conformations that the ligand can adopt prior to complex formation. One method of achieving this is to fix two of the ligating atoms in a rigid plane, with the other two donor moieties appended to this rigid plane and available to provide the correct coordination geometry. The pendent donors must be designed in such a way that they are long enough to form a coordinate bond, but not too long to allow unwanted complex geometries. There are several reported examples of this design, which are in general based on the rigid phenanthroline backbone. Systems with donor groups linked directly to the 2 and 9 positions of 1, 10-phenanthroline via a methylene group have been studied (figure 1.15).[45] The metal-complex equilibrium has been studied for the methyl and phenyl substituted phosphinic acids (15, R = Me and Ph). For the methyl derivative (15, R = Me) the order of complex stability is Zn > Ni > Cu and for the phenyl substituted acid (15, R = Ph) Cu > Zn > Ni. In an attempt to increase the propensity for selective tetrahedral complexation, ligand (16) has also been synthesised, however the

solution complexation behaviour was only given a cursary examination.[46] It was found that the ligand prefered to bind the zinc ion in a 2:1 manner, forming a N_4-bound zinc complex with no carboxylate participation.

Many more examples based on N-substituted 1,2-ethyl and 1,3-propyl diamine backbones have been investigated.[47, 48] However because of the number of conformations which can be adopted by the ligand prior to complexation (due to the non-rigid backbone) they have been unsuccessful in their objective of imposing tetrahedral coordination.

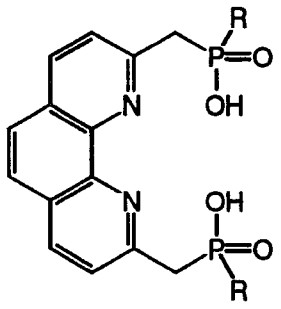

(**15**) R = Me, Ph, Benzyl

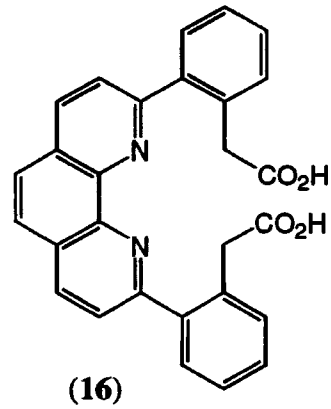

(**16**)

Figure 1.15 Phenanthroline based [2 - 2] ligands

[2 - 2]$_2$ ligand arrangement

Examples of ligand architectures which can adopt a [2 - 2]$_2$ conformation are few and far between. The only succesful application of this design is based on a functionalised 2,2' -bis(benzimidazole) (figure 1.16).[49]

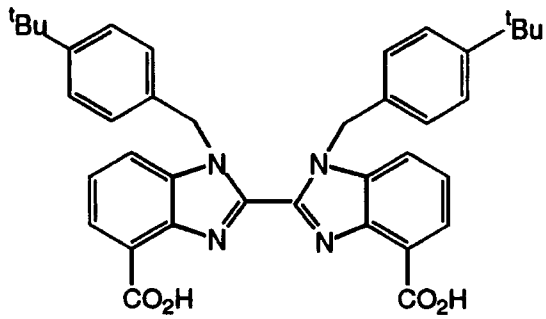

(**17**)

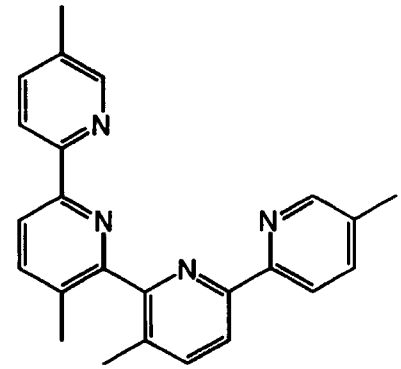

(**18**)

Figure 1.16 [2 - 2]$_2$ geometry 2, 2'-bis(benzimidazole) ligand (17) and a quaterpyridine (18)

With bulky N-alkyl substituents, the dihedral angle between the two benzimidazole moities is close to 90°. Incorporation of anionic donors into the 4 and 4' positions allows the formation of two tetrahedral binding sites. Indeed the ligand forms neutral dimeric

complexes with Zn^{2+} and shows selective, cooperative binding to zinc(II) over copper(II) and nickel(II). These ligand systems are similar to complexes formed with quaterpyridines which have been used as prototype helicating agents with copper(I), wherein two orthogonal bipyridyl groups chelate alternately with copper(I) to produce a helical chain.[50]

[3 + 1] ligand arrangement

In this arrangement three of the donor atoms are incorporated into a basal plane. The metal sits above this plane and the fourth pendant donor binds to form the tetrahedron. Previous exmaples of the [3 + 1] structural type have focussed on the use of 1,5,9-triazacyclododecane ($12N_3$) as the base plane with a fourth donor group attached to the ring. The length of the group attaching the fourth donor group must be carefully selected, such that it coordiantes effectively to the metal without allowing competive binding to solvent molecules or other anions. Appended $12N_3$ macrocycles have been synthesised by Kimura (19)[51] and Moore (20)[52] (figure 1.17).

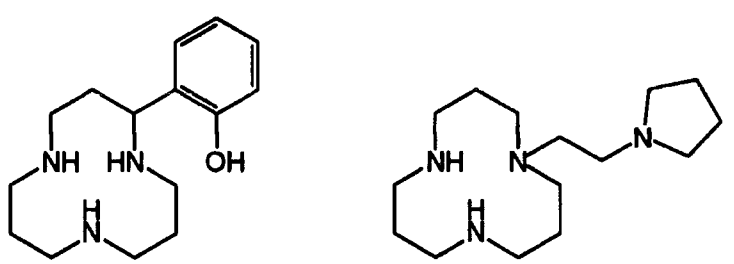

(19) **(20)**

Figure 1.17 Kimura's and Moore's $12N_3$ based [3 + 1] ligands

In these two examples the pendent arm is inadequate at filling the fourth coordination site, which results in cleft formation. This produces a distorted trigonal pyramidal complex with the fifth coordination site filled by solvent molecules or counter ions.

In an attempt to improve on the design two other $12N_3$ based ligand systems have been studied (figure 1.18).[53] The N-linked ligand (21) forms strong complexes with Cu^{2+} and Zn^{2+} ($LogK_{ML}$ = 18.7 and 14.1 repectively) in which phenolate participation was demonstrated, whereas the C-linked ligand (22) forms much weaker complexes with Cu^{2+}, Ni^{2+} and Zn^{2+} ($LogK_{ML}$ = 10.2, 7.32 and 6.11 respectively) in which phenolate participation was absent. The degree of phenolate participation was determined by comparing the magnitude of the extinction coefficient for the charge transfer band at 418nm in the copper complexes of both ligands.

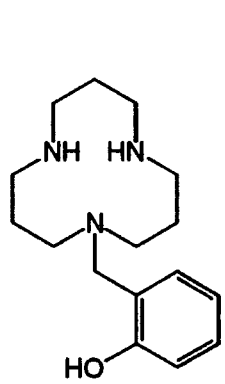

(21)

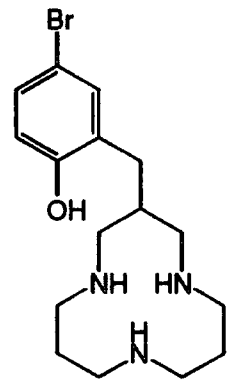

(22)

Figure 1.18 Improved [3 + 1] ligand architecture.

[1 + 3] ligand arrangement

In this ligand geometry three donor groups are attached to a fourth donor to give a trisubstituted monodentate ligand. There have been many examples of this type of ligand class, with 'tren' being a classic example. This ligand is not able to impart any geometric constraints on ligand geometry. Although it coordinates to zinc in a tetrahedral fashion, coordination to other transition metals results in a range of complex geometries. Ligands based on tris(pyrazolylborate) have been studied as selective ligands for zinc. This class of ligands does not strictly fall into the [1 + 3] class as the trisubstituted boron atom is unable to participate in metal coordination. However due to the sterically demanding nature of the ligand there is only room for one further coordination site, thus resulting in a tetrahedral geometry for zinc. Vahrenkamp has studied various substituted tris(pyrazolylborate) zinc complexes as models for phosphate esterases (figure 1.19).[54]

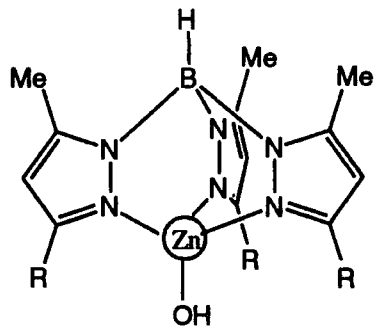

R = 3-pyridyl

(23)

Figure 1.19 Tris(pyrazolylborate) zinc complex as a model for phosphate esterases

Reaction of the zinc hydroxide complexes (23) with phosphate esters resulted in rapid hydrolysis to produce the corresponding phosphorus acids. Isolation of the solid complexes revealed a coordinated phosphate anion in the solid state. Investigation of a

number of complexes showed that zinc adopted tetrahedral coordination geometry in each case.

A final example of a predesigned tetrahedrally coordinating ligand based on 3,7-diaxabicyclo[3,3,1]nonane (given the trivial name, bispidine) is examined. Although it does not strictly fall into any of the described ligand types it is sufficiently interesting to warrant inclusion.

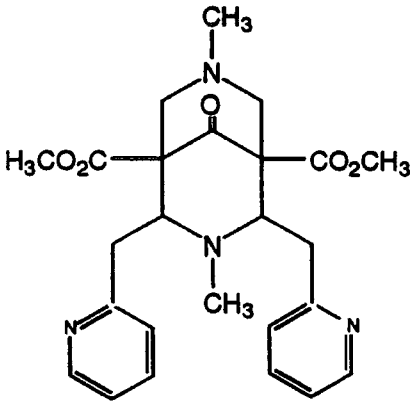

(24)

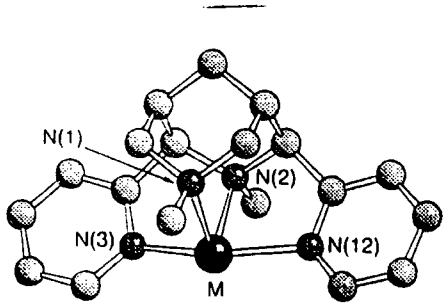

(25)

Figure 1.20 rigid tetradentate bispidine ligand (24) and molecular model of tetrahedral complex (25)

Comba and coworkers have shown that pyridyl appended bispidine ligands (24) present an extremely rigid tetrahedral array of donor atoms (figure 1.20).[55] The formation of two six membered chelate rings with the two pyridyl pendent arms is critical in achieving this geometry. Analysis of the corresponding ligand without the methylene spacers enforces trigonal-pyramidal coordination geometries in preferance to the desired tetrahedral geometry.

1.4 Ligand Design Requirements

There are a number of strategies which can be used to influence complex selectivity and stability in the design of a new ligand system. The correct choice of donor atom, chelate ring size and control of the ligand geometry are the most important parameters in designing a new system.[56]

Donor atom selection

Selection of the correct donor atom for a given system can lead to an increase in complex stability. Observation of many inorganic reactions between Lewis acids and bases lead Pearson[57] to introduce the concept of Hard and Soft Acids and Bases (HSAB) or type A or B acids described by Schwarzenbach[58] and Ahrland.[59] He noted that hard acids formed stronger bonds (and reacted more quickly) with hard bases, and

soft acids formed stronger bonds (and reacted more quickly) with soft bases. Using this observation he was able to classify metal centres as either hard (class a), soft (class b) or borderline (Figure 1.21).

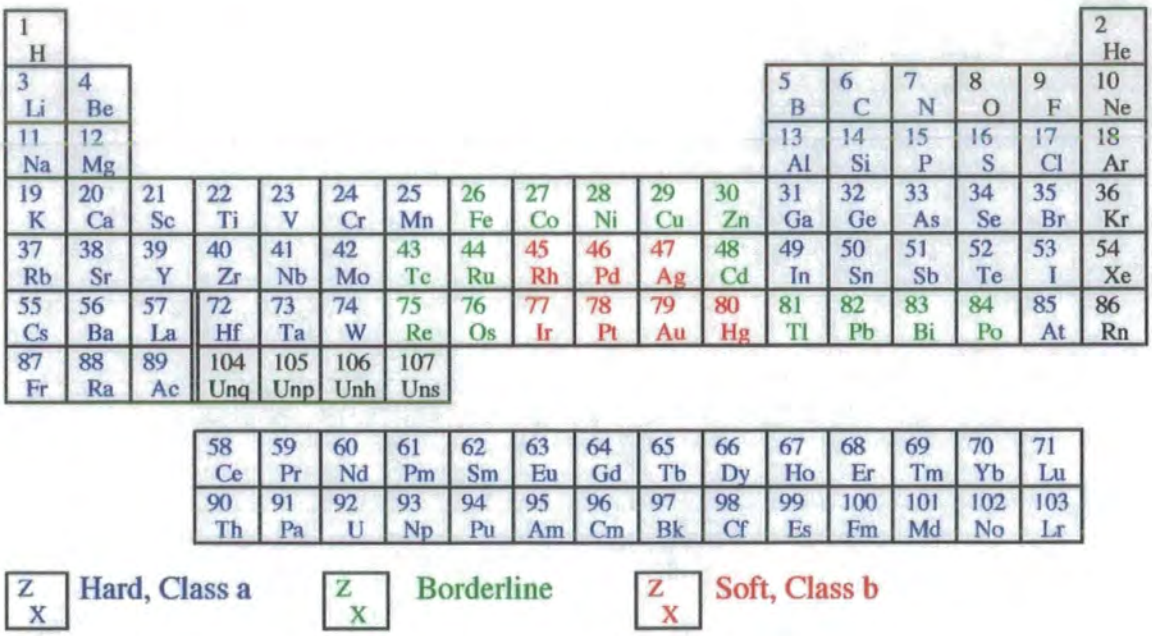

Figure 1.21 Pearsons classification of metal centres in their common oxidation states.

It follows therefore that by matching a complementary Lewis acid (metal centre) with Lewis bases (donor atoms) the complex stability can be optimised. Zinc is classified as a borderline acceptor, and as such should tolerate both hard and soft donor groups. However during the extraction stage in the hydrometallurgic recovery of zinc there are several other metals present, amongst these the ferric ion (hard) (*vide supra*, section 1.2.2). It is possible to discriminate against coordination to these harder ions by choosing more polarisable donating groups for zinc, hence disfavouring complexation to harder acceptors. For example, comparing formation constants between a hard acceptor (Ca^{2+}) and a borderline acceptor (Zn^{2+}) and changing a non-polarisable donor (neutral oxygen) for a more polarisable donor (nitrogen) increases the complex stability for the borderline acceptor (Table 1.6).

Ligand	$LogK_{Ca(II)L}$	$LogK_{Zn(II)L}$
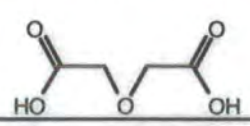	3.38	3.61
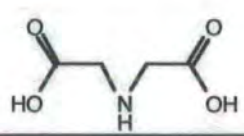	2.59	7.15

Table 1.6 $LogK_{ML}$ constants (298K, H_20, I = 0.1) for Ca and Zn[60]

The HSAB concept provides an elementary guide to donor atom selection but charge and steric bulk are also contributory factors. Generally the coordination number increases with metal ion radius. For example first row transition metals favour 4, 5 or 6 coordinate complexes, whereas larger cations such as the lanthanide ions can accommodate higher coordination numbers. This is a combination of charge and steric interactions, for smaller metal cations increased coordination by anionic donors results in a large repulsive coulombic interactions. As the coordination number increases destabilising steric interactions also become more important, while larger cations can accommodate this increase.

Chelate effects

Complex stability is enhanced if the ligating groups form chelate rings compared to the analogous monodentate ligands. This is a thermodynamic effect and is related to the change in entropic contributions to the free energy of complexation. There is little difference in the enthalpic contributions to the free energy between chelating and non-chelating ligands. The predominant cause of this effect is the large change in entropy resulting from the release of the bound ligands upon complexation with a polydentate ligand (Table 1.7).

	NH_3	en	dien	tren
$Log\beta ZnL_{CN4}$	9.65	10.62		12.03
$Log\beta ZnL_{CN6}$	9.08	17.71	18.6	

Table 1.7 Stability constants for 4 and 6 coordinate Zn complexes (298K, H_2O, I = 0.1)[60]

The size of the chelate ring formed on complexation has a profound effect on the complex stability and selectivity for a given metal. Generally an increase in the chelate ring size leads to a decrease in the overall complex stability. This is chiefly an enthalpic effect associated with the increased steric strain and repulsion of the dipoles of the donor groups. However with larger chelate rings (greater than seven) the entropic contribution becomes more significant, as organisation prior to metal binding has a detrimental effect on the energy of complexation. Simple molecular mechanics calculations have been used to provide a rationale to explain these observations (figure 1.22).[56] For six membered chelate rings the lowest energy conformation is a chair like structure, in which all torsional, diaxial and eclipsing interactions are minimised. For a chair like chelate to form, the metal-donor bonds need to be short and the bite angle will be large. Smaller metal cations adopt lower coordination numbers will have short metal-donor atom bond lengths and a large bite angle, and hence favour six membered chelate

rings. For five membered chelate rings the donor groups need to adopt longer bond lengths and smaller bite angles which favours larger metals due to their ability to accommodate higher coordination numbers.

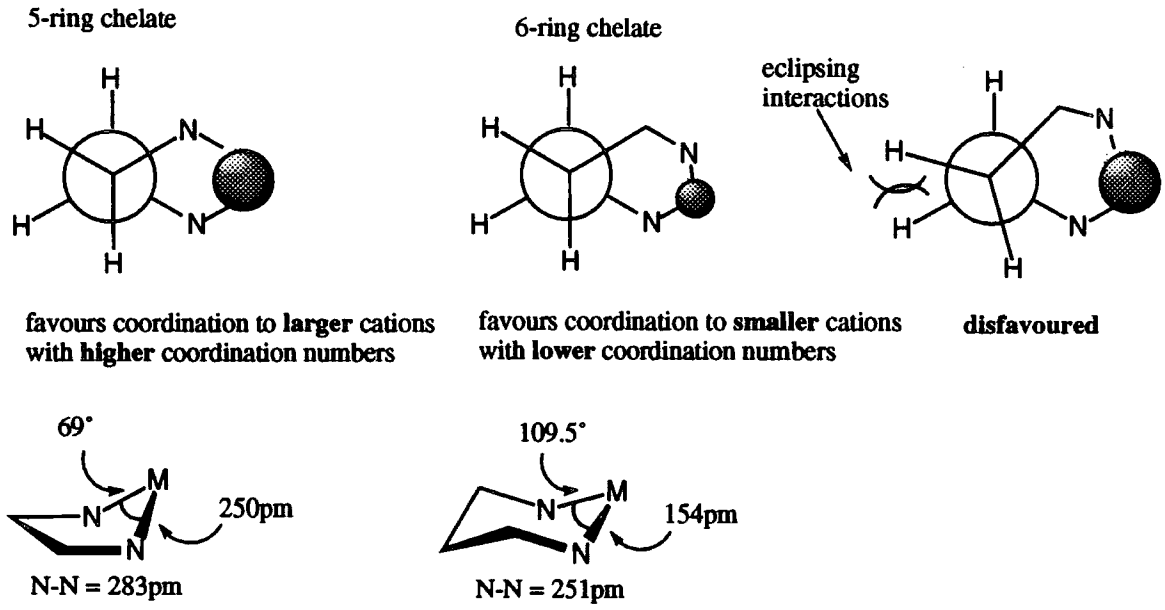

Figure 1.22 Dimensions required for minimum strain energies in chelate rings.

Geometric constraints

By imposing certain geometrical constraints on the ligand architecture it is also possible to impart a degree of selectivity for the zinc ion. As mentioned previously, zinc has a $[Ar]3d^{10}$ electronic structure and as such does not benefit from crystal field stabilisation energies in complex formation. A tetrahedral geometry can be imposed by producing a ligand which forms strong metal-donor atom bonds, which will have shorter metal-donor bond lengths, thereby promoting the required tetrahedral geometry by minising steric interactions. If the ligand is designed to be predisposed to form a tetrahedral array of donor atoms, there will only be a small change in entropy on complexation. Therefore there will be a proportionately larger net enthalpic contribution to the free energy of complexation and hence an increase in the free energy of complexation. A ligand with a predefined geometry should also discriminate against the formation of other, undesirable, coordination geometries, such as square planar, octahedral and trigonal bipyramidal, due to the prohibitively large steric penalties involved in the adoption of these geometries.

1.5 Ligand Design and Target Ligands

Using the design criteria outlined above it is possible to design ligand systems which should favour binding to the zinc atom, whilst discriminating against coordination to larger and harder cations. Using geometrical constraints, discrimination over near

neighbours in the transition series should be possible, thus upsetting the usual order of transition metal complex stability, the Irving-Williams series.[28]

In order to accomplish this task the proposed ligand systems need to possess strong Lewis basic donor groups, which should shorten the metal-ligand bond length and hence promote tetrahedral geometries (*vide supra*). In order to achieve this, the target compounds are to be based around aromatic heterocycles which have strongly coordinating heteroatoms e.g. pyridyl, quinolinyl and benzimidazole based ligand architectures. To produce systems which form charge neutral complexes (a necessity for extraction into organic solvents) with zinc, the ligands must have anionic donor groups, one in the case of bidentate ligands and two for tetradentate systems. The anionic donor needs to be complementary to the donor atom preference for zinc and have a pK_a low enough to be considered for use in hydrometallurgy. The ideal candidates to fulfil these criteria are the phosphorus acids, and in particular phosphinic acids, which have significantly lower pK_as than their carboxylate counterparts (see chapter 2.2). The pentavalency at phosphorus also provides an additional site for modification of the lipophilicity and fine tuning of the acidity of this function.

Although attachment of phosphorus acids to aromatic heterocycles has been examined in the past, the methods currently available for their introduction have generally been non-specific and are not tolerant of other functionalities in the molecule. A preliminary investigation into methods towards forming carbon-phosphorus and phosphorus-nitrogen bonds was undertaken in order to discover an attractive method for the introduction of these moieties. This aspect is described in chapter two.

All of the factors described above relate to thermodynamic contributions to complex formation. It should also be remembered that the rate of complex formation and the kinetic stability of the complex are also important. If the rate of formation is slow and the complex is kinetically labile, then its applicability to the hydrometallurgic recovery of zinc will be limited.

1.6 Scope of Work

The work presented in this thesis concerns the synthesis of tailored ligands for the selective solvent extraction of aqueous zinc ions. Using the design criteria and principles of coordination chemistry outlined above, several ligand systems have been designed and synthesised which explore the $[2 - 2]_2$, [2 - 2] and [2 + 2] binding geometries. Preliminary investigations into the formation of phosphinic acids will be exploited in the synthesis of these systems.

Chapter two covers a brief review of synthetic methodology directed towards the formation of C-P and N-P bonds. Included in this description are a number of model studies performed with the same aim in mind. The stability and ease of formation of the C-P and N-P bond are also considered and contrasted.

Chapter three concerns the synthesis of several benzimidazole based ligand systems, which have phosphinic acids as the anionic donor groups and form six-membered chelate rings with metal ions (figure 1.23).

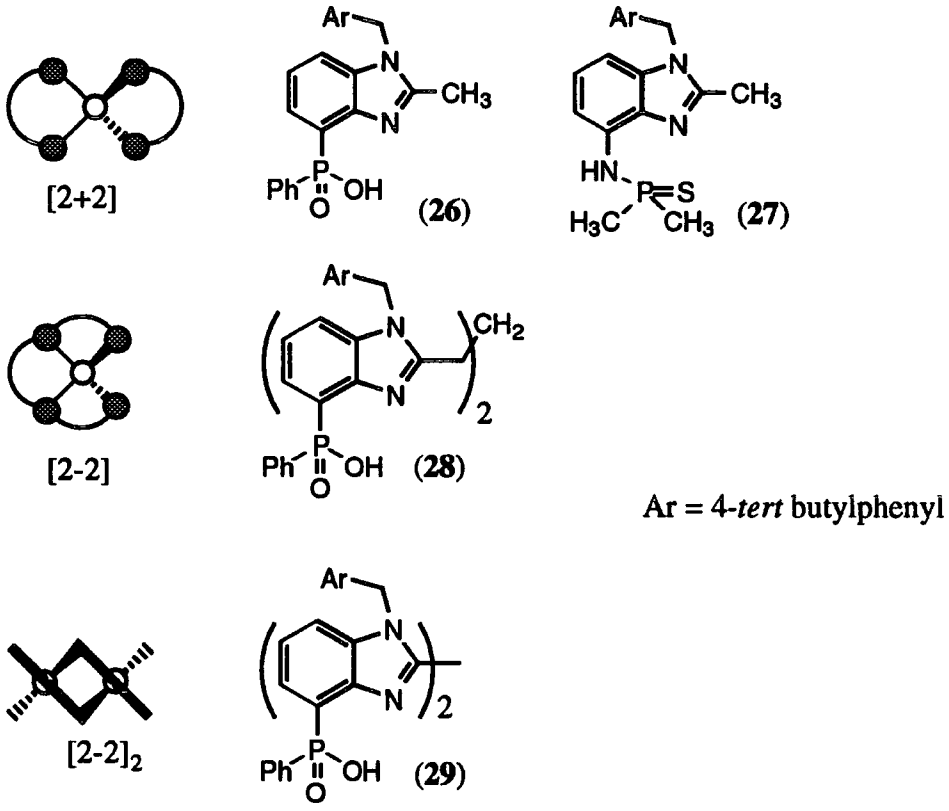

Figure 1.23 Binding geometries and ligands examined in chapter three

Systems based on a monobenzimidazole moiety (26), which is expected to form 2:1 complexes with tetrahedral zinc are discussed. Bisbenzimidazoles involving a 2, 2' (29) and a trimethylene linkage (28) are presented which form 2:2 and 1:1 stoichiometries respectively with zinc. A final benzimidazole based system with a thiophosphoramide donor group (27), possessing a seven ring chelate is also investigated. In all four ligand systems the lipophilicity can easily be varied by manipulation of the N-alkyl substituent or the nature of the phosphorus substituent. The problems associated with the synthesis of these ligands are discussed, along with an investigation into their coordination chemistry.

Chapter four describes a bidentate ligand systems based on C-8 substituted quinolines (30) and (31) (figure 1.24). The synthesis of the ligands (30) and (31) is described along with an investigation into the solution coordination chemistry. Variation of the steric

bulk at the C-2 position is examined with regard to the imposition of a good tetrahedral geometry for divalent zinc.

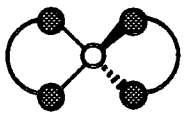

[2+2]

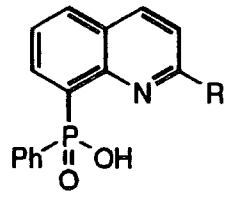

(**30**) R = H
(**31**) R = CH_3

Figure 1.24 Binding geometries and ligands examined in chapter four

Chapter five describes a bidentate ligand system based on a C-6 substituted pyridine (figure 1.25).

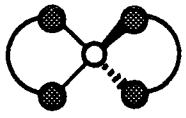

[2+2]

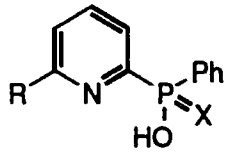

(**32**) R = H, X = O
(**33**) R = CH_3, X = O
(**34**) R = CH_3, X = S

Figure 1.25 Binding geometries and ligands examined in chapter five

Three ligands were synthesised (32), (33) and (34), which are designed to bind to zinc in a [2+2] coordination mode. The effect of increasing the steric bulk at the C-2 position to impose tetrahedral geometry is examined and a thiophosphinic analogue (34) has been synthesised to probe the effect of the more acidic group.

Chapter six details experimental procedures and methods.

1.7 References

1. R. F. Tylecote; 'History of Metallurgy', The Metals Society, London, 1976, 182
2. C. B. Alcock, 'Principles of Pyrometallurgy', Academic Press, London, 1970, pp 1886-9
3. N. N. Greenwood and A. Earnshaw; 'Chemistry of the Elements', Pergamon Press, Oxford, 1984, pp 246-7
4. C. K. Gupta and T. K. Mukherjee; 'Hydrometallurgy in Extraction Processes', CRC Press Inc. USA, 1990, **1**, pp 1-2
5. J. E. Huheey; 'Inorganic Chemistry', Harper Collins Publishers Inc. New York, 1983, 354,
6. C. K. Gupta and T. K. Mukherjee; 'Hydrometallurgy in Extraction Processes', CRC Press, Inc. USA, 1990, **1**, pp 35-56
7. G. Egget, W. R. Hopkins, T. W. Garlick and M. J. Ashley; AIME meet, New York, Feb. 1975
8. D. C. Cuperetino; 'Ion Exchange and Solvent Extraction', SCI conference, Belgrave House, London, 11th March 1998

9. P. W. Atkins; 'Physical Chemistry', Oxford University Press, Oxford, 1990, pp 906-919
10. F. Habashi; *Chem. Eng. News*, 1982, **8**, 46
11. C. K. Gupta and T. K. Mukherjee; 'Hydrometallurgy in Extraction Processes', CRC Press, Inc. USA, 1990, **2**, pp 78-80 & 132-134
12. E. D. Nogueira, J. M. Regiffe and P. M. Blythe; *Chem. Ind.*, 1980, 63
13. C. I. Sainzdiaz, H. Klocker, R. Marr and H. J. Bart; *Hydrometallurgy*, 1996, **42**, pp 1-11
14. N. Miralles, A. M. Sastre, M. Aguillar and M. Cox; *Solvent Extrac. Ion Exch.*, 1992, **10**, 51
15. N. B. Devi, K. C. Nathsarma and V. Chakravortty, *Hydrometallurgy*, 1997, **45**, 169
16. S. Amer and A. Luis; *Revista De Metalurgia*, 1995, **31**, 351
17. R. F. Dalton and R. Price; 'The Cuprex Process-a new chloride-based hydrometallurgic process for the recovery of copper', Ch. 42, in 'Separation Processes in Hydrometallurgy', Ed. G. A. Davies, Ellis Horwood Ltd, Chicester, 1987
18. P. Tasker; 'Novel Extractants', SCI conference, London, 15th March 1995
19. S. Wigetors and J. Rydberg; *Acta Chem. Scand. A*, 1980, **34**, 313
20. C. J. Matthews, T. A. Leese, D. Thorp and J. C. Lockhart; *J. Chem. Soc., Dalton Trans.*, 1998, **1**, 79
21. T. J. Donohoe, R. R. Harji, P. R. Moore and M. J. Waring; *J. Chem. Soc., Perkin Trans. 1*, 1998, **4**, 819
22. R. Gupta; '*Fundamentals of Polymers*', Mc. Graw-Hill Publishing Company, New York, 1997
23. D. E. Fenton; 'Biocoordination Chemistry', Oxford University Press, Oxford, 1997
24. A. Werner; *Z. Anorg. Chem.*, 1893, **3**, 267
25. L. Pauling; 'The Nature of the Chemical Bond', 3rd Ed., Cornell University Press, New York, 1960
26. H. Bethe; *Ann. Physik*, 1929, **3**, 135
27. (i) J. H. Van Vleck; *Phys. Rev.*, 1932, **41**, 208 (ii) J. H. Van Vleck; *J. Chem. Phys.*, 1935, **3**, 803
28. H. M. N. H. Irving and R. J. P. Williams; *J. Chem. Soc.*, 1953, 3192
29. P. George and D. S. McClure; *Prog. Inorg. Chem.*, 1959, **1**, 381
30. J. K. Weddell, A. L. Allred and D. Meyerstein; *J. Inorg. Nucl. Chem.*, 1980, **42**, 219
31. H. Sigel and R. B. Martin; *Chem. Soc. Rev.*, 1994, 83
32. (i) R. H. Prince; 'Zinc and Cadmium' Ch. 56, *Comprehensive Coordination Chemistry*, Eds. G. Wilkinson, R. D. Gillard, J. A. McCleverty, Elsevier, 1987

(ii) D. W. Sharp; 'Transition Metals Part 1' in *Inorganic Chemistry Series 2*, Ed. M. J. Emeléus, Butterworth and Co, London, 1975 (iii) M. J. Mays; 'Transition Metals Part 2' in *Inorganic Chemistry Series 2*, Ed. M. J. Emeléus, Butterworth and Co, London, 1975

33. E. Kimura, M. Yamaoka, M. Morioka and T. Koike; *Inorg. Chem.*, 1986, **25**, 3883
34. T. Koike, E. Kimura, I. Nakamura, Y. Hashimoto and M. Shiro; *J. Am. Chem. Soc.*, 1994, **116**, 4764
35. I. Coldham; *J. Chem. Soc., Perkin Trans. 1*, 1998, **7**, 1343
36. M. Kitamura, M. Yamakawa, H. Oka, S. Suga and R. Noyori; *Chem. Eur. J*, 1996, **2**, 1173
37. A. G. M. Barrett and K. Kasdorf; *J. Am. Chem. Soc.*, 1996, **118**, 11030
38. J. Bjerrum and C. K. Jorgensen; *Rev. Trav. Chim.*, 1956, **75**, 658
39. H. Siegel and R. B. Martin; *Chem. Soc. Rev.*, 1994, 83
40. G. F. Smith and W. H. McCurdy Jr.; *Anal. Chem.*, 1952, **24**, 371
41. G. Stephens, H. L. Fenkel Jr. and W. M. Spinelli; *Anal. Chem.*, 1974, **46**, 692
42. P. Gonzalezduarte, R. March, J. Pons, W. Clegg, L. Cucurullsanchez, A. Alvarezlarena and J. F. Pinella; *Polyhedron*, 1996, **15**, 2747
43. O. Saied, M. Simard and J. D. Wuest; *Organometallics*, 1998, **17**, No. 6, 1128
44. F. Connac, N. Hadaddi, Y. Lucchese, M. Dartiguenave, L. Lamande, M. Sanchez, M. Simard and A. L. Beauchamp; *Inorganica Chimica Acta*, 1997, **153**, No.1, 107
45. G. B. Bates, E. Cole, D. Parker and R. Kataky; *J. Chem. Soc., Dalton Trans.* 1996, 2693
46. G. B. Bates and D. Parker; *Tetrahedron Lett.*, 1996, **37**, 267
47. M. A. M. Easson and D. Parker; *Tetrahedron Lett.*, 1997, **38**, 6091
48. E. Cole Ph. D Thesis, University of Durham, 1993
49. G. B. Bates, D. Parker and P. A. Tasker; *J. Chem. Soc., Perkin Trans. 2.*, 1996, **6**, 1117
50. J. M. Lehn, A. Rigault, J. Siegel, J. Harrowfield, B. Chevier and D. Moras; *Proc. Natl. Acad. Sci. USA*, 1987, **87**, 2565
51. E. Kimura, M. Yamaoka, M. Morioka and T. Koike; *Inorg. Chem.*, 1986, **25**, 3883
52. N. W. Alcock, A. C. Benniston, P. Moore, G. A. Pike and S. C. Rawle; *J. Chem. Soc., Chem Commun.*, 1991, 701
53. G. B. Bates and D. Parker; *J. Chem. Soc., Perkin Trans. 2.*, 1996, **6**, 1109
54. K. Weis, M. Rombach, M. Ruf and H. Vahrenkamp; *Eur. J. Inorg. Chem.*, 1998, **2**, 263
55. P. Comba, B. Nuber and A. Ramlow; *J. Chem. Soc., Dalton Trans.*, 1997, 347
56. R. D. Hancock and A. E. Martell; *Chem. Rev.*, 1989, **89**, 1875

57. R. G. Pearson; *J. Am. Chem. Soc.*, 1963, **85**, 3533

58. G. Schwarzenbach; *Adv. Inorg. Radiochem.*, 1961, **3**, 257

59. S. Ahrland, J. Chatt and N. R. Davies; *Q. Rev. Chem. Soc.*, 1958, 12

60. R. M. Smith and A. E. Martell; 'Critical Stability Constants' Vol 1 to 6, Plenum Press, London

Chapter Two

Introduction to Phosphorus Chemistry

2 Introduction to Phosphorus Chemistry

A rationale for the need to incorporate phosphinic acids into the target compounds is given (2.1), followed by a comparison between carboxylic and phosphorus based acids, highlighting key differences in their chemistry (2.2). Methods are reviewed detailing methods currently available for constructing aromatic carbon-phosphorus bonds, and some model reactions which have been performed (2.3). Synthetic procedures for constructing phosphorus-nitrogen containing ligands are covered focussing on the acid lability of this bond (2.4).

2.1 The need for Phosphinic Acids

For a ligand system to be an efficient agent for the hydrometallurgic recovery of zinc, the pK_a of the anionic donor needs to be as low as possible. Also the lipophilicity of the complex needs to be varied to allow solubilisation of the metal complexes in organic media. For these two facts alone, phosphinic acids offer an attractive solution to the problem; firstly they have pK_as which are lower than the corresponding carboxylic acids (see below), and secondly the pentavalency at phosphorus allows variation of the lipophilicity without compromising the pK_a or the geometry of the coordination site. The use of a phosphinic acid gives a larger chelate 'bite' angle upon complexation (figure 2.1). The angle formed between the metal and the two donors (nitrogen and phosphinate) is less acute for phosphinates than the angle produced by the corresponding carboxylate analogoue. The C-P and the P-O bond of the phosphinic acid (185 and 150ppm respectively) are longer than the corresponding C-C and C-O bonds of the carboxylate (154 and 125ppm respectively).[1] This should result in a complex which is less strained in the phosphinic acid case than in the carboxylate, especially in the case of the more rigid heterocyclic based ligands which are described in this work.

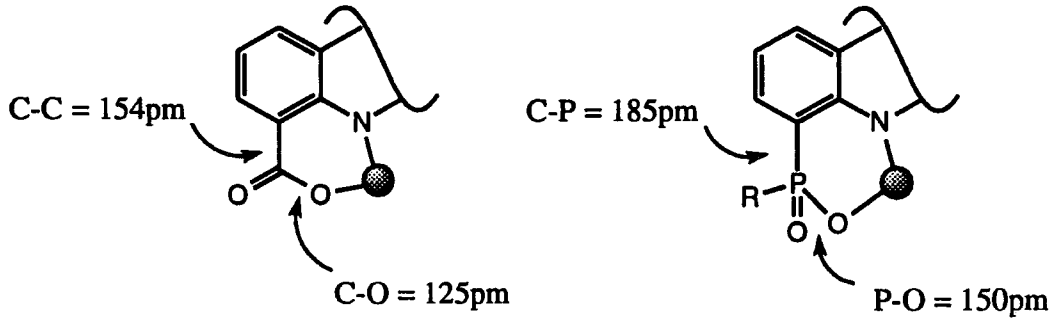

Figure 2.1 Comparison of chelate bite angles formed by aza-carboxylate and aza-phosphinates

2.2 Comparison of Phosphinic and Carboxylic Acids

It has been established that for a ligand to be an efficient and selective extractant for zinc, over a wide pH range, the anionic donor groups need to be more acidic than carboxylic acids.[2] To this end the envisaged use of phosphinic or thiophosphinic acids as the preferred donors, which have lower pK_as than carboxylic acids will satisfy these requirements (figure 2.2).[3] There are a large number of precedents for this, as many extractants currently in use are based upon substituted phosphorus acids and their derivatives.[4]

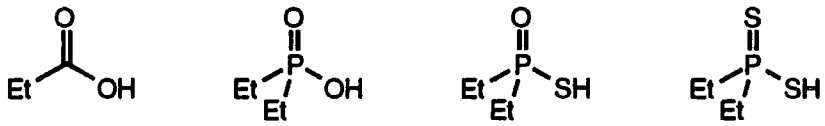

pK_a	4.67	3.29	2.54	1.71

Figure 2.2 pK_as of carboxylic and phosphorus acids.[3]

The use of phosphinic acids is attractive due to the pentavalency at the phosphorus atom, which allows facile variation of ligand lipophilicity and minor modifications to the pK_a.

We anticipated that the formation of the phosphinic acid functionality would be the determining factor in our synthetic routes. A search of the literature reveals a number of methods currently available to produce phosphinic acids directly attached to an aromatic ring and analogous systems with a nitrogen spacer. Also a number of model reactions were performed and these are discussed briefly.

2.3 Phosphinic Acids Linked Directly to an Aromatic Ring

Conceptually the simplest method for the formation of a carbon phosphorus bond is reaction of an anionic aromatic fragment with PCl_3 (35).

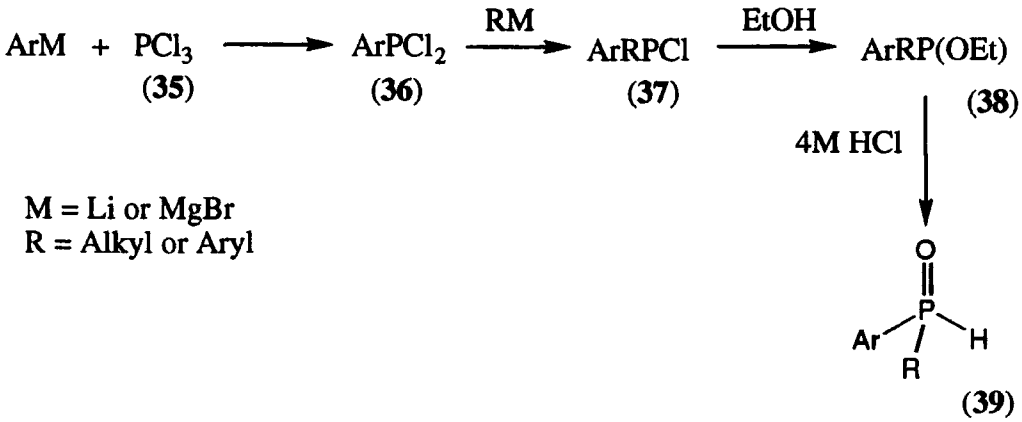

Scheme 2.1 Formation of phosphonous acid (39) from phosphorus trichloride

Once this has been accomplished addition of a further carbon nucleophile should give the disubstituted phosphinous chloride (37), which can be functionalised to the ethoxyphosphine (38) and hydrolysed to give the phosphonous acid (39) (scheme 2.1).[5]

However there are several problems associated with the above scheme, namely that it requires two sequential additions of carbon nucleophiles to the phosphorus centre. Controlling the addition to give monosubstitution in both cases will be problematical unless an excess of the phosphorus containing species is used. This would not be an atom efficient process, as the aromatic fragment would be an advanced ligand fragment. As such this process was not considered to offer a realistic route to the target molecules.

The classic method for the synthesis of phosphinate esters, the precursors of phosphinic acids, is the Arbusov reaction,[6] in which a phosphite (40) is reacted with an alkyl bromide (41) to produce a substituted diethyl alkylphosphinate (42) (scheme 2.2)

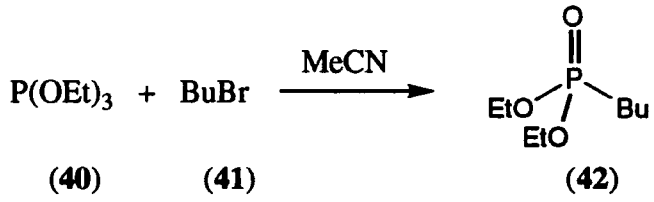

Scheme 2.2 Arbusov reaction between triethylphosphite and butylbromide

The Arbusov reaction can be extended for incorporation into our heterocyclic based ligand systems. For example, reaction of an anionic aromatic ligand fragment with diethoxy chlorophosphine (43) will give a diethyl arylphosphite which should in turn be able to undergo the Arbusov reaction to give the desired phosphinate ester (44) (scheme 2.3)

This modified reaction has been attempted in previous work,[7] however separation of the intermediates from the final compound proved very difficult and so this methodology was also considered inappropriate.

M = Li or MgBr R = Alkyl or Aryl

Scheme 2.3 Modified Arbusov reaction

An alternative method was envisaged which involved reaction of the ligand fragment with a mixed phosphine fragment. To produce the required substituted phenylphosphinic acids, the necessary phosphine fragment would have to be chloroethoxyphenylphosphine (47). This mixed phosphine can be synthesised by a metathetical reaction between equimolar amounts of dichlorophenylphosphine (45) and diethyl phenylphosphonite (46) in the absence of solvent at 0°C (scheme 2.4).[8]

$$\underset{\textbf{(45)}}{PhPCl_2} + \underset{\textbf{(46)}}{PhP(OEt)_2} \xrightarrow{0°C} \underset{\textbf{(47)}}{2\ PhP(OEt)Cl}$$

Scheme 2.4 Disproportionation reaction to produce the mixed phosphine (47)

With this mixed phosphine in hand a number of model studies were performed in order to assess the viability of such methodology in the synthesis of the desired ligand systems. The model studies were directed with a view to producing ligand substituted phenyl phosphinic and thiophosphinc acids, with phenyl lithium as a model for the aromatic fragment. Reaction of phenyl lithium (48) with chloroethoxyphenylphosphine (47) at -78°C gave ethyl diphenylphosphonite (49) as the sole product. Ethyl diphenylphosphonite was used in subsequent studies. Hydrolysis of ethyl diphenylphosphonite with concentrated hydrochloric acid followed by neutralisation and extraction into ether gave diphenylphosphonous acid (50) as the sole product by ^{31}P NMR (δ_P 19 ppm). Hydrolysis using a non-acidic method,[9] trimethylsilylbromide in ether also gave the phophonous acid (50) as the sole product (scheme 2.5)

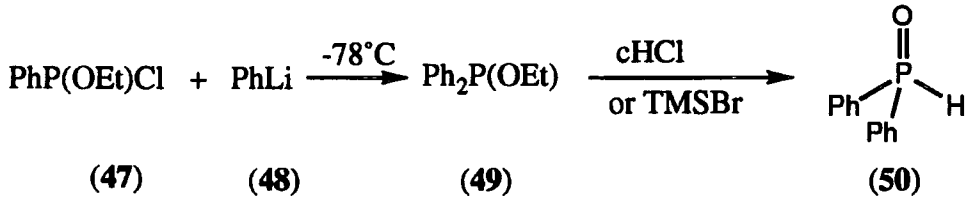

(47) **(48)** **(49)** **(50)**

Scheme 2.5 Synthesis of diphenyl phosphonous acid (50)

Phosphonous acids exist as an equilibrium mixture of the P(V) (50) and the P(III) (51) species, because of this equilibrium it is possible to further oxidise to the corresponding phosphinic or thiophosphinic acids (by addition of oxygen or sulfur).[10] Reaction of diphenyl phosphonous acid (50) with crushed elemental sulfur (S_8) in chloroform at 40°C followed by filtration to remove excess sulfur gave diphenyl thiophosphinic (52) as a single species, as deduced by ^1H and ^{31}P (δ_P 76 ppm) NMR (scheme 2.6)

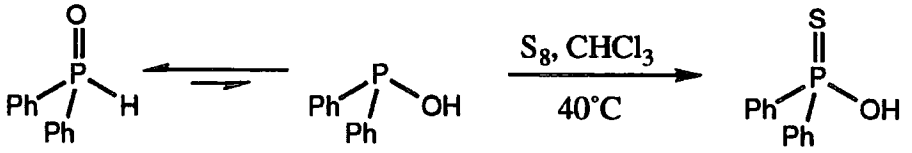

(50) (51) (52)

Scheme 2.6 Sulfur insertion with phosphonous acids

A slightly different methodology was also employed in an attempt to produce the thiophosphinic acid derivatives. This involved sulfur insertion into the intermediate ethyl diphenylphosphonite (49) P(III) species. Sulfur insertion was carried out by an analogous procedure to that above, to produce ethyl diphenylphosphinesulfide (53) as the sole species (δ_P 81 ppm) (scheme 2.7). However hydrolysis of the intermediate phosphine sulfide with either concentrated lithium hydroxide, hydrochloric acid or trimethylsilyl bromide failed.

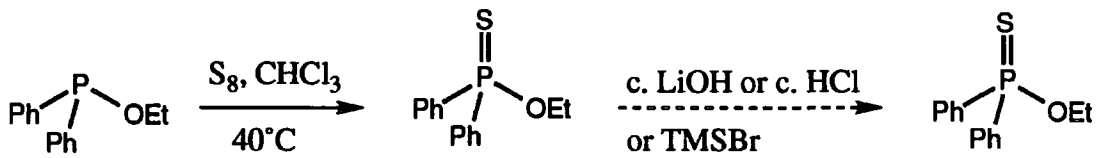

(49) (53)

Scheme 2.7 Attempted hydrolysis of ethyl diphenylphosphinesulfide (53)

In fact the only reported literature example to date for thiophosphinate ester hydrolysis involves use of activated esters such as para-nitrophenol derivatives, often requiring catalytic procedures with enzymes[11, 12] or extremely high pH.[13]

A conceptually different approach was also investigated to produce dithiophosphinic acids directly. This involved the use of Lawesson's reagent (54), a popular thionating agent, which has been used extensively in the synthesis of thioamides, thioketones, thioesters and sulfur containing heterocycles.[14] It has also been employed in the mild reduction of esters and amides to the corresponding ethers and amines by conversion to the thio-ether or amide followed by sulfur removal with Raney nickel.[15] Lawesson's reagent (54) a phosphine sulfide cyclic dianhydride should be ring opened with two equivalents of either Grignard or lithiate species to give the alkyl or aryl substituted dithiophosphinc acid.[16] Reaction between a suspension of Lawesson's reagent (54) in dichloromethane and either methyl or phenyl magnesium bromide at -78°C gave a colourless solution. An aqueous acidic work-up produced the methyl (55) and phenyl substituted (56) dithiophosphinic acids, in quantitative yield, as the sole species (δ_P = 52 and 56 ppm respectively) (scheme 2.8).

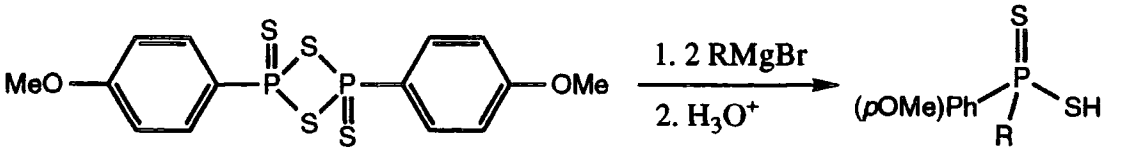

R = CH_3 or Ph (54) (55) R = CH_3 (56) R = Ph

Scheme 2.8 Additions of methyl and phenyl Grignard to Lawesson's reagent (54)

The corresponding reaction between Lawesson's reagent and commercial lithiate species (methyl, butyl and phenyl) failed to give the dithiophosphinic acids cleanly, as deduced by ^{1}H and ^{31}P NMR. Reaction of freshly prepared lithiate species (phenyl, 4-methylphenyl and 4-methoxyphenyl) again gave a complex mixture of phosphorus species.

A final method investigated relied upon a disconnection between the aromatic C-P bond. This requires an aryl bromide and an appropriately functionalised P-H containing species as synthons in a palladium (0) catalysed cross coupling reaction. Reactions of this type have been reported by Xu and Huang[17] and Hirao[18] who used either $Pd(PPh_3)_4$, $Pd(PPh_3)_2Cl_2$ or $Pd(OAc)_2$ as the pro-catalyts to couple aryl bromides with alkyl-aryl or alkyl-alkyl phosphinous esters (57). These reactions yielded ethyl alkyl-aryl or alkyl-alkyl phosphinates (58) with a high degree of tolerance for other functional groups in the molecule (scheme 2.9).

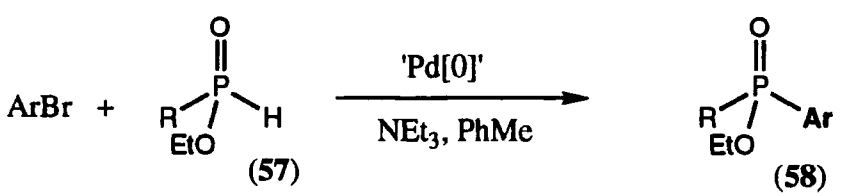

R = Alkyl or aryl

Scheme 2.9 Palladium catalysed 'P-H' insertion reaction.

An added advantage for this approach to carbon-phosphorus bond formation is the ease of synthesis of the alkyl-aryl or alkyl-alkyl phosphinous esters. This allows variation of the lipophilictiy of the target compounds without compromising the binding avidity or pK_as of the acids. The phosphonous esters (57) can be produced by simply dropping ethanol, at 0°C, onto a suitably substituted dichloro alkyl or aryl phosphine,[19] which can in turn be synthesised by adding excess phosphorus trichloride to the required Grignard species (scheme 2.10).

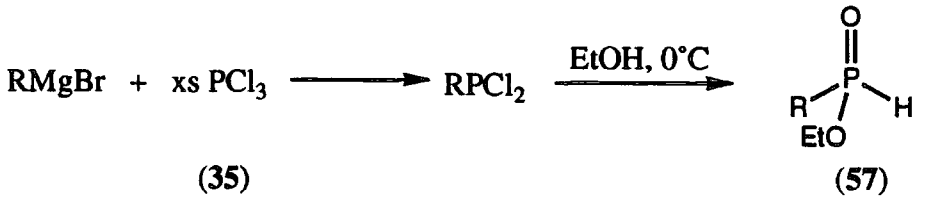

(35) (57)

R = Alkyl or aryl

Scheme 2.10 Synthesis of ethyl-aryl or ethyl-alkyl phosphinous esters (57)

2.4 Phosphinic Acids Linked by a Nitrogen Spacer to an Aromatic Ring

Phosphinic acids linked to an aromatic ligand fragment via a nitrogen spacer were also investigated. Aniline was used as a model for the ligand fragment. A similar strategy was envisaged for the production of the aryl phosphinic amides as for the preceding study. Synthesis of aryl or alkyl phosphoramidite esters should be possible from chloroethoxyphenylphosphine and a functionalised amine. The opportunity exists for equilibrium between the P(III) trivalent pyramidal amido (59) form and the P(V) tetrahedral imidol (60) form as in the previous examples of phosphonous acids (57) (scheme 2.11)

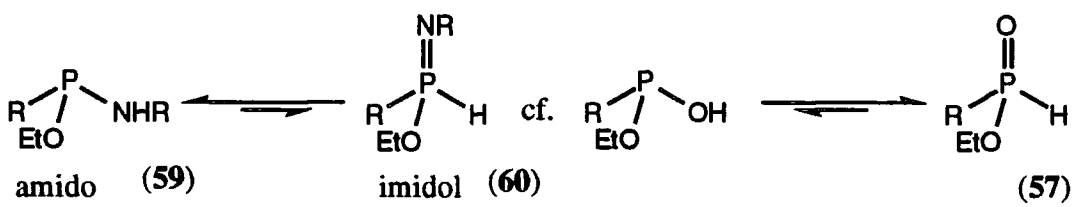

amido (59) imidol (60) (57)

Scheme 2.11 Tautomeric equilibrium between amido (59) and imidol forms (60)

However in contrast to the phosphonous acids, the phosphoramidite esters exist mainly in the amido form. The position of this equilibrium can be influenced by the nature of the R substituent on nitrogen and its ability to influence the hydrogen bonding ability of the amine.[20]

Reaction of aniline (61) with chloroethoxyphenylphosphine (47), prepared as above, in the presence of triethylamine gave ethyl phenylphosphoramidite (62) (δ_P 106 ppm) following precipitation of the triethylamine salts by ether. Unlike the phosphonous acids, hydrolysis of the phosphoramidite esters did not produce the corresponding phosphonous amidite acids. Hydrolysis using either concentrated lithium hydroxide, hydrochloric acid or trimethylsilyl bromide gave phenyl phosphonic acid (63) in all three cases, as deduced by ^{31}P NMR (scheme 2.12).

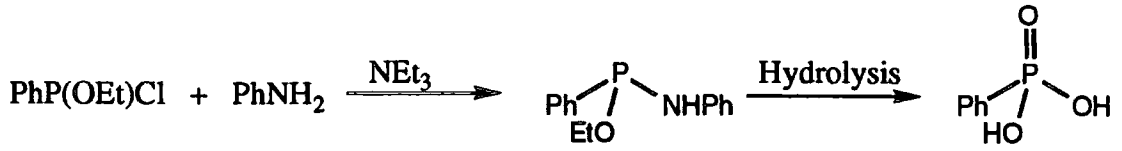

(47) (61) (62) (63)

Hydrolysis conditions; c. HCl, c. LiOH or TMSBr

Scheme 2.12 Synthesis of ethyl phenylphosphoramidite (62) and hydrolysis to phenyl phosphonic acid (63)

Sulfur insertion into the intermediate amido compound should give the corresponding phosphine sulfide (64). Hydrolysis of this compound should be easier than the corresponding thiophosphinates due to the anchimeric assistance provided by the neighbouring amide functionality. Sulfur insertion was carried out as with the previous examples by heating ethyl phenylphosphoramidite (62) with crushed sulfur in chloroform at 40°C. This gave ethyl phenylthiophosphine amide (64) as the sole product (δ_P 67 ppm) following removal of the excess sulfur by filtration. Attempted hydrolysis of the P(V) intermediate using either concentrated lithium hydroxide, hydrochloric acid or trimethylsilylbromide failed to give the desired acid and only unreacted starting material was recovered (scheme 2.13).

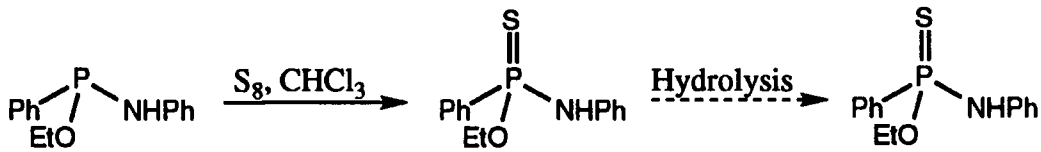

(62) (64)

Hydrolysis conditions: c. LiOH, c. HCl or TMSBr

Scheme 2.13 Sulfur insertion and attempted hydrolysis of phosphine sulfide (64)

Lawesson's reagent has also been used to produce dithiophosphinic acid amides by the reaction of primary or secondary amines with the dimeric anhydride.[21, 22] Reaction of a suspension of Lawesson's reagent in dichloromethane with aniline resulted in complete solution after 16 hours at room temperature. ^{31}P NMR (δ_P 65 ppm) and combustion analysis indicated that the desired dithiophosphinc acid had formed, however mass analysis failed to give the molecular ion of the adduct. This gave concern that the product of the reaction was a 1:1 salt rather than a discrete species, as such this methodology was not pursued any further.

The extreme acid sensitivity of the P-N bond suggests that its use as a donor group in the hydrometallurgic recovery of metals is not a viable proposition.

2.5 References

1. D. Parker, 'Imaging and Targeting', Ch.17, *Comprehensive Supramolecular Chemistry*, Eds. J. M. Lehn, D. N. Reinhoudt, Pergamon, Oxford, 1996
2. G. Cole and D. Bauer; *Rev. Inorg. Chem.*, 1989, **10**, 121
3. D. E. C. Corbridge, '*Phosphorus: An Outline of its Chemistry, Biochemistry and Technology*'. 4th Ed., Elsevier (1990), Ch. 4 & 7
4. (i) E. D. Nogueira, J. M. Regiffe and P. M. Blythe; *Chem. Ind.*, 1980, 63 (ii) N. Miralles, A. M. Sastre, M. Aguillar and M. Cox; *Solvent Extrac. Ion Exch.*, 1992, **10**, 51 (iii) N. B. Devi, K. C. Nathsarma and V. Chakravortty, *Hydrometallurgy*, 1997, **45**, 169 (iv) S. Amer and A. Luis; *Revista De Metalurgia*, 1995, **31**, 351
5. K. Sasse, '*Phosphorus Compounds*', in Vol. 12 of E. Muller, '*Methoden der Organishen Chemie*', Thieme, Stuttgart, 1963
6. A. A. Petrov, A. V. Dogadina, B. I. Ionin, V. A. Garibina and A. A. Leonov; *Russ. Chem. Rev.* 1983, **52**, 1030
7. G. B. Bates, *Synthesis of Tetrahedrally Coordinating Ligands*, Ph. D. Thesis, University of Durham, 1995, 69
8. D. E. C. Corbridge, '*Phosphorus: An Outline of its Chemistry, Biochemistry and Technology*'. 4th Ed., Elsevier (1990), p 329
9. C. E. McKenna, M. T. Higa, N. H. Cheung and M. C. McKeena; *Tetrahedron Lett.*; 1977, **2**, 155
10. D. E. C. Corbridge, '*Phosphorus: An Outline of its Chemistry, Biochemistry and Technology*'. 4th Ed., Elsevier (1990), 315
11. P. K. Danikhel and Purnanand; *Indian J. Chem.*, Sect A., 1990, 29 (A) (9) 256
12. R. Honeycult, L. Ballantine, H. Le Baron, D. Paulson, V. Sein, C. Ganz and G. Milad, *ACS Symp Ser*, 1984, **259**, 343; *Chem Abs.* 101 : 224809n
13. W. Steurbaut, W. Dejonckheere and R. H. Kips, *Meded. Fac. Landbouwnet Rijksuniv Gent.*, 1980, **45** (4) 943; *Chem. Abs.* 94 : 78413x
14. M. P. Cava and M. I. Levonson; *Tetrahedron*, 1985, **41**, No. 22, 5061
15. R. A. Cherkasov, G. A. Kutyrev and A. N. Pudovik; *Terahedron*, 1985, **41**, No. 13, 2567
16. K. Diemert and W. Kuchen; *Angew. Chem., Int. Ed. Engl., Edit*, 1971, **10**, No. 7, 539
17. Y. Xu, Z. Li, J. Xia, H. Guo and Y. Huang; *Synthesis*, 1983, 377
18. T. Hirao, T. Masunaga, Y. Ohshiro and T. Agawa; *Synthesis*, 1981, 56
19. B. A. Arbusov and N. I. Rizpolozhensky; *Izv. An. SSSR, OKhn*, 1952, 843

20. D. E. C. Corbridge, 'Phosphorus: An Outline of its Chemistry, Biochemistry and Technology'. 4th Ed., Elsevier (1990), 403
21. E. Fluck and R. M. Reinisch; *Chem. Ber.*, 1962, **45**, 1388
22. E. Fluck and H. Binder; *Z. Anorg. Chem.*, 1967, **354**, 113

Chapter Three

Benzimidazole Derived Ligands

3 Benzimidazole Derived Ligands

The design, synthesis and coordination properties of a new class of phosphinic acid appended benzimidazole based ligand systems is presented. Design of the new target ligands is discussed with regard to their ability to coordinate selectively to zinc. Incorporation of the phosphinic acid moiety is contrasted with previous examples bearing carboxylate donors. The synthetic schemes and difficulties experienced in producing the four new ligand systems are presented. The coordination chemistry of each of the ligands is discussed using evidence obtained from ^{31}P and ^{1}H NMR, ESMS, liquid-liquid extraction, uv and fluorescence spectroscopy. The chapter will be split into two sections; the first concerns the synthesis and coordination properties of ligands based on the monobenzimidazole skeleton while in the second section ligand architectures constructed from 2-2' and propyl linked bis(benzimidazoles) are examined.

3.1 Benzimidazoles

Benzimidazoles and bis(benzimidazoles) are compounds structurally derived from the mono-cyclic imidazole ring system. Benzimidazole (65) was first prepared in 1872 by Hobrecker,[1] and the first bis(benzimidazole) (66) was reported 56 years later by Phillips (figure 3.1).[2] The synthesis of benzimidazoles and bis(benzimidazoles) has been extensively reviewed elsewhere.[3, 4, 5]

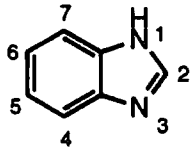

(65)

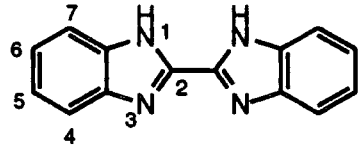

(66)

Figure 3.1 Structure of benzimidazole (65) and 2-2' bis(benzimidazole) (66)

The benzimidazole ring system features in many different active compounds such as the pharmaceutical thiabendazole (67), which is active against nematodal infections, and fungicides such as benomyl (68) (figure 3.2).

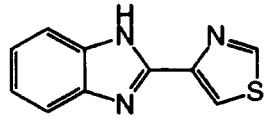

(67)

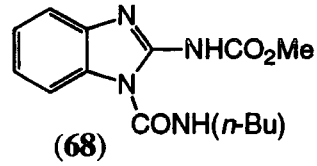

(68)

Figure 3.2 Structures of thiabendazole (67) and benomyl (68)

Benzimidazole is known to be a key component of vitamin B_{12} in the form of 5, 6-dimethyl-1-(α-D-ribofuranosyl) benzimidazole (69) figure (3.3).[6]

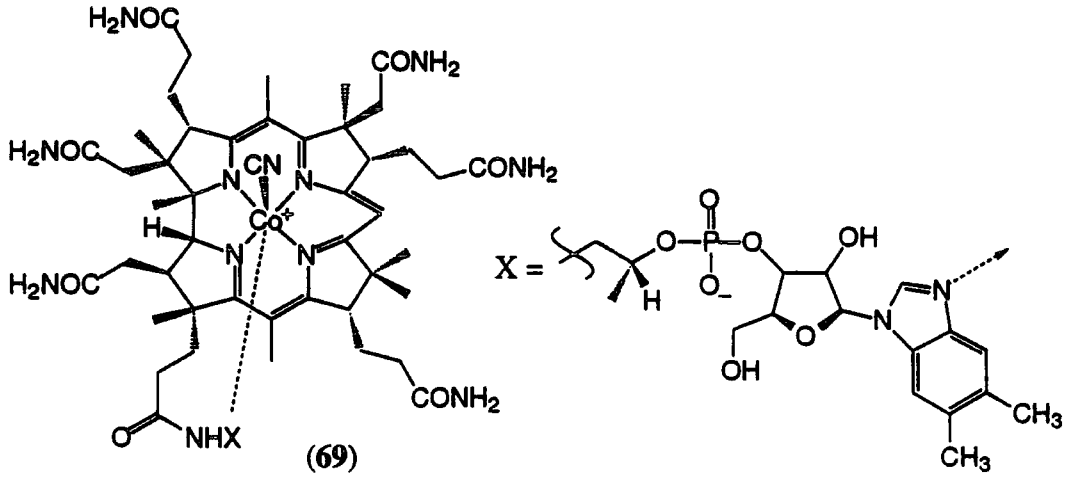

(69)

Figure 3.3 Structure coenzyme B_{12} (69)

Bisbenzimidazoles are usually linked by the 2-2' junction but examples containing 2,4- and 2,5- linkages are known. The two benzimidazole units may be linked directly or via a spacer, which can be either aliphatic or aromatic. Currently there are no bis(benzimidazoles) used commercially.

3.2 Previous aspects of benzimidazole zinc coordination

Benzimidazole and bis(benzimidazole) zinc coordination chemistry has been widely studied. There are examples of monobenzimidazole and bis(benzimidazole) ligands with spacers in the 2-2' position, however there are relatively few examples of directly linked 2-2' bis(benzimidazoles) which have been used to coordinate to zinc. Most of the reported complexes have employed 2,2'-bis-1H-benzimidazole (66) and generally involve second or third row transition metals such as gold,[7] palladium,[8] ruthenium,[9] silver[10] or rhodium.[11]

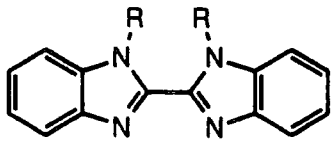

(8) R = Aliphatic

(7) R= OC(O)-alipahtic

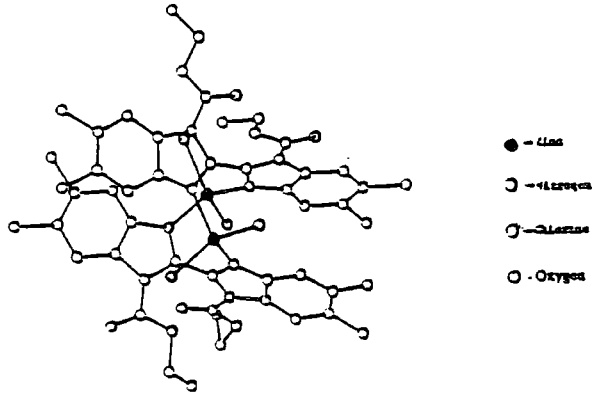

(70)

Figure 3.4 Zinc coordinating benzimidazoles (7) and (8) and structure of (70) zinc complex

Two examples of N-substituted 2,2'-bis(benzimidazoles) have been reported which coordinate to zinc forming dimeric complexes of the form $L_2Zn_2Cl_4$ in the solid state. In each case the zinc ions are in a tetrahedral environment.[12, 13] The coordination sphere of zinc is completed by four benzimidazole nitrogen atoms and four chloride ions (figure 3.4). A recent example of a mono-benzimidazole system designed for zinc coordination is shown below.[14] The ligand (71) was produced by a simple synthetic route from 1-H-benzimidazole in high yield, and complexation with zinc bis(hexamethyldisilylazide) (72) in diethylether produced the three coordinate zinc complex (73) (scheme 3.1). Analysis of the solid state structure shows zinc in a planar N_3 coordination environment, with a 'T' shape coordination geometry, having two short amido Zn-N bonds (188nm) and a longer benzimidazole Zn-N bond (207nm). This complex was prepared in order to study coordinatively unsaturated zinc compounds in catalytic methanol synthesis, for the reaction between hydrogen and carbon monoxide.

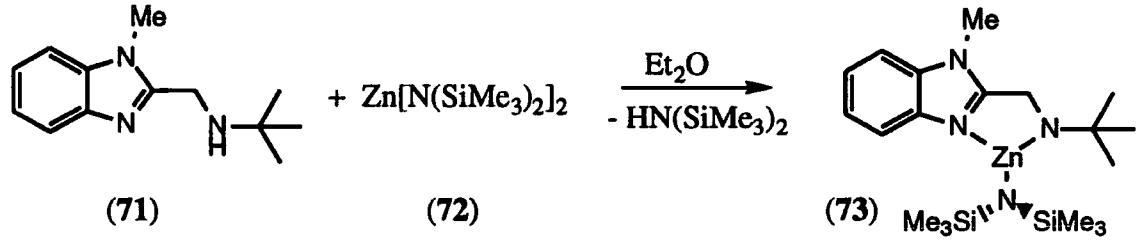

(71) (72) (73)

Scheme 3.1 Preparation of (73) zinc complex

Several research groups have looked at heteroatom substituted bis(1,3 propandiyl) benzimidazoles, which were prepared with a view to producing biomimetic model complexes. The donor atom sets for these ligands have been chosen to mirror those found in known zinc metalloenzymes for example; N_3 in carbonic anhydrase and thermolysin, N_3O in carboxypeptidase and β-lactamase and NS_2 in alcohol dehydrogenase.[15] Lockhart *et al.* have prepared (74) and (75) which differ only in the heteroatom in the trimethylene bridge and complex formation was achieved using zinc perchlorate.[16] For both ligands, analysis of the solid state structure reveals that zinc possesses a bound water atom, which may implicated in the catalytic activity of the enzyme, either by ionisation or by displacement of the solvent molecule. With ligand (75), which offers an N_2O donor set for zinc it was found that in the solid state (76) zinc is in a pseudo-trigonal bypyramidal geometry with the three donor atoms coordinating and the remaining coordination sites filled by water and a solvent molecule (acetonitrile) (figure 3.5). In contrast, ligand (74) which has an N_2S donor set produces a different coordination mode to zinc. Binding of the sulfur atom in the thioether bridge is absent and zinc adopts a pseudo-tetrahedral coordination geometry (77) with two coordinated counter ions (chloride) (figure 3.5) in the solid state.

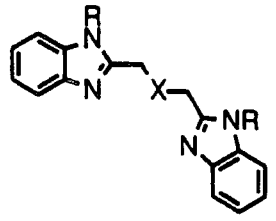

(74) R = Me, X = S

(75) R = H, X = O

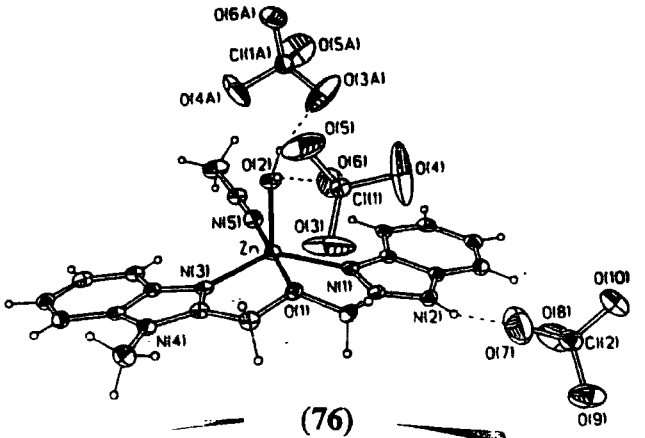

(76)

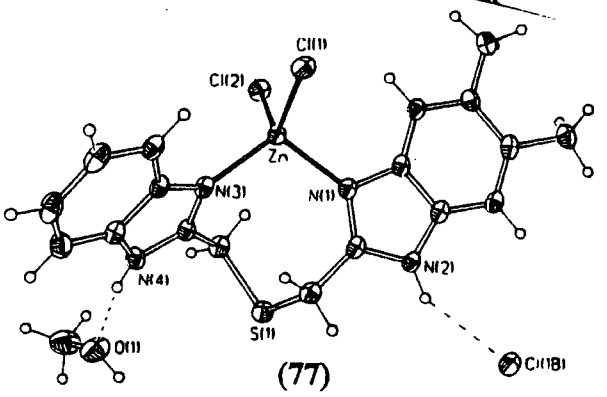

(77)

Figure 3.5 Crystal structures of (74) and (75) as their zinc complexes

Krebs and co-workers have investigated the coordination properties of a tris-benzimidazole ligand (78) derived from nitrilotriacetic acid, in which the zinc complex was produced by reaction of the ligand with zinc(II) thiocyanate in isopropanol.[17] Analysis of the solid state structure shows zinc in a distorted trigonal bypyramidal coordination geometry (79), with an extremely long Zn-N_{amine} bond (254nm) and a coordinated thiocyanate counter ion (figure 3.6).

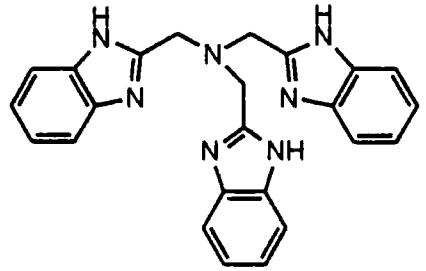

(78)

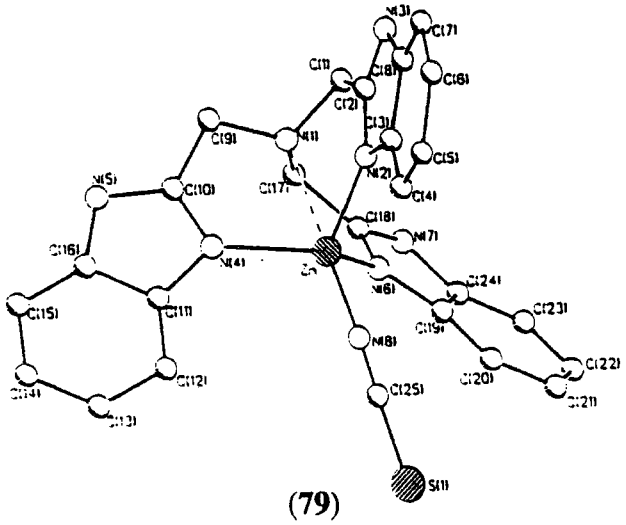

(79)

Figure 3.6 Ligand (78) and zinc complex of N-tris(2-benzimidazolylmethyl)amine (79)

3.3 Design of monobenzimidazole ligand

In the initial section of this chapter, bidentate ligand systems based on the [2+2] architecture will be considered (figure 3.7). Using the design methodology outlined in chapter one, two ligands should bind to the metal centre and through the correct design of the system unwanted coordination geometries should be prevented. The ligand (26) presents an NO donor set from a benzimidazole nitrogen and a phosphinic acid, and is expected to bind to zinc as a bidentate ligand in a 2:1 fashion in the putative pseudo-tetrahedral complex (figure 3.7).

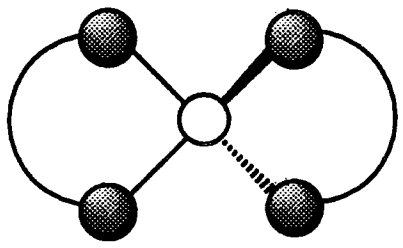

[2+2]

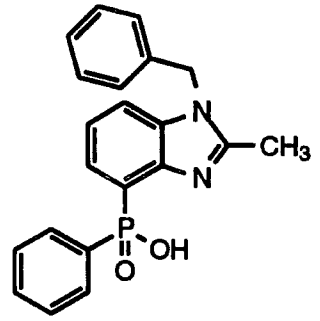

(**26**)

Figure 3.7 Diagrammatic representation of [2+2] ligand geometry and target ligand (26)

Molecular Modelling

Molecular modelling of the zinc complex was performed using the Sybyl 6.3 programme (Tripos UK Ltd.) at Zeneca Specialties, Blackley. Charge distribution of the complex was calculated using MNDO force field routines and the structures minimised with the AM1 force field (figure 3.8). The model shows tetrahedral zinc (green central ion) with two chelating bidentate benzimidazole ligands as the lowest energy structure. The methyl substituent in the C-2 position will prevent formation of other coordination geometries, particularly square planar and octahedral. Attempts to place the ligands in a square planar or trigonal bipyramidal coordination geometry resulted in a structure that minimised itself to a tetrahedral arrangement. The two phenyl substituents on the phosphinic acid are oriented in and out the plane of the page, indicating that substitution in the *para* position of the phenyl ring will not have a detrimental effect on the binding.

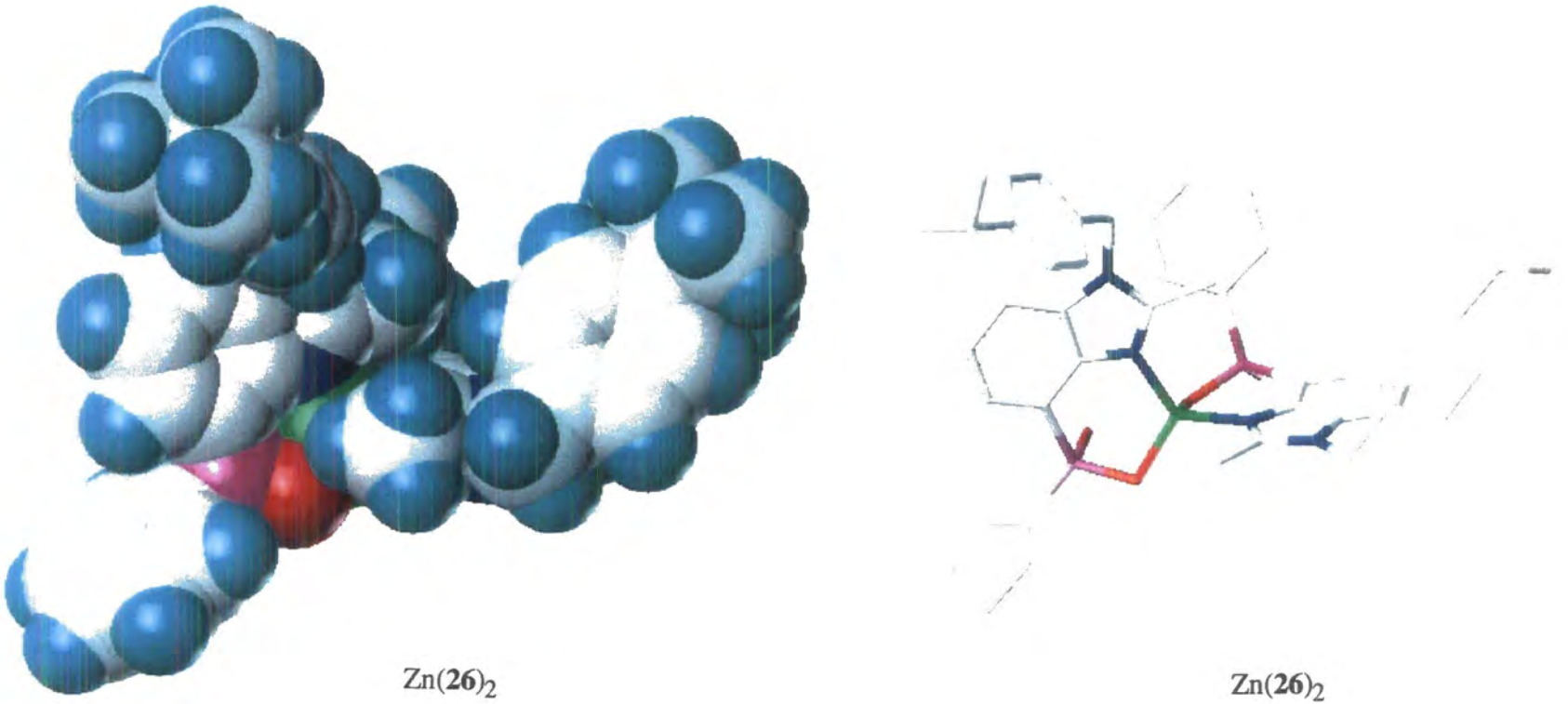

Figure 3.8 Molecular model showing the tetrahedral zinc complex of ligand (26), space filling (left) and line drawing (right)

Ligand architecture

The ligand system (26) is based on the benzimidazole ring system, although imidazoles are generally found to be coordinated to zinc in metalloenzymes via the amino acid histidine. Functionalisation of imidazole is problematic and the benzimidazole ring system is more easily manipulated which should also impart extra rigidity to the ligand. The strong bond formed between the benzimidazole nitrogen and zinc may shorten the Zn-N bond length, thereby promoting tetrahedral geometries by minimising steric interactions.[18, 19] The phosphinate donors should help promote coordination to zinc at low pH, crucial for an efficient hydrometallurgic extractant.[20] Choice of the correct substituent in the 2-position of the ring is critical in ensuring a good tetrahedral geometry. If the substituent is too bulky, then steric hindrance will inhibit complex formation, while if the substituent is too small, discrimination against other coordination geometries will be limited. From molecular modelling studies (*vide supra*) the methyl group satisfies these criteria. Binding of the phosphinate oxygen and the proximate nitrogen atom to zinc will form a six-ring chelate, which tends to favour coordination to smaller metal ions.[21]

The lipophilicity of the complex can be easily be varied without compromising the binding ability of the ligand. The N-alkyl substituent can easily be modified to produce lipophilic analogues by further substitution in the *para* position. Alternatively the pentavalency of the phosphorus atom can be exploited. The synthesis of lipophilic phosphinate substituents allows variation of the lipophilicity on the 'south' side of the molecule, which will aid solubilisation in the commercial kerosene based solvents used in the hydrometallurgic recovery of metals.

3.4 Synthesis of Benzimidazole-4-phenylphosphinic acid Ligand

Retrosynthetic analysis of the target compound (26) is shown below (scheme 3.2).

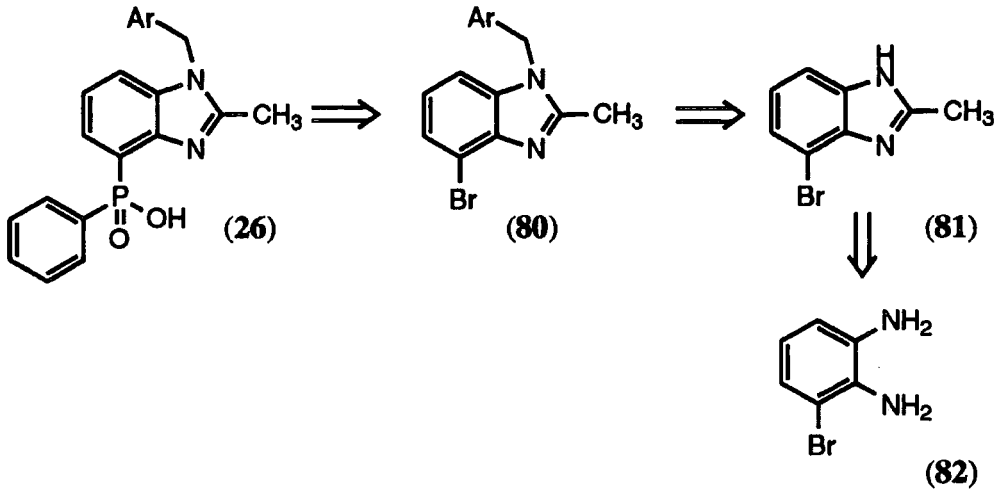

Scheme 3.2 Retrosynthetic analysis of monobenzimidazole ligand (26)

Disconnection of the phosphinic acid functionality followed by subsequent removal of the N-benzyl substituent (readily introduced by N-alkylation with a suitable benzylic bromide) gives the parent benzimidazole (81). Disconnection from the benzimidazole (81) to the diamine (82) provides a simple starting point for the synthetic scheme. Potential problems with this synthetic route involve the introduction of the C-P bond, as discussed in chapter two. The use of the mild and selective palladium catalysed cross-coupling reaction should provide a solution to this. Selective introduction of the N-alkyl substituent is also potentially problematic: alkylation of the 2-methyl-4-bromobenzimidazole can, in principle, occur at either the 1 or 3 position as the proton can reside on either of the two nitrogen atoms. Alkylation of benzimidazole moieties proceeds via a S_E2' mechanism. Therefore the 4-bromo substituent should provide enough steric bulk to direct alkylation to the desired nitrogen atom. The literature contains a number of examples of this type of selective alkylation. The alkylation of 2,6-dimethyl-4-nitrobenzimidazole (83) with butyl bromide and sodium hydride to give exclusively 2,6dimethyl-1-butyl-4-nitrobenzimidazole (84), provides a good example (scheme 3.3).[22]

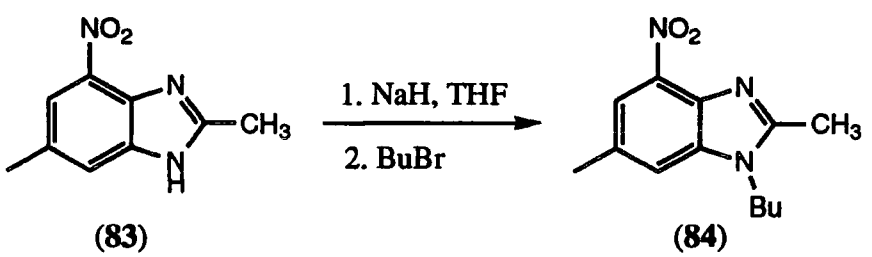

(83) **(84)**

Scheme 3.3 Selective N-alkylation of benzimidazole (83)

Finally, disconnection of the benzimidazole to the substituted diamine should proceed easily in the forward manner, using the standard Phillips procedure for benzimidazole synthesis.[23]

Synthesis of 3-bromo-1, 2-diaminobenzene.

The key compound in the production of the bromobenzimidazole is 3-bromo-1,2-diaminobenzene(82). Several different routes were attempted before a satisfactory synthesis was obtained. The first approach attempted (scheme 3.4) involved the direct nitration of 2-bromoaniline (85) with 4-nitro-4-methyl-2,3,5,6-tetrabromo-2,5-cyclohexadiene-1-one (86) following the procedure of Guette.[24] The driving force for this reaction is the re-aromatisation of the dienone (86) which can be recovered and reused simply by treatment with nitric acid. The reaction does not require the use of protic media, negating the need to protect 2-bromoaniline (85). Protonation of the amine would result in a highly deactivated aromatic system in which the ammonium ion would be *meta* directing.

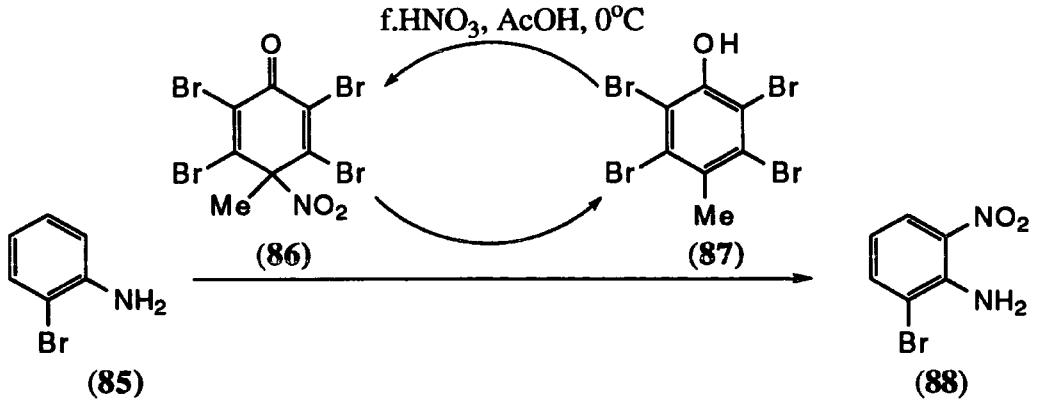

Scheme 3.4 Nitration of 2-bromoaniline (85)

This method produced a mixture of *ortho* and *para* isomers which were separated by flash chromatography giving only a small amount of the desired *ortho*-nitrated product (23%).

Nitration was also attempted in acidic media, which necessitated protection of the amine as its acetamide derivative (89). N-Alkylation was accomplished using acetic anhydride and a catalytic amount of concentrated sulphuric acid. The first method attempted involved nitration at 0°C with a mixture of concentrated nitric and sulphuric acids. However this produced predominantly the *para* nitrated product and chromatographic separation yielded only 2-bromo-6-nitroaniline and 2-bromo-6-nitro-N-acetylaniline as a 1:1 mixture.

Next, nitration was attempted with stoichiometric amounts of acetic acid and fuming nitric acid. This afforded only starting materials, even after extended reaction times. The method of Smith was also attempted, which involved pre-forming the nitronium ion with acetic anhydride and fuming nitric acid followed by the addition of the protected amine.[25] Again this method only gave unreacted starting material.

The successful nitration method (scheme 3.5) involved the formation of the nitronium ion with a 5:4 v/v mixture of fuming nitric acid and trifluoroacetic acid with 1% added water. The reaction was initiated with gentle heating between each addition of 2-bromo-N-acetylaniline. The reaction time was considerably shorter than previously reported methods,[26] being complete within 16 hours. Precipitation by pouring the nitration mixture onto ice gave the *ortho* and *para* nitrated products as a 1:1 mixture. The two isomers could be separated by recrystallisation from chloroform at 0°C, giving the *ortho*-nitrated product (90) as a white crystalline material. Scaling up the reaction had no detrimental effect either on the reaction times or on the ratio of *ortho* to *para*

nitrated products. In fact batches of up to 100g can be successfully nitrated without any detrimental effects on the yield, rate and without raising undue safety concerns.

Hydrolysis of the 4-nitro N-acetyl derivative (90) with a hydrochloric acid-ethanol mixture (33% v/v) gave 2-bromo-6-nitroaniline (88) as bright yellow crystals. The nitro group was then reduced using tin(II) dichloride dihydrate in concentrated hydrochloric acid at 110°C, to yield the required bromo-diamine (82) as a pale yellow solid in 43% overall yield. Reduction of the nitro group was also attempted using catalytic hydrogenation and transfer hydrogenation conditions. Neither of these methods gave the target compound, unreacted starting material being recovered on work-up, in each case.

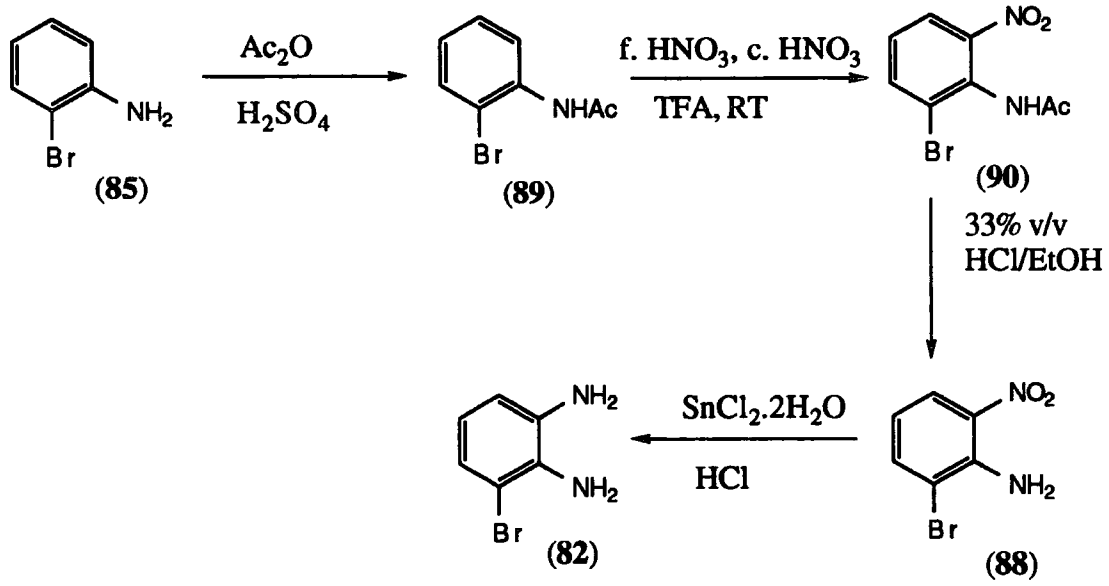

Scheme 3.5 Successful synthesis of 3-bromo-1,2-diaminobenzene (82)

4-Bromo-2-methylbenzimidazole (81) was produced by a modified Phillips procedure.[23] Condensation of the bromo-diamine (82) with excess acetic anhydride at 120°C for two hours and removal of the residual acetic anhydride under reduced pressure followed by acid hydrolysis gave the desired benzimidazole (81) as an off-white solid in 89% yield.

N-Alkylation of 4-bromo-2-methylbenzimidazole (81) was accomplished in DMF using caesium carbonate as the base. It was found necessary to ensure that both the benzimidazole and caesium carbonate were rigorously dry prior to performing the reaction. As expected, the bromide substituent provided enough steric bulk to direct N-alkylation (scheme 3.6) to the least hindered side of the molecule. The regio-chemistry was confirmed by a ^1H NOE experiment showing an enhancement only between the benzylic CH_2 and H-7 of the benzimidazole ring.

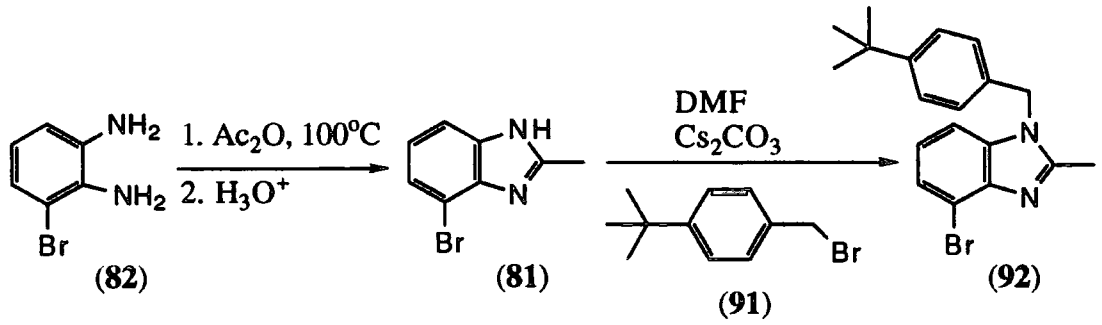

Scheme 3.6 N-alkylation of 4-bromobenzimidazole (81)

Introduction of the phosphinic acid function

With the bromo substituted benzimidazole (92) in hand, application of a number of the model reactions discussed earlier (Ch 2.3) was investigated. Conceptually the simplest method for introduction of the phosphorus atom is to produce an anionic site on the benzimidazole skeleton and react this with an electrophilic source of phosphorus.

Halogen-lithium exchange was attempted in an analogous manner to that of a previous study with 2-2' bis(benzimidazoles).[26] The bromo-benzimidazole (92) was dried under vacuum at 80°C for eighteen hours to remove all traces of water then dissolved in anhydrous THF. n-Butyl lithium was added dropwise at -78°C and the mixture kept at this temperature for three hours (scheme 3.7).

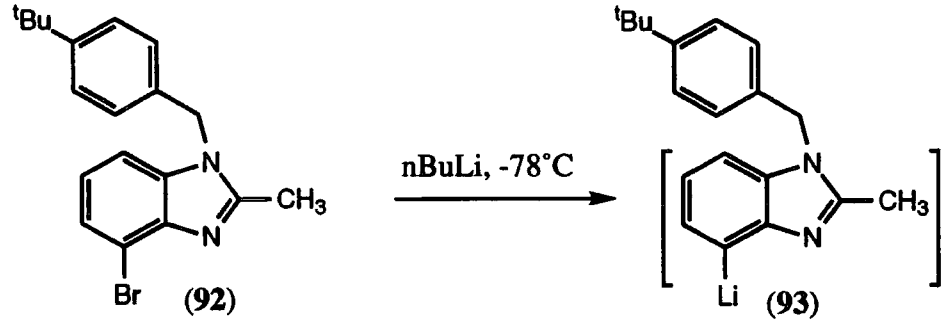

Scheme 3.7 Lithiation of monobenzimidazole (92)

The supposed 4-lithio benzimidazole (93) was then allowed to react with a variety of electrophilic agents in order to obtain an anionic donor group at the four position of the benzimidazole ring. Quenching with chloroethoxyphenylphosphine (47) (prepared freshly, chapter 2 section 2.3), carbon dioxide or carbonyl sulfide followed by an aqueous acidic workup gave a dark coloured solid in all cases. The products were subject to analysis by NMR (^{31}P and ^{1}H), ESMS and HPLC. None of the desired product was detected (scheme 3.8).

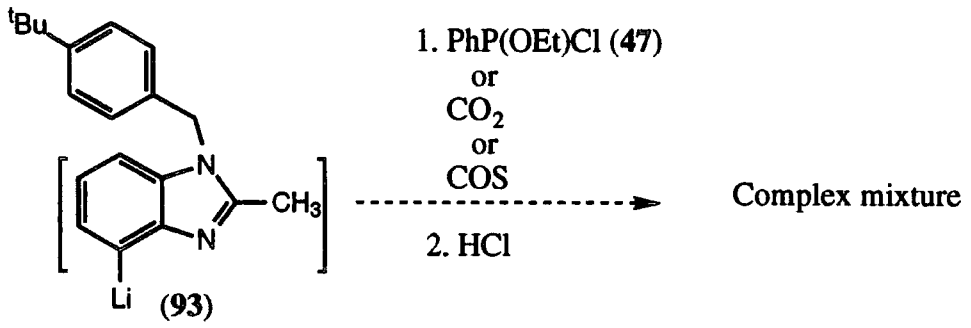

Scheme 3.8 Attempted electrophilic quenching of lithio-benzimidazole (93)

The apparent failure of the lithiation can perhaps be explained by competitive deprotonation of the 2-methyl substituents protons. This position is similar in nature to a simple ethanoate ester. As such, deprotonation should be facile under these reaction conditions, producing a stabilised carbanion. Formation of this proposed intermediate followed by an electrophilic quench could account for the complex reaction mixture obtained.

In an attempt to overcome this problem and negate the use of a basic reagent to form a metallated benzimidazole, Grignard formation was attempted. Magnesium turnings were activated by stirring vigorously under vacuum at 100°C and suspended in THF with a single crystal of iodine. A solution of 4-bromo-1-(4-*tert* butylbenzyl)-2-methylbenzimidazole (92) was slowly added to the magnesium suspension with gentle heating. The mixture was heated at 70°C for sixteen hours and dry solid Lawesson's reagent (54) added and the mixture heated for a further two hours. Following an aqueous acidic work-up, only starting materials were recovered (scheme 3.9). Subsequent attempts at Grignard formation followed by quenching with CO_2 or D_2O again gave only unreacted staring materials, indicating that Grignard formation is rather difficult.

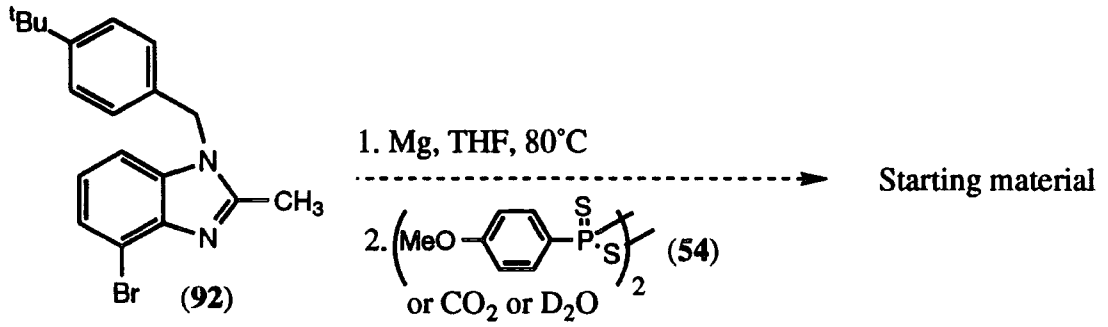

Scheme 3.9 Attempted formation of Grignard and electrophilic quench

As formation of either the lithiate or Grignard derivatives of the bromo-benzimidazole appeared to be hampered by competing reactions or lack of reactivity, the palladium catalysed cross coupling reaction with phosphinous esters was investigated (chapter 2 section 2.3). Using the procedure of Xu and Huang, it is possible to cross couple aryl bromides with alkyl-aryl phosphinous esters using either $Pd(PPh_3)_4$, $Pd(PPh_3)_2Cl_2$ or $Pd(OAc)_2$ as the pro-catalyst.[27] Tetrakis(triphenylphosphine)palladium(0) was prepared according to the procedure of Coulson by reaction of a suspension of palladium dichloride in dimethyl sulfoxide with triphenylphosphine at 140°C, followed by reduction with hydrazine.[28]

4-Bromo-1-(4-*tert* butylbenzyl)-2-methylbenzimidazole (92) was rigorously dried prior to dissolution in dry toluene and triethylamine and ethylphenylphosphinite (94) were added to the solution. The mixture was degassed twice and tetrakis-(triphenylphosphine)palladium(0) added to the reaction mixture, which was heated at 120°C for sixteen hours. Purification by flash chromatography gave the product phosphinate ester (95) in 62% yield as a white powder (scheme 3.10).

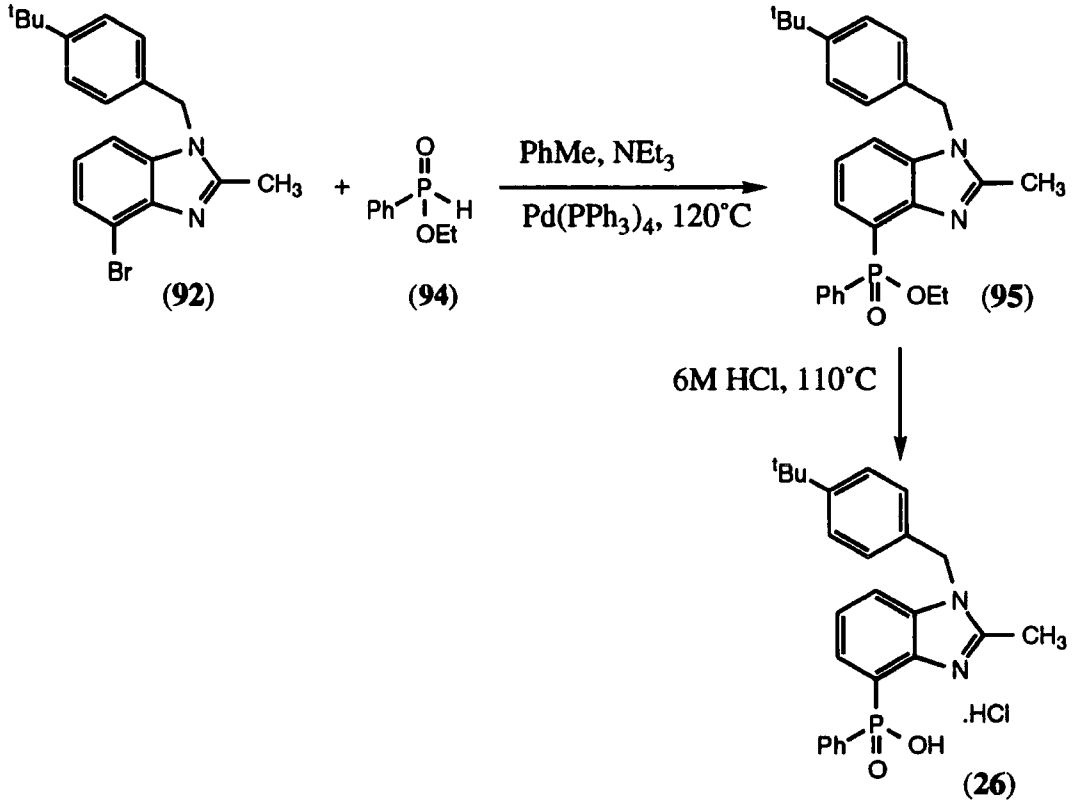

Scheme 3.10 Cross coupling of 4-bromobenzimidazole (92) and ethyl phenylphosphinite (94)

Conversion to the target acid (26) was simply achieved by hydrolysis of the phosphinate ester (95) in hydrochloric acid (6M) which was removed by lyophilisation to give the product (26) as its hydrochloride salt in 24% overall yield (scheme 3.10).

3.5 Solution complexation behaviour

In solution various equilibria can exist when metal ions are present, involving differently protonated mononuclear species (equations 3.1 to 3.4). With the addition of a metal to the ligand, all these equilibria may not necessarily occur to any significant extent and some may be neglected. Formation of an ML_2 complex must proceed via formation of a ML complex. However, the relative proportions of these in solution will depend on the relative magnitude of K_1 and K_2. If the ligand forms a 2:1 complex and further metal is added there is the possibility that this may react further to form two ML complexes, which is K_1/K_2.

$$M + L \overset{K_1}{\rightleftharpoons} ML \qquad \text{eqn. 3.1}$$

$$ML + L \overset{K_2}{\rightleftharpoons} ML_2 \qquad \text{eqn. 3.2}$$

$$ML + H \overset{K_3}{\rightleftharpoons} MLH \qquad \text{eqn. 3.3}$$

$$ML_2 + M \overset{K_1/K_2}{\rightleftharpoons} 2ML \qquad \text{eqn. 3.4}$$

Where possible all solution complexation behaviour was monitored in 100% methanol solution to maintain consistency between the data.

3.5.1 ^{31}P NMR titrations

Phosphorus NMR titrations will provide information regarding the participation of the phosphinic acid in complexation. Analysis of the data obtained from this technique gives an insight into the nature of the equilibria involved in solution.

NMR titrations for the phosphinic acid appended benzimidazole ligand (26) were carried out in a mixture of deuteriated solvents (25% CD_3OD, 75% $CDCl_3$) with a 0.04M ligand solution and 0.4M solution of metal triflates (Zn, Cd, Ni and Cu). In all cases the titrations were performed in a single NMR tube with incremental additions of the more concentrated metal solution. Owing to the much greater concentration of this solution it is possible to neglect changes in the ligand concentration within the range studied. Each sample was analysed by ^{31}P NMR spectroscopy between addition of each aliquot of the metal solution.

Zinc

With increasing metal to ligand ratios, there was an observed shift in the phosphorus signal to higher frequency. A single exchange broadened peak was observed, indicating that bound and unbound species were in fast exchange on the NMR timescale(101MHz, 293K). Plotting the shift in phosphorus resonance against the metal to ligand ratio (M/L) gave a titration curve (figure 3.9). Non-linear least squares analysis for a 1:1 stoichiometric complex[29, 30] gave an equilibrium stability constant of $LogK_{Zn} = 5 \pm 0.1$ (see appendix A). There is a positive deviation of the experimental curve away from the theoretical curve at M/L < 1, suggesting that ML_2 formation may be occurring en route to a stronger ML complex.

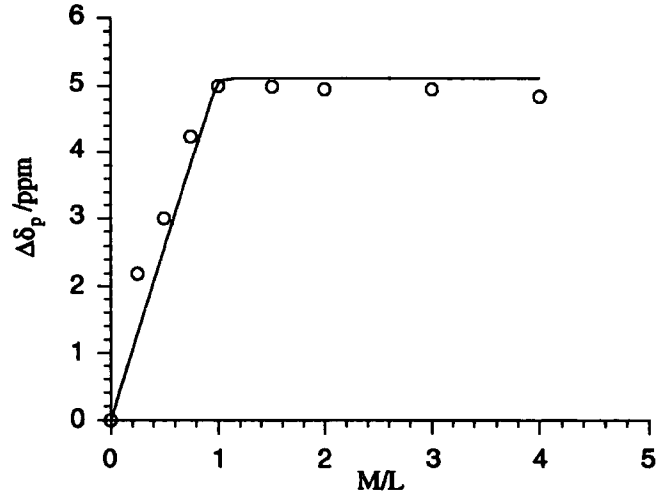

Figure 3.9 ^{31}P NMR titration with $ZnTf_2$ and (XX) (293K, 25% CD_3OD, 75% $CDCl_3$)

Job's Method of Continuous Variations

Using Job's method it is possible to determine the predominant stoichiometry in solution. Experimentally this involves preparing different combinations of the metal and ligand, such that the total concentration is constant (see appendix B). Plotting the complex concentration (given by eqn. 3.5), where δ_{obs} = the observed chemical shift, δ_L = the chemical shift of the ligand and δ_{MmLn} = the limiting chemical shift of the complex, against the percentage of ligand present provides a curve which gives the stoichiometric ratio at the turning point (figure 3.10):[31]

$$[M_m L_n] = \frac{[L](\delta_{obs} - \delta_L)}{(\delta_{M_m L_n} - \delta_L)} \qquad \text{eqn. (3.5)}$$

From the above curve it is clear there is a turning point at a ligand percentage of 66%, indicating that the complex stoichiometry in solution is predominantly 2:1.

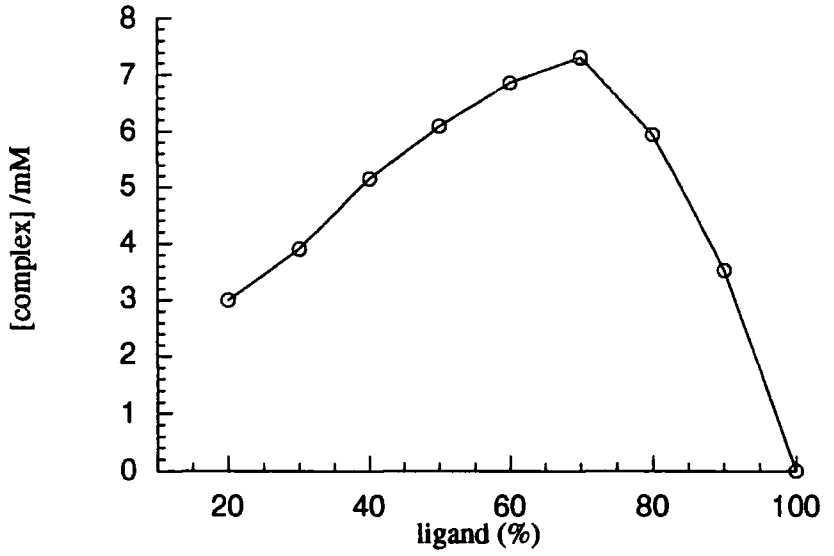

Figure 3.10 Job's plot of (26) plus zinc (293K, 25% CD_3OD, 75% $CDCl_3$)

Cadmium

With increasing metal to ligand ratios, there was an observed shift in the phosphorus signal to higher frequency. There was a single exchange broadened peak, indicating that bound and unbound species were in fast exchange on the NMR time scale(101MHz, 293K). Plotting the shift in phosphorus resonance against the metal to ligand ration (M/L) gave a titration curve (figure 3.11).

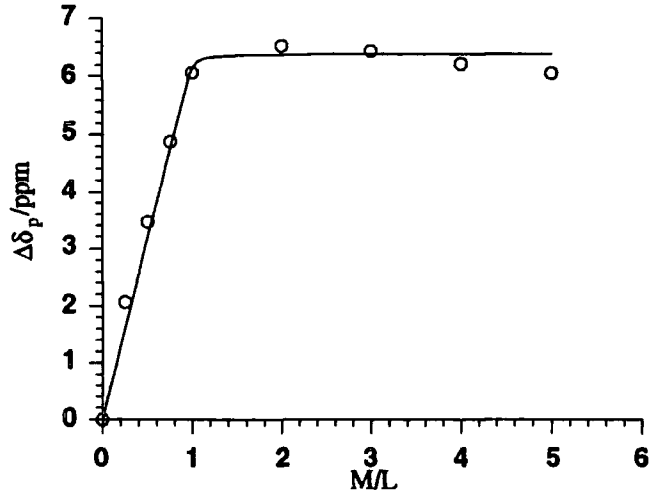

Figure 3.11 ^{31}P NMR titration with $CdTf_2$ and (26) (293K, 25% CD_3OD, 75% $CDCl_3$)

Non-linear least squares analysis for a 1:1 stoichiometric complex[29, 30] gave an equilibrium stability constant of $\log K_{Cd} = 4.2 \pm 0.1$. The form of the titration curve suggests that with cadmium the species formed in solution when excess metal is present is a 1:1 complex.

3.5.2 Fluoresence titrations

Background

Although investigation of the solution chemistry by phosphorus NMR is an extremely useful tool, it only provides insight into the properties of the phosphinic acid donor. Shifts in the spectrum upon addition of metal imply that the acid is indeed binding to the metal. This technique does not provide a method for investigating how the nitrogen donor in the benzimidazole ring is interacting with the metal. Fluorescence and visible/ultraviolet spectroscopy can be used to probe this interaction. The coordination of the benzimidazole nitrogen atom to a proton or metal ion will cause a perturbation of the chromophore molecular orbitals, and hence may effect the emission and absorption characteristics of the system. These changes in the spectroscopic properties will manifest themselves as changes in emission/absorption intensity and/or a shift in the wavelength.

pH Titration

Although potentiometric methods are often used for the accurate determination of acidity constants, this method is unsuitable for use at pH values below 3 and above 9. This is because the response of the pH electrode is not reliable at these extremes. Fluorometric determination of acidity constants does not suffer from this drawback as the change in fluorescence intensity or the wavelength shift are the important parameters.

Variations in fluorescence intensity were monitored as a function of pH for 1-(*tert* butylbenzyl)-2-methylbenzimidazole-4-phenylphosphinic acid (26). The titrations were started at low pH by addition of trifuoroacetic acid and moved to higher pH by incremental addition of sodium hydroxide solution. The variation in intensity was then monitored as a function of pH between 1 and 10. A selection of the spectra at various pH values are shown (figure 3.12).

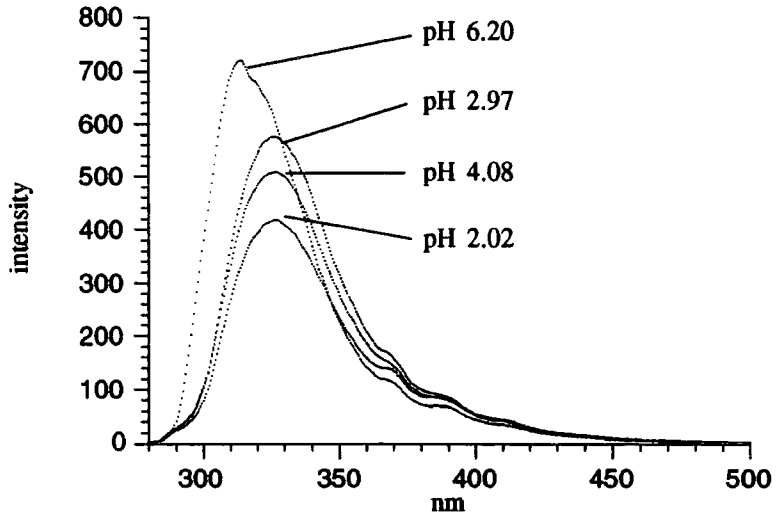

Figure 3.12 Variation of fluorescence intensity as a function of pH for (26) (90% H_2O, 10% MeOH, λ_{ex}=270nm, λ_{em}=280-500nm)

As is evident from the above spectra there is not only a change in emission intensity, but also a shift in the emission wavelength. This change is consistent with a combination of internal charge transfer (ICT) and the pertubation of the frontier orbitals on protonation. Protonating the nitrogen atom causes a change in the relative energies of the HOMO and LUMO of the system.* Both the HOMO and the LUMO are lowered in energy when the nitrogen atom is protonated relative to the free species. The energy gap between the frontier orbitals is greater for the unprotonated system, resulting in a higher energy, blue-shifted emisson.

In the excited state the dipole moment of the molecule is likely to be more pronounced than in the ground state. This dipole causes the solvent shell to reorganise around the molecule and because emission occurs over a longer timescale, the excited state relaxes to a modified ground state.[32] Evidence for the ICT was confirmed by recording the fluorescence emission spectra in solvents of increasing polarity (THF, CH_2Cl_2, MeCN, MeOH and H_2O, with polarities of 0.21, 0.31, 0.46, 0.76 and 1.0 on the E_T[30] scale[33]) with an associated red-shifted emission. By plotting the variation in fluorescence intensity versus pH, information regarding the pK_a of both the phosphinic acid and benzimidazole nitrogen can be gained. A plot of the fluorescence emission intensity at both 326 and 308nm against pH is shown below (figure 3.13).

* Energies of the HOMO for the benzimidazole and benzimidazolium cation are -8.87 and -13.51 eV and the LUMO energies -0.09 and -5.20 eV respectively. Calculated using MOPAC and the AM1 force field on the Cache program

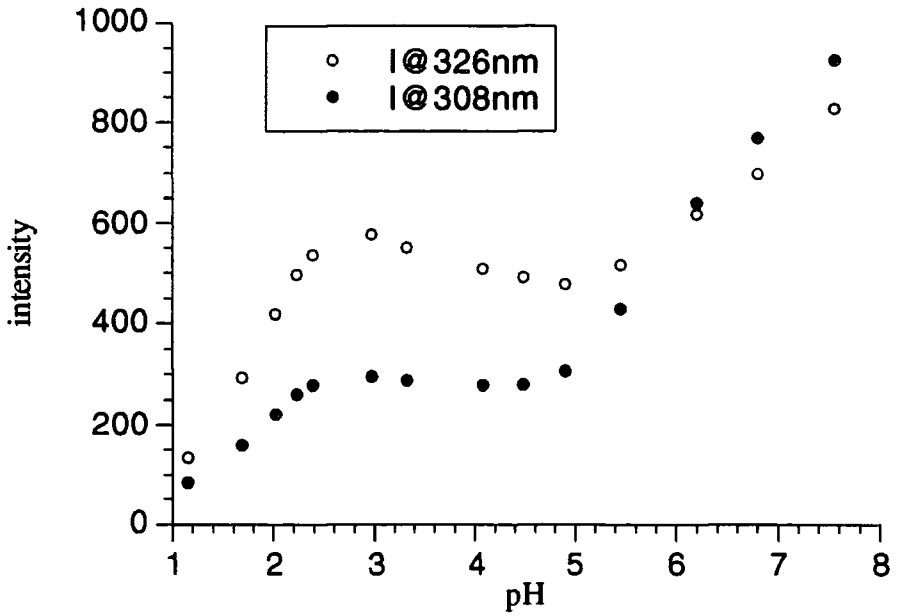

Figure 3.13 Change in fluorescence intensity vs. pH at 326 and 308nm for the benzimidazole (26) (90% H_2O, 10% MeOH, λ_{ex}=270nm, λ_{em}=280-500nm)

From the variation in fluorescence intensity it can be seen that for 1<pH<3 the fluorescence intensity is increasing almost linearly with increasing pH. At a pH less than 3 both the benzimidazole nitrogen and the phosphinic acid are protonated (figure 3.14, (96)).

As the pH rises there will be diminishing amounts of this species present in solution and at a pH of approximately 3 there will be predominantly the tautomer (97) which will be stabilised by the polar solvent. The intensity of fluorescent emission will be at a maximum for this portion of the profile as the possibility now exists for extended conjugation and hence an increase in the intensity. This is due to rigidity of this intermediate, which allows for either the phosphinate oxygen double bond or the phenyl ring to become coplanar with the benzimidazole. For this to happen the six membered ring containing the proton cannot be planar.

As the pH continues to rise (i.e. 3<pH<5.5) the intensity of emission falls off again at 326nm. The proportion of the mono-protonated benzimidazole (99) and its zwitterionic tautomer (97) will decrease (figure 3.14). As the concentration of (97) falls there will be more of the mono-anionic species (98) present in the solution. This species cannot place either the phenyl ring or the phosphinate oxygen double bond coplanar with the benzimidazole ring because the lone pairs on the oxygen atoms have to placed out of plane with the lone pair of the benzimidazole nitrogen.

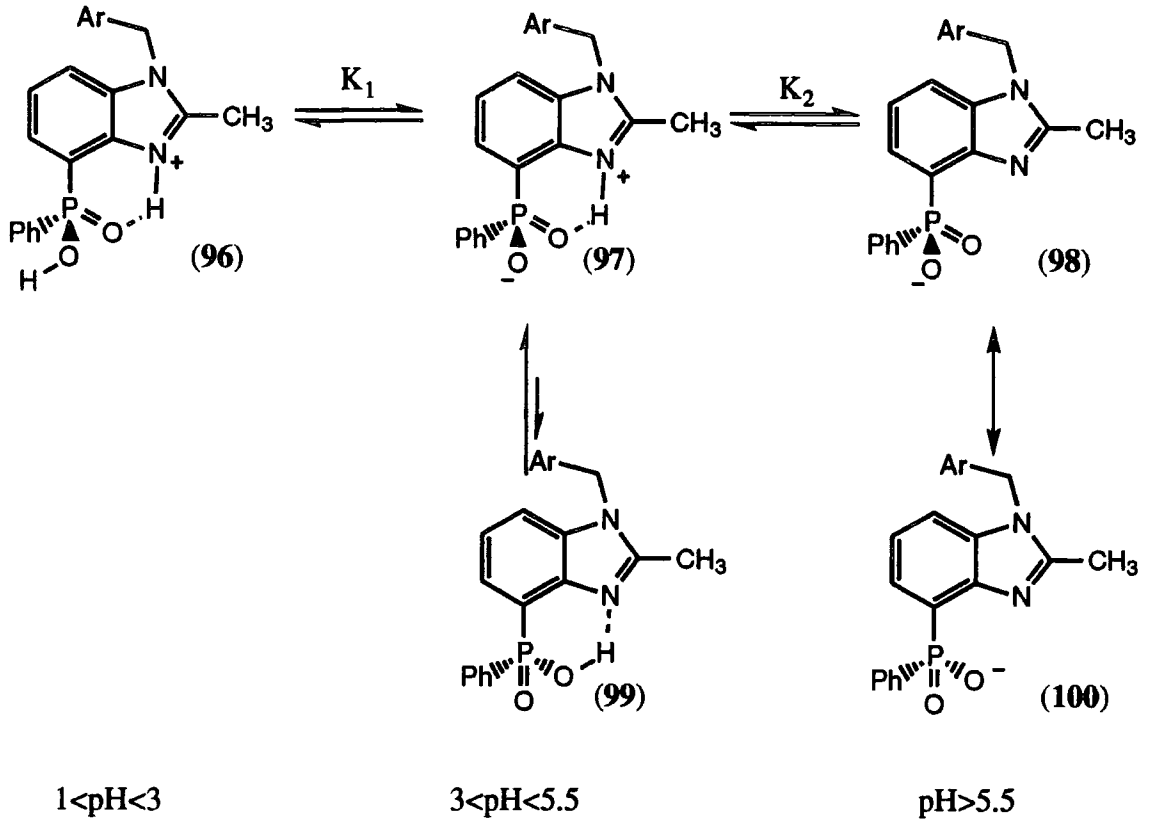

Figure 3.14 Species present in solution at various pH

Hence the fluorescent intensity falls off to a minimum. By inspection of the pH profile the pK_as of the phosphinic acid and benzimidazole nitrogen are approximately 3 and 5.5 respectively. It must be remebered that the pKa values estimated by this method correspond to the singlet , S_1, excited state values which should be fairly close to the ground state values. The values estimated are in accordance with literature values for benzimidazole (pK_a 5.5)[34] and diphenyl phosphinic acids (pK_a c. 2.9).[35]

Zinc fluorescence titration

In order to investigate the complex stoichiometry in solution further it is necessary to monitor the interaction of the benzimidazole ring with added zinc ions. To achieve this examination of the change in fluorescence emission intensity upon addition of incremental portions of the metal ion is a useful probe. The variation of fluorescence intensity (λ_{ex}=270nm, λ_{em}=280-500nm, slits 3nm) with added zinc is shown in figure 3.15.

The pH of the ligand solution to which the zinc was added was measured to be 4.40. As such, the ligand exists mainly as the charge neutral zwitterionic form (ie 97 in figure 3.14) and will have a proton involved in a predominantly covalent bond with the benzimidazole nitrogen.

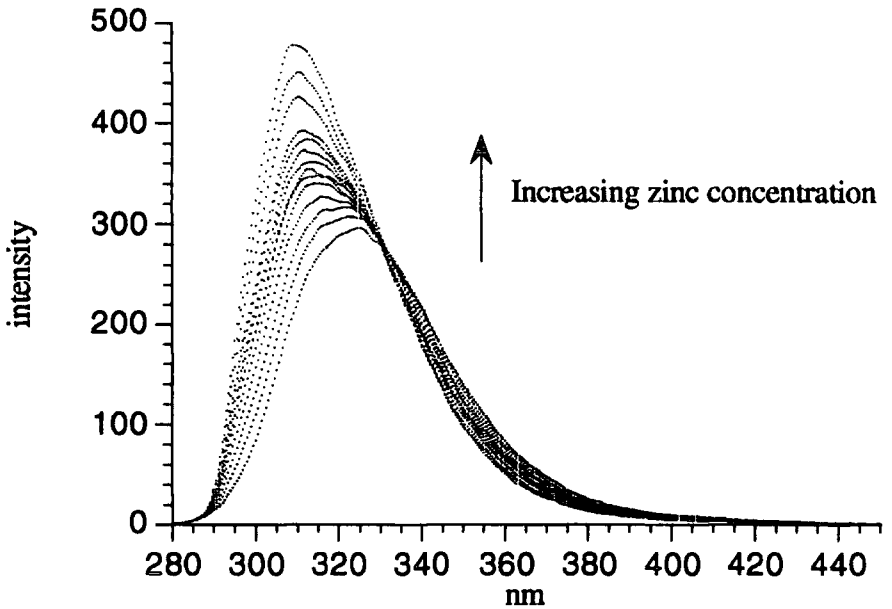

Figure 3.15 Variation of fluorescence intensity for (26) with $Zn(ClO_4)_2$ addition (95% MeOH, λ_{ex}=270nm, λ_{em}=280-500nm)

In this state, the electronic transition responsible for the fluorescence is likely to be a π-π^* type. As more zinc is added the proton is displaced by the metal participating in a dative bond with nitrogen atom. This change in the nature of the bond allows the ground state molecular orbital to be more easily oxidised than when the proton was present. The origins of this change lie in the effect that metal coordination has on the frontier orbitals of the system and an associated ICT affect (*vide supra*). As with the pH titration, coordination of zinc will cause a lowering of the energies of both the LUMO and the HOMO. However, the relative change density for zinc will be larger than for the proton because of the increased charge of the metal.

There is also a chelation enhanched fluorescence (CHEF) effect. When the ligand forms a chelate ring with the metal this restricts internal modes of vibration and rotation, which allows prolonged extended conjugation in the system, leading to a shift (15nm) in the observed fluorescence emission.[36] This increased rigidity of the system also accounts for an increase in the fluorescence intensity. Generally speaking, the more rigid a system the less efficient the non-radiative deactivation pathways because they involve a distortion of the molecule.

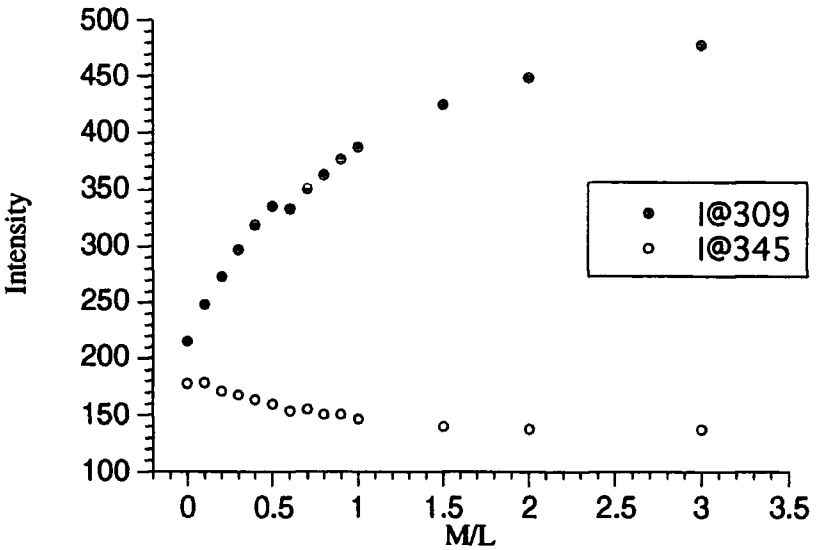

Figure 3.16 Variation of fluorescence intensity for (26) with increasing zinc concentration (95% MeOH, λ_{ex}=270nm, λ_{em}=280-500nm)

To deduce the stoichiometry in solution a plot of intensity against metal to ligand ratio is shown at 309 and 345nm (figure 3.16).

Examination of the fluorescent intensity plot (figure 3.16) shows that as the metal to ligand ratio increases, a new band with an emission maximum at 309nm grows in, whilst emission at 345nm decreases. The emission at 345nm, corresponding to the free ligand diminishes with increasing zinc concentration, whilst the emission from the complex at 309nm (shifted by 36nm) increases. Two effects contribute to this shift in wavelength, the lowering of the HOMO and LUMO energies causes a shift in the emision wavelength to higher energy and there is also the possibility for internal charge transfer to occur (*vide supra*). The plot of emission intensity against metal to ligand ratio shows this trend at both 309 and 345nm. In both cases the form of the curve indicates that at this concentration (10μmol) the ligand appears to be forming a weak ML complex.

3.5.3 UV measurements

Stock solutions of the ligand (26) and the metal salts of cobalt, copper, nickel, zinc and ferric perchlorates in methanol (1mmol) were prepared. To 1ml of the ligand solution was added 1ml of the appropriate metal salt solution and the mixture diluted with methanol to make a final, total concentration of 0.01mmol. A comparison of the uv spectra of the free ligand and the one to one mixture of ligand (26) and zinc(II)perchlorate is shown below (figure 3.17).

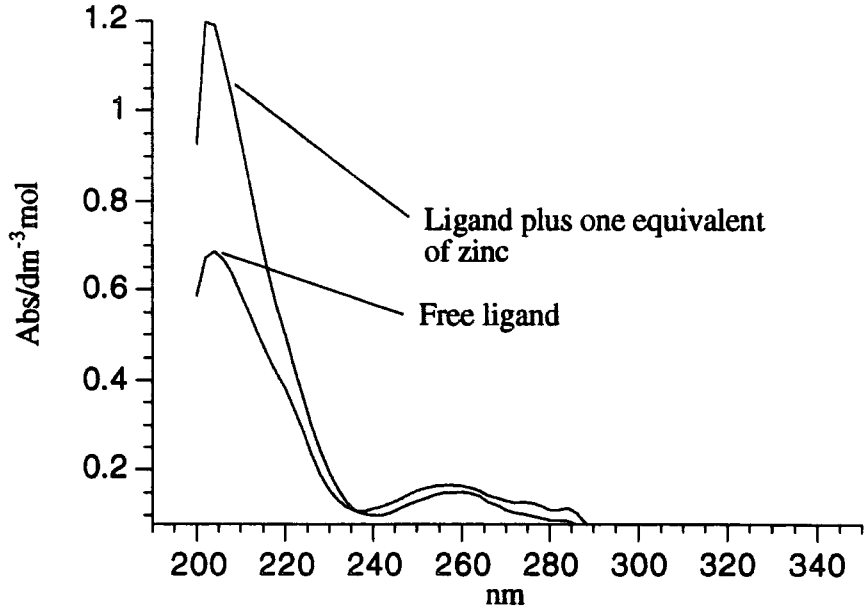

Figure 3.17 Comparison of uv spectra for ligand (XX), as free and zinc complexed species (CH_3OH, 298K)

Benzimidazoles possess characteristic absorption bands, which resemble those of substituted benzene derivatives. The short and long wavelength absorption bands correspond to transitions in the imidazole and aryl rings respectively.[37, 38] Coordination of the zinc atom has a profound effect on the absorption spectrum with a large increase in the absorption for the phenyl ring at 205nm (ε_L = 6810dm^3mol^{-1} and ε_{LZn} = 11900dm^3mol^{-1}), whereas the longer wavelength absorption is relatively unchanged between 257 and 277nm (ε_L = 1690dm^3mol^{-1} and ε_{LZn} = 1500dm^3mol^{-1} at 257nm and ε_L = 1210dm^3mol^{-1} and ε_{LZn} = 980dm^3mol^{-1} at 277nm). A summary of the uv absorption bands are given below, in the presence nickel, zinc, cobalt, copper and iron (table 3.1).

With zinc, copper, nickel and cobalt perchlorates the absorption spectra for the complexes are all similar, indicating that the ligand adopts similar geometries in solution with all metals. Ligand to metal charge transfer bands were also detected for iron, copper and cobalt at 389, 314 and 308nm respectively. Cobalt was used to probe the geometry of the complex, with tetrahedral cobalt having an absorption at 666nm (ε = 600 dm^3M^{-1}), whereas octahedral cobalt absorbs at 454nm (ε = 6 dm^3M^{-1}). In the case of this ligand, no absorption band around 660nm was observed suggesting that the ligand was not forming a tetrahedral cobalt complex, under the experimental conditiions.

Ligand		Zinc(II)		Copper(II)		Nickel(II)	
λ / nm	ε / dm^3M^{-1}	λ / nm	ε / dm^3M^{-1}	λ / nm	ε / dm^3M^{-1}	λ / nm	ε / dm^3M^{-1}
204	6690	202	11900	210 (s)	13960	207 (s)	12636
218	4310	257	1510	219	15000	224	13800
252	1570	272	1090	259	1106	254	1603
276	1270	280	850	276(s)	950	273 (s)	1157
282	1900			314	595	282 (s)	901

Ligand		Cobalt (II)		Iron (III)	
λ / nm	ε / dm^3M^{-1}	λ / nm	ε / dm^3M^{-1}	λ / nm	ε / dm^3M^{-1}
204	6690	207 (s)	12060	214	13480
218	4310	219	13280	259	6680
252	1570	254	1530	278 (s)	4520
276	1270	275 (s)	1104	328 (s)	1120
282	1900	282	861	389	808
		308	297		

Table 3.1 UV absorption of ligand (26) in the presence of Zn, Cu, Ni, Co and Fe perchlorates (CH_3OH, 298K)

3.5.4 Electrospray mass spectrometry studies

The solution complexation behaviour of this ligand was further studied using electrospray mass spectrometry (ESMS). ESMS is a relatively new technique which has been used to study the nature of molecular and ionic species in solution.[39] The atmospheric inlet allows information to be obtained about weakly bound species in solution, providing that the ionisation process does not perturb the species.[40] The ionisation process is not fully understood, which makes quantitative analysis unreliable. Qualitative analysis is possible for a given ligand and its complexes, and information regarding the affinity for a particular metal can be estimated.

Complexation and electrospray analysis for 1-(*tert* butylbenzyl)-2-methylbenzimidazole-4-phenylphosphinic acid (26) was carried out in 100% methanol

with the perchlorate salts of zinc, nickel, copper and ferric. A stock solution of the ligand and the metals were prepared (1mmol) and complex solutions of 1:1 stoichiometry made up. These solutions were diluted to make final concentrations of 0.01mmol, and their ESMS spectra recorded in positive and negative ionisation modes. The ESMS$^+$ spectra produced the best results showing complexes associated with a proton or sodium cation in most cases.

Zinc

In the presence of zinc ions, the major species observed was the protonated ML_2 complex. The observed spectrum is in excellent agreement with the theoretical isotope pattern for $[L_2ZnH]^+$ (figure 3.18). Presumably the ML_2 complex is protonated on the benzyl substituted nitrogen atom.

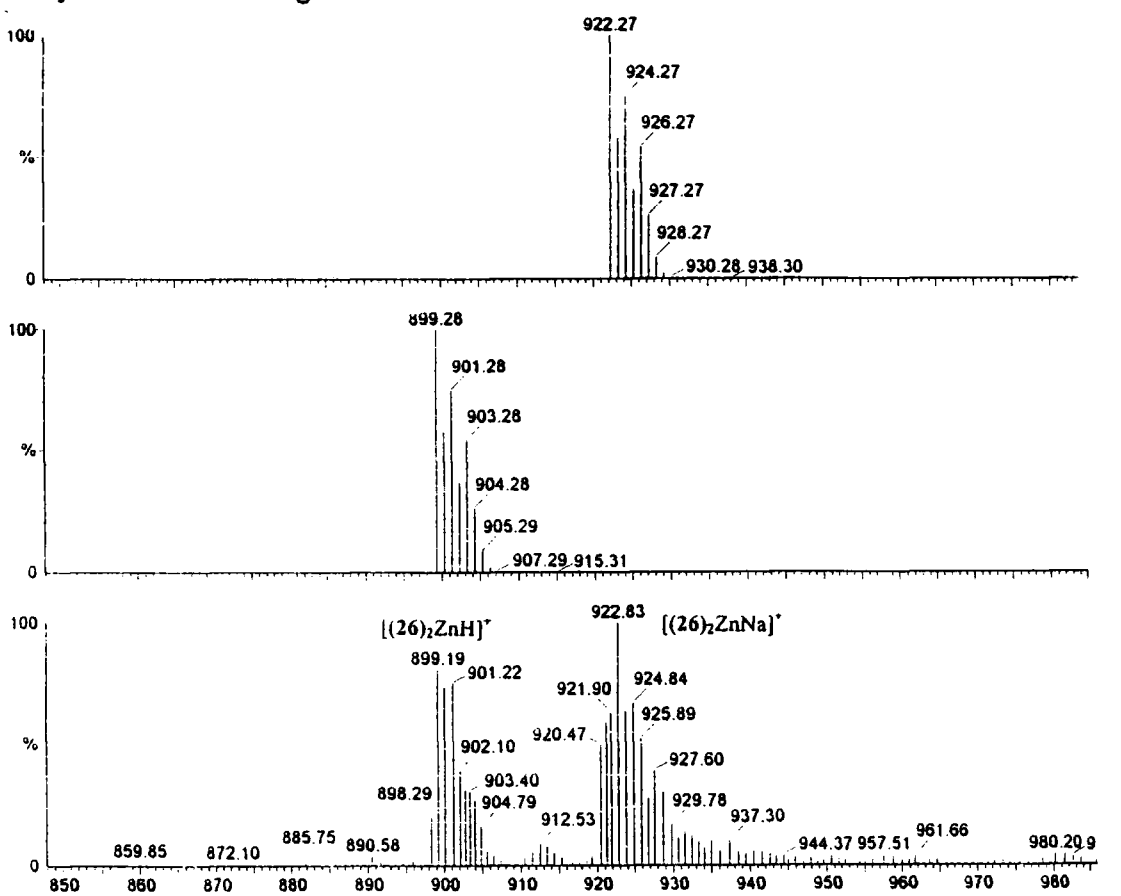

Figure 3.18 ESMS$^+$ spectrum of $[(26)_2ZnH]^+$ (lower) with isotope model (top)

Copper and nickel

In contrast to the spectrum obtained for the zinc complex the predominant species observed in the electrospray is the protonated ligand (100% in both cases), with smaller amounts of the $[L_2MH]^+$ species being observed (33 and 9.5% for copper and nickel

respectively). The $[L_2MH]^+$ species (67 and 6.84% respectively) was also observed in each case.

Iron

For iron no signals corresponding to bound species were observed, whether operating in positive or negative ionisation modes. The only species detected in each case was the free, unbound ligand.

A summary of the species detected by ESMS for the ligand plus zinc, copper, nickel and ferric perchlorates is shown below (table 3.2)

Metal	Species	Obs. Mass	Calc. Mass	Rel. Intensity
Zinc	$[LH]^+$	419.25	419.88	73%
	$[L_2ZnH]^+$	899.65	899.28	100%
	$[L_2ZnNa]^+$	922.83	922.27	89%
Copper	$[LH]^+$	419.27	419.88	100%
	$[L_2CuH]^+$	898.10	898.43	33.5%
	$[L_2CuNa]^+$	920.28	920.63	67%
Nickel	$[LH]^+$	419.27	419.88	100%
	$[L_2NiH]^+$	893.24	893.37	9.5%
	$[L_2NiNa]^+$	915.23	915.65	6.84%
Iron	$[LH]^+$	419.27	419.88	100%
	No complex species observed			

$ESMS^+$, cone voltage 30V, source temperature 60°C

Table 3.2 Summary of species observed in ESMS for (26)

3.5.5 Liquid-liquid extraction

In order to assess the ability of the ligand (26) to transport zinc ions across an aqueous-organic interface extractions tests were performed by C. Chartroux at the University of Dresden. Investigations were performed in micro-reaction vials in buffered aqueous media (298K, pH 2) and chloroform.[41] For ligand (26), the percentage extraction of

Hg(II), Ni(II), Zn(II) and Co(II) is represented below (figure 3.19). These metals were chosen as they were the ones available at the time

The distribution of each metal ion in the organic and aqueous phases was determined using radio-isotopes of each metal (Ch.6.1). It is clear from the figure that zinc is selectively transported into chloroform over nickel, mercury and cobalt. The pronounced selectivity over nickel and cobalt arises from a combination of geometric and donor atom preferences. For nickel virtually no metal was transported across the liquid interface, even after shaking for two hours, presumably reflecting nickel's slow rate of complex formation.

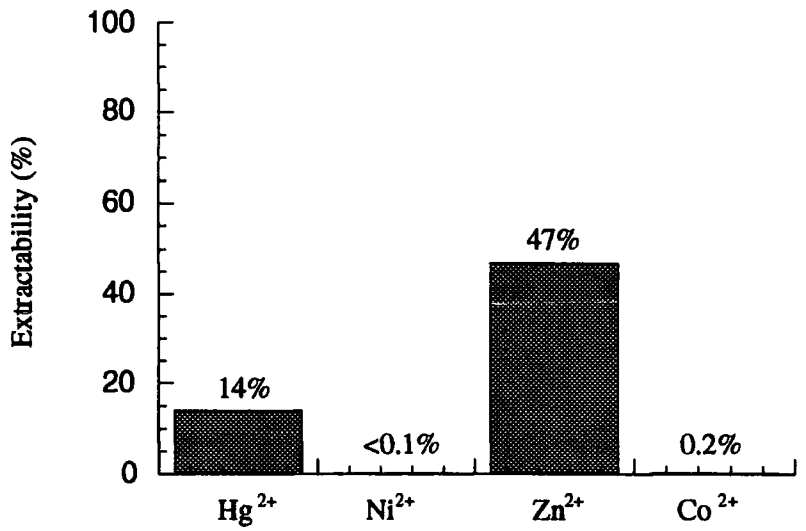

Figure 3.19 Extractability of Hg^{2+}, Co^{2+}, Zn^{2+} with (26), $[M]=10^{-4}moldm^{-3}$, $[L]=10^{-3}moldm^{-3}$ ($CHCl_3$, 293K)

3.6 Dimethylthiophosphoryl based Ligand System

Background

In naturally occurring zinc-containing metalloenzymes the coordination environment generally consists of one of three groups of donor sets, either N_3O in carbonic anhydrase and thermolysin, N_2O_2 in carboxypeptidase and β-lactamase or N_2S_2 in alcohol dehydrogenase.[42] In the monobenzimidazole phosphinic acid (26) ligand system (*vide supra*) the donor set available to zinc upon formation of a ML_2 complex is N_2O_2. Obviously this is not the only preferred coordination environment for the zinc ion and an N_2S_2 donor set is an attractive alternative. With this in mind, simple conversion of the monobenzimidazole ligand (26) described above to the corresponding

thiophosphinic acid should make available this particular donor set. Model studies (Ch. 2.3) showed that it is possible to convert appended phosphinic acids into the corresponding thiophosphinic acid derivatives. However from earlier work,[43] the formation of the thiophosphinates is not a trivial matter and that the stability of thiophosphinic acids in the presence of metals is questionable. Desulfurisation of the thiophosphinic acid to the corresponding phosphinic acid is a particular problem and copper is known to mediate this process rapidly and irreversibly. An alternative donor group is a dialkyl or diaryl thiophosphoramide, which should coordinate through the sulfur atom. The ability of the donor set to act efficiently is intimately related to the pK_a of the nitrogen proton: the lower the pKa the more likely it is to present an anionic donor.

Ligand Design

The design of a dialkylthiophosphoryl ligand mirrors that of the phosphinic acid appended monobenzimidazole (section 3.2). The only difference is the method of attachment of the potentially anionic donor group, the target ligand (27) is shown below (figure 3.20). In this system an eight membered chelate ring will be formed upon complex formation. This larger sized chelate ring may decrease the stabilty of complex by having a large positive entropy contribution to the free energy of complexation.

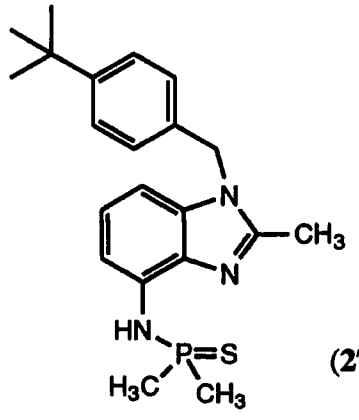

(27)

Figure 3.20 Target dimethylthiophosphoryl based ligand (27)

The retrosynthetic analysis is very similar to that for the phosphinic acid derived ligand (section 3.4) with the only difference being the incorporation of an amino group in place of the bromine atom. The same design features also apply to this system; incorporation of the 2-methyl substituent should impose steric restrictions in the complex and the benzyl group can be modified to tune the lipophilicity of the complex.

Availability of dialkyl and diarylthiophosphoryl precursors

There are many of examples of disubstituted phosphonothioic halides known in the literature (figure 3.21). Derivatives are known with alkyl (C_1-C_{20}), cycloalkyl (C_5 and

C_6), aryl, bromide and chloride but generally their synthesis has lacked specificity, producing a mixture of $R_2P(S)X$ and $RP(S)X_2$.[44] A number of routes to the dimethyl and diphenyl bromides and chlorides via their respective bis(phosphine sulfides) derivatives are known.[45]

Figure 3.21 Some disubstituted phosphonothioic halides

3.7 Ligand synthesis

As with the pervious benzimidazole based ligand system, the compound required prior to benzimidazole formation is a substituted *ortho*-diaminobenzene derivative. In this case the required intermediate is 3-nitro-1,2-diaminobenzene (102). The synthesis of 3-nitro-1,2-diaminobenzene (102) was accomplished by the selective reduction of one nitro group of 2,6-dinitroaniline (101) under three atmospheres of hydrogen with a palladium on carbon catalyst.[46] Condensation of the diamine with acetic anhydride followed by acid hydrolysis gave the 3-nitro substituted benzimidazole (103) in moderate yield (58%).

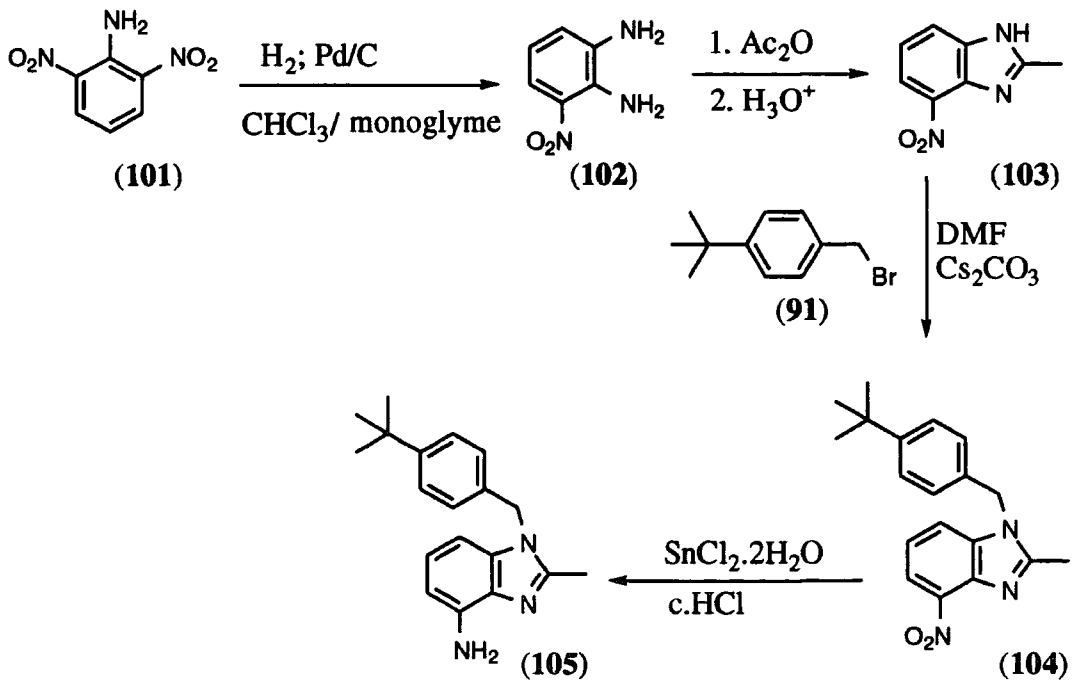

Scheme 3.11 Synthesis of N-alkylated 4-amino-benzimidazole (105)

As the NH proton on benzimidazoles can, in principle, reside on either nitrogen atom, then alkylation can in theory occur in either position. However the steric bulk provided by the *ortho* nitro group directs alkylation to the least sterically hindered side of the molecule. Therefore, N-alkylation with 4-tert-butylbenzyl bromide (91) in DMF using caesium carbonate as the base gave the required benzimidazole (104) in near quantitative yield. The nitro functionality was then reduced with tin(II) chloride dihydrate in concentrated hydrochloric acid to give the 4-amino benzimidazole (105), as a pale brown crystalline solid (scheme 3.11).

The 4-amino-benzimidazole (105) was then converted to its thiophosphoramide derivative (27), by reaction of the amino benzimidazole (105) with bromodimethylphosphine sulfide (108). The bromophosphine reagent was prepared by the action of bromine on tetramethyldiphosphine disulfide (107). The disulfide was prepared according to the procedure of Parshall by the reaction of trichlorophosphine sulfide (106) with an excess of methyl magnesium bromide at -15°C (scheme 3.12).[47]

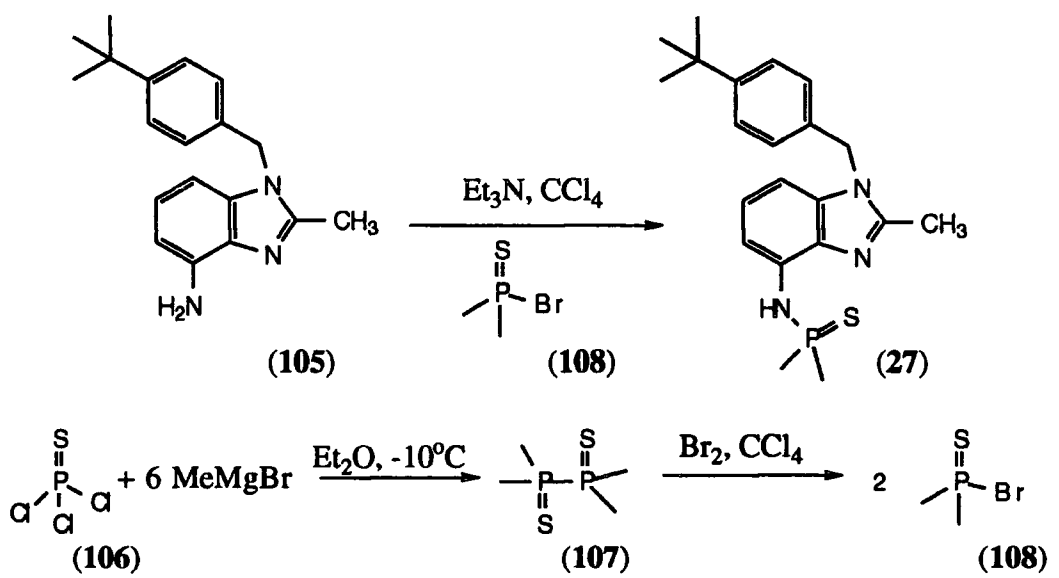

Scheme 3.12 Synthesis of the thiophosphoramide ligand (27)

This reaction can be capricious and has to be attempted with caution as there is a considerable induction period. Following addition of a small portion of methyl magnesium bromide the reaction was monitored to observe initiation (indicated by a slight rise in temperature) and further addition should be maintained at a temperature of -10°C. The amino benzimidazole and bromodimethylphosphine sulfide were then coupled in anhydrous carbon tetrachloride with triethylamine as the base. The reaction could be conveniently followed by phosphorus NMR spectroscopy (δ_p product (27) = 55ppm, δ_p bromo derivative (108) = 62ppm and δ_p dimer (107) = 35ppm). The solvent was removed and the triethylamine salts washed out with water giving the desired ligand in 22% overall yield (scheme 3.12).

3.8 Solution complexation behaviour

3.8.1 ^{1}H NMR titrations.

The complexation of metal triflates (Zn^{2+}, Cd^{2+}, Pb^{2+}) with 1-(4-tert-butyl)benzyl-2-methyl-(4-aminodimethylphosphinesulfide)-benzimidazole (27) was examined by ^{1}H NMR spectroscopy (25% CD_3OD, 75% $CDCl_3$). All NMR titrations were carried out in single tubes, and a metal triflate solution (0.4M) was added to a ligand solution (0.04M). Each sample was examined by ^{1}H NMR and the change in chemical shift ($\Delta\delta_H$)relative to the free ligand was plotted against the M/L ratio.

Lead

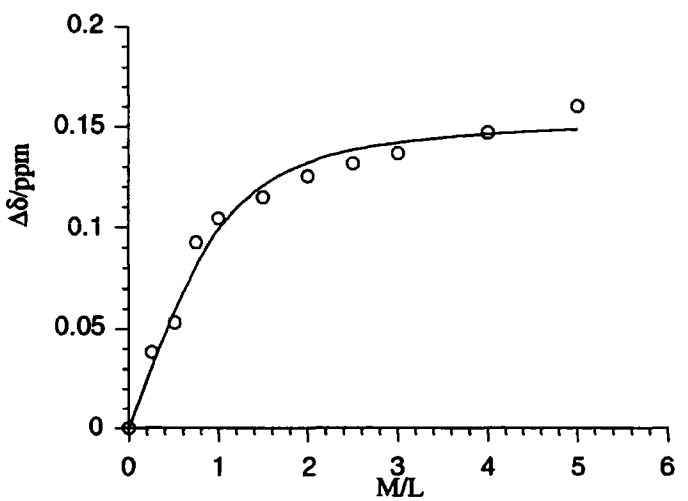

Figure 3.22 Ligand (27) plus $PbTf_2$ NMR titration curve (25% CD_3OD, 75% $CDCl_3$, 293K)

With increasing metal to ligand ratio, a shift in the methylene NCH_2Ar proton resonance to higher frequency was observed. In contrast, with addition of the metal triflate there was relatively little shift in the C-2 methylene resonance, and very little loss of signal resolution, with only a slight line broadening ($\omega_{1/2}$=6.5Hz) of the two protons ortho to the benzimidazole nitrogen atoms. A non-linear least squares analysis[29, 30], for the binding isotherm for formation of an ML complex gave a stability constant of 113 ± 20 (figure 3.22). However a similar analysis for a ML_2 complex gave a poor fit.

Zinc

For zinc, a different set of spectra were obtained. Following addition of the zinc triflate to the free ligand, spectral resolution was lost. The three separate proton signals on the benzimidazole ring coalesced to give an exchanged broadened signal, and the P-methyl group doublet also broadened into a single peak ($\omega_{1/2}$=31Hz). A non-linear least squares analysis[29, 30] for an ML complex gave a stability constant of 56 ± 11 (figure 3.23). Attempts to fit the data for ML_2 complex formation were unsuccessful, owing to a lack of data points. The loss of resolution in the proton spectrum for zinc is consistent with a complex formation which is in very rapid exchange with the unbound species. Attempts to try and slow down the exchange process were made. Variable temperature NMR spectra (-40°C, $CDCl_3$) of the mixture at M/L ratios of 0.5 and 1.5 were examined. No observable change was observed.

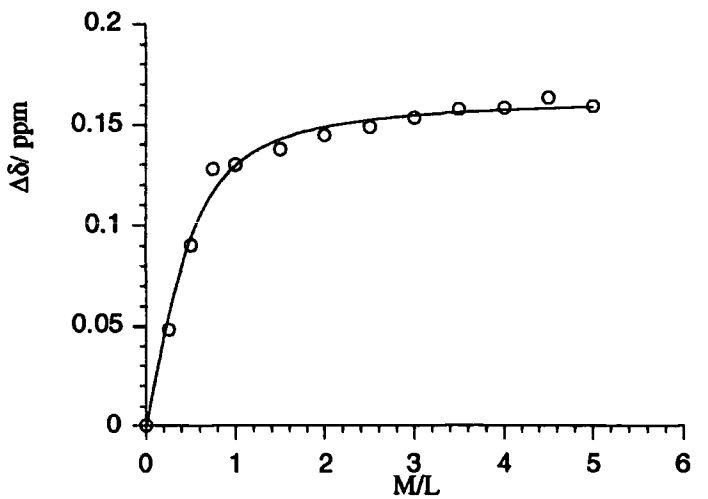

Figure 3.23 Ligand (27) plus $ZnTf_2$ NMR titration curve (25% CD_3OD, 75% $CDCl_3$, 293K)

Cadmium

For cadmium, a shift to higher frequency of the NCH_2Ar signal was observed upon addition of the metal triflate (figure 3.24). The non-linear least squares analysis[29, 30] could only fit the data for a ML complex, and gave a meaningless result when fitted with the equation for ML_2 formation. The data obtained for the cadmium system seemed to suggest that at low M/L ratios, formation of a relatively strong 2:1 (CdL_2) complex is occurring followed by some form of mixed 1:1 and 2:1 species. A weakly bound and rapidly exchanging species was observed at higher M/L ratios ($1.0<M/L\leq5$). At M/L ratios of less than one, two separate P-methyl doublets were observed in the ^1H NMR spectrum, consistent with a strongly bound and unbound species in slow

exchange on the NMR time scale, which implies a formation constant greater than logK=5.5 (which would be infered from a static complex on the NMR timescale). When M/L>1 the two P-methyl doublets ($\omega_{1/2}$=16Hz) coalesce and all of the ring proton resolution is lost, consistent with the complex reacting with further metal to produce rapidly exchanging ligand and complex species, with an overall equilibrium constant less than logK = 5.5.

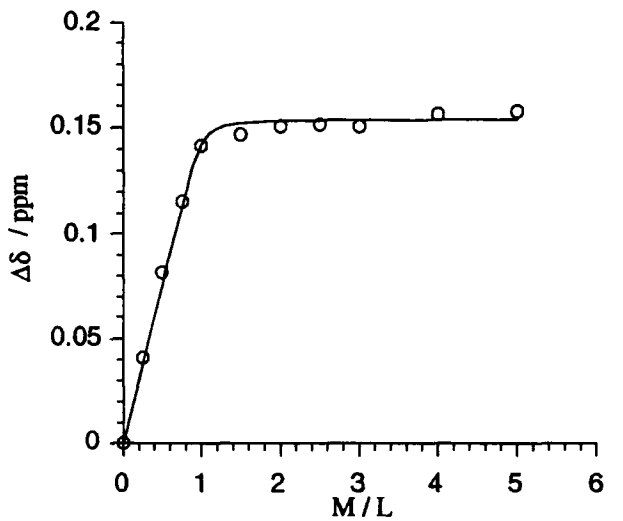

Figure 3.24 Ligand (27) plus $CdTf_2$ NMR titration curve (25% CD_3OD, 75% $CDCl_3$, 293K)

3.8.2 ESMS speciation studies.

A stock ligand (27) solution (0.15 mmol) was prepared in a mixed solvent of 70% methanol and 30% dichloromethane. To 1 ml of the ligand solution was added the required amount of a methanolic metal triflate solution to make the required 1:1 or 2:1 metal to ligand ratio.

For lead, copper and nickel the major peaks observed are for the free ligand (see table 3.3). With only relatively minor amounts of signals corresponding to metal bound species

For zinc the major species observed was a 2:1 complex of the deprotonated ligand and zinc (table 2.1). Excellent agreement was observed between the experimental and theoretical isotope patterns (see figure 3.25). In contrast to the information deduced from the NMR titration result, there seemed to be no sign of any 1:1 complex formation.

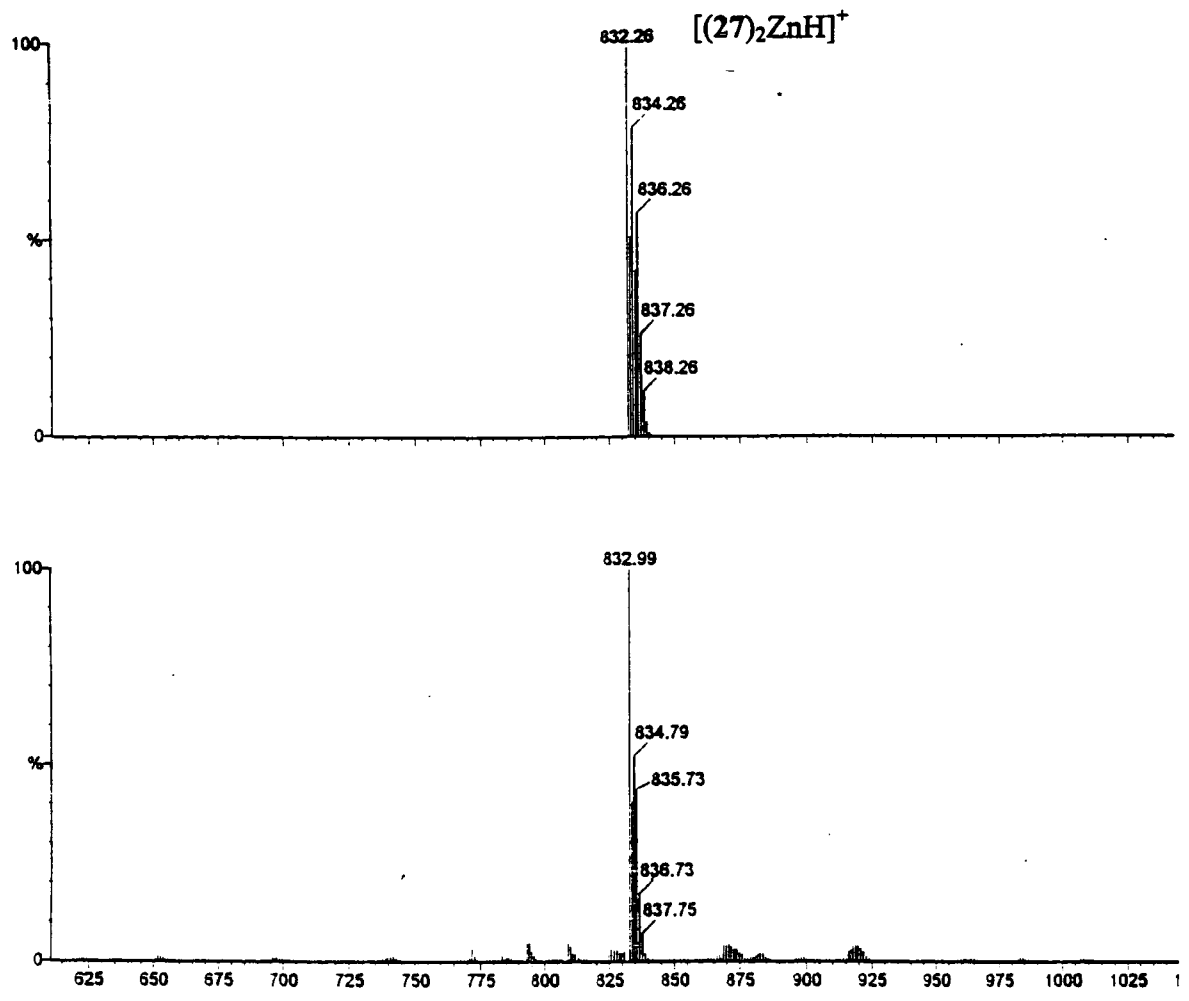

Figure 3.25 ESMS spectrum of $[(27)_2Zn]$ with theoretical spectrum below.

For cadmium more complicated behaviour was observed. The major peak corresponds to the 2:1 complex (table 2.1). In comparison to zinc, higher order species were also detected, e.g. $[L_3CdTf]$. The occurrence of the L_3Cd complex perhaps reflects cadmium's larger ionic radius (r_i 0.95Å) compared to that of the zinc ion (r_i 0.75Å). This larger radius allows higher coordination numbers to be attained, as such formation of an ML_2 complex does not impose enough steric restriction to prevent ML_3 complex formation.

A summary of the major species detected in the ESMS experiment, with the observed and calculated masses is shown below (table 3.3).

Complex + ligand	Observed Species.	Observed Mass.	Calculated Mass.
Pb	LH^+	386.3	
	$[L_2Pb\text{-}H]^+$	976.8	976.35
Ni	LH^+	386.3	
	$[L_2Ni\text{-}H]^+$	827.1	827.3
	$[L2NiTf]^+$	977.4	977.24
Cu	LH^+	386.3	
	$[L_2Cu\text{-}H]^+$	833.1	832.3
Zn	$[L_2ZnH]^+$	833.9	833.7
	$[L_2ZnH(OH_2)_2]^+$	870.8	870.7
Cd	$[L_2CdH]^+$	882.7	882.3
	$[L_2CdH(OH_2)_2]^+$	918.7	918.4
	$[L_3CdTf]^+$	1414.1	1414.4

$ESMS^+$, cone voltage 30V, source temperature 60°C

Table 3.3 ESMS speciation, major peaks underlined (solvent 30% methanol, 70% dichloromethane, cone voltage = 60v).

3.8.3 Zn pH extraction isotherm

In order to assess the ligands ability to extract zinc across an aqueous-organic interface a working model for zinc extraction was performed. The method chosen was designed to be as similar as possible to the industrial process of hydrometallurgy.

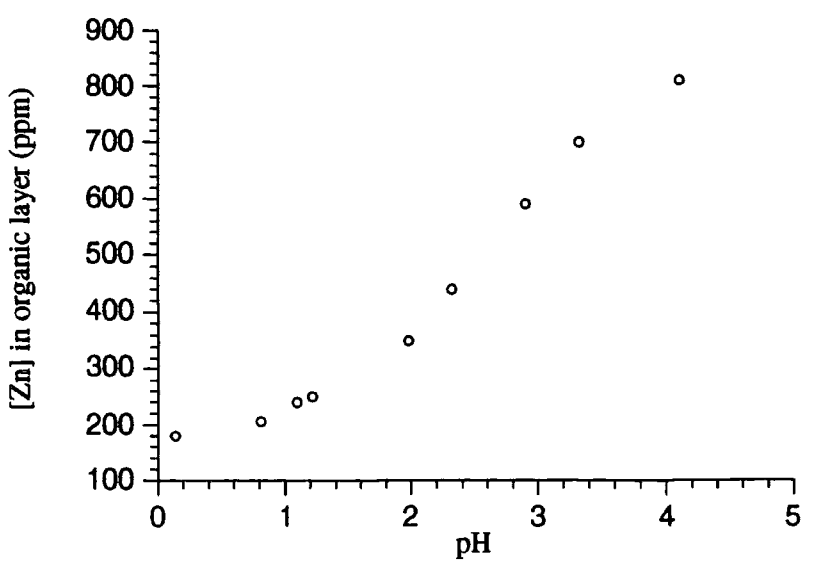

Figure 3.25 Zn pH extraction isotherm for ligand (27) (CH_2Cl_2, $[ZnCl_2]$ = 0.5M, [27] = 0.1M, 298K)

The ligand (27) was dissolved in Analar dichloromethane to give a 0.1M solution, which was partitioned into 8 Eppendorf tubes. An equal volume of zinc chloride solution was added to each tube with an increase in the pH of the zinc chloride solution between each addition. Measurements were taken over the pH range 0.14 to 4.10, as at pH values greater than 4.5 zinc hydroxide formation complicates the extraction test. Each tube was mixed for five minutes, and the organic phases separated and the metal content determined by atomic absorption spectroscopy. From the extraction curve (figure 3.25) the aqueous acidity at which 50% of the maximum amount of zinc is extracted ($pH_{1/2}$) was found to be pH 2.8. The stability constant determined by ^1H NMR titrations (section 3.9.1) indicated that weak binding was occurring with zinc. As the binding is weak there is no sharp point of inflection in the extraction isotherm plot. As the $pH_{1/2}$ value is greater than 2.5 then this ligand is unsuitable as a hydrometallurgic extractant as it operates at a pH above that which ferric hydroxide precipitates.

3.9 2-2' Bis(benzimidazole) bis-phosphinic acid ligand

Introduction

There have been two reported examples of 2-2' bis(benzimidazoles) which bind to zinc in a tetrahedral manner (figure 3.26).[12, 13] From the crystal structure both ligands form dimeric complexes with two zinc atoms, binding via the benzimidazole nitrogen atoms with the free coordination sites filled by chloride counter ions. In the solid state each bis(benzimidazole) unit adopts a 90° twist angle about the 2-2' linkage which creates the tetrahedral coordination sites.

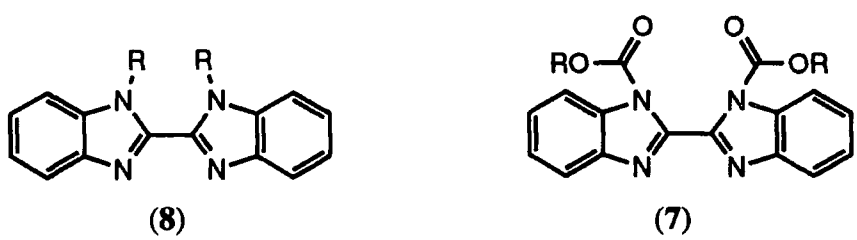

(8) (7)

Figure 3.26 Bis(benzimidazole) ligands (7) and (8)

3.10 Improved ligand design

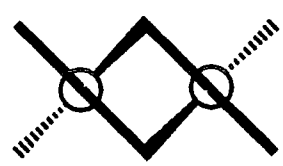

$[2\text{-}2]_2$

Figure 3.27 $[2\text{-}2]_2$ ligand geometry

Systems based on the $[2\text{-}2]_2$ architecture will be examined in this section (figure 3.27). Two mutually perpendicular coordination planes may be defined when the dihedral angle between the benzimidazole subunits is close to 90°. Examination of the solid state structure of (7) and (8) (Ch. 3.2) shows the coordinated chloride ions completing the tetrahedral geometry of zinc. Incorporation of anionic donor groups in the 4 and 4' positions of the bis(benzimidazole) structure allows six-ring chelate formation (favouring small ions)[21] with the 3 and 3' benzimidazole nitrogen atoms, and therefore the possibility of formation of charge neutral L_2Zn_2 complexes. With this in mind previous work has focused on incorporation of carboxylate donors in the 4 and 4' positions (17) (figure 3.28).[26] This work will attempt to improve on previous work by substituting the carboxylate donor for the phosphinic acid functionality (figure 3.28).

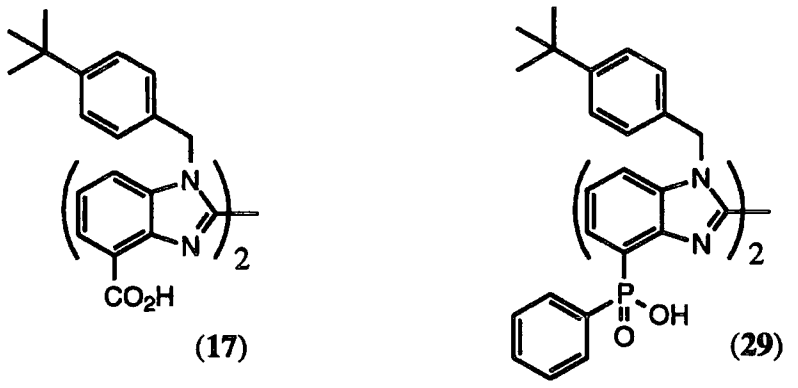

Figure 3.28 Previous 4,4' substituted bis(benzimidazole) (17) and improved design (29)

As with the previous bis(benzimidazole) ligand (17) incorporation of the N-alkyl substituent serves two purposes; the ligands preferred binding conformation is imposed by the bulky benzyl groups and the lipophilicity can be varied without compromising the binding sites. Use of the phosphinic acid donor should allow metal coordination at a lower pH than for the analogous carboxylates, due to the lower pKa of the phosphinic acids relative to carboxylic acids (Ch. 2.2).[20]

3.11 Ligand synthesis

Earlier routes towards the synthesis of substituted 2-2' bis(benzimidazoles) examined a variety of methods. Several attempts were made with 3-substituted *ortho*-diaminobenzene (109) which had an anionic donor group already in place. Attempted coupling of these compounds used extremely forcing conditions which generally resulted in decarboxylation of the molecule (scheme 3.13). Protonation of the intermediate bis-acid (111) followed by decarboxylation resulted in recovery of the unsubstituted bis(benzimidazole) (113).[48]

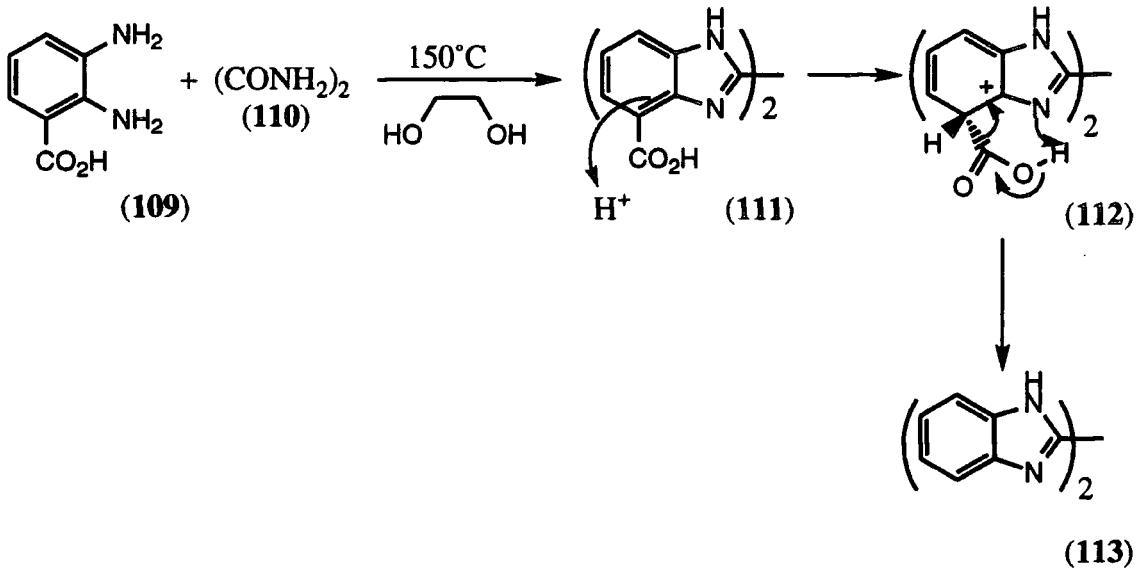

Scheme 3.13 Decarboxylation of bis(benzimidazole) (111)

Attempts to modify this procedure, either by carrying out the reaction in the presence of potassium carbonate, performing it at lower temperatures, or by microwave activation failed to give the desired product.

1,2-Diaminobenzene is known to react with methyl trichloroacetimidate, $Cl_3C(NH)OMe$ (114), to produce the parent bis(benzimidazole).[49] Attempted coupling with this and (109) failed to give any of the desired material. A strategy similar to that described above (Ch. 3.4) was employed. Incorporation of a bromo substituent into the diamine should allow formation of the bis(benzimidazole), followed by subsequent transformation to the desired anionic donor group.

Reaction of diaminobromobenzene (82) with half a molar equivalent of methyl trichloroacetimidate (114) was initiated by the addition of a few drops of concentrated hydrochloric acid in methanol. Initially, the addition of acid is needed to form the intermediate 2-trichloromethyl derivative. However, unless base is added the reaction will stop at this stage. Base deprotonates the 2-trichloromethyl-benzimidazole followed by loss of HCl, and reaction with a second diaminobromobenzene (82) unit produces the 4-4'-dibromo-bis(benzimidazole) (115) in 75% overall yield (Scheme 3.14).

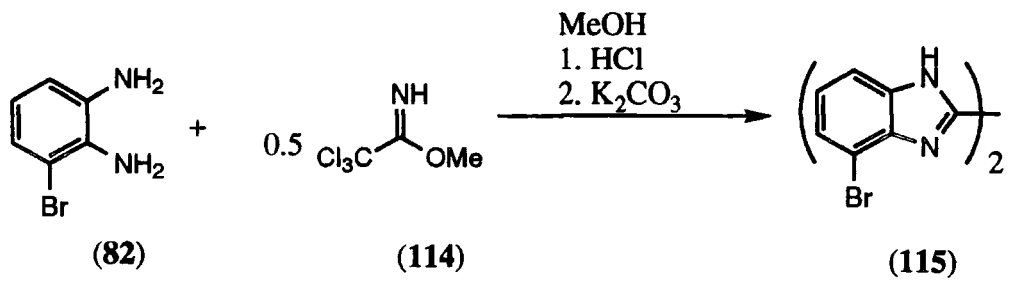

Scheme 3.14 Coupling of diaminobromobenzene (82) to produce (115)

The dibromo(bisbenzimidazole) (115) was found to be insoluble in methanol, allowing simple purification by boiling in methanol and filtering, allowing the pure material to be recovered as a yellow solid.

The bromine substituent provided enough steric bulk to direct N-alkylation to the distant nitrogen using 4-tert-butylbenzyl bromide (91) in DMF, with caesium carbonate as the base. The substituted product (116) had a low solubility in DMF and was isolated by precipitation with methanol. Recrystallisation from chloroform gave a white solid (scheme 3.15).

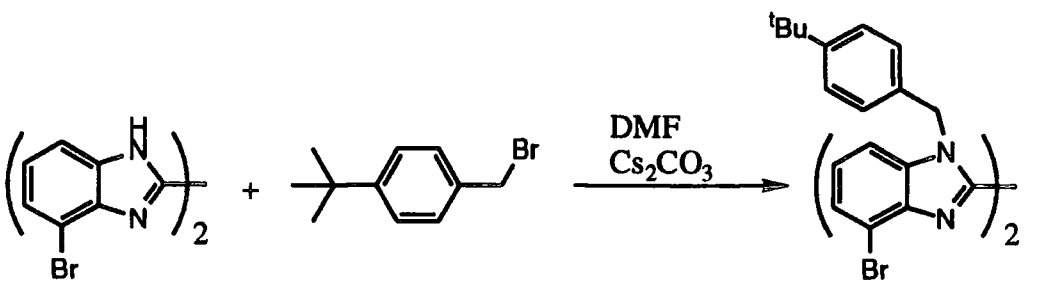

(115) **(91)** **(116)**

Scheme XX Selective N-alkylation of 4, 4'-dibromobis-1H-benzimidazole (115)

From previous work[26] it is known that formation of the lithio-bis(benzimidazole) is possible by reaction of a slurry of the N-alkylated dibromo-bis(benzimidazole) in THF at -78°C with butyl lithium. The reaction is slow, due to the limited solubility in the reaction solvent, but quenching of the resulting species with dry carbon dioxide gave the dicarboxylated benzimidazole (17) in 60% yield. From earlier model studies (Ch. 2.3), it should be possible to produce phosphinic and thiophosphinic acids by reaction between chloroethoxyphenylphosphine (47) and the lithio bis(benzimidazole) (117), followed by acid hydrolysis and sulfur insertion to give the desired product (118). The dilithiate of dibromo-bis(benzimidazole) (117) was produced in an analogous way to previous work.[26] Quenching the solution with chloroethoxyphenylphosphine (47), and without isolation of the intermediates, followed by acid hydrolysis and sulfur insertion gave a pale yellow gum. Proton and phosphorus NMR analysis indicated that traces of the desired species were present, however separation using either column chromatography or HPLC failed to give any product (118) (scheme 3.16). An alternative approach was explored using the trans-metallation of the intermediate lithiate followed by reaction with half a molar equivalent of Lawesson's reagent. The lithiate was generated in the usual way, but anhydrous magnesium bromide was added to the solution in order to produce the corresponding Grignard species. Reaction of the resulting solution with a suspension of Lawesson's reagent (54) in THF, which was

seen to go into solution upon addition, followed by acidic work up gave only a trace of the desired dithiophosphinic acid as deduced by analysis of an electrospray mass spectrum of the crude reaction mixture (scheme 3.16). This mixture also could not be separated by either column or high performance liquid chromatography. Since it is known that the dilithio-bis(benzimidazole) (117) reacts with carbon dioxide,[26] it was decided to attempt reaction of the lithiate with carbonyl sulfide to produce the bis-thiocarboxylic acid. However when dry carbonyl sulfide was bubbled through the lithiate solution, and after an aqueous acidic work up no sign of the mono or bis thiocarboxylic acid was present in proton NMR or mass spectra of the crude reaction mixture (scheme 3.16).

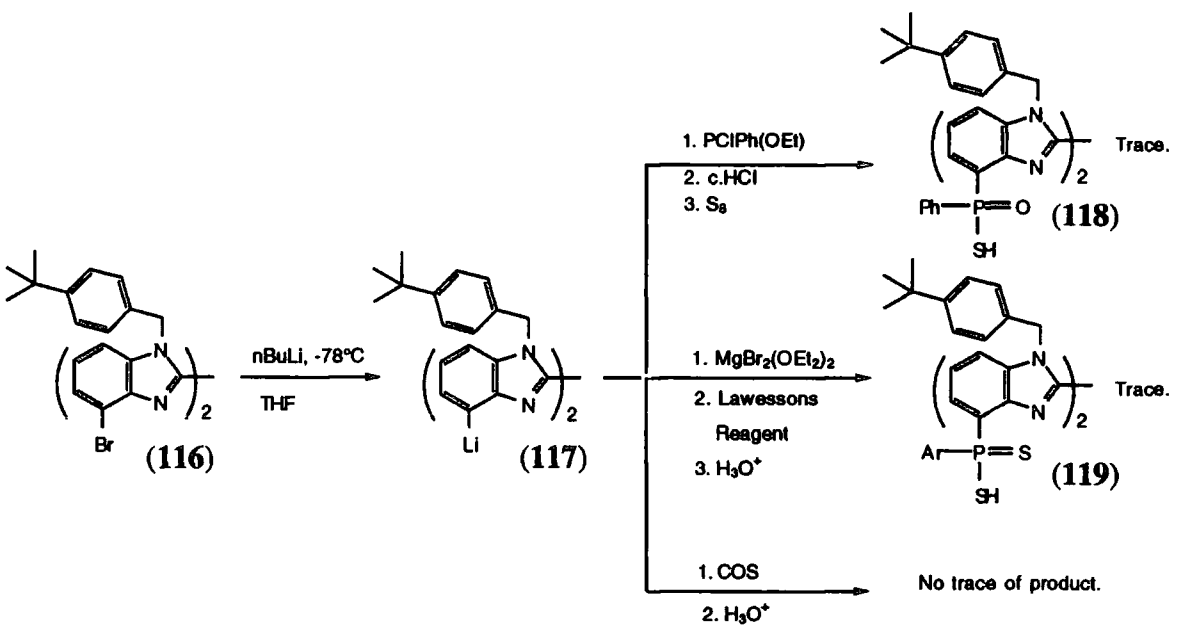

Scheme 3.16 Reactions of dilithio-bis(benzimidazole) (117)

As formation of either the lithiate or Grignard derivatives of the dibromo-bis(benzimidazole) (116) seemed to be hampered by competing reactions or lacked reactivity the last of the surveyed model reactions was attempted (chapter 2 section 2.3).

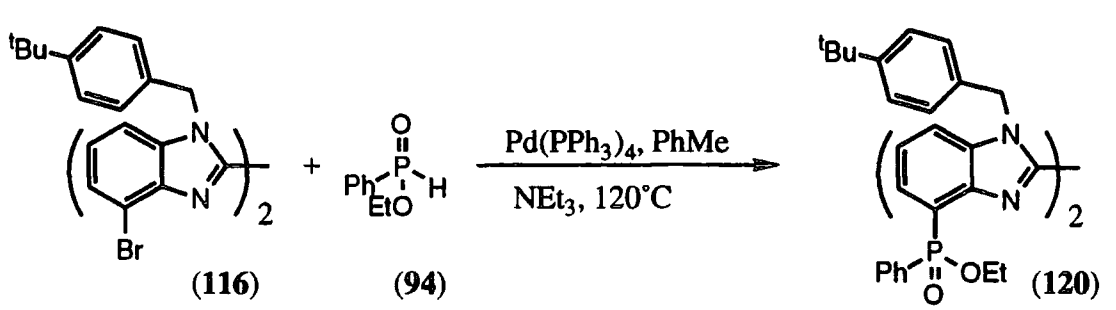

Scheme 3.17 Synthesis of bisphosphinate ester (120)

The phosphinate functionalities were introduced in an analogous manner to that described above (*vide supra*), by palladium catalysed coupling with ethylphenylphosphonite (94) in the presence of $Pd(PPh_3)_4$ and triethylamine.[27] Purification by flash chromatography gave the bis phosphinate ester (120) in 52% yield (scheme 3.17).

NMR analysis of bisphosphinate ester

^1H and ^{31}P analysis of the bisphosphinate ester (120) revealed a number of interesting splitting patterns. Analysis of the ^1H-^1H COSY spectrum allowed assignment of the aromatic protons (figure 3.29).

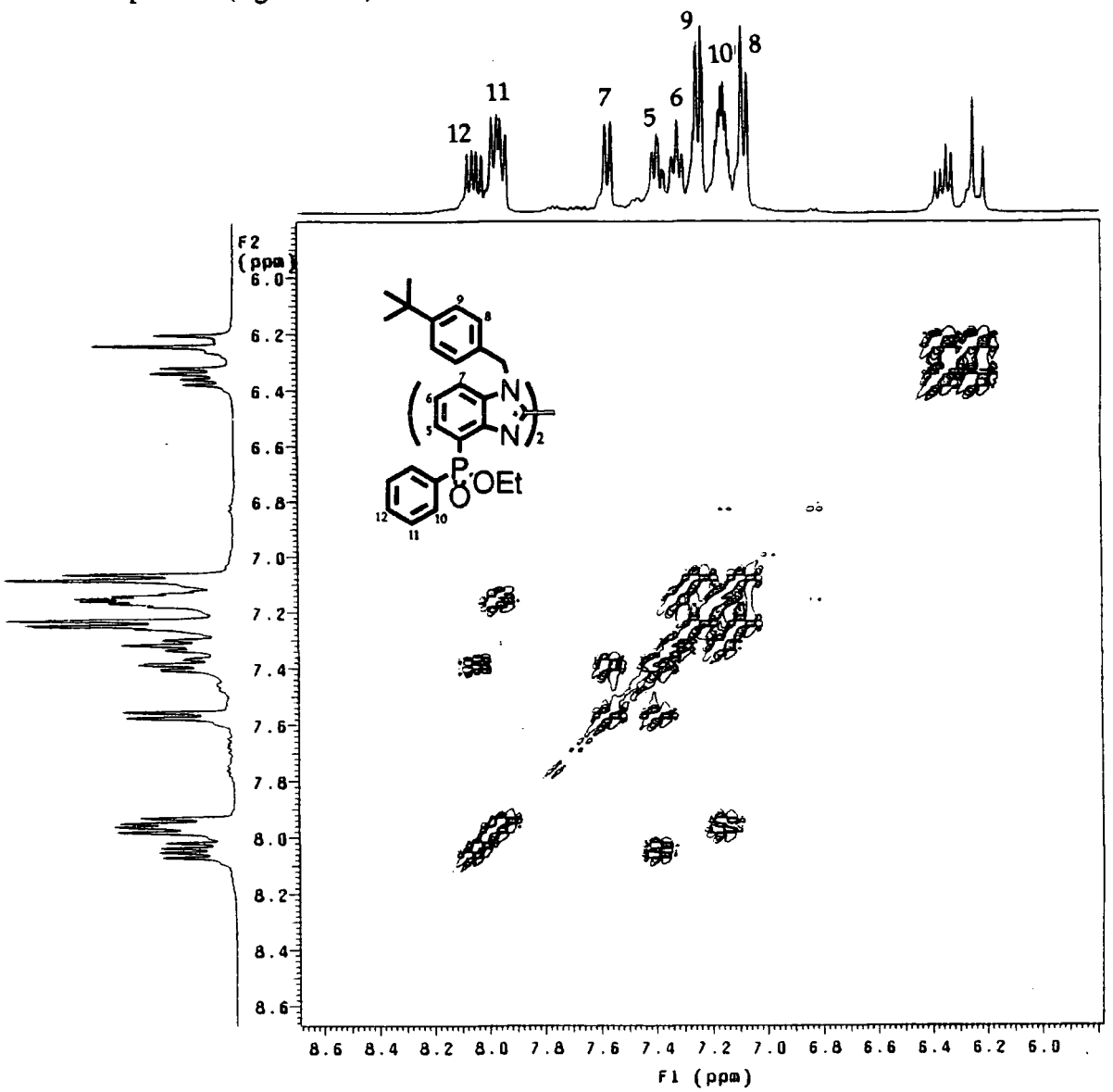

Figure 3.29 ^1H-^1H COSY of bisphosphinate (120)

The signal resulting from the benzylic protons (6.2 - 6.4ppm) produced an unusual splitting pattern. It was unclear if this was due to a conformational effect or some long range coupling to phosphorus. Proton-phosphorus coupling across up to 7 bonds has been observed in other systems.[50] In order to determine whether this pattern was caused by this a $\{^{31}P\}$-^{1}H spectrum was recorded (figure 3.30). Although coupling due to phosphorus is lost in the aromatic region, none of the structure in the benzylic signals was lost.

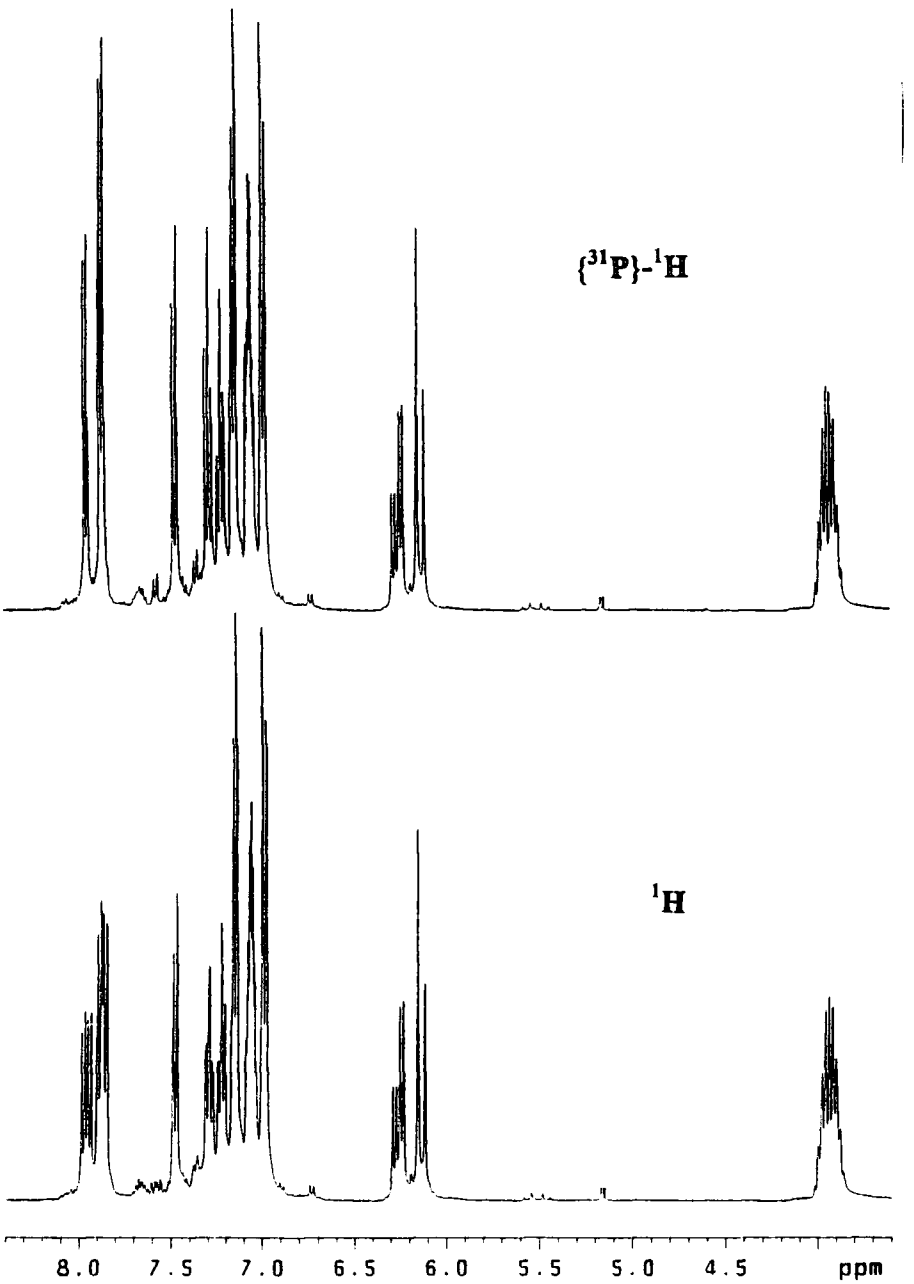

Figure 3.30 $\{^{31}P\}$-^{1}H spectrum of bisphosphinate (120)

The above spectrum implies that this unusual signal is due to a conformational effect. At room temperature the phenylphosphinic acid substituent prevents any rotation about the 2-2' bond and locks the benzyl substituents in one position in space. This rigidity causes the two benzylic protons to be in magnetically different environments and results

in a geminal coupling producing two overlapping AB quartets for the RR/SS and SR diastereomers. In an attempt to try and induce movement variable temperature (VT) NMR was performed in d_2-tetrachloroethane (d_2-TCE) which allows temperatures of up to 120°C to be reached. Comparison of the spectra at ambient temperature and 120°C shows a surprising result (figure 3.31). The quartet centered at 6.3ppm collapses, whereas the quartet centered at 6.28ppm remains intact. This difference in properties stems from the differing physical properties of the diastereomers in solution. The oppurtinity exists for the chirality at phosphorus to be R or S and R or S about the 2-2' bond. Rotation of the RSS diasteriomer magnetically inverts the benzylic protons, resulting in a singlet. When the RSR diasteriomer rotatates about the central 2-2' bond the benzylic protons remain in the same magnetic environment, resulting in the AB quartet. Comparison of the aromatic region of the spectrum at ambient temperature and 120°C shows a decrease in the line width at higher temperatures, which is a viscosity effect. As the temperature increases the solvent becomes less viscous and the molecules can rotate in solution at a higher rate, this increase in internal motion will have the effect of increasing T_2. As line width is proportional to $1/T_2$, then an increase in relaxation rate will cause a corresponding decrease in linewidth.

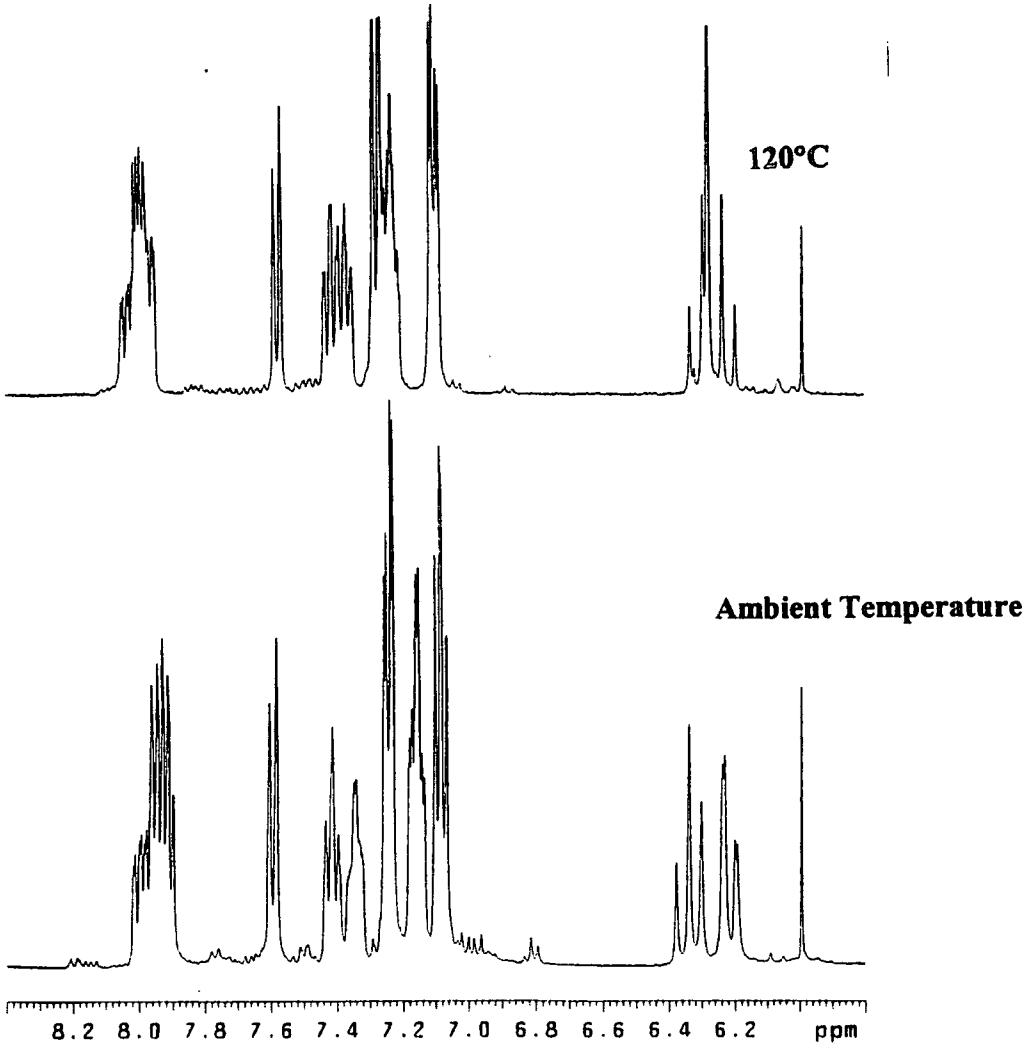

Figure 3.31 VT NMR of (120) at ambient temperature and 120°C

Attempted hydrolysis of bisphosphinate ester

Initial attempts to hydrolyse the bisphosphinate ester (120) were hampered by the insolubility of the compound in common solvents used for hydrolysis. Dissolution of the ester (120) in 1, 4-dioxane followed by addition of concentrated hydrochloric to make a final acid concentration of 6M and heating at 110° resulted in precipitation of a white solid (scheme 3.18). The solid was isolated by centrifugation washed with water and dried under vacuum. The product was found to be insoluble in all known organic and protic solvents. Combustion analysis confirmed that ester hydrolysis had occurred and that the di-hydrochloride salt (29) had formed.

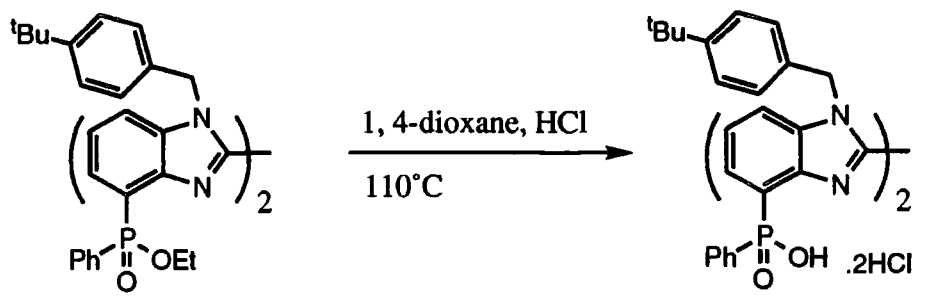

(120) (29)

Scheme 3.18 Acid hydrolysis of bis-ester (120)

In an attempt to try and solubilise the ligand a suspension of the solid was heated in methanol with zinc acetate. Filtering the solution and examination of the filtrate by ^{1}H NMR revealed no sign of any organic species.

In order to try and overcome the problem of insolubility of the free acid, hydrolysis was attempted using a methanolic solution (1M) of tetrabutylammonium hydroxide. Heating a mixture of the diester (120) with a ten fold excess of tetrabutylammonium hydroxide and analysis of the solution by ^{31}P NMR spectroscopy showed that ester hydrolysis had occurred.

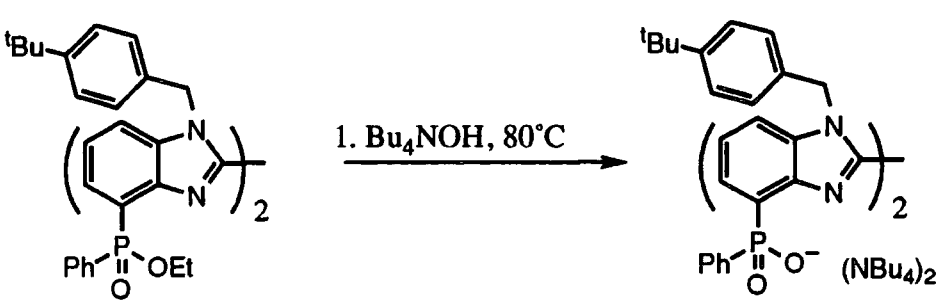

(120) (121)

Scheme 3.19 Alkaline hydrolysis of (120)

Loss of the two singlets at 32.2 and 32.3ppm and formation of a singlet at 16ppm was observed. Isolation of the pure compound was not achieved. Neutralisation of the mixture and extraction into chloroform gave a product which still contained an excess of tetrabutyl ammonium salts. Column chromatography on silica gel did not provide enough resolution to separate the mixture and the product eluted with the ammonium salts (scheme 3.19).

In order to try and produce a more soluble analogue of the 2,2'-bis(benzimidazole) ligand (29) several variations were synthesised in order to achieve this goal. By incorporating 3,5-di(*tert* butyl)phenyl and 3,5-dimethoxyphenyl benzylic substitutents into the molecule it was hoped that that the solubility in nonpolar solvents would be increased. However, neither of these two derivatives produced a more soluble bis(phosphinic acid). An alternative strategy was also attempted by varying the phosphorus substituent. Use of ethyl (2-ethylhexyl)phosphonite (222, Ch. 5.5.5) was expected to alleviate the rigidity imposed by the phenyl substituent in the above system. Unfortunately attempts to cross couple this phosphine with the dibromo-bis(benzimidazole) (116) failed when using either $Pd(PPh_3)_4$, $Pd(OAc)_2$ or elevated temperatures.

3.12 A trimethylene spaced bis(benzimidazole) ligand.

Introduction

The earlier sections in this chapter have discussed bidentate ligands, in which binding of one ligand to a metal centre did not promote coordination of a second ligand. As such, the metal ion has a number of free coordination sites which can accommodate either solvent molecules or counter-anions, such as chloride or sulfate. Coordination of such anions will result in a charged complex which will not be transported efficiently across an aqueous-organic interface. In an attempt to overcome these difficulties, a tetradentate ligand system (28) was designed which can bind cooperatively all four donor atoms to form a charge neutral complex which may transport zinc ions selectively and efficiently across a liquid-liquid interface.

3.13 Ligand design

The problems highlighted in the previous sections with bidentate ligands serve to emphasise the difficulties inherent in relying on ML_2 complex formation. Formation of these complexes is concentration dependent in both the metal and the ligand. There is also the possibility that ML and ML_3 complex stoichiometries may form in solution. An

alternative approach based on the [2-2] geometry was investigated with a view to overcoming these difficulties (figure 3.32).

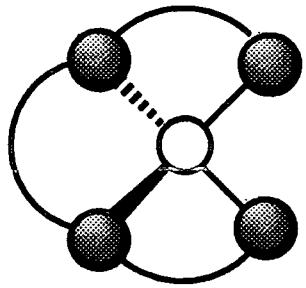

Figure 3.32 Diagrammatic representation of [2-2] ligand architecture

In this system the two sets of two donor atoms are held together with a semi-rigid backbone. This contrasts with other systems based on the [2-2] geometry (see Ch. 1.3.5), where two donor atoms are held together in the same plane by a rigid backbone possessing two chelating pendent arms. The target molecule (28) was based on a bis(benzimidazole) substructure, with two phosphinic acid appended benzimidazole units held together by a trimethylene chain in the 2 and 2' positions. The general structure is shown below (figure 3.33).

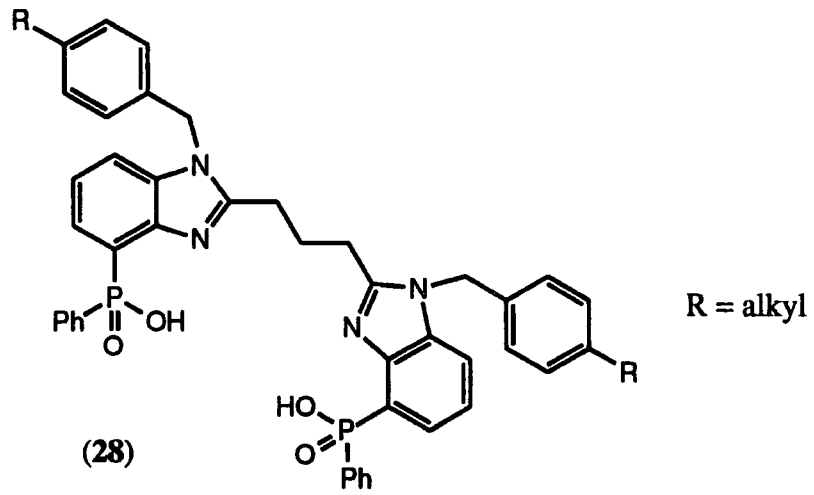

(28)

Figure 3.33 Target ligand system (28)

The donor set presented by the ligand is an N_2O_2 type, analogous to that of carboxypeptidase and β-lactamase, and should therefore be complementary to the zinc atom.[41] Formation of two-six ring chelates, between the phosphinate oxygens and nitrogen atoms and an eight membered chelate leads to 1:1 complex formation with tetrahedral zinc. The incorporation of an eight membered chelate ring is generally considered to be unfavourable for stable complex formation to occur, due to the positive entropy contribution to the free energy of complexation. The phosphinic acid was chosen in preference to the carboxylic acid for the same reason as for the

monobenzimidazole ligand (26) (Ch. 3.3), namely the lower pK_a compared to the corresponding carboxylate. Use of phosphinic acids as donors should also help to discriminate against coordination to the cupric ion. It has been noted by others that anionic phosphinates are good σ donors for charge dense ions such as magnesium and calcium, but disfavour coordination to copper (II).[51, 52]

The lipophilicity of the complex can be modified as in the previous benzimidazole examples (Ch. 3.3 and 3.9). Variation of the N-alkyl substituent will lead to a ligand which has a highly lipophilic 'north' side to the molecule, which may not aid extraction capabilities. Modification of the lipophilicity around the phosphinic acid function may also help to reduce the molecular dipole and aid dissolution of the complex in organic solvents.

Molecular modelling

Molecular modelling of the zinc complex was performed as previously described (Ch. 3.3). The model shows tetrahedral zinc (green central sphere) with two chelating benzimidazoles with the propyl chain connecting these two subunits (figure 3.34). The linking C_3 chain only adopts an ideal gauche confirmation when the metal ion adopts a tetrahedral coordination geometry. For other geometries, particularly square planar, prohibitive steric penalties are imposed. If the complex forms other geometries the only realistic stoichiometry is an ML_2 type complex. If this were the case, then the complex would have two eight ring chelates, which would be extremely unfavourable energetically, with large positive entropy contributions to the free energy of complexation, disfavouring complex formation. The only other possibility for complex formation is helicate formation. This may occur while still maintaining a tetrahedral coordination site without imposing any severe steric penalties.

3.14 Ligand synthesis

As for 1-(*tert* butylbenzyl)-2-methylbenzimidazole-4-phenylphosphinic acid (26) the same retrosynthetic steps can be applied to the bis(1,3-propyl)benzimidazole-4,4'-bis(phenylphosphinic acid) ligand (28), involving a disconnection back to 3-bromo-1,2-diaminobenzene (82). The only difference between the two systems is in the coupling methodology to produce the bis(benzimidazole). Various methods were attempted prior to discovery of a successful, high yielding process.

The initial stratergy involved the simple condensation between glutaric acid (122) and 3-bromo-1,2-diaminobenzene (82) in toluene under Dean-Stark conditions (scheme 3.20)

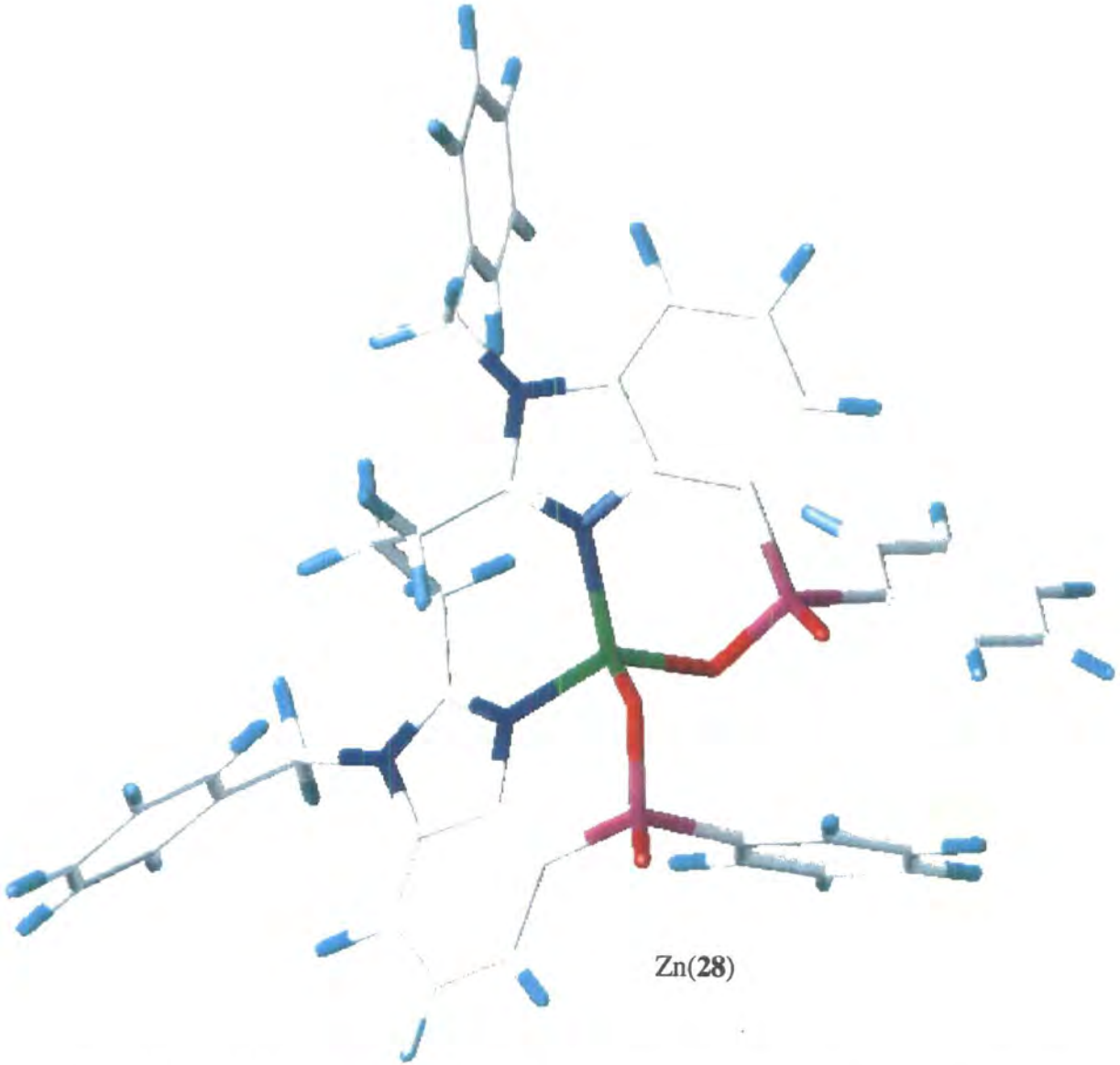

Figure 3.34 Molecular model showing the tetrahedral zinc complex of ligand (28)

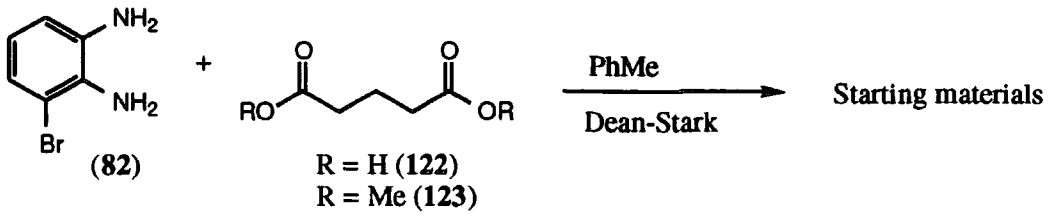

Scheme 3.20 Attempted Dean-Stark condensation to from bis(benzimidazole) skeleton

This process did not yield the desired product and only unreacted starting materials were recovered following removal of the toluene under reduced pressure. In an attempt to increase the reactivity of the acid group the methyl ester (123) was prepared by stirring in methanol for 16 hours at room temperature with a catalytic amount of sulfuric acid. Neutralisation and extraction into dichloromethane gave the di-ester (123) in near quantitative yield. Condensation between the diester (123) and the *ortho*-diamine (82) was attempted in an analogous manner to that for glutaric acid (122); once again only starting materials were recovered. Repeating the reaction in the melt at 150°C for 18 hours again resulted only in unreacted materials. As a last resort, a Woods metal bath was employed to generate forcing conditions; a mixture of dimethylglutarate (123) and 3-bromo-1,2-diaminobenzene (82) was heated in the melt at about 250°C for 3 hours. The dark solid isolated proved to be intractable and this approach was abandoned.

The classic Phillips procedure was then investigated.[23] This involves heating a mixture of the amine in hydrochloric acid (4M) with the desired acid at reflux temperature. Reaction of the diamine (82) with half a molar equivalent of glutaric acid (122) again only produced staring materials, even after prolonged reaction (scheme 3.21).

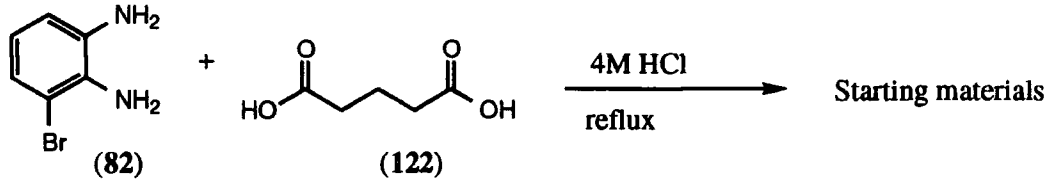

Scheme 3.21 Attempted Phillips condensation

Another common approach to benzimidazole formation which only involves the formation of a single bond (the 1, 2 (or 2, 3) bond) has been widely applied to analogous systems. This method involves ultimately forming a suitably functionalised 2-(N-acylamino)- or 2-(N-arylamino)-arylamine, which can be cyclised by thermolysis.[53, 54] The attempted reaction between bis-(acid chloride) of glutaric acid (122), which was formed in dichloromethane using oxalyl chloride with a catalytic amount of DMF, was added a solution of 3-bromo-1,2-diaminobenzene (82) in

dichloromethane. There was an immediate discoloration of the solution and an intractable solid was recovered after work up, presumably due to competing polymer formation (scheme 3.22).

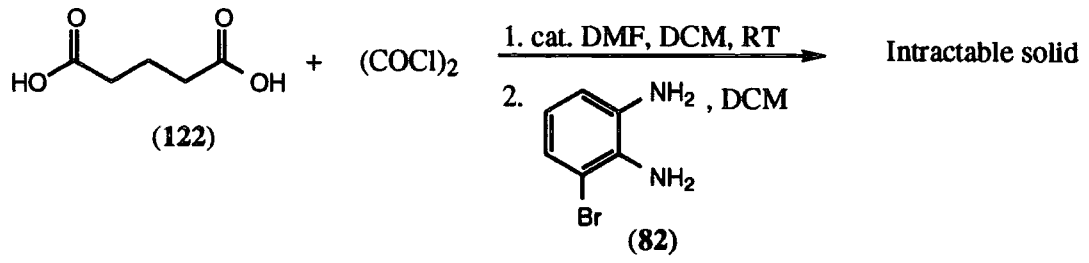

Scheme 3.22 Attempted formation of bis(N-acetylated)-diamine

This approach can be extended to use functionalised 2-nitroacylaminoarenes, which should prevent the problems of supposed polymer formation encountered with the previous route.[54] Once formed, the 2-nitroacylaminoarenes can be cyclised in reducing media such as tin and acetic or hydrochloric acids, tin(II) chloride and hydrochloric acid or heterogeneous hydrogenation methods.

Using this approach, glutaric acid (122) was converted to its bis-(acyl chloride) using oxalyl chloride and a catalytic amount of DMF in a similar manner to that described above. 2-Bromo-6-nitroaniline (88) was added as a solution in dichloromethane to the acid chloride solution. Again immediate discoloration of the solution occurred and following aqueous acidic work-up only an intractable solid was recovered, indicating that polymer formation had again occurred (scheme 3.23).

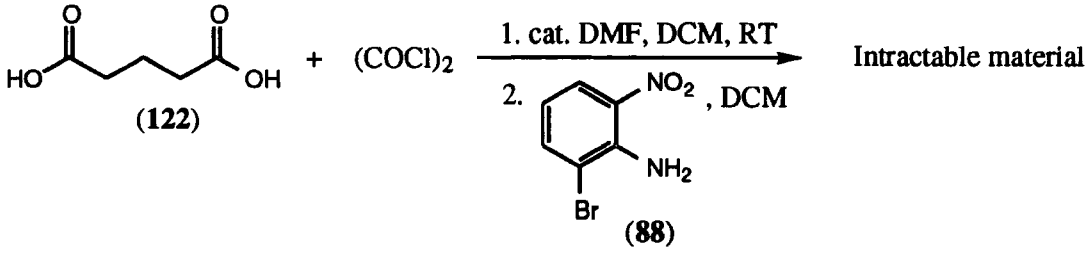

Scheme 3.23 Attempted formation of bis-(6-nitroacetyamino) derivative

A milder coupling method was adopted from peptide chemistry, (1,1'-dimethylaminopropyl)-3-ethylcarbomide hydrochloride (EDCI) was used as a mild method of coupling carboxylic acids with amines. EDCI is preferable to the more classical reagent DCC (dicyclohexylcarbodiimide) because the product from the coupling procedure is water soluble and can be easily removed with an aqueous wash. Reaction of 2-bromo-6-nitroaniline (88) with glutaric acid (122) in the presence of a molar equivalent of EDCI and an acyl carrier reagent (pyridine) in dichloromethane at

room temperature again, only gave unreacted starting materials. Even prolonged reaction or performing the same procedure under reflux conditions failed to give the desired product (scheme 3.24).

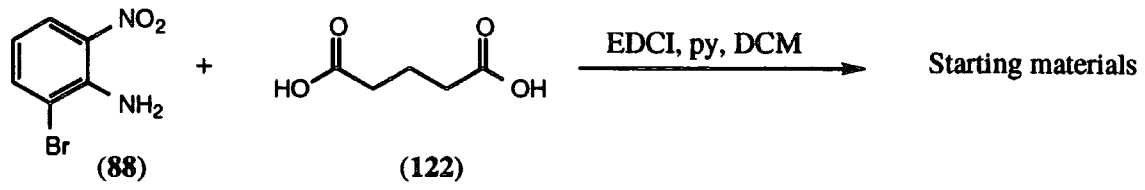

(88) (122)

Scheme 3.24 Attempted EDCI mediated coupling methodology

As concomitant formation of the bis(benzimidazole) architecture appears to be hampered by either a lack of reactivity or competing side reactions, a new approach was sought. This involved the sequential formation of each benzimidazole unit using a funtionalised C_5 chain. This chain needs to designed in such a way so that the C-1 and C-5 positions are at different oxidation levels and can be independently manipulated or orthogonally protected.

To a freshly prepared solution of anhydrous sodium methoxide was added δ-valerolactone (124) and the solution refluxed for 3 hours. The mixture was poured into water and extracted with diethylether.

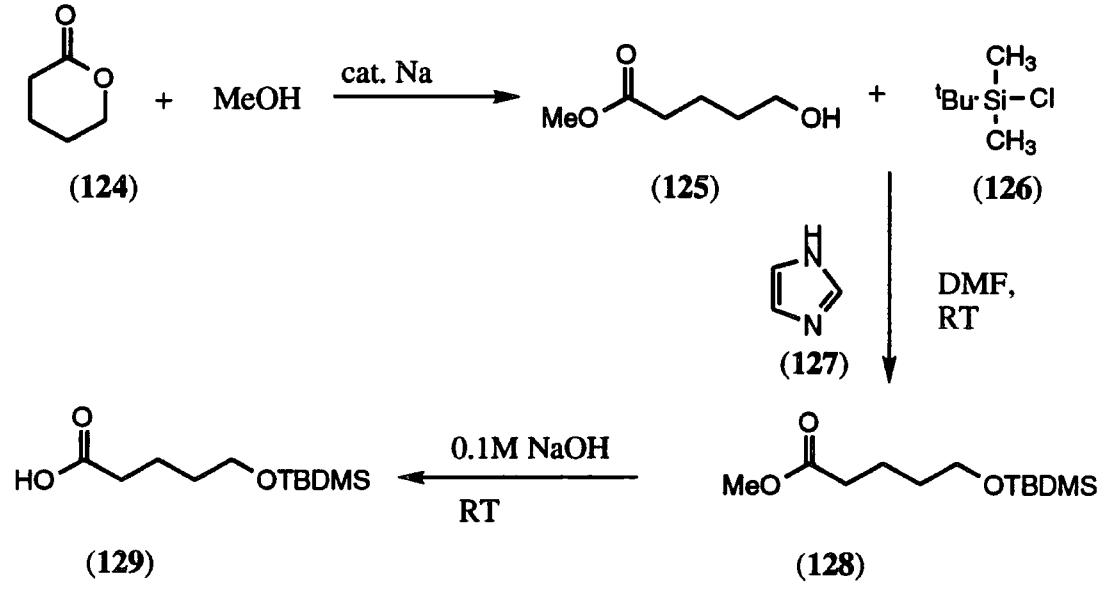

Scheme 3.25 Preparation of protected hydroxy ester (128) and acid (129)

Removal of the solvent gave methyl-5-hydroxypentanoic acid (125) in 68% yield. Protection of the hydroxyl group was affected using *tert* butyl dimethylsilyl chloride (126) in DMF with imidazole (127) acting as the base (scheme 3.25). With the TBDMS protected hydroxy ester (128) the five carbon chain has two oxygen functionalities at

two different oxygenation levels. Therefore condensation with one molar equivalent of diamine (82) should produce a hydroxy functionalised benzimidazole. This can be deprotected, oxidised and a second diamine condensed to form the required bis(benzimidazole). The ester was also hydrolysed in sodium hydroxide (0.1M) to produce the free acid (129) in quantitative yield, the acid could then in principle, be used in a Phillips type condensation in parallel to the above procedure.

Attempted condensation of the protected ester (128) with one molar equivalent of 3-bromo-1,2-diaminobenzene (82) in toluene under Dean-Stark conditions failed to give the desired product. Changing the solvent to *para*-xylene and repeating the procedure again failed to yield the target compound, even after prolonged reaction (scheme 3.26).

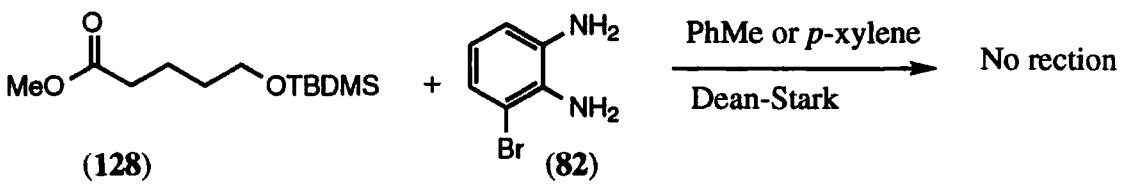

Scheme 3.26 Attempted condensation with protected ester (128)

A Phillips type condensation was attempted with the protected hydroxy acid (129) in the hope that condensation and concomitant deprotection of the silyl group would occur.[23] Heating a 1:1 mixture of the acid (129) and 3-bromo-1,2-diaminobenzene (82) at 120°C failed to produce the desired product on work-up. Only 5-hydroxy pentanoic acid (130) and unreacted diamine (82) were recovered (scheme 3.27).

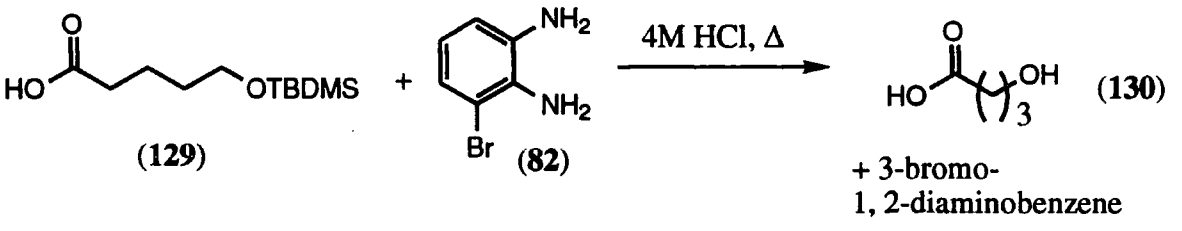

Scheme 3.27 Attempted Phillips type condensation

Another variant on the same methodology focused on the production of ethyl-4-cyano butyrate (132), which was synthesised by reaction of ethyl-4-bromobutyrate (131) with potassium cyanide at 100°C in DMSO.[56] Isolation of the product was achieved by pouring the mixture into water and extraction with diethylether to produce a brown oil, which was further purified by distillation under pressure to give a colourless oil in 66% yield (scheme 3.28).

(131) (132)

Scheme 3.28 Preparation of ethyl-4-cyanobutyrate (132)

The condensation between ethyl-4-cyano butyrate (132) and a molar equivalent of 3-bromo-1,2-diaminobenzene (82) was attempted following using the procedure of Leavitt.[57] Heating the two reagents in polyphosphoric acid 180°C for 6 hours, gave a bright orange solid after aqueous work-up and treatment with activated carbon (scheme 3.29). Analysis of the product by ^{1}H and ^{13}C NMR revealed that indeed the benzimidazole product had formed, but analysis of the carbon spectrum showed no sign of the nitrile signal. Mass spectrometry showed a bromine isotope pattern indicative of two bromine atoms in the molecule (1:2:1 intensity) indicating that the ultimate target, the propyl spaced bis-benzimidazole (133) had formed, with some unreacted ethyl-4-cyanobutyrate (132) still present.

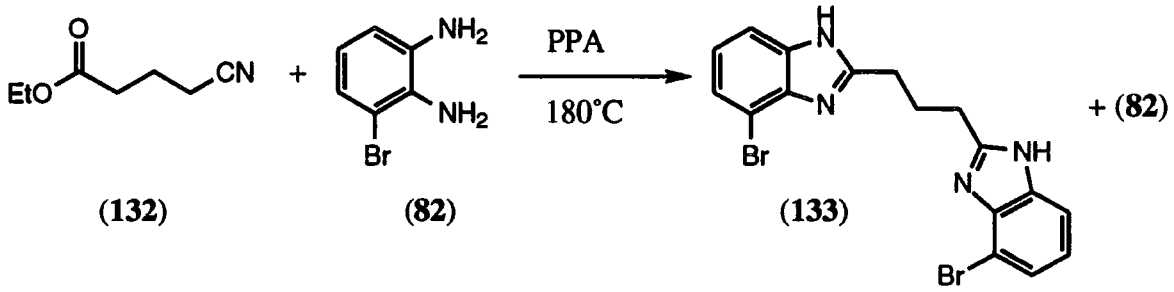

(132) (82) (133)

Scheme 3.29 Condensation reaction between ethyl-4-cyanobutyrate (132) and diamine (82)

Repeating the most simple procedure, by reaction between dimethylglutarate (123) and the bromo-diamine (82) in PPA at 180°C produced the 4,4'-dibromo-bis(benzimidazole) (133) in moderate yield (59%) following the same procedure as above (scheme 3.30). Presumably the success of this procedure relates to the high effective acid concentration Many reactions which require very high temperatures may proceed cleanly at much lower temperatures in PPA.

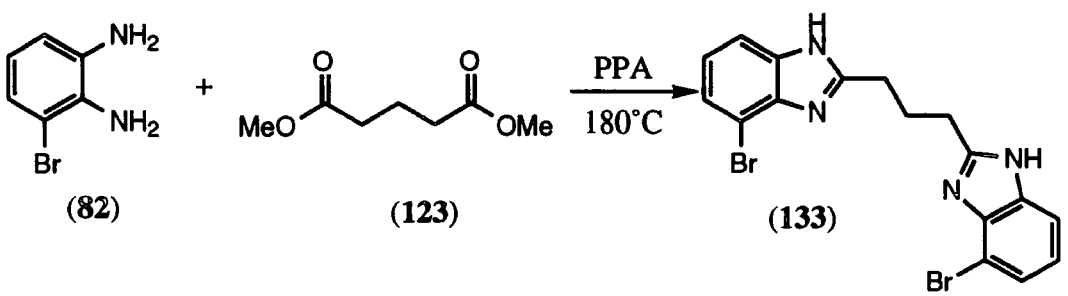

(82) (123) (133)

Scheme 3.30 Reaction of dimethylglutarate (123) and 3-bromo-1,2-diaminobenzene (82) to produce (133)

With the 4, 4'-dibromo-bis(benzimidazole) (133) to hand, the same methodology for the introduction of the N-alkyl substituent and the phosphinic acid moieties can be employed as for the monobenzimidazole case (section 3.4).

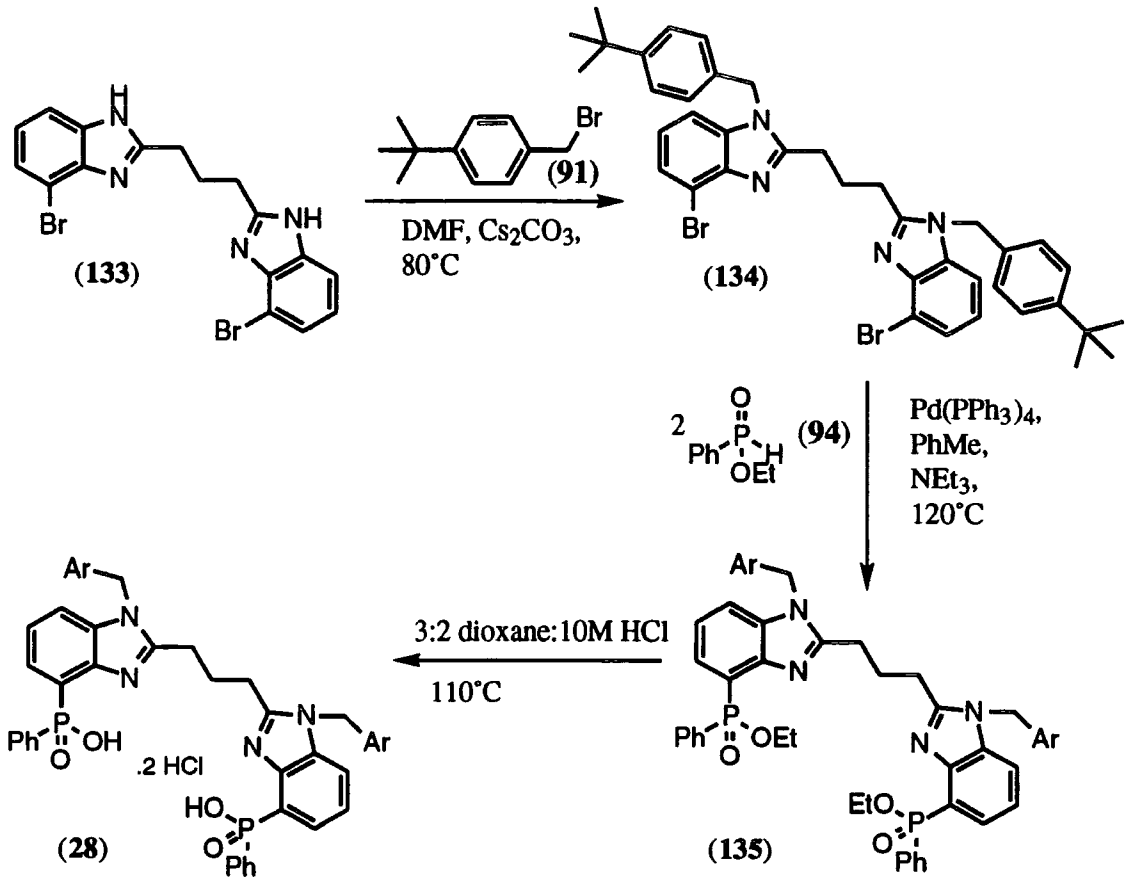

Scheme 3.31 Synthesis of target ligand (28)

Alkylation of the bis(benzimidazole) (133) was carried out in an analogous manner to the previous two examples, in DMF at 80°C with caesium carbonate as the base. The same selectivity for alkylation was observed as in the previous cases (*vide supra*), to give 4,4'-dibromo-1,1'-di(*tert* butylbenzyl)-2,2'-bis(1,3 propyl)bis(benzimidazole) (134). Cross coupling the dibromo compound (134) with two equivalents of ethylphenylphosphonite (94) in toluene with tetrakis(triphenylphosphine)palladium(0) catalysis gave the crude bis-phosphinate ester (135).[27] Purification by flash chromatography gave the pure product (135) as a pale orange solid in reasonable yield (62%). Ester hydrolysis was conducted in a 3:2 mixture of 1,4-dioxane and hydrochloric acid (10M), reaction at 110°C followed by lyophilisation gave the target ligand (28) as its dihydrochloride salt in overall 16% yield (scheme 3.31).

3.15 Solution complexation behaviour

Solution complexation behaviour was examined using ^{31}P NMR titration, fluorescence spectroscopy, uv, electrospray mass spectrometry and liquid-liquid extraction.

3.15.1 ^{31}P NMR titration

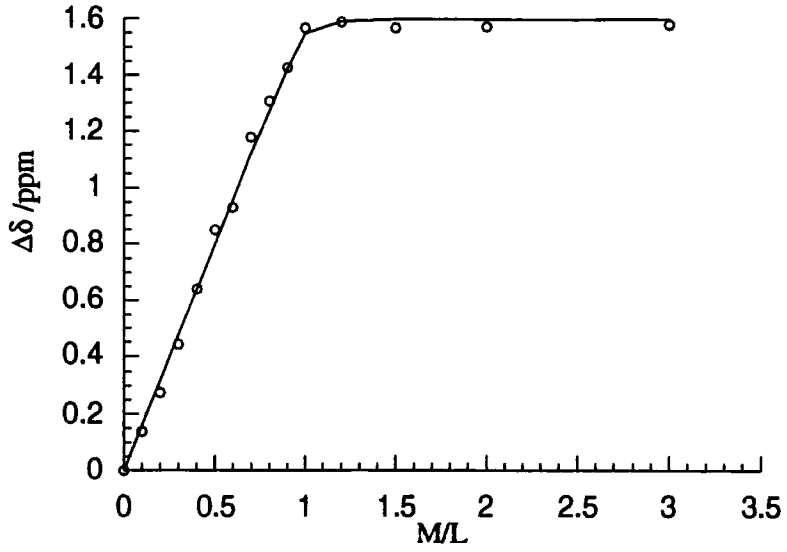

Figure 3.34 ^{31}P NMR titration of (28) with $ZnTf_2$ (25% CD_3OD, 75% $CHCl_3$, 293K)

There was an observed shift in the phosphorus signal to higher frequency with increasing metal to ligand ratios. A single exchange-broadened peak was observed, indicating that bound and unbound species were in fast exchange on the NMR time scale (101MHz, 293K). Plotting the shift in phosphorus resonance against the metal to ligand ratio (M/L) gave a titration curve (figure 3.34). Non-linear least squares analysis for a 1:1 stoichiometric complex (appendix A)[29, 30] gave an equilibrium stability constant of $LogK_{ZnL} = 5 \pm 0.1$. The ligand therefore forms a relatively strong ML complex with zinc, indicated by the sharp turning point at M/L=1.

3.15.2 Fluoresence spectroscopy titrations

pH titration

Variations in fluorescence intensity were monitored as a function of pH for 1, 1'-di(*tert* butylbenzyl)-bis(1, 3 propyl)benzimidazole-4, 4'-bis(phenylphosphinic acid) (28) starting at low pH and moving to high pH by incremental addition of sodium hydroxide solution. The variation in intensity was then monitored as a function of pH between 1

and 12. A selection of the spectra (λ_{ex}=290nm, λ_{em}=300-550nm, slits 2.5nm) at various pH values are shown below (figure 3.35).

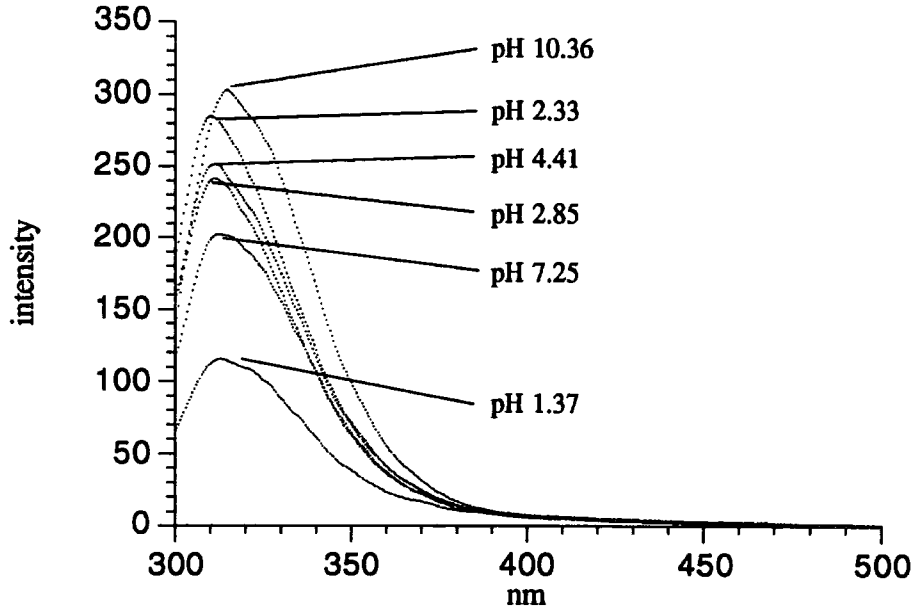

Figure 3.35 Variation in fluorescence intensity with pH for ligand (28) (λ_{ex}=290nm, λ_{em}=300-550nm, 90% H_2O, 10% CH_3OH, 298K)

From the change in intensity with pH it is evident that there is mainly a variation in intensity without a concomitant shift in the emission maximum. Above pH 8 there is a small shift in the wavelength of emission, by about 8nm to longer wavelength. The shift in wavelength is consistent with protonation causing a shift in the energies of the frontier orbitals, which accounts for the slight wavelength shift at high pH as described previously. Plotting the change in intensity against pH at 314nm reveals information regarding the different protonation states of the ligand (figure 3.36).

The pH profile of the trimethylene spaced bis(benzimidazole) ligand (28) is similar in form to that of the mono benzimidazole system (26). This implies that the presence of two benzimidazole subunits in the ligand does not significantly influence the pK_as of either the phosphinic acids or the nitrogen atoms. For this ligand, the two subunits can be regarded as behaving independently, and the same acid-base equilibria apply for this ligand as with the monobenzimidazole ligand (26) (section 3.5.2 scheme 3.14). The increase in fluorescence intensity between pH 1 and 3 may be ascribed to deprotonation of the phosphinic acid, allowing the phosphinate oxygen to participate in coplanar conjugation with the heterocyclic ring. With the subsequent decrease in intensity between pH 3 and 6 due to the loss of the rigid chelate ring formed between the phosphinate and the nitrogen atom.

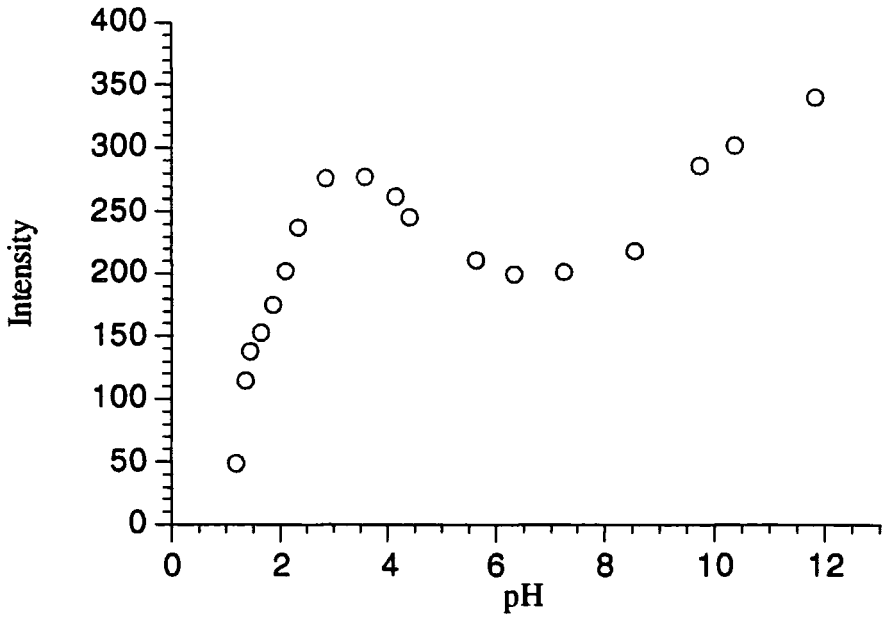

Scheme 3.36 Variation in fluorescence intensity at 314nm against pH for ligand (28) (λ_{ex}=290nm, λ_{em}=300-550nm, 90% H_2O, 10% CH_3OH, 298K)

By inspection of the curve the pK_a of the phosphinic acid functionality can be estimated to be 3 and the benzimidazole nitrogen around 5.5. Again, it must be remembered that these values are excited state values, which should be fairly close to the ground state values.

Zinc fluorescence titration

In order to investigate the complex stoichiometry in solution further, it is necessary to monitor the interaction of the benzimidazole ring with added zinc ions. Examinination of the change in fluorescence intensity upon addition of incremental portions of zinc ions should provide a useful probe. The variation of fluorescence intensity (λ_{ex}=290nm, λ_{em}=300-550nm, slits 2.5nm)with addition of zinc is shown below (figure 3.37).

The observed fluorescence intensity increases with addition of zinc. In the absence of zinc the ligand exists predominantly as it's zwitterionic form (the pH of the solution was measured to be 4.5) and the benzimidazole nitrogen will exist mainly in the zwitterionic form (Ch. 3.5.2 figure 3.14). In this, state the electronic transition responsible for the fluorescence is likely to be a π-π^* transition. As zinc is added the proton is progressively displaced by participation of the metal in a dative bond with the nitrogen atom. This change in bond order modifies the energy of the frontier orbitals (Ch. 3.5.2) and may be responsible for the observed changes. There is also an associated CHEF effect when the ligand binds to the metal, where the more restricted modes of internal

vibration and rotation lead to an increase in the observed emission intensity.[36] Associated with this is an ICT effect which contributes to changes in the observed emission spectrum, as described above (Ch. 3.5.2).[32]

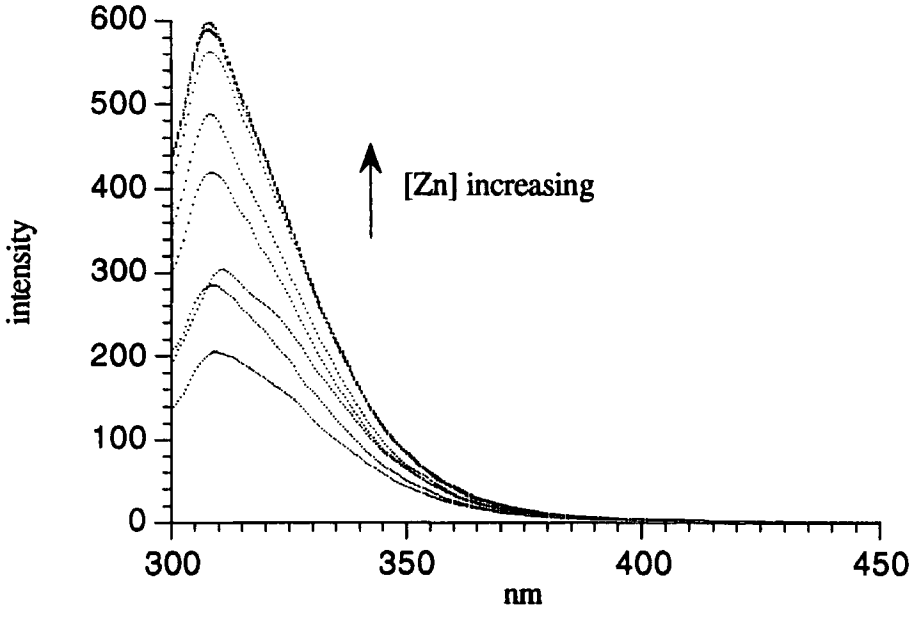

Figure 3.37 Variation in fluorescence intensity for (28) with incremental addition of $Zn(ClO_4)_2$ (λ_{ex}=290nm, λ_{em}=300-550nm, 10% H_2O, 90% CH_3OH, 298K)

To deduce the complexstoichiometry in solution a plot of intensity against metal to ligand ratio is shown below at 309nm (figure 3.38). From the form of the curve the ligand seems to be forming an ML_2 complex with zinc at this concentration, which is contrary to evidence from ^{31}P NMR titrations (Ch. 3.15.1), ESMS (Ch. 3.15.4) and liquid-liquid extraction data (Ch. 3.15.5). There is a possible explanation for the data obtained from the fluoresence studies, by comparing the equilibrium constants (eqn. 3.1 and 3.2):

$$M + L \overset{K_1}{\rightleftharpoons} ML \qquad K_1 = \frac{[ML]}{[M][L]} \qquad \text{eqn. 3.1}$$

$$ML + L \overset{K_2}{\rightleftharpoons} ML_2 \qquad K_2 = \frac{[ML_2]}{[ML][L]} \qquad \text{eqn. 3.1}$$

Initially there is an excess of ligand in the solution and as metal is added the ligand forms an ML_2 complex, therefore the observed increase in fluorescence intensity will reach a maximum at M/L=0.5. However with further addition of metal to the solution,

an ML complex is formed from the ML_2 complex, as shown by NMR and liquid-liquid extraction. If this is the case then there will be no further increase in the observed fluorescence intensity as all the nitrogen atoms in the system will still be coordinated to the metal. Hence, there will be no further change to the aromatic chromophore at higher M/L ratios which results in the levelling off the observed curve.

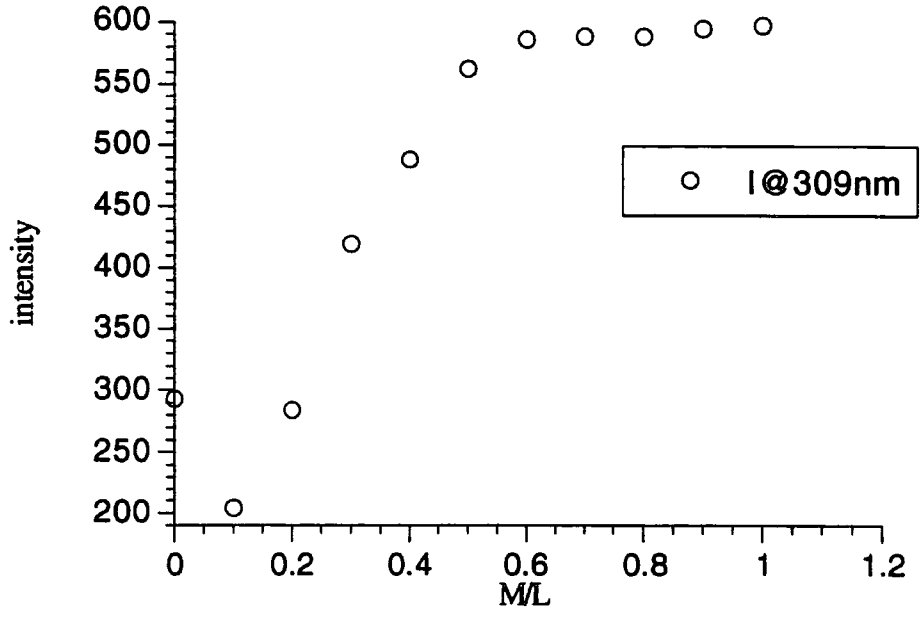

Figure 3.38 Variation of intensity for (28) against M/L at 309nm (λ_{ex}=290nm, λ_{em}=300-550nm, 10% H_2O, 90% CH_3OH, 298K)

3.15.3 UV measurements

Stock solutions of the ligand (28) and the metal salts of cobalt, copper, nickel, zinc and ferric perchlorates in methanol (1mmol) were prepared. To 1ml of the ligand solution was added 1ml of the appropriate metal salt solution and the mixture diluted with methanol to make a final, total concentration of 0.01mmol.

As has been mentioned before (*vide supra* Ch. 3.5.3), benzimidazoles possess characteristic absorption bands, which resemble those of substituted benzene derivatives. The short and long wavelength absorption bands correspond to transitions in the imidazole and aryl rings respectively.[37, 38] Coordination of the zinc ion has a significant effect on the absorption spectrum with a large increase in the absorption for the high energy transition at 207nm (ε_L = 14817dm^3mol^{-1} and ε_{LZn} = 20066dm^3mol^{-1}), whereas the longer wavelength absorption is relatively unchanged between 259 and 290nm (ε_L = 13927dm^3mol^{-1} and ε_{LZn} = 18860dm^3mol^{-1} at 290nm and ε_L = 915dm^3mol^{-1} and ε_{LZn} = 1426dm^3mol^{-1} at 277nm). A comparison of the uv spectra of

the free ligand and the one to one mixture of ligand (28) and zinc(II)perchlorate is shown below (figure 3.39).

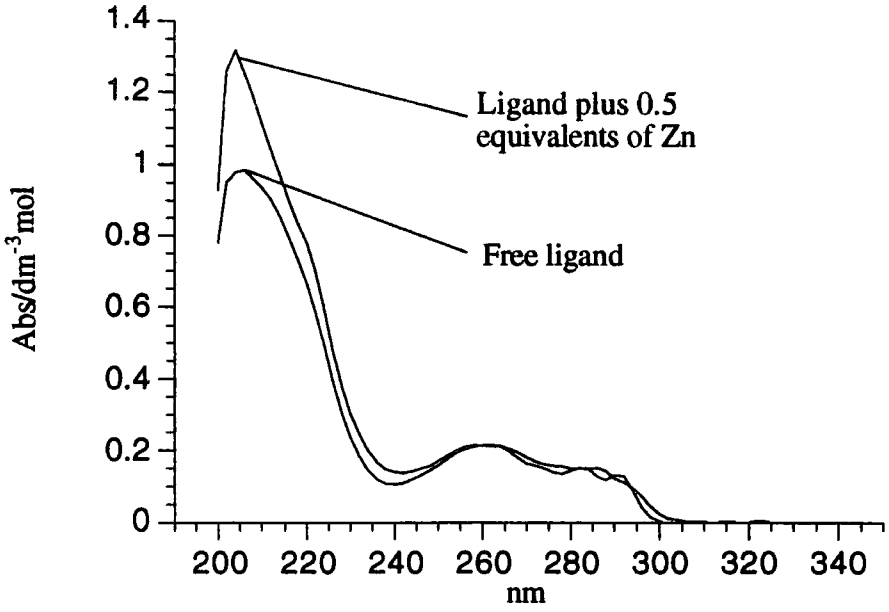

Figure 3.39 Comparison of ligand (28) and Zn complex (λ_{ex}=290nm, λ_{em}=300-550nm, 90% H_2O, 10% CH_3OH, 298K)

A summary of the uv absorption bands are give below in the presence of nickel, zinc, cobalt, copper and iron salts (table 3.4).

With zinc, copper, nickel and cobalt the absorption spectra for the complexes are all similar. The extinction coefficients for all measurements is roughly double that of the monobenzimidazole ligand (26) at the same concentration, due to the presence of two benzimidazole subunits per ligand, which gives an effective concentration of benzimidazole chromophore of 0.02mmol.

Ligand		Zinc(II)		Copper(II)		Nickel(II)	
λ / nm	ε / dm^3M^{-1}	λ / nm	ε / dm^3M^{-1}	λ / nm	ε / dm^3M^{-1}	λ / nm	ε / dm^3M^{-1}
207	14817	213(s)	20066	214 (s)	24266	208 (s)	22406
216 (s)	15753	224	21333	224	27126	224	25526
259	13927	259	18860	261	21266	264	19400
290	915	280	1426	279	1753	282	1500
		290 (s)	1240	290 (s)	1453		

Ligand		Cobalt (II)		Iron (III)	
λ / nm	ε / dm^3M^{-1}	λ / nm	ε / dm^3M^{-1}	λ / nm	ε / dm^3M^{-1}
207	14817	219	25933	216	47933
216 (s)	15753	261	17600	261	22693
259	13927	282	1420	281	1786
290	915				

Table 3.4 UV absorption of ligand (28) in the presaence of Zn, Cu, Ni, Co and Fe perchlorates (CH_3OH, 298K)

3.15.4 Electrospray Mass Spectrometry

Complexation and electrospray analysis was carried out with the above ligand (28) using the metal ions of zinc, copper, nickel and ferric as their perchlorate salts. A stock solution of the ligand in methanol was prepared with a concentration of 10μM and metal solutions of 100μM. Although ESMS is not a quantitative technique, comparison of the relative intensities of the major peaks gives a qualitative order of the selectivity for the given metals. Complex solutions were prepared as one to one mixtures and $ESMS^+$ and $ESMS^-$ spectra recorded. The negative ion ESMS spectra produced the best results, often in complexes associated with chloride or perchlorate counter ions.

Copper

For copper, peaks corresponding to $[LCuCl]^-$ and $[LCu(ClO_4)]^-$ were observed as the major peaks, with relative intensities of 73 and 41% respectively. However these were less intense than other spectra recorded at the same concentration.

Nickel

For nickel an extremely weak signal due to complexed ligand was observed, with $[LNiCl]^-$ and $[LNi(ClO_4)]^-$ being the only species detected. The relative intensities of these two signals was 5 and 3% respectively. The implication of these two weak signals is that the nickel complex is much less stable, or is formed much more slowly than the corresponding copper complex under these conditions.

Zinc

With zinc a slightly different spectrum was observed. Major peaks corresponding to the 1:1 complexes, $[LZn]^+$, $[LZnCl]^+$ and $[LZn(ClO_4)]^+$ with relative intensities of 100, 77 and 33% respectively were observed. The 100% abundance of the molecular ion of the complex suggests that the zinc complex may be more abundant than the corresponding copper or nickel complexes, in the electrospray environment. Excellent agreement between the observed spectrum and the theoretical isotope pattern was observed (figure 3.40)

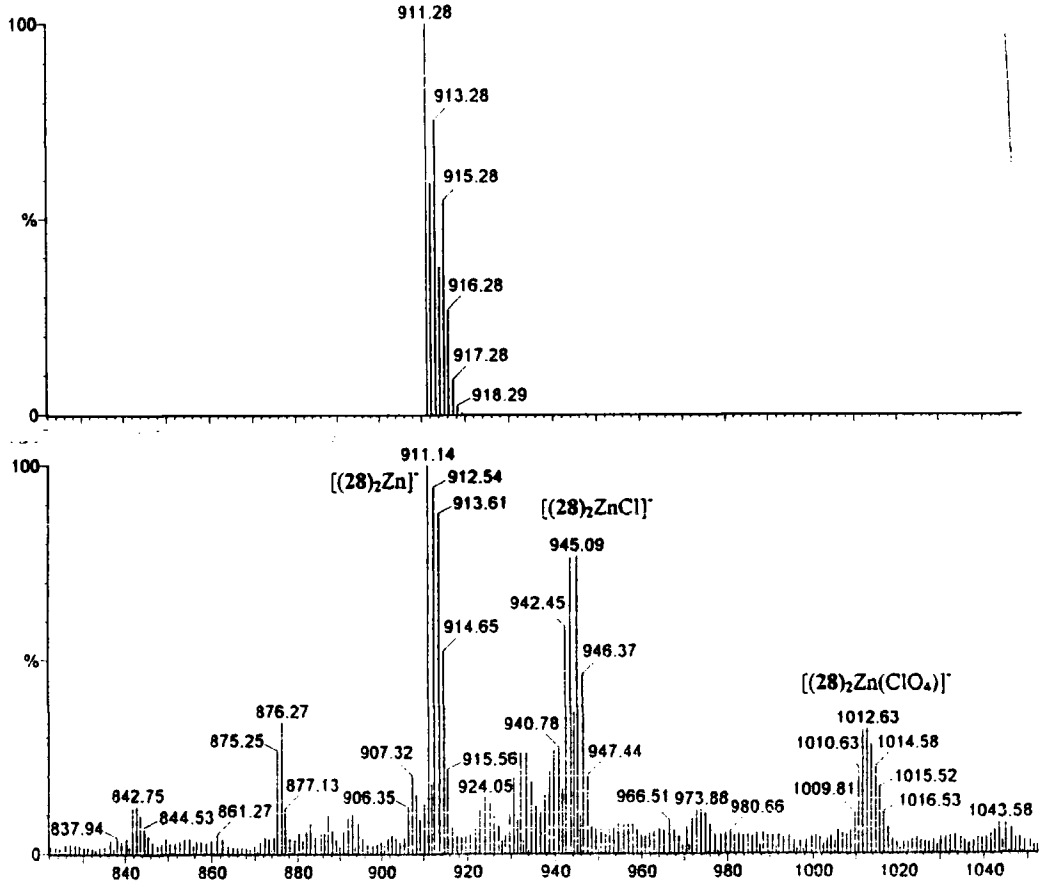

Figure 3.40 ESMS spectrum of $[(28)Zn]^+$ with theoretical isotope pattern above

Iron

With iron no metal complexes signals were observed. Indicating that this ligand is unable to adopt a geometry complimentary to iron's preferred coordination geometry.

Summary of ESMS data

The major species observed for all four metal ions studied are summarised below (table 3.5), with the observed and calculated masses and the relative intensities of the given species.

Metal ion	Species	Observed Mass	Calculated Mass	Relative Intensity
Zn	$[LZn]^-$	911.14	911.28	100%
	$[LZnCl]^-$	945.09	945.36	77%
	$[LZn]^-/2$	456.26	456.15	56%
	$[LZn(ClO_4)]^-$	1012.63	1012.84	33%
Cu	$[[LCuCl]^-$	943.95	943.24	73%
	$[[LCu(ClO_4)]^-$	1008.6	1008.77	41%
Ni	$[LNiCl]^-$	938.76	938.74	5%
	$[LNi(ClO_4)]^-$	1004.63	1004.32	3%
Fe	No complex species observed			

ESMS$^-$, 60°C source temperature, 30V cone voltage.

Table 3.5 Summary of major species observed with (28) in the presence of zinc, copper, nickel and iron perchlorates

3.15.5 Liquid-liquid extraction

Liquid-liquid extraction experiments were performed on ligand (28) by C. Chartroux at the University of Dresden, Germany in micro-reaction vials in buffered aqueous media (298K, pH 2) and chloroform, using the metal salts of $HgCl_2$, $Ni(NO_3)_2$, $ZnCl_2$ and $Co(NO3)_2$.[40] The results of the extraction studies are shown below (figure 3.41)

From the figure it is evident that zinc is almost totally transported into the organic phase, with the ligand (28) transporting about 75% of the available cobalt and mercury into chloroform. The ligand transports negligible quantities of nickel across the liquid interface, reflecting the ligands low coordination preference for this metal.

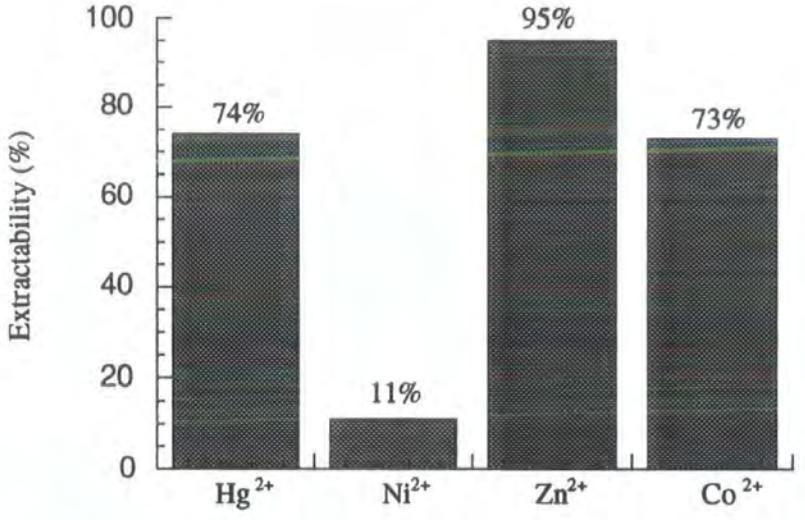

Figure 3.41 Extracatability of Hg^{2+}, Co^{2+}, Zn^{2+} and Ni^{2+} with (28), $[M]=10^{-4}moldm^{-3}$, $[L]=10^{-3}moldm^{-3}$ ($CHCl_3$, 298K)

Information regarding the overall stoichiometry of complexation was also obtained by measuring the ratio of cation concentrations in the organic phase (D_m), as a function of the ligand concentration in the organic solvent (C_{ligand}) for mercury, zinc and cobalt (figure 3.42).

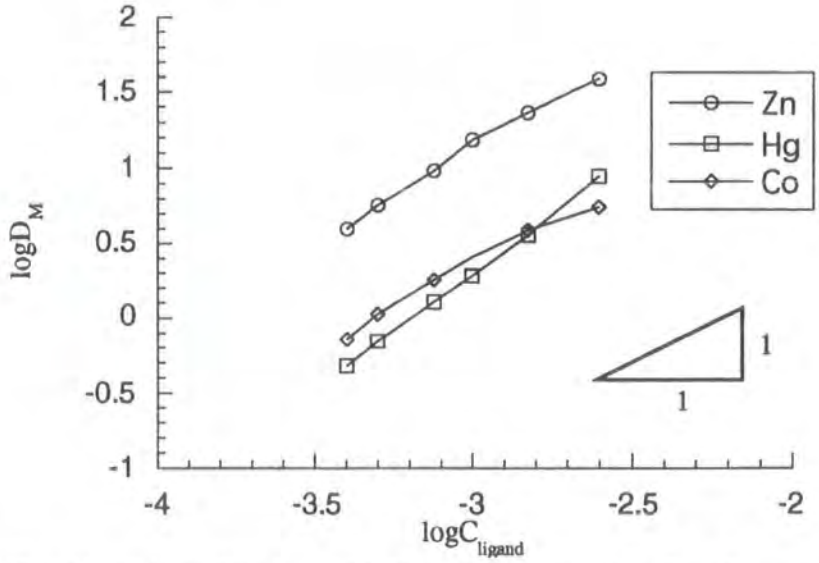

Figure 3.42 Variation of $logD_m$ with ligand concentration ($logC_{ligand}$) for the extraction of Hg^{2+}, Co^{2+}, Zn^{2+} with (28), $[M]=10^{-4}moldm^{-3}$ ($CHCl_3$, 298K)

From the data for the zinc and cobalt extractions, slopes of near unity were obtained, consistent with 1:1 complex formation, with a suggestion of a small degree of 2:1 complex formation. For mercury a slightly more complex case was observed, analysis of the slope indicates that both 1:1 and 2:1 complex formation is occurring in the organic phase. There have been previous examples of bis(1,3-propyl)benzimidazoles, which do not possess anionic donors binding to large metal cations in a 2:1 manner.[58, 59] It is possible to analyse the form of the curve by an iterative least squares procedure to obtain an estimate of the stability constant of (28) with mercury, cobalt and zinc, this is tabulated below (table 3.6).[31]

Metal	$\log\beta_{ML}$	$\log\beta_{ML2}$
Hg	3.0	3.1
Co	3.4	1.4
Zn	4.1	1.4

Table 3.6 Formation conatants for (28) derived from liquid-liquid extraction

There is a pronounced selectivity for zinc over both mercury and cobalt ions using the partitioning method of analysis. Selectivity for zinc over mercury may be related to the large ionic radius of mercury (1.02Å) relative to zinc (0.75Å), restricting six-ring chelate formation for the larger ion and enforcing a 2:1 coordination mode on the complex via coordination to four benzimidazole nitrogens. The preference for zinc over cobalt of the metal may be due to the choice of donor atoms in the ligand. Cobalt is a hard acceptor and prefers hard donors (Ch 1.4), therefore coordination to the N_2O_2 donor set of the ligand will be more favoured for the borderline zinc ion.

With nickel, accurate measurements were not possible as the system did not reach equilibrium, even after mechanical shaking for two hours. Extraction of nickel with (28) was attempted at pH 2.1 and 2.7, and in both cases shallow curves were obtained, which could not be analysed to determine a stability constant (figure 3.43).

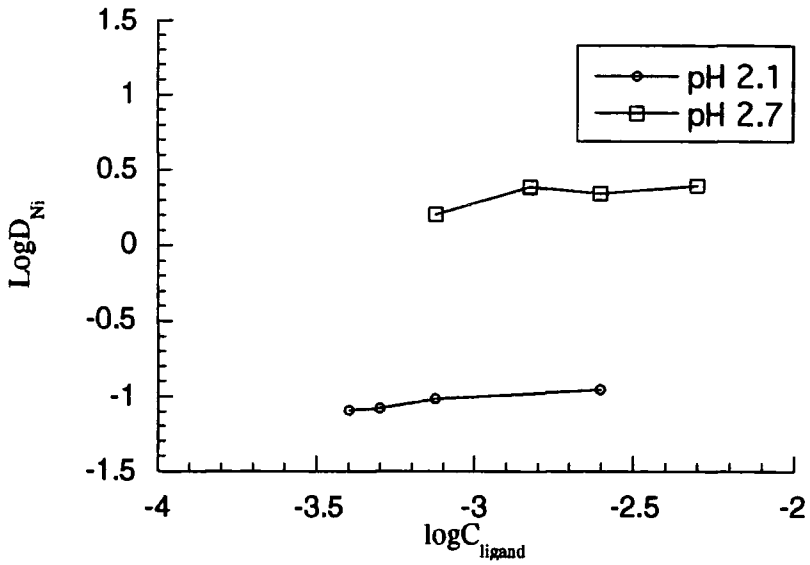

Figure 3.43 Variation of $logD_{Ni}$ with ligand concentration ($logC_{ligand}$) for the extraction of Ni^{2+} with (28), $[M]=10^{-4}moldm^{-3}$ ($CHCl_3$, 298K)

3.16 Summary and Conclusions

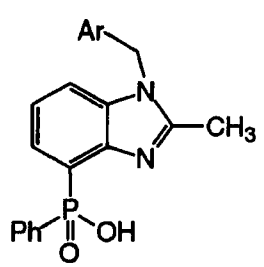

(26)

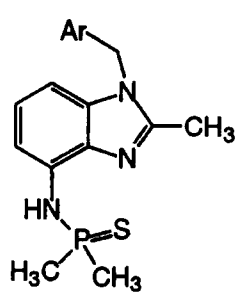

(27)

Ar = 4-(*tert* butyl)phenyl

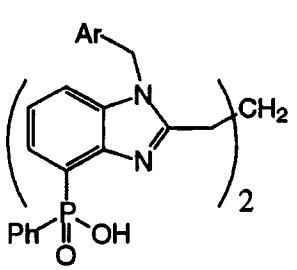

(28)

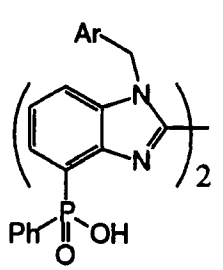

(29)

Figure 3.44 Structure of ligands (26), (27), (28) and (29)

Viable synthetic routes to all four of the described ligand systems have been, which allowing variation of the steric bulk and lipophilicity of the ligands (figure 3.44). For

the mono-benzimidazole phosphinic acid ligand (26), solution coordination chemistry studies show that with excess metal present, the ligand tends to form ML complexes, consistent with NMR data. However the predominant species in solution is the ML_2 complex (ESMS and Job plot). Evidence from fluorescence studies imply a weak ML complex, formation of which is consistent with data obtained from the ^{31}P NMR titrations. Overall, in the presence of excess zinc ions the ligand forms ML complex species, whereas when the ligand is in excess over the metal ML_2 species predominate. Liquid-liquid extraction tests show that zinc is transported selectively over cobalt, mercury and nickel from an aqueous phase into chloroform.

For the ligand system based on the thiophosphoramide donor (27), ^{1}H NMR titrations indicate that weak ML complex formation is occurring in solution, as deduced by the ill defined turning point in the titration curve, and the continued, steady rise in $\Delta\delta$. Electrospray studies indicate that the ligand forms ML_2 species predominantly under these experimental conditions. Solvent extraction studies across a pH range show that the ligand is able to extract zinc, but at a pH that is too high for use in the hydrometallurgic recovery of zinc.

A synthetic route towards the 2,2'-bis(benzimidazole) ligand (29) has been developed, unfortunately isolation of the free acid was hampered by insolubility or difficulties in purification.

An efficacious route to the trimethylene spaced bis(benzimidazole) ligand (28) has been developed, which allows modification of the lipophilicity at either the phosphorus atom or the N-alkyl substituent. In solution the ligand initially forms a weakly N_4 bound ML_2 complex when in excess over the metal. This is apparent from the stability constant obtained by liquid-liquid extraction and the zinc fluorescence titration, where a maximum fluorescence emission intensity is obtained at M/L=0.5. When more metal is added a strong ML complex is formed, as shown by the ^{31}P NMR data ($\log\beta_{ML}=5 \pm 0.1$ $moldm^{-3}$). Reasonable agreement was obtained with the stability constant obtained from the partitioning studies ($\log\beta_{ML} = 4.1$ $moldm^{-3}$). Evidence from the ESMS experiment support these conclusions, where only ML species were observed.

3.17 References

1. F. Hobrecker; *Ber.*, 1872, **5**, 920
2. M. A. Phillips; *J. Chem. Soc.*, 1928, 2393
3. P. N. Preston; *Chem. Rev.*, 1974, **74**, 279
4. P. N. Preston, D. M. Smith and G. Tennant; 'Benzimidazoles and Congeneric Tricyclic Compounds', Vol. 40 and 41, *The Chemistry of Heterocyclic*

compounds, Eds. A. Weissberger and E. C. Taylor, John Wiley and Sons, Chichester, 1981

5. M. R. Grimmett; '*Imidazole and Benzimidazole Synthesis*', Academic Press, London, 1997
6. T. L. Gilchrist; '*Heterocyclic Chemistry*' , Longman Scientific and Technical, Harlow, 1992, 303
7. R. Usón, J. Gimeno, J. Formies, F. Martinez and C. Fernandez; *Inorg. Chim. Acta*, 1982, **63**, 91
8. R. Usón, J. Gimeno, L. A. Oro, J. M. de Ilarduya, J. A. Cabezo, A. Tiripicchio and M. T. Camellini; *J. Chem. Soc., Dalton Trans.*, 1983, 1729
9. M-A. Haga; *Inorg. Chim. Acta*, 1983, **75**, 29
10. R. Usón, A. Laguna and J. A. Bhad; *J. Organomet. Chem.*, 1983, **256**, 341
11. R. Usón, L. A. Oro, M. A. Ciriano, M. M. Naval, M. C. Apreda, C. Foces-Foces, F. H. Cuno and S. Garcia-Blanco; *J. Organomet. Chem.*, 1983, **256**, 331
12. D. P. Devonald, A. J. Nelson, P. M. Quan and D. Stewart; '*Process for the Extraction of Metal Values and Novel Metal Extractants*', Europe Pat. 0196153 B1 (1986)
13. R. F. Dalton, A. Burgess and P. M. Quan; *Hydrometallurgy*, 1992, **30**, 385
14. M. S. Chinn and J. Chen; *Inorg. Chem.*, 1995, **34**, 6079
15. I. Bertini, C. Luchinat, W. Maret and M. Zeppezauer, eds., '*Zinc Enzymes*', Brikhauser, Boston, 1986
16. C. J. Matthews, W. Clegg, S. L. Heath, N. C. Martin, M. N. Stuart Hill and J. Lockhart; *Inorg. Chem.*, 1998, **37**, 199
17. C. Nazikkol, R. Wegner, J. Bremer, B. Krebs; *Z. Anorg. Allg. Chem.*, 1996, **622**, 329
18. J. Bjerrum and C. K. Jorgensen; *Rev. Trav. Chim.*, 1956, **75**, 658
19. H. Siegel and R. B. Martin; *Chem. Soc. Rev.*, 1994, 83
20. (i) N. B. Devi, K. C. Nathsarma and V. Chakravortty, *Hydrometallurgy*, 1997, **45**,169 (ii) S. Amer and A. Luis; *Revista De Metalurgia*, 1995, **31**, 351
21. R. D. Hancock and A. E. Martell; *Chem. Rev.*, 1989, **89**, 1875
22. R. E. Lyle and J. L. La Mattina; *J. Org. Chem.*, 1975, **40**, 438
23. M. A. Phillips; *J. Chem. Soc.*, 1953, 1143
24. M. Lemaire, A. Guy, P. Boutin and J. P. Guette; *Synthesis*, 1989, 761
25. K. Smith, A. Musson and G. A. DeBoos; *J. Chem. Soc., Chem .Commun.*, 1996, 469
26. G. B. Bates; '*Tetrahedrally Coordinating Ligands*', Ph.D. Thesis, University of Durham, 1995
27. Y. Xu, Z. Li, J. Xia, H. Guo, and Y. Huang; *Synthesis*, 1983, 377
28. D. R. Coulson; *Inorg. Synth.*, 1972, **13**, 121

29. L. Collie, J. E. Denness, D. Parker, F. O'Carroll and C. Tachon; *J. Chem. Soc., Perkin Trans. 2*, 1993, 1747
30. K. A. Connors; '*Binding Constants, The Measurement of Molecular Complex Stability*', John Wiley and Sons, New York, 1987
31. A. Job; *Annales de Chimie* (10th Series), 1928, **9**, 113
32. A. P. de Silva, H. Q. N. Gunaratne, T. Gunnlaugsson, A. J. M. Huxley, C. P. McCoy, J. T. Rademacher and T. E. Rice; *Chem. Rev.*, 1997, **97**, 1515
33. C. Reichardt; '*Solvents and Solvent Effects in Organic Chemistry*', VCH, Weinheim, 1988, p 365
34. R. M. Smith and A. E. Martell; 'Critical Stability Constants' Vol 1 to 6, Plenum Press, London
35. D. E. C. Corbridge, '*Phosphorus: An Outline of its Chemistry, Biochemistry and Technology*'. 4th Ed., Elsevier (1990), Ch. 4 & 7
36. M. H. Hutson, K. W. Haider and A. W. Czarnik; *J. Am. Chem. Soc.*, 1988, **110**, 4460
37. D. J. Rabiger and M. M. Joulié; *J. Org. Chem.*, 1964, **29**, 476
38. G. Leandri, A. Mangini, F. Montanari and R. Posserini; *Gazz. Chim. Ital.*, 1955, **85**, 769
39. J. B. Fenn, M. Mann, C. K. Meng, S. F. Wong and C. M .Whitehouse; *Science*, 1989, **246**, 64
40. M. Dole, L. L. Mack, R. L. Hing, R. C. Mobley, L. D. Ferguson and M. B. Alice; *J. Chem. Phys.*, 1979, **71**, 4451
41. H. Stephan, K. Gloe, T. Krüger, C. Chartroux, R. Neumann, E. Weber, A. Möckel, N. Woller, G. Subklew and M. J. Schwuger; *Solvent Extraction Research and Development, Japan*, 1996, **3**, 43
42. D. E. Fenton; '*Biocoordination Chemistry*', Oxford University Press, Oxford, 1997
43. M. A. M. Easson; '*Synthesis of Tailored Ligands for Radiopharmaceutical Applications*' Ph.D. Thesis, University of Durham, 1997
44. A. D. F. Toy and E. G. Uhing, U.S. Patent 4,076 (C1. 260-543; CO7F9/04), 28 Feb. 1978, Appl. 502, 702
45. K. A. Pollart and H. J. Harwood; *J. Org. Chem.*, 1962, **27**, 4444
46. T. Entwhistle; *J. Chem. Soc., Perkin Trans. 2*, 1975, 1300
47. G. W. Parshall; *Org. Synth.*, 1965, **45**, 102
48. G. B. Bates, D. Parker and P. A. Tasker; *J. Chem. Soc., Perkin Trans. 2.*, 1996, **6**, 1117
49. G. Holan, E. C. Samuel, B. C. Ennis and R. W. Hinde; *J. Chem. Soc.*, 1962, 571
50. S. Berger, S. Braun and H. O. Kalinowski; '*NMR of the Non-Metallic Elements*', Wiley Interscience, Chichester, 1997, 917-920

51. (i) K. Bazakas and I. Lukes; *J. Chem. Soc., Dalton Trans.*, 1995, 113 (ii) I. Lukes, K. Bazakas, P. Hermann and P. Vojtisek; *J. Chem. Soc., Dalton Trans.*, 1992, 939
52. (i) K. P. Pulukkody, T. J. Norman, D. Parker, L. Royle and C. J. Broan; *J. Chem. Soc., Perkin Trans. 2*, 1993, 605 (ii) C. J. Broan, K. H. Jankowski, R. Kataky, and D. Parker; *J. Chem. Soc., Chem. Commun.*, 1990, 1738
53. J. B. Wright; *Chem. Rev.*, 1951, **48**, 397
54. P. N. Preston and G. Tennant; *Chem. Rev.*, 1972, **72**, 627
55. (i) S. Takahashi and H. Kano; *Chem. Pharm. Bull.*, 1963, **68**, 12971 (ii) S. M. Hussain, A. M. El-Reedy and S. A. El-Sherabasy; *J. Heterocycl. Chem.*, 1988, **25**, 9
56. E. Leete and J. A. McDonell; *J. Am. Chem. Soc.*, 1981, **103**, 654
57. D. W. Hein, R. J. Alheim and J. J. Leavitt; *J. Am. Chem. Soc.*, 1957, **79**, 427
58. C. J. Matthews, W. Clegg, M. R. J. Elsegood, T. A. Leese, D. Thorp, P. Thornton and J. C. Lockhart; *J. Chem. Soc., Dalton Trans.*, 1996, 1531
59. K. Ogawa, K. Nakata and K. Ichikawa; *Bull. Chem. Soc. Jpn.*, 1997, **70**, 2925

Chapter Four

Quinoline Derived Ligand Systems

4 Quinoline Derived Ligand Systems

Two ligand systems based on the quinoline ring system, appended with phosphinic acid functionalities are presented. An introduction to quinolines is presented (4.1), followed by a brief discussion on previous aspects of quinoline zinc coordination chemistry and some zinc fluorophores (4.2). The design (4.3) and synthesis (4.4) of the new ligand systems is described, followed by an introduction to their solution coordination chemistry (4.5), which was studied using NMR, fluorescence and UV spectroscopy, ESMS, potentiometry and liquid-liquid extraction.

4.1 Quinolines

Quinoline (136) was first isolated by distillation from coal tar by Runge in 1834.[1]

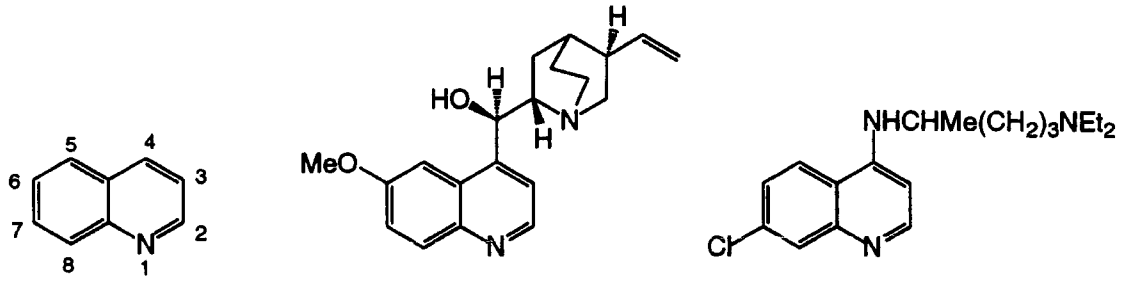

(**136**) Quinoline (**137**) (**138**)

Figure 4.1 Structure of quinoline (136) and some related compounds

Quinine (137) is a naturally occuring alkoloid which has been traditionally used as an antimalarial drug, and to give tonic it's bitter flavour. The quinoline skeleton has also been used as a basis for synthetic antimalarial drugs, of which chloroquine (138) is an example (figure 4.1). Quinoline has also formed the basis for fluorescence sensors for the zinc ion *in vivo*, this is covered below (4.2) and has been reviewed elsewhere.[2]

4.2 Zinc Coordination Chemistry and Fluorescence Probes

There is a surprising lack of literature relating to ligands derived from the quinoline ring system applied to zinc coordination chemistry. Perhaps this is because synthesis of designed and specific ligands is not a trivial matter. Quinoline tends to undergo electrophilic attack in the 3- position and nucleophilic attack in the 2- and 4- positions. Therefore incorporation of donor groups is less easy in the eight position compared to the 2-, 3- or 4- positions.

8-Hydroxy-2-methylquinoline (140) and 8-hydroxyquinoline (139) are two commercially available bidentate ligands which have been used to study zinc coordination chemistry (figure 4.2).

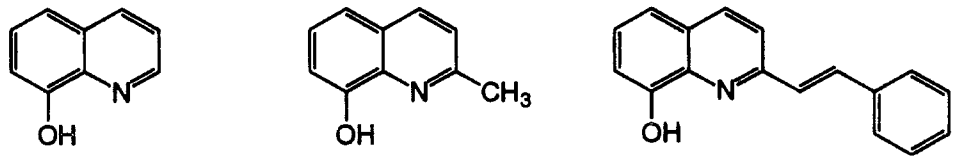

(139) **(140)** **(141)**

Figure 4.2 8-Hydroxyquinoline (139), 2-methyl-8-hydroxyquinoline (140) and ligand (141)

The coordination chemistry of these ligands with first row transition metals follows the Irving-Williams series. For 8-hydroxyquinoline (139), logβ values for the ML complexes of nickel, copper and zinc of 9.3, 12.5 and 8.5 have been determined.[3] A structural variant on the previous two ligands has been prepared by Kido, with a styryl group attached at the C-2 position (141).[4] This was synthesised to be a fluorescent sensor for zinc, the ligand emits orange light upon complexation. The orange colour results from extended conjugation of the quinoline system into the styryl group. The authors did not report the effect of this bulky substituent on the coordination properties of this ligand, or on the selectivity over the first row transition metals.

A zinc fluorophore based on a quinoline sulfonamide was designed and synthesised (143) by Lincoln *et al.* (figure 4.3), and has been used extensively for cellular studies.[5, 6] This ligand was the first fluorescence probe to visualise intracellular zinc ions in living cells. An ester group was incorporated in (142), so that after uptake of the charge neutral ligand into the cell, the anionic form (143) is produced by an intracellular esterase, leading to retention of the complex in the cell. Analysis of the zinc complex by fluorometric titration showed that both 1:1 and 2:1 complexes were formed with stability constants of $\log K_{ML}=6.84$ and $\log K_{ML_2}=7.06$ respectively, however the structures of these species were not determined. A 20-fold enhancement in fluorescence was observed on addition of 1μM zinc solution to a 2μM solution of the ligand, while fluorescence was unaffected in the presence of other biologically relevant cations (Ca^{2+}, Mg^{2+}, Cu^{2+}, Fe^{2+}, Fe^{3+}, Mn^{2+} and Co^{2+}). This is a very promising start to sensing zinc in intracellular situations, as the binding affinity for zinc is not large enough to sense zinc in tightly bound zinc-enzymes or zinc-finger proteins. To examine the concentration of bound zinc in enzymes and proteins a much higher formation constant with zinc is required, because the effective concentration of unbound zinc ions is much smaller.

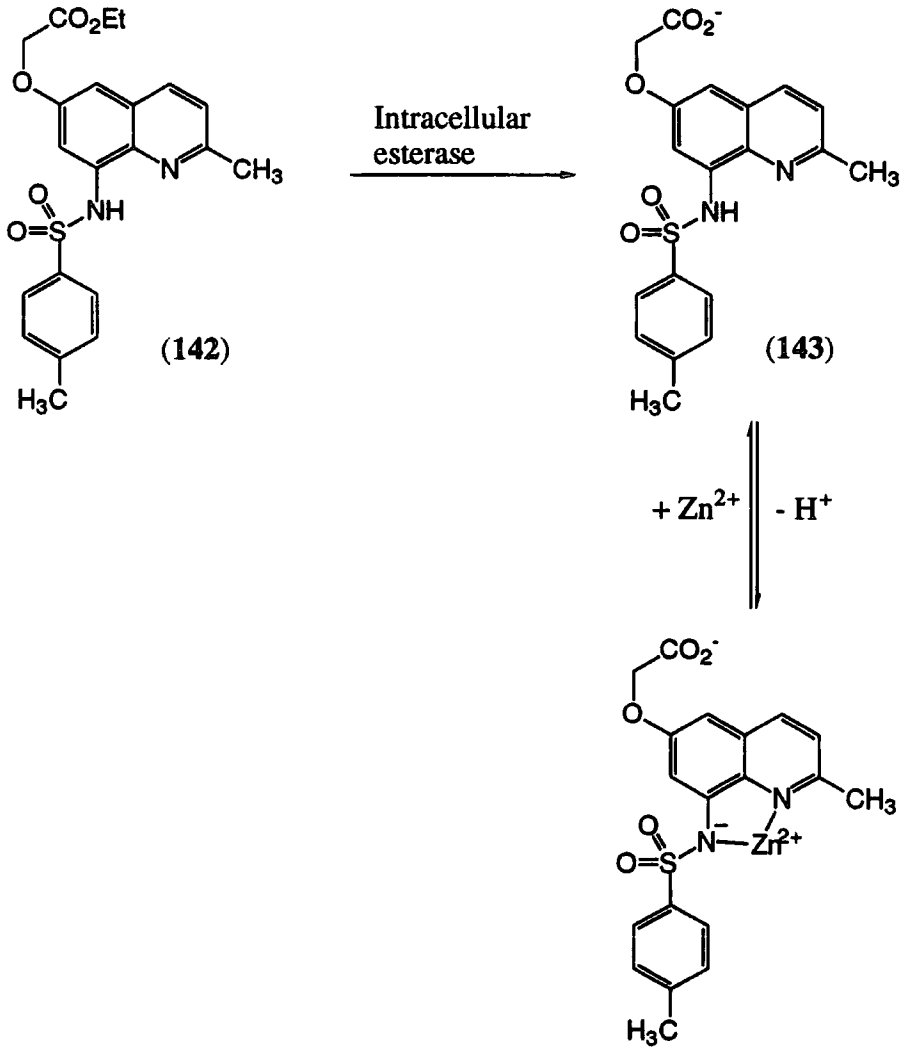

Figure 4.3 Lincoln's zinc probe (142) in intracellular trapping mechanism

Thompson and co-workers observed that 5-(di-methylamino)-1-naphthalenesulfonamide (dansylamide, 144) bound strongly to zinc-finger proteins with a concomitant change in the fluorescent emission.[7]

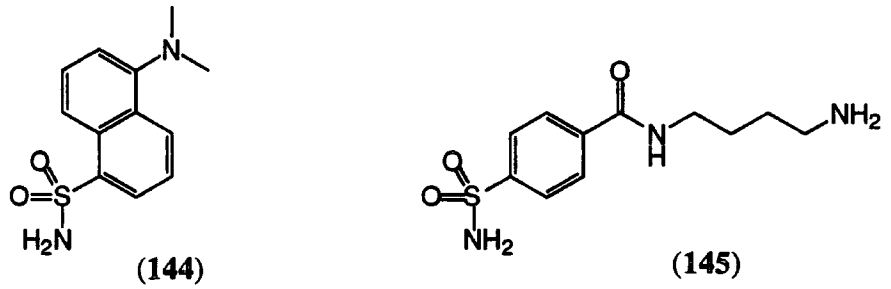

Figure 4.4 Structure of dansylamide (144) and potential sensor (145)

Dansylamide (144) was used as a first generation fluorescent sensor, which was used to generate the second generation structure (145) from an iterative structure-based search of the X-ray crystallographic data base with (144) as the starting ligand (figure 4.4).

Attachment of a fluorescent dye (fluorescein) to the conjugate gave a potential flourescent probe for strongly bound zinc. The dansylamide portion of the ligand was shown to bind strongly to the active site in carbonic anhydrase and the observed fluorescence shown to be highly dependent on the concentration of zinc.

Another sensor based on dansylamide (144) has recently been developed by Kimura.[8] This system takes advantage of the strong complexes formed between divalent zinc and $12N_4$, and since it is based on a tetraazamacrocyle, the ligand and its complexes are water soluble (figure 4.5).

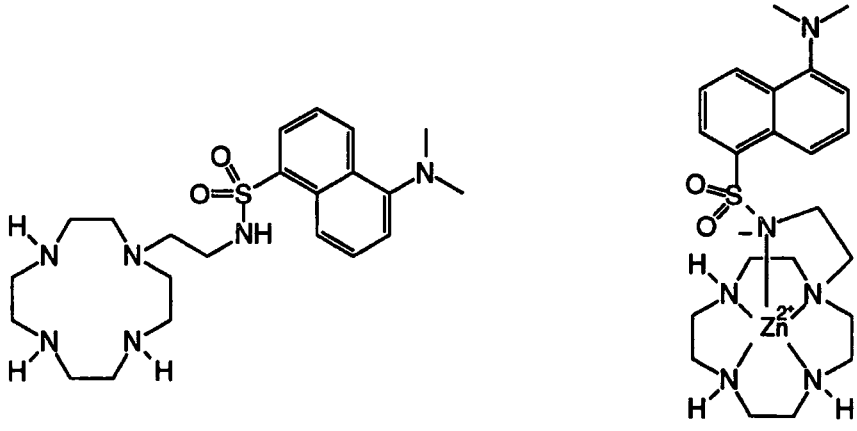

(146) **(147)**

Figure 4.5 Kimura's zinc fluorophore (146) and it's zinc complex (147)

The formation constant for the 1:1 complex was determined to be $\log K_{ML}$=20.8 by potentiometric methods, which makes it a good candidate for sensing strongly bound zinc in enzymes and proteins. The zinc complex (147) showed a blue-shifted emission (λ_{em}=490nm, by 30nm) with a 10-fold increase in intensity in the presence of a molar equivalent of zinc. Titration of (146) with human carbonic anhydrase showed a larger blue-shift (λ_{em}=478nm, by 42nm) coupled with a 15.3-fold increase in intensity.

4.3 Design of New Ligand System

Using the criteria for ligand design described in chapter one (1.4), a ligand system (30) and (31) was designed based on the quinoline moiety. The ligand has a phosphinic acid functionality and presents an NO donor set, which can interact with tetrahedral zinc in a [2 + 2] coordination mode (figure 4.6). The ligand is predisposed to form a six-ring chelate with metal ions, favouring coordination to smaller ions such as zinc.[9] The advantages of using phosphinic acids as the anionic donor have been highlighted elsewhere and the method of attachment has been covered in detail (*vide supra*).

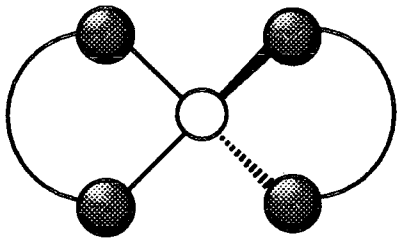

[2+2]

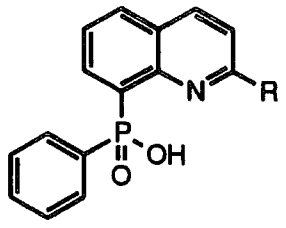

R = H (**30**)
R = Me (**31**)

Figure 4.6 Diagrammatic representation of [2 + 2] ligand geometry and target ligands (30) and (31)

Use of a heterocycle with two six-membered rings should contrast well with the benzimidazole ligands (chapter 3) which contain a six-five ring system. The change in the orientation of the nitrogen lone pair and proximity of the C-2 substituent will have a marked effect on the complex selectivity, stoichiometry and stability.

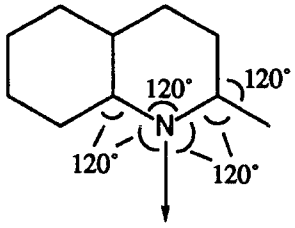

Quinoline type

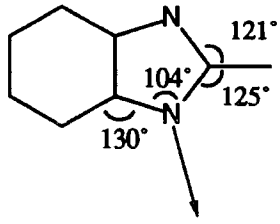

Benzimidazole type

Figure 4.7 Structural variations between quinoline benzimidazole systems

As the quinoline system is formed from two aromatic rings, all bond angles are approximately 120°. By contrast the crystal structure of benzimidazole shows that the angle between the C-4 position and the C-N bond has increased to 130° and the C-2 substituent is moved away from the nitrogen lone pair, relative to the quinoline ring.[10] This result is also inferred from considerations of elementary geometry (figure 4.7). The donor atom set chosen for this ligand is suitable for strong binding, as it mimics many zinc containing enzymes (see Ch. 3.6). Using borderline Lewis bases should help discriminate against coordination to harder interferent ions, and the strong Lewis basicity of the nitrogen atom may shorten the Zn-N bond.[11]

Modification of the lipophilicity of the quinoline derived system without compromising the binding site is not as easily accomplished as for the benzimidazole ligands. The potential sites for modification are substitution of the quinoline ring, extension of the C-2 position, or manipulation of the phosphinic acid functionality.

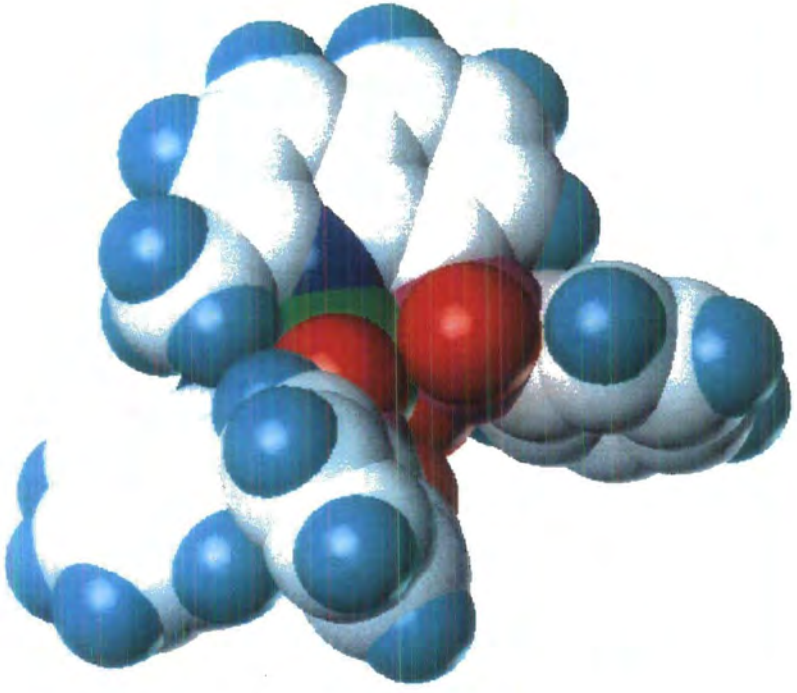

$Zn(\mathbf{30})_2$

$Zn(\mathbf{30})_2$

Figure 4.8 Molecular model showing the tetrahedral zinc complex of ligand (30), space filling (left) and line drawing (right)

Molecular modelling

Molecular modelling of the zinc complex was performed as described previously (Ch. 3.3). The model shows tetrahedral zinc (green central ion) with two chelating 8-(2-methylquinolinyl)phenylphosphinic acid (31) ligands at their minimum energy structure (figure 4.8). The methyl substituent in the C-2 position prevents formation of other coordination geometries, particularly square planar and octahedral. The two phenyl substituents on the phosphinic acid are oriented in and out the plane of the page, indicating that substitution in the *ortho* position of the phenyl ring will have a minimal effect on metal binding.

4.4 Synthesis

Retrosynthetic analysis of the target ligands (30) and (31) is shown below (figure 4.9).

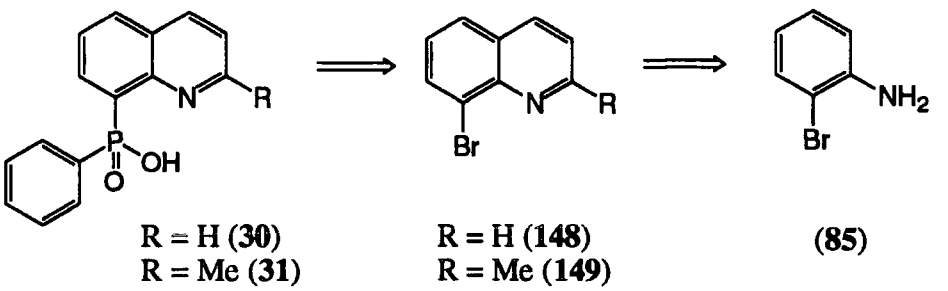

Figure 4.9 Retrosynthetic analysis of target ligands (30) and (31)

Disconnection of the C-P bond to the substituted 8-bromo quinoline (148) and (149) is followed by deconstruction of the quinoline ring system to give the readily available starting material 2-bromoaniline (85). The forward steps involve formation of the quinoline ring; this may be problematic when R is bulkier than hydrogen, as a mixture of constitutional isomers may be formed (1 or 4 substitution patterns). Synthesis of the final 8-phosphinic acid is then envisaged via the coupling methodology described previously (Ch. 3.4), using the palladium catalysed cross-coupling procedure which proved to be a versatile means of introducing this functionality for the benzimidazoles.

There are several methodologies available for the synthesis of quinoline rings, particularly the Skraup,[12] Doebner-Miller[13] and Combes procedures.[14] The Skraup synthesis involves heating a substituted aniline and glycerol (or a derivative) with sulfuric acid. However, this method tends to give a mixture of regio-isomers. The Doebner-Miller synthesis negates the need to use a glycerol derivative and reaction between an α,β-unsaturated aldehyde and aniline (or a derivative) gives the quinoline ring in moderate yield. One might expect that a mixture of isomers would result upon condensation of crotonaldehyde (151) with aniline (150). However, mechanistic studies

with crotonaldehyde (151) showed that only the 2-isomer predominates.[15] This is consistent with initial conjugate addition of crotonaldehyde (151) and subsequent ring closure to form the quinoline. It has been shown that the Schiff base formed from crotonaldehyde (151) and aniline (150) undergoes cyclisation in acidic solution to produce only the 2-methyl derivative and not the 4-methyl product. On this basis an alternative mechanism has been proposed (scheme 4.1).[15]

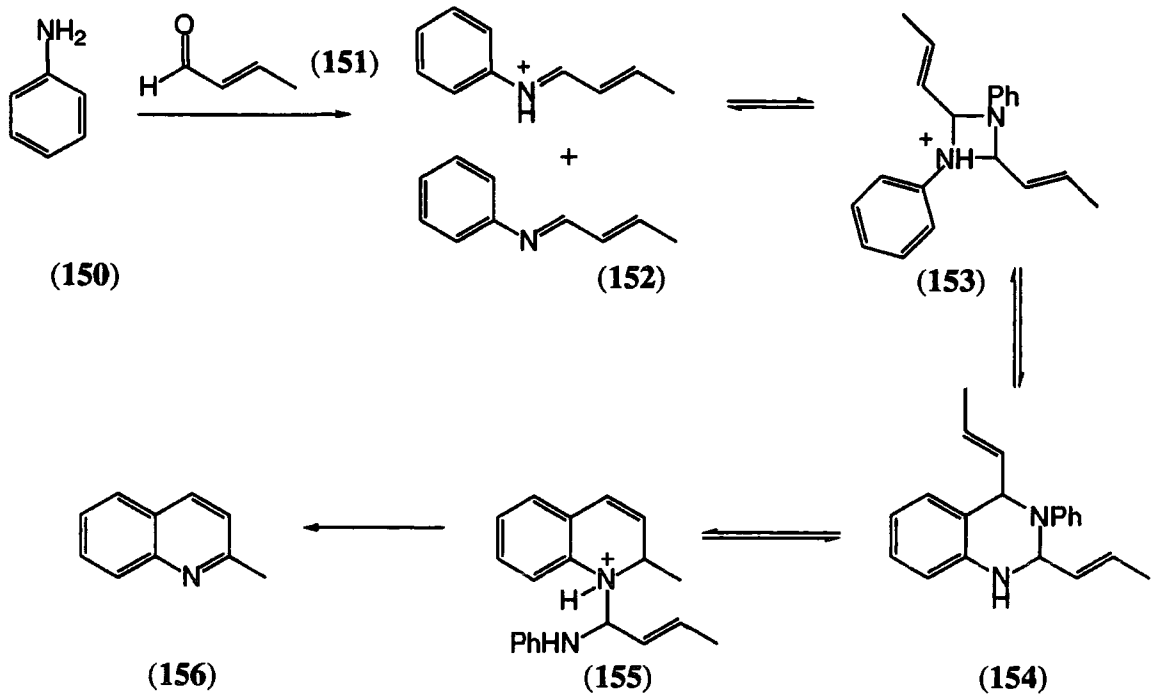

Scheme 4.1 Mechanism of Doebner-Miller quinoline synthesis

A mixture of Schiff bases (152) exists in the reaction mixture, these cyclise to produce the intermediate 1,3-diazetinium ion (153), which then undergoes nucleophilic attack from the proximate phenyl ring to give (154). Rearrangement gives the N-alkyl derivative (155) and oxidative elimination produces the substituted quinoline (156) and Schiff base (152).

Although the Doebner-Miller synthesis gives exclusively the 2-substituted products the reaction mix is often contaminated with varying amounts of unreacted aniline, N-alkylamines and 1,2,3,4-tetrahydroquinaldine. In addition isolation of the desired material can be tedious and often lowers the recovery of the product. An improved method of preparation of quinolines has been reported which involves formation of a zinc complex of the quinoline in the reaction mixture, which selectively precipitates and can easily be isolated.[16]

Using this improved methodology both 8-bromo-2-methylquinoline and 8-bromoquinoline were prepared in high yield. Acrolein (157) or crotonaldehyde (151) were added dropwise to a refluxing solution of 2-bromoaniline (85) in hydrochloric acid (6M), and the reaction followed by tlc. When the reaction was complete a single molar equivalent of zinc(II) chloride was added to the dark solution. Upon standing at room temperature yellow crystals of the 2:1 zinc complex (158) and (159) precipitated from the reaction mixture. 8-Bromo-2-methylquinoline (149) was isolated in 66% yield, following addition of concentrated ammonia and extraction into diethylether. 8-Bromoquinoline (148) was isolated in a similar manner and further purified by short path distillation under reduced pressure to give the pure compound as a pale oil in 56% yield (scheme 4.2).

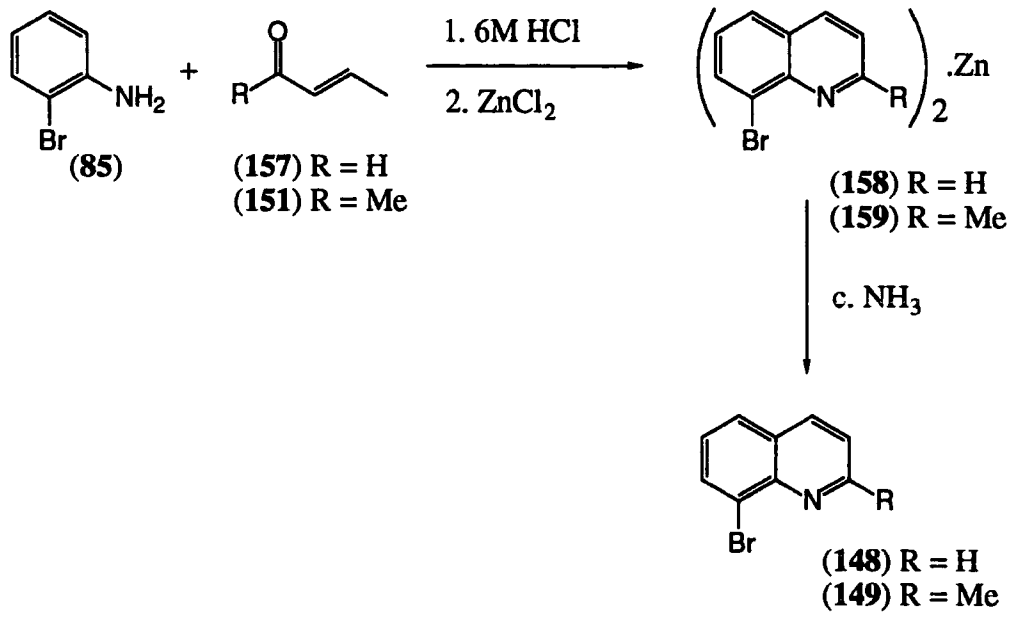

Scheme 4.2 Preparation of 8-bromo-2-substituted quinolines (148) and (149)

Transformation of (148) and (149) to the corresponding ethyl phenylphosphinate derivative was then achieved in an analogous manner to that described in chapter three, by a palladium catalysed coupling with ethylphenylphosphonite (94) in the presence of $Pd(PPh_3)_4$ and triethylamine.[17] Purification of the products by flash chromatography gave the phosphinate esters (160) and (161) in 68 and 54% yields respectively. Subsequent hydrolysis of the esters using hydrochloric acid (6M) proceeded to completion after 20h under reflux. Lyophilisation gave the target ligands (30) and (31) as their hydrochloride salts in near quantitative yield for both compounds (scheme 4.3).

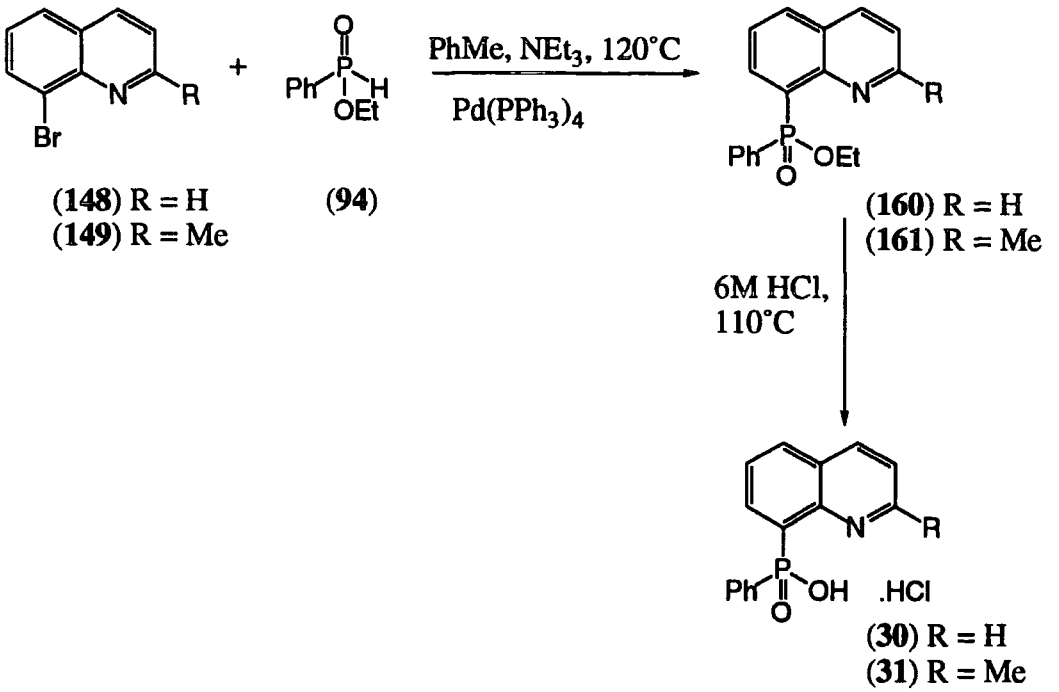

(**148**) R = H
(**149**) R = Me

(**94**)

(**160**) R = H
(**161**) R = Me

(**30**) R = H
(**31**) R = Me

Scheme 4.3 Synthesis of target ligands (30) and (31)

An alternative synthetic strategy which would allow easy modification of the lipophilicity of the compounds, was pursued in parallel to this approach. Such a strategy would become essential if the ligands showed promise as candidates for the hydrometallurgic recovery of zinc. The second approach was designed to allow formation of the C-P bond early in the synthesis, allowing diversity to be maximised.

There are many methods available for forming aryl-phosphorus bonds, most of which require extremes of temperature or pressure. Amongst these Grabiak and co-workers reported a modified Arbrozov reaction between *ortho*-iodotoluene and diethoxy methylphosphine which proceeds at 200°C, catalysed by anhydrous nickel(II)chloride.[18] Grabiak also reported a similar procedure which used irradiation to produce the phosphinate ester from *ortho*-iodobenzylamide.[19] A more amenable method was described by Cadogan via nucleophilic displacement of a nitro group in 1,2-dinitrobenzene.[20]

Reaction of diethoxyphenylphosphine (46) with 1,2-dinitrobenzene (162) at room temperature in acetonitrile gave ethyl (2-nitrophenyl)phenylphosphinate (163) in 74% yield following vacuum distillation of the crude oil. Reduction of this material was carried according to the procedure of Chubb, using iron powder in aqueous ammonium chloride to give ethyl (2-aminophenyl)phenylphosphinate (164) in 83% yield (scheme 4.4).[21]

It was envisaged that reaction of the phosphinate appended aniline derivative (164) with a suitably functionalised α,β-unsaturated aldehyde under modified Doebner-Miller

conditions would give the desired quinoline with concomitant hydrolysis of the phosphinate ester.

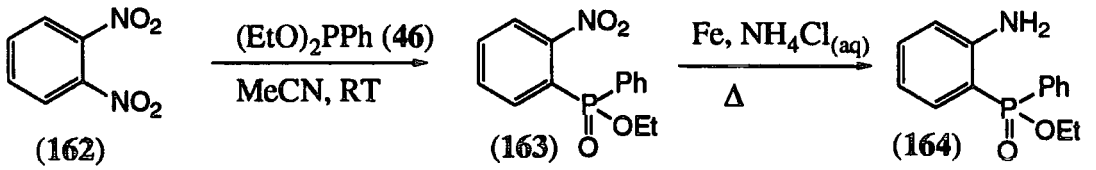

Scheme 4.4 Preparation of 2-(ethyl phenylphosphonate)-aniline (164)

The lipophilic α,β-unsaturated ester (167) was easily prepared by Wittig reaction between carboxyethyl(triphenylphosphine) ylide (165) and undecenal (166). Reduction with two molar equivalents of DIBAL-H in DCM at -78°C gave the corresponding alcohol (168) in 97% yield. Attempts to prepare the aldehyde from this alcohol by the Swern oxidation gave moderate yields (66%).[22] The use of PCC supported on alumina resulted in a drammatic increase in the isolated yield (94%) of the aldehyde (169) (scheme 4.5).[23]

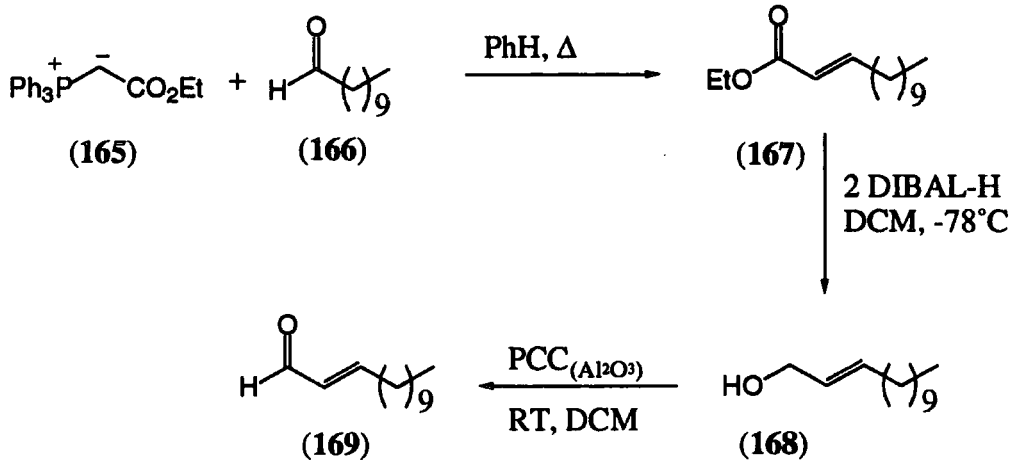

Scheme 4.5 Synthesis of lipophilic α, β-unsaturated aldehyde (169)

Reaction of the α,β-unsaturated aldehyde (169) with a solution of refluxing ethyl (2-aminophenyl)phenylphosphinate (164) in hydrochloric acid (6M) did not give any of the desired product. NMR analysis revealed that hydrolysis of the phosphinate ester had proceeded, but that formation of the quinoline had not occurred. Repeating the reaction with hydrochloric (10M) acid diluted with 1,4-dioxane did not give the target quinoline compound. This implies that phosphinate ester hydrolysis occurs more quickly than the cyclisation step and that the phosphinate itself is unreactive. This alternative strategy is clearly unsuitable, and alternatives will need to be investigated should these ligands prove suitable for zinc extraction.

4.5 Solution Coordination Chemistry

The solution complexation behaviour of 8-(quinolinyl)phenylphosphinic acid (30) and 8-(2-methylquinolinyl)phenylphosphinic acid (31) was assessed using a variety of techniques namely, ^{31}P NMR, fluorescence and UV spectroscopy, ESMS and potentiometry. Ideally all speciation studies would be carried out in 100% methanol to allow fair comparison within the data set. In solution various equilibrium processes can occur which are detailed schematically below (equations 4.1 to 4.4)

$$M + L \overset{K_1}{\rightleftharpoons} ML \qquad \text{eqn. 4.1}$$

$$ML + L \overset{K_2}{\rightleftharpoons} ML_2 \qquad \text{eqn. 4.2}$$

$$ML + H \overset{K_3}{\rightleftharpoons} MLH \qquad \text{eqn. 4.3}$$

$$ML_2 + M \overset{K_1/K_2}{\rightleftharpoons} 2ML \qquad \text{eqn. 4.4}$$

4.5.1 ^{31}P NMR Titrations

NMR titrations were performed as described in the experimental section (Ch. 6.1). Analysis of the form of the obtained curve provides information about how the phosphinic acid interacts with zinc in solution. If the metal competes effectively with the proton to bind to the acid, then a different shift in the spectrum will be seen, as the electron density in the P-O bond changes.

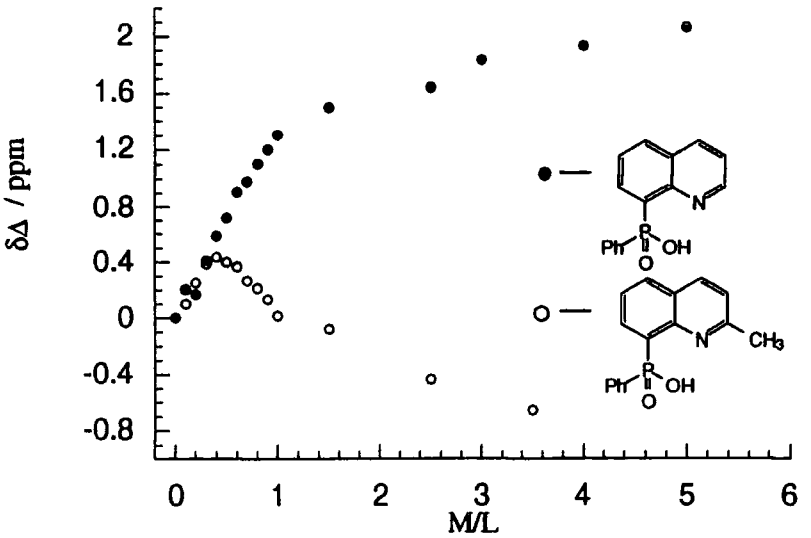

Figure 4.10 ^{31}P NMR titration of 8-(quinolinyl)phenylphosphinic acid (30) and 8-(quinolinyl)phenylphosphinic acid (31) with $ZnTf_2$ (25% CD_3OD, 75% $CDCl_3$, 293K)

Upon addition of zinc to 8-(quinolinyl)phenylphosphinic acid (30) a shift of the ^{31}P signal to lower frequency was observed. There was only a single exchange broadened peak for all examined M/L ratios, indicating that the metal is in fast exchange with the ligand on the NMR timescale. A plot of the change in chemical shift against increasing metal to ligand ratio is shown (figure 4.10). It is evident that in the region 0<M/L<1 there is a linear increase in the curve and at higher ratios (M/L>1) the slope of the curve is more shallow. This implies that the complex is forming a weak ML complex at this concentration. The ML complex formation is governed by K_1 (eqn. 4.1).

$$M + L \underset{}{\overset{K_1}{\rightleftharpoons}} ML \qquad K_1 = \frac{[ML]}{[M][L]} \qquad \text{eqn. 4.1}$$

If K_1 is small then there should be a significant amount of unbound ligand in solution. Therefore as more metal is added the system must respond by driving the equilibrium to the right. For 8-(quinolinyl)phenylphosphinic acid (30) the form of the curve implies a weak ML complex, this accounts for the shallow curve at M/L ratios greater than 1.

Addition of zinc triflate to a solution of 8-(2-methylquinolinyl)phenylphosphinic acid (31) produced a significantly different profile to that of the unsubstituted ligand (30) (figure 4.10). In the region 0<M/L<0.5 the signal shifts to lower frequency, whereas for M/L>0.5 there is a pronounced shift back to higher frequency. In all regions only one exchange broadened signal was observed, indicating that the complex is in fast exchange on the NMR timescale. From the observation of the form of the curve on addition of zinc it appears that for 0<M/L<0.5 there seems to be ML_2 formation, indicated by the turning point at M/L=0.5. At higher M/L ratios formation of a ML complex seems to predominate.

$$M + L \underset{}{\overset{K_1}{\rightleftharpoons}} ML \qquad K_1 = \frac{[ML]}{[M][L]} \qquad \text{eqn. 4.1}$$

$$ML + L \underset{}{\overset{K_2}{\rightleftharpoons}} ML_2 \qquad K_2 = \frac{[ML_2]}{[ML][L]} \qquad \text{eqn. 4.2}$$

$$ML_2 + M \underset{}{\overset{K_1/K_2}{\rightleftharpoons}} 2\,ML \qquad \frac{K_1}{K_2} = \frac{[ML]^2}{[ML_2][M]} \qquad \text{eqn. 4.4}$$

This ligand initially forms an ML_2 complex which is present in solution until M/L=0.5. At M/L ratios higher than this there is a change in the gradient of the curve (figure 4.10), this change is due to the formation of ML complex species from the ML_2 species already in solution. For an ML complex to form from a solution containing ML_2

complexes, K_4 (eqn. 4.4) must be the driving force, that is as more metal is added the ML_2 complex reacts further to produce two ML complexes.

Although no quantitative comparison can be made between the two ligands, a qualitative statement about their respective stability constants can be made from the extent of the shift in observed curves. For 8-(quinolinyl)phenylphosphinic acid (30) the relative value for the ML_2 formation constant is much smaller than the ML_2 formation constant for 8-(2-methylquinolinyl)phenylphosphinic acid (31). For the ML formation constants the opposite is true. For the unsubstituted derivative (30) $K_1 > K_2$, which accounts for the sharp rise in $\Delta\delta$, followed by a much shallower increase. For the 2-methyl derivative $K_2 > K_1$ therefore as [M] increases then $[ML_2]$ must decrease in order to keep $K_1.K_2$ constant. However, the formation of a ML complex from a ML_2 complex is driven by a relatively large K_1/K_2 value (eqn. 4.4) which drives the equilibrium to the right.

From the NMR titration evidence it would appear that the 2-methyl substituted ligand (31) is forming a weak ML_2 complex, which readily reacts further to form two ML complexes upon addition of more metal, whereas the unsubstituted ligand (30) forms a stronger ML complex. Phosphorus NMR gives information regarding the coordination behaviour of the phosphinic acid moiety in solution, but does not provide any information regarding the participation of the nitrogen donor.

4.5.2 Fluorescence Spectrofluorimetry

To examine the degree to which the heterocyclic ring participates in zinc binding, it is necessary to probe the aromatic system directly. Fluorescence spectroscopy affords a tool to probe the aromatic system, which provides the major chromophore in the system. As the fluorescence emission spectra is also sensitive to variation in pH, the protonation constants can also be determined using this method. This method is complimentary to potentiometry (section 4.5.5) which will be described later.

pH fluorescence titration

Variations in fluorescence intensity were monitored as a function of pH for 8-(quinolinyl)phenylphosphinic acid (30) and 8-(2-methylquinolinyl)phenylphosphinic acid (31) starting at low pH by addition of trifluoroacetic acid and moving to high pH by incremental addition of sodium hydroxide solution. The variation in intensity was then monitored as a function of pH between 1 and 10.

8-(Quinolinyl)phenylphosphinic acid (30)

For ligand (30) a selection of the fluorescent emission spectra (λ_{ex}=290nm, λ_{max}=300-550nm, slits 8nm and a scan speed of 120nmmin^{-1}) at various pH values is shown below (figure 4.11).

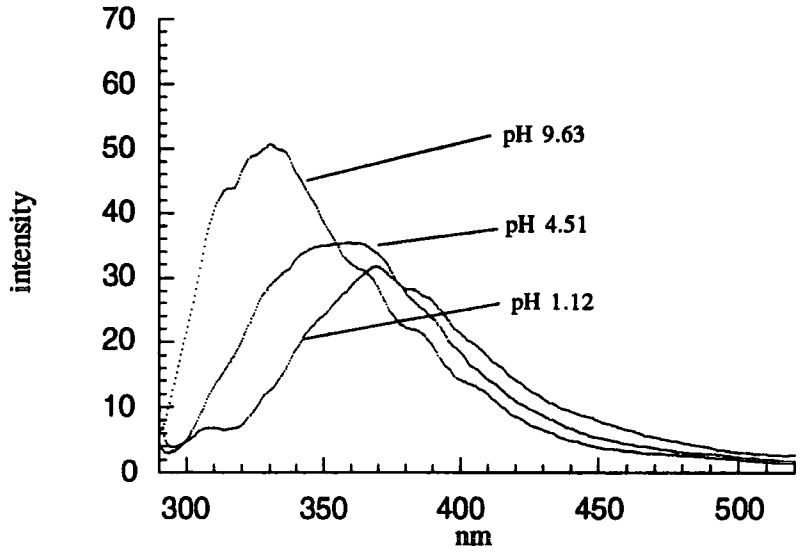

Figure 4.11 Variation in fluorescence emission at various pH values for (30) (λ_{ex}=290nm, λ_{max}=300-550nm, 90% H_2O, 10% MeOH, 293K)

It is evident that there is a marked change in the fluorescence emission spectra at both low and high pH. Comparing the emission at pH 1.12 with that at 9.63, shows a large increase in the fluorescence intensity and a shift in the emission wavelength of 40nm towards the blue region of the spectrum. A plot of the change in emission intensity at 328nm is shown below (figure 4.12).

The fluorescence of quinoline (λ_{max}=360nm) is extremely weak unless the solvent is capable of forming hydrogen bonds. In non-polar solvents fluorescence intensity is negligible, because the n-π^* transition is weak due to the quenching of the excited state by the nitrogen lone pair. The quinolinium cation shows a shift in the emission spectra to longer wavelength of about 40nm.[24] This is due to a combination of internal charge transfer (ICT) and the perturbation of the frontier orbitals on protonation. In the excited state the dipole moment of the molecule is likely to be more pronounced than in the ground state. This dipole causes the solvent shell to reorganise around the molecule and because emission occurs over a longer timescale the excited state relaxes to a modified ground state.[25] The existence of an ICT excited state has been demonstrated in analogous systems, where in solvents of increasing polarity (CH_2Cl_2, Et_2O, MeCN,

MeOH and H_20) a bathochromic shift was observed in λ_{max}.[26] Protonating the quinoline nitrogen causes both the HOMO and the LUMO to be lowered in energy relative to the unprotonated species.* This change in the relative energies of the frontier orbitals results in a shift in the wavelength and intensity of emission.

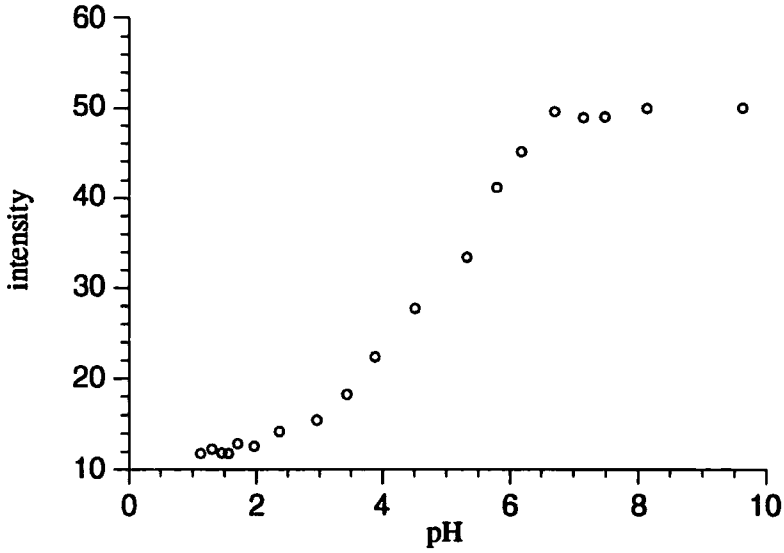

Figure 4.12 Variation in fluorescence intensity at 328nm for (30) (λ_{ex}=290nm, λ_{max}=300-550nm, 90% H_2O, 10% MeOH, 293K)

From observation of the change in intensity at 328nm, it seems that a number of processes are occurring in solution. Between pH 1 and 4 there is a an increase in intensity which rises again from pH 4 reaching a maximum at about pH 6. A summary of the possible species present in solution is shown below (figure 4.13). At low pH values below 3 the singly charged cation is exclusively present in solution (170). As the pH rises and the phosphinic acid is deprotonated, there exists the possibility for extended conjugation into the phosphinate system, accounting for the slight rise in emission intensity. At pH 4 the species present predominantly in solution is the zwitterionic form (171), which is in equilibrium with the charge neutral species (173). The zwitterionic species still resembles the quinolinium cation, and as such fluorescent emission is similar to that that observed for the protonated species (170). As the pH rises above 4 the anionic species (172) begins to be present in solution; this resembles free quinoline. A number of processes are working in conjuction to produce the observed increase and shift in emission intensity. Both the effect of protonation and internal charge transfer cause this change in the emission, as described above.

* The HOMO and LUMO energies were calculated on the Cache program using MOPAC with the AM1 force field. The HOMO and LUMO energies of quinoline were calculated to be -9.24 and -0.65 eV respectively.The quinolinium cation HOMO and LUMO energies were determined to be -13.76 and -5.93 eV respectively.

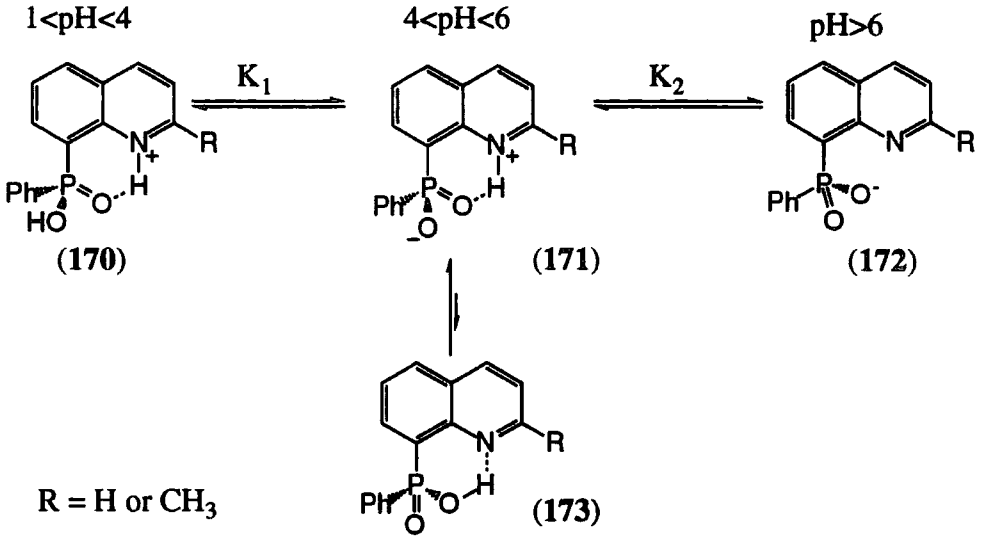

Figure 4.13 Species present in solution at different pH values for (30) and (31)

From the pH dependent changes at 328nm the pK_a values for the phosphinic acid and the quinoline can be estimated. The first rise in intensity is due to the deprotonation of the phosphinic acid and is about pH 2.4 (pK_1 figure 4.12). The second rise is due to deprotonation at nitrogen, which can be estimated to occur about pH 4.8 (pK_2 figure 4.12). Of course these values relate to the pKa of the singlet excited state. These values are likely to be close to the value of the ground state which are about 2.8 for aromatic-phenylphosphinic acids and approximately 4.8 for quinoline.[3]

8-(2-Methylquinolinyl)phenylphosphinic acid (31)

A selection of fluorescence emission spectra (λ_{ex}=290nm, λ_{max}=300-550nm, slits 8nm and a scan speed of 120nmmin^{-1}) at different pH values is shown below (figure 4.14).

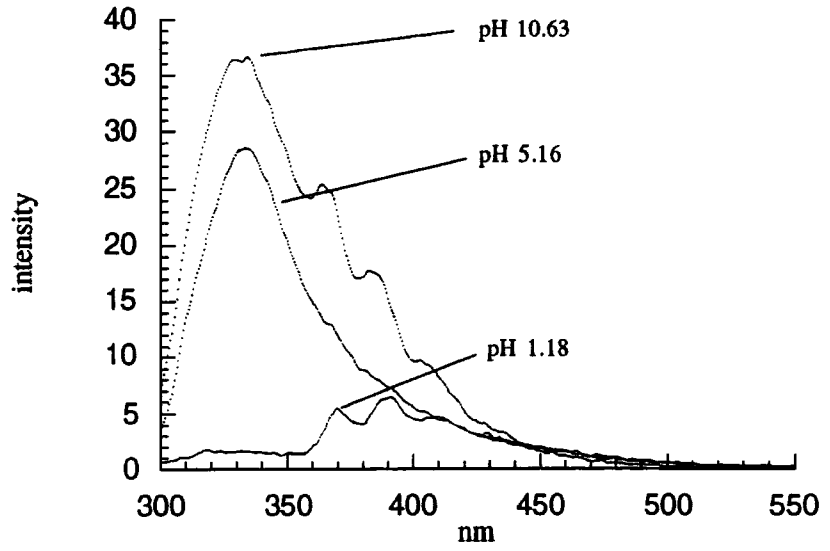

Figure 4.14 Variation in emission spectra for (31) at different pH (λ_{ex}=290nm, λ_{max}=300-550nm, 90% H_2O, 10% MeOH, 293K)

As in the previous example (*vide supra*) there is a striking difference in the emission spectra at low and high pH. Not only is there a change in emission intensity but a large shift to shorter wavelength (58nm) upon basification of the solution. Plotting the change in intensity at 378nm against pH gives information regarding the pK_a as in the above example (figure 4.15).

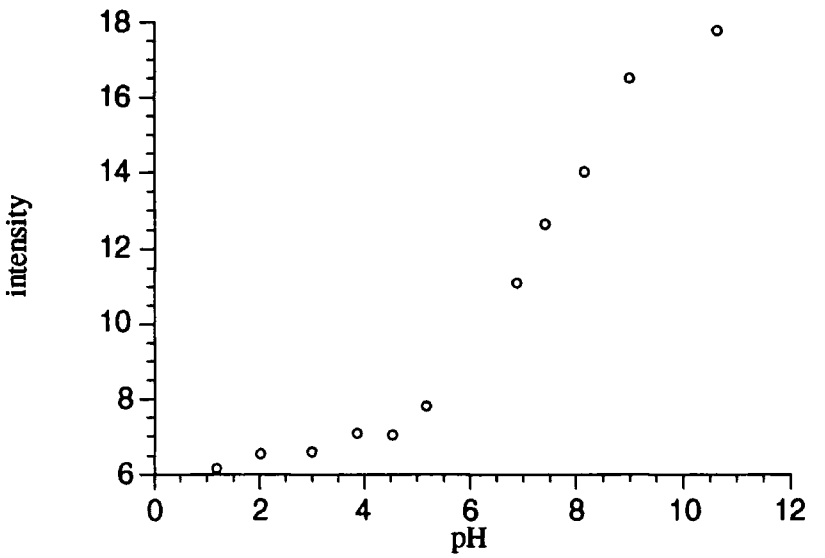

Figure 4.15 Change in emission intensity at 378nm vs. pH for (31) (λ_{ex}=290nm, λ_{max}=300-550nm, 90% H_2O, 10% MeOH, 293K)

There is a gradual rise in intensity between pH 1 and 4 with a much larger rise between pH 5 and 9. Again, this change can be related to the pH dependent speciation (figure 4.13). The small rise in intensity between pH 0 and 4 is due to the deprotonation of the phosphinic acid, which may allow further conjugation of the quinoline ring into the phosphinate system and give rise to an increase in the intensity of fluorescent emission. The more rapid rise between pH 5 and 9 is due to the disappearance of the zwitterionic form (figure 4.13, 171) which is effectively the quinolinium cation and subsequent formation of the free quinoline nitrogen. The pK_a of the quinoline nitrogen is about 7.5 (pK_2 figure 4.15). The increase in pK_a for the quinoline nitrogen is due to the proximate methyl group, which has a small positive inductive effect. This has been observed in analogous systems, e. g. for 8-hydroxy quinoline (139) and 2-methyl-8-hydroxyquinoline (140) the pK_as are 4.99 and 5.63 respectively.[3]

Zinc fluorescence titrations

As mentioned above fluorescence spectroscopy can be used to probe the interaction between the quinoline nitrogen and zinc ions in solution. This method is complementary to the ^{31}P NMR titrations, and a clearer picture regarding the participation of both donor groups should result.

For 8-(quinolinyl)phenylphosphinic acid (30) the fluorescent emission spectra (λ_{ex}=280nm, λ_{em}=290-550nm, slits=8nm and scan speed of 120nmmin^{-1}) with addition of zinc perchlorate is shown below (figure 4.16).

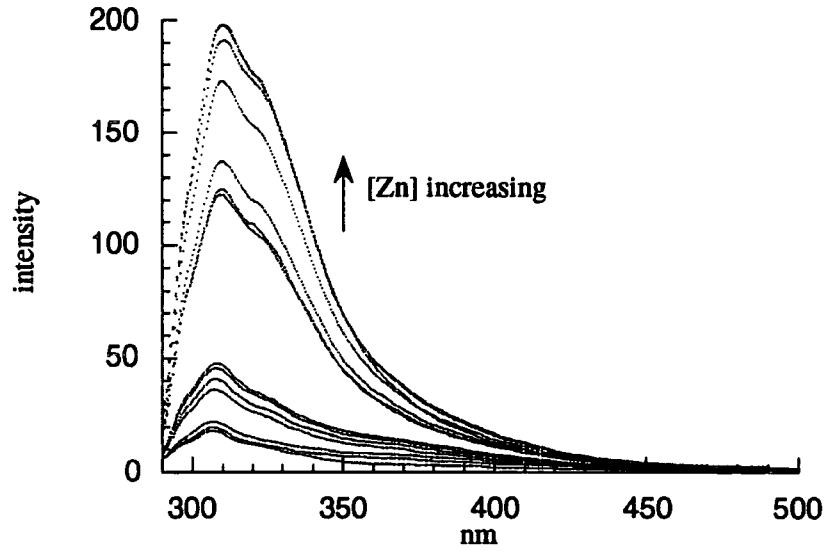

Figure 4.16 Variation in fluorescence with incremental addition of $Zn(ClO_4)_2$ to (30) (λ_{ex}=290nm, λ_{max}=300-550nm, 10% H_2O, 90% MeOH, 293K)

The intensity of emission at 310nm increases with addition of zinc, without any significant shift in the absorbance maximum. The experiment was carried out at pH 5.4, where the ligand exists mainly in the anionic form (figure 4.13, 171). With addition of zinc, the solvent shell is displaced and a dative bond is formed to the nitrogen atom. Although this should have little effect on the electron density in the Zn-N bond compared to the N-H hydrogen bond, there is a marked difference in fluorescence intensity. In 1988 Czarnik and co-workers reported chelation-enhanced fluorescence (CHEF) with 9, 10-bis(2, 5-dimethyl-2, 5-diazahexyl)anthracene, where coordination of zinc resulted in a 14 fold increase in fluorescence intensity.[25, 27] The origins of the CHEF effect lies in the restricted internal vibration and rotation modes imposed on the bidentate ligand upon chelation. This restricted internal motion allows prolonged, extended conjugation of the system and hence gives rise to an increase in the observed fluorescence intensity. In this case there is an eleven fold increase in fluorescence

intensity when M/L=3, relative to free ligand. Coordination of zinc to the nitrogen will also modify the relative energies of the frontier orbitals, in a similar manner to that of the proton. As zinc is a divalent cation the extent to which the HOMO and LUMO will be lowered in energy will be more pronounced compared to the effect for protonation. This change may account for the larger increase in fluorescence intensity observed in the zinc isotherm relative to the pH titration.

Plotting the change in intensity against metal to ligand ratio at 310nm gives an indication of the stoichiometry of the complex (figure 4.17).

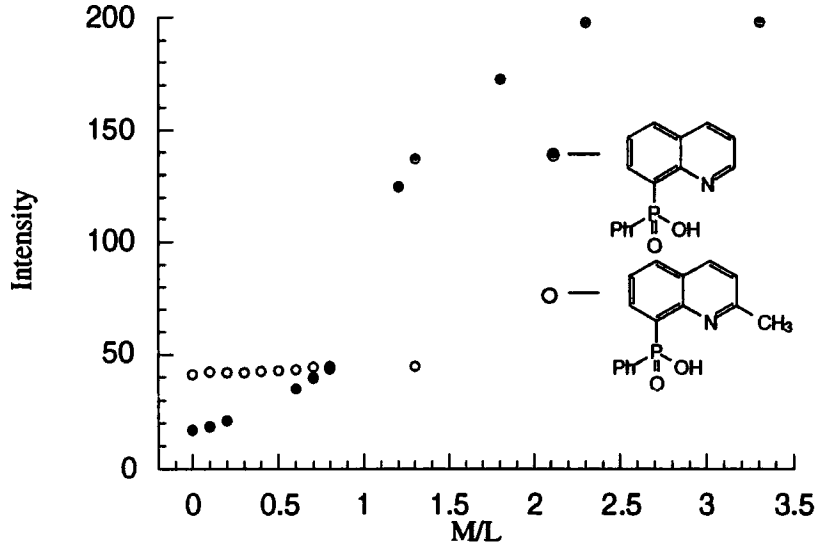

Figure 4.17 Variation in fluorescent intensity at 310nm for (30) and (31) with $Zn(ClO_4)_2$ (λ_{ex}=290nm, λ_{max}=300-550nm, 10% H_2O, 90% MeOH, 293K)

A steady rise in the fluorescence intensity is observed with a sharp increase in the intensity at 1:1 stoichiometry. At M/L>1 the intensity continues to rise. The form of the change in intensity and the fact that there is a sharp increase at M/L = 1 is consistent with formation of 1:1 complex in solution, with participation of the quinoline nitrogen.

The titration of 8-(2-methylquinolinyl)phenylphosphinic acid (31) with zinc was carried out in exactly the same manner as with 8-(quinolinyl)phenylphosphinic acid (30). In this case the intensity does not change upon addition of zinc perchlorate even at high M/L ratios. This implies that the quinoline nitrogen is not coordinating to zinc at this concentration. Performing the same experiment in aqueous media also gave the same result. A plot of the change in intensity for (31) with incremental addition of zinc is contrasted with the unsubstituted ligand on the same scale for comparison (figure 4.17).

From the fluorescence and NMR data, it would appear that the unsubstituted ligand (30) is binding to zinc in a 1:1 stoichiometry with participation of the quinoline nitrogen (174), whereas the 2-methyl derivative (31) appears to form 2:1 complexes without participation of the quinoline nitrogen. An alternative coordination mode must be operating. The 2-methyl substituent is sterically inhibiting chelate ring formation between the phosphinate and the proximate quinoline nitrogen. Presumably the ligand must be binding through both the phosphinic acid groups only (figure 4.18).

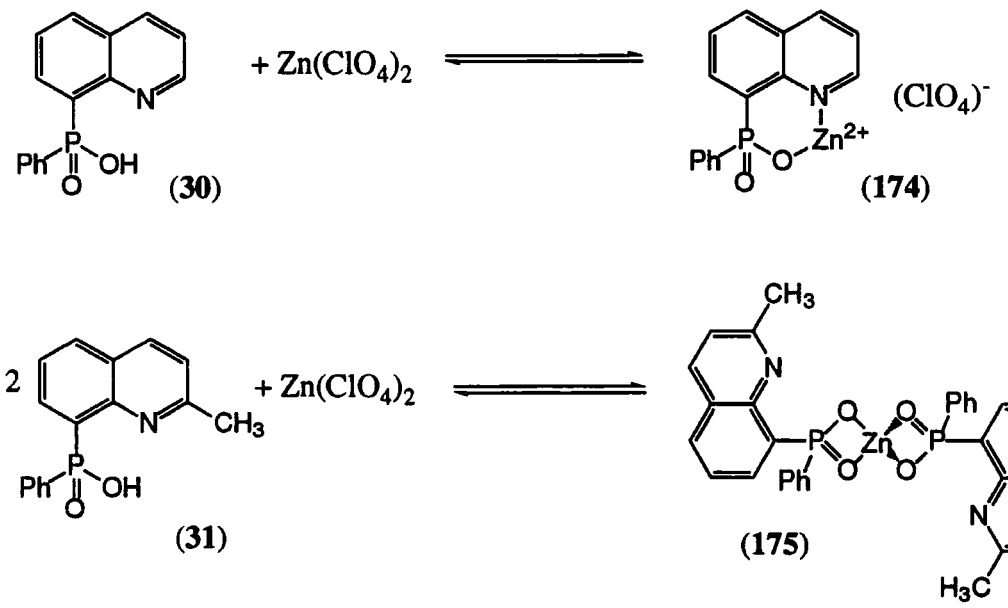

Figure 4.18 Possible coordination modes for (30) and (31) with zinc

The proposed coordination mode is a 2:1 complex with binding to zinc solely through the phosphinate donors (175). Phosphinates are known to bind to zinc in this manner, and D2EHPA, HEH[EHP] and HDOP have been shown to coordinate in this mode (Ch. 1.2.3).[28, 29] Carboxylates also bind to zinc in a bidentate manner with the solid state structure of zinc(II) acetate revealing bridged acetates with tetrahedra of zinc ions.[30] Examples of other such binding modes with phosphinic acid derivatives have been reviewed in detail elsewhere.[31]

4.5.3 UV Spectroscopy

Investigation of the ligands and the metal complexes by UV spectroscopy provides a tool to probe the aromatic system in the ground state. If the quinolinyl nitrogen is bound to the metal then there may be a change in the absorption spectrum relative to the uncomplexed ligand. Fluorescence and UV spectroscopy were carried out at the same concentrations for purposes of comparison.

8-(Quinolinyl)phenylphosphinic acid (30)

In polar solvents free quinoline has three absorption bands, 228nm (E_1 band), 265nm (E_2 band) and 313nm (B band) which are attributable to π–π^*, π–π^* and n-π^* respectively.[32] Comparison of the ligand (30) to quinoline shows hypsochromic shifts of approximately 30nm for the E bands, whereas the B band is relatively unaffected.

With addition of one equivalent of copper and zinc, there is a slight change in the absorption spectra. The two π–π^* transitions experience a slight hyperchromic shift, whereas the B band is blue shifted by about 10nm, indicating that coordination to the quinoline nitrogen is affecting the n-π^* transition.

With the addition of nickel and cobalt there is an observed hyperchromic shift for both the π–π^* bands. But the n-π^* transition is unaffected relative to the free ligand.

With the addition of one equivalent of iron(III) perchlorate a substantially different spectrum was obtained. A large hyperchromic shift was observed for the E_1 band, with concomitant disappearance of the E_2 band. The transition responsible for the n-π^* absorption again experiences a large hyperchromic shift. A comparison of the UV absorption spectra of the ligand (0.1mM) and the iron complex (0.02mM) is shown below (figure 4.19).

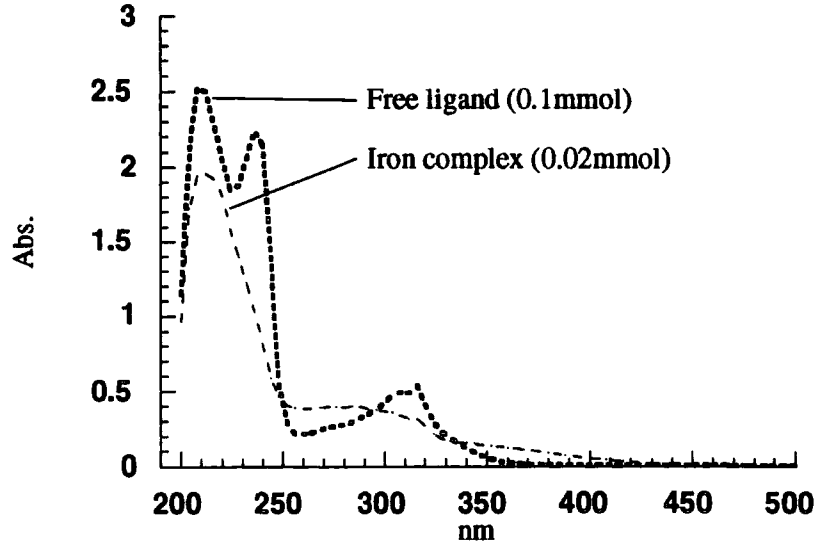

Figure 4.19 Comparison of free ligand (30) and iron complex (MeOH, 298K)

The results for the UV absorption maxima for the free ligand (30) and the complexes with zinc, copper, nickel, cobalt and iron (III) are summarised below, giving the absorption maxima and molar extinction coefficients (table 4.1).

Ligand		Zinc		Copper	
λ_{max}/nm	ε/dm^{3}M^{-1}	λ_{max}/nm	ε/dm^{3}M^{-1}	λ_{max}/nm	ε/dm^{3}M^{-1}
208	25300	211	26900	211	29000
235	22300	232	22600	232	25050
305	4780	291	4410	296	7180
315	5200	305	4900	305 (s)	7300

Nickel		Cobalt		Iron	
λ_{max}/nm	ε/dm^{3}M^{-1}	λ_{max}/nm	ε/dm^{3}M^{-1}	λ_{max}/nm	ε/dm^{3}M^{-1}
211	28400	211	27700	211	97500
235	25200	235	24900	275 (s)	20500
306	5420	305	5420	308	18000
317 (s)	5100	315 (s)	5400	319	7445

Table 4.1 UV absorption maxima for (30) as the free ligand and in the presence of metal salts (MeOH, 298K)

8-(2-Methylquinolinyl)phenylphosphinic acid (31)

As mentioned above, in solution free quinoline has three absorption bands, 228nm (E_1 band), 265nm (E_2 band) and 313nm (B band) which are attributable to π–π^*, π–π^* and n-π^* respectively. Comparison of the ligand (31) to quinoline shows hypsochromic shifted E bands by approximately 25nm in both cases, while the B band is relatively unaffected.

With the addition of zinc, copper, nickel and cobalt to 8-(2-methylquinolinyl) phenylphosphinic acid (31) there is no change (within experimental limits) in any of the absorption bands in the complexes compared to the free ligand. This suggests that the quinoline nitrogen is not binding under these conditions.

With iron a spectrum similar to that obtained for (30) was observed. A large hyperchromic shift was observed for the E_1 band, with concomitant disappearance of the E_2 band. The transition responsible for the n-π^* absorption again experiences a large hyperchromic shift. In this case the quinoline nitrogen must be bound.

The results for the UV absorption maxima for the free ligand (31) and the complexes with zinc, copper, nickel, cobalt and iron (III) are summarised below, giving the absorption maxima and molar extinction coefficients (table 4.2).

Ligand		Zinc		Copper	
λ_{max}/cm^{-1}	ε/dm^3M^{-1}	λ_{max}/cm^{-1}	ε/dm^3M^{-1}	λ_{max}/cm^{-1}	ε/dm^3M^{-1}
215	29900	213	29500	212	31200
239	30520	239	29300	239	31500
311 (s)	9600	311 (s)	8600	308 (s)	8500
317	10790	319	9700	319	9600

Nickel		Cobalt		Iron	
λ_{max}/cm^{-1}	ε/dm^3M^{-1}	λ_{max}/cm^{-1}	ε/dm^3M^{-1}	λ_{max}/cm^{-1}	ε/dm^3M^{-1}
212	27700	212	27600	218	47500
239	26400	237	26900	275 (s)	9300
310 (s)	7100	311 (s)	7500	308	8500
317	8290	319	8100	319	8750

Table 4.2 UV absorption maxima for (31) as the free ligand and in the presence of metal salts (MeOH, 298K)

4.5.4 Electrospray Mass Spectrometry

ESMS analysis of the complexation behaviour of 8-(2-methylquinolinyl) phenylphosphinic acid (31) and 8-(quinolinyl)phenylphosphinic acid (30) with zinc, copper, nickel and ferric ions was carried out using their perchlorate salts. A stock solution of the ligand in methanol was prepared with a concentration of 1mM and metal solutions of 1mM. Complex solutions were prepared as one to one mixtures and diluted to make a final concentration of 0.01mmol, and their ESMS spectra recorded in both positive and negative ionisation modes. The $ESMS^+$ spectra produced the best results, with protonated complexes being observed.

8-(Quinolinyl)phenylphosphinic acid (30)

Zinc

For zinc the major species observed was the protonated ligand, at 100% intensity. Signals corresponding to the protonated ML_2 complex were observed, but at very low relative intensity (5%). The $[L_2H]^+$ complex was also observed, again at very low relative intensity (4.6%).

Nickel and Copper

With nickel and copper a slightly different species distribution was observed. In both cases the most abundant peak corresponded to the protonated ligand. However, for both nickel and copper, species corresponding to $[LM]^+$ were seen, with relative intensities of 6.6 and 6% respectively. The $[ML_2H]^+$ complex for both metals was much more abundant than for the zinc system, with relative intensities of 13.3 and 14% for nickel and copper respectively. An excellent correlation between the observed isotope pattern for $[NiL_2H]^+$ and the calculated theoretical isotope distribution is shown below (fig. 4.20)

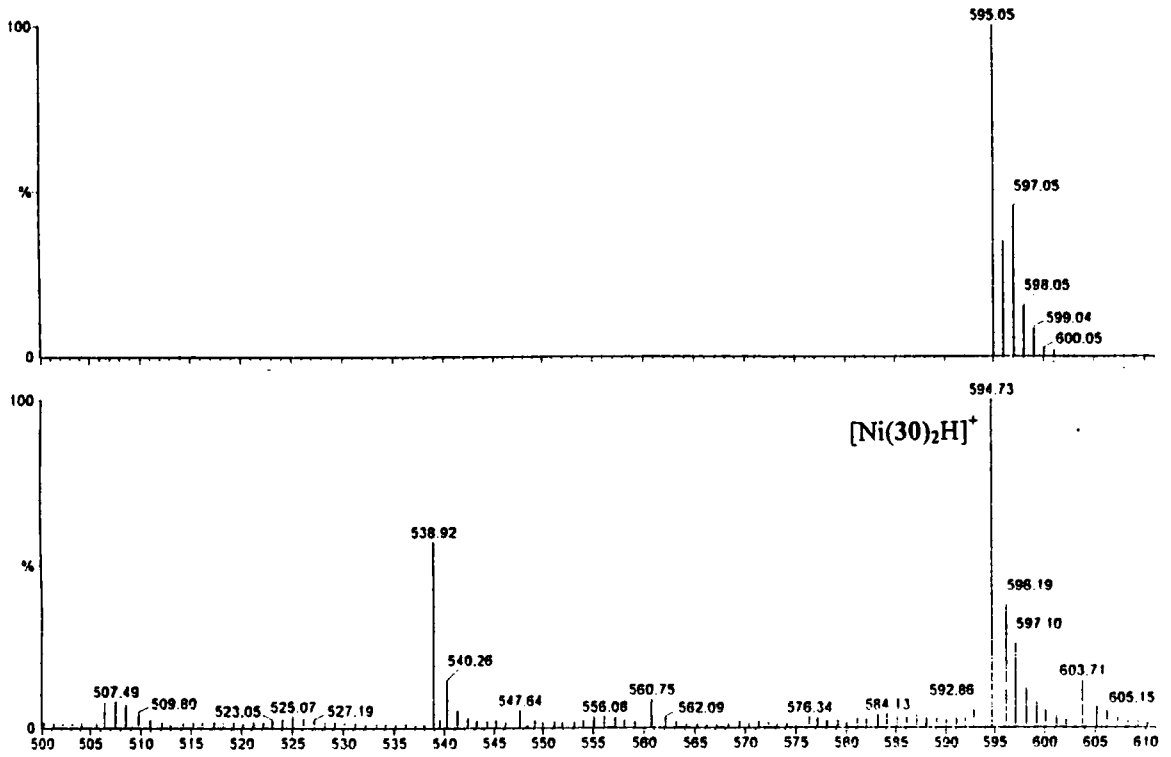

Figure 4.20 Oberserved spectrum for $[Ni(30)_2H]^+$ (below) and isotope pattern (above)

Iron

For iron the protonated ligand was still the most abundant species present. Signals corresponding to $[LFeCl]^+$, $[L_2Fe]^+$ and $[L_3FeH]^+$ were also detected. with relative abundance of 7.3, 2.6 and 0.5% respectively

A summary of the species, the observed and calculated masses and relative intensities is shown below (table 4.3).

Metal	Species	Obs. Mass	Calc. Mass	Rel. Intensity
Zn	$[LH]^+$	269.95	270.07	100%
	$[L_2H]^+$	538.87	539.12	4.8%
	$[L_2ZnH]^+$	600.81	601.04	5%
Cu	$[LH]^+$	269.97	270.07	100%
	$[LCu]^+$	330.94	331.09	6%
	$[L_2H]^+$	538.90	539.12	2.6%
	$[L_2CuH]^+$	599.74	600.04	14%
Ni	$[LH]^+$	269.99	270.07	100%
	$[LNi]^+$	325.92	326.24	6.66%
	$[L_2H]^+$	538.92	539.12	7%
	$[L_2NiH]^+$	594.73	595.05	13.3%
Fe	$[LH]^+$	269.99	270.07	100%
	$[LFeCl]^+$	354.97	355.31	7.3%
	$[L_2Fe]^+$	592.22	593.05	2.7%
	$[L_3FeH]^+$	862.41	862.11	0.5%

$ESMS^+$ cone voltage 30V, source temperature 60°C

Table 4.3 Summary of species observed in ESMS for (xx30

By comparing the relative abundances of the $[ML_2H]^+$ complexes observed in the spectra the following order of abundance is observed:

$$Cu \approx Ni > Zn > Fe$$

Desolvation of the complexes has been shown to be an important factor when considering relative ESMS intensities.[33] Correlation of the desolvation energies for the

various complex species in solution is not a realistic possibility, therefore quantitative analysis between the observed relative intensities is not possible.

8-(2-Methylquinolinyl)phenylphosphinic acid (31)

Zinc, copper and nickel

Similar spectra were observed with all three divalent metal ions in the ESMS experiment. The most abundant signal in all cases was the protonated ligand, $[L_2MH]^+$ were also detected, with relative abundance of 6, 9.3 and 31.3% respectively for zinc, copper and nickel. An excellent correlation between the observed isotope pattern for $[CuL_2H]^+$ and the calculated theoretical isotope distribution is shown below (fig. 4.21)

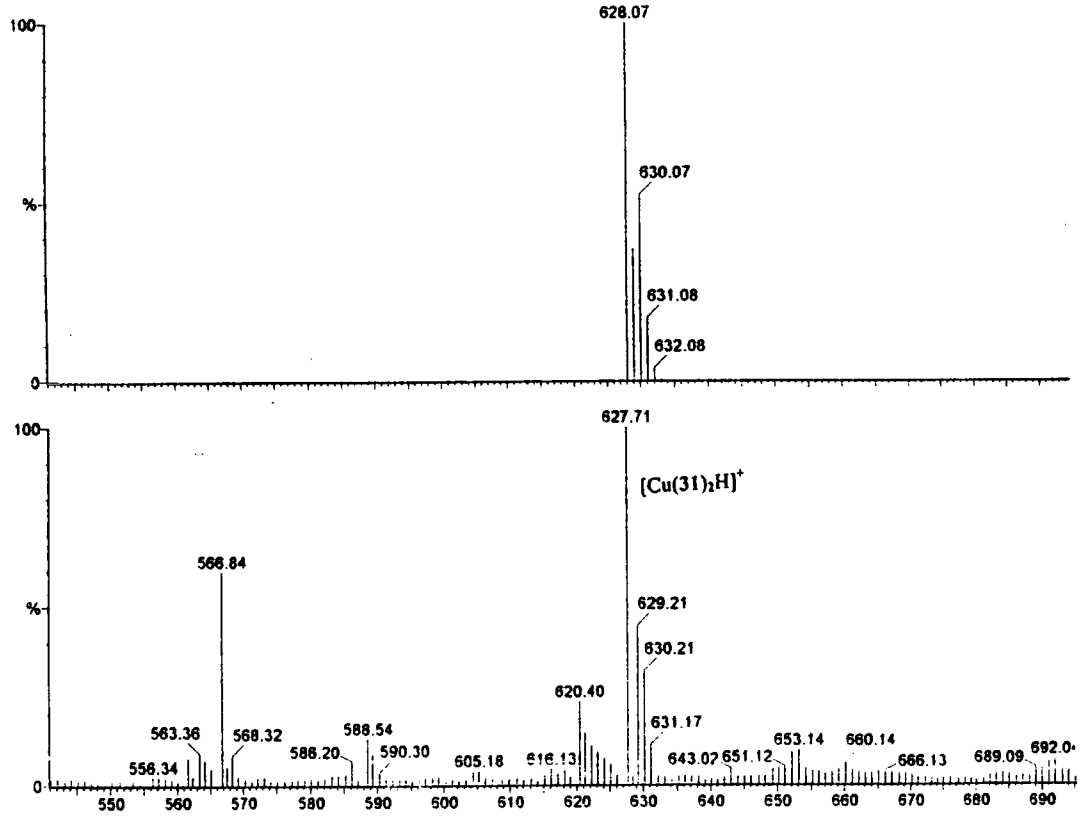

Figure 4.21 Oberserved spectrum for $[Cu(31)_2H]^+$ (below) and isotope pattern (above)

Iron

For iron the sole species detected in the ESMS spectra of the 1:1 mixture of ligand and ferric perchlorate was the protonated ligand. No signals corresponding to complexed ligand were seen.

A summary of the species, the observed and calculated masses and relative intensities is shown below (table 4.4).

Metal	Species	Obs. Mass	Calc. Mass	Rel. Intensity
Zn	$[LH]^+$	284.00	284.08	100%
	$[L_2H]^+$	566.84	567.96	2.8%
	$[L_2ZnH]^+$	628.52	629.07	6%
Cu	$[LH]^+$	283.98	284.08	100%
	$[L_2H]^+$	566.84	567.96	6%
	$[L_2CuH]^+$	627.71	628.07	9.33%
Ni	$[LH]^+$	283.99	284.08	100%
	$[L_2H]^+$	538.92	567.96	4.66%
	$[L_2NiH]^+$	622.72	623.08	31.3%
Fe	$[LH]^+$ No complex species observed	283.99	284.08	100%

$ESMS^+$ cone voltage 30V, source temperature 60°C

Table 4.4 Summary of species observed in ESMS for (31)

For 8-(2-methylquinolinyl)phenylphosphinic acid (31) the only complex species observed were with the divalent metal ions, nickel, copper and zinc. Comparison of the relative intensities for the 2:1 complex gives the following order of abudance:

$$Ni > Cu > Zn$$

This is the same relative order as for the previous ligand (*vide supra*).

4.5.5 Potentiometry

The protonation constants and metal ligand stability constants for nickel, copper and zinc were determined using pH-metric titrations were performed at the University of Newcastle for 8-(2-methylquinolinyl)phenylphosphinic acid (31), followed by an iterative least-squares analysis carried out by Dr. Ritu Kataky at the University of Durham.

Protonation constants

All titrations were carried out in a water thermostatically temperature controlled cell (c. 5cm^3 capacity) and the contents mixed with a magnetic stirrer. The experiments were performed at 25°C at a constant ionic strength (I = 0.1 Me_4NNO_3) using tetramethylammonium hydroxide as the base (0.05 mol dm^{-3}). The latter solution was calibrated by titration against a standard solution of hydrochloric acid (0.02 mol dm^{-3}). Incremental additions to the cell were controlled by a PC program ('Molspin'), which allowed the volume to be added and the time between additions to be adjusted. The results are tabulated and presented together with pK_a values for similar ligands systems (table 4.5).

Ligand		pK_1	pK_2
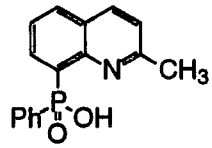	**(31)**[a]	2.94	7.49
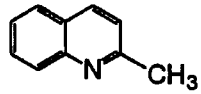	**(176)**[b]	5.61	
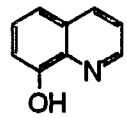	**(139)**[b]	4.99	9.66
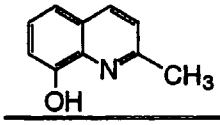	**(140)**[b]	5.63	10.04

a. This work b. reference 3.

Table 4.5 Protonation constants for substituted quinolines (I = 0.1, H_2O, 298K)

The values obtained by potentiometry are in close agreement with those obtained by fluorescence spectroscopy (section 4.5.1). The protonation constants, pK_1 and pK_2, refer to stepwise protonation of the ligand to form LH (171) and LH_2^+ (170) (figure 4.22)

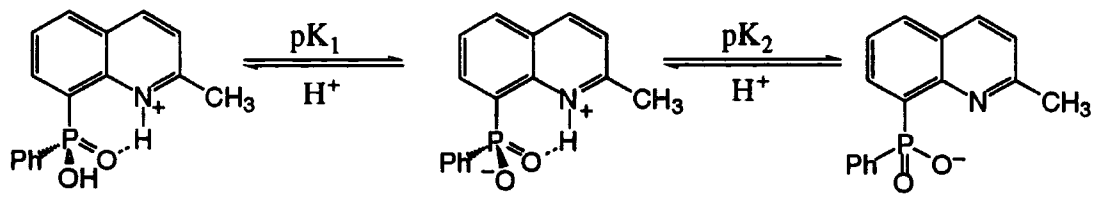

LH_2^+, (**170**) LH, (**171**) L^-, (**172**)

Figure 4.22 Protonation constants for ligand (31)

The speciation diagram shows the percentage distribution of ligand species (LH_2^+, LH and L^-) in solution as a function of pH (figure 4.23). At pH values less than 2 the sole species in solution is LH_2^+ (170), whereas at pH 7.4 there is a 50% mixture of LH (171) and L^- (172).

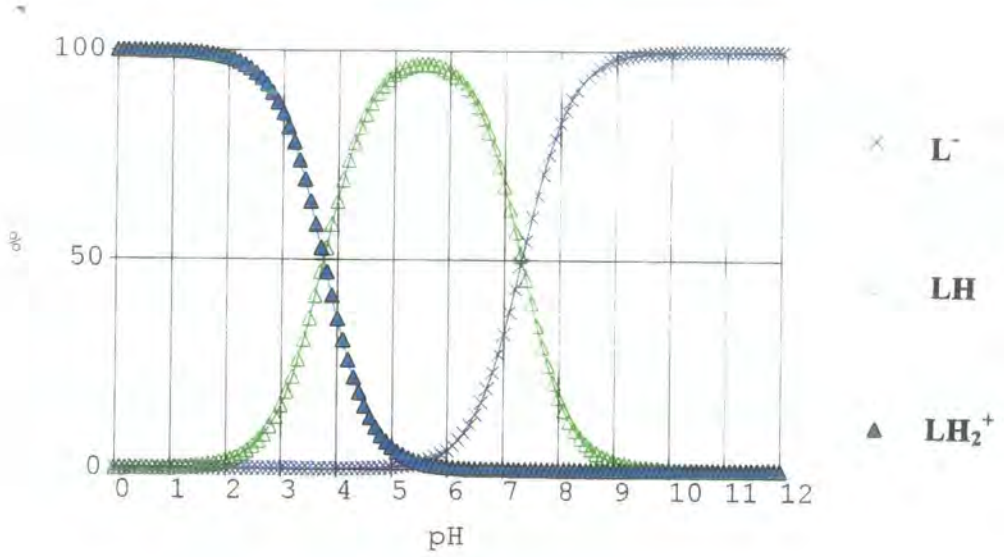

Figure 4.23 Speciation diagram of ligand (31) as a function of pH (I = 0.1, H_2O, 298K)

Comparison of similar ligands

Comparing the nitrogen protonation values for 2-methylquinoline (176), 8-hydroxyquinoline (139) and 2-methyl-8-hydroxyquinoline (140) reveals a difference in value attributable to positive induction effect of the methyl group. The higher value for the nitrogen protonation constant for ligand (31) is due to the proximate phosphinic acid functionality. Deprotonation of the intermediate zwitterionic form (171) not only involves breaking the N-H bond but also the hydrogen bond to the phosphinate oxygen, but also disrupting the strong electrostatic attraction between the nitrogen atom and phosphinate oxygen.

Metal-ligand stability constants

Metal nitrate solutions of nickel, copper and zinc were prepared in purite water. The exact metal concentration was determined by atomic absorption spectroscopy prior to use. The titrations were carried out at the University of Newcastle and analysed by an iterative least-squares procedure, performed by Dr. Ritu Kataky of the University of Durham. The logβ values for successive formation of ML and ML_2 complexes was

determined using the protonation constants obtained above with the 'Superquad' program (table 4.6).

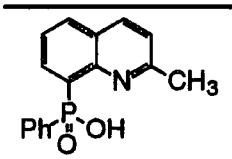 (31)	$Log\beta_{ML_2}$
Nickel	10.3
Copper	8.2
Zinc	Not observed

Table 4.6 Stabilty constants for nickel and copper with (31) (I = 0.1, H_2O, 298K)

The data obtained from the zinc titration could not be fitted to either 1:1 or 2:1 complex stoichiometries. The only stoichiometry which gave a satisfactory fit was a $L_2Zn_2(OH)_2$ with a formation constant of $\log K_{L_2Zn_2(OH)_2}=9.8$. A possible coordination mode for this stoichiometry is depicted below (figure 4.24).

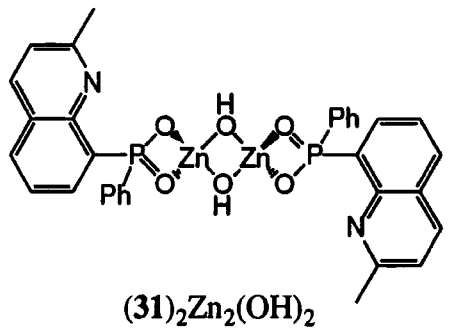

$(31)_2Zn_2(OH)_2$

Figure 4.24 Proposed coordination mode of $(31)_2Zn_2(OH)_2$

A comparison of metal stability constants of related ligand systems is given below (table 4.7). Comparison of the 8-(quinolinyl)phosphate ligand (177) to 8-(2-methylquinolinyl) phenylphosphinic acid (31) reveals a much larger formation constant for the 2:1 complex stoichiometry for both nickel and copper. This may be due to seven ring chelate formation of the former ligand (177). In fact, the equilibrium constants for 8-(quinolinyl)phosphate (177) suggest that the phosphinate is binding without participation of the quinoline nitrogen. For 8-hydroxyquinoine (139) and ligand (178) the order of stabilty for nickel, copper and zinc follows the Irving-Williams series.[35] This order of stabilty arises because the two ligands (139) and (177) were not designed with any geometric constraints or donor atom preference in mind.

Ligand		Nickel		Copper		Zinc	
		$Log\beta_{ML}$	$Log\beta_{ML_2}$	$Log\beta_{ML}$	$Log\beta_{ML_2}$	$Log\beta_{ML}$	$Log\beta_{ML_2}$
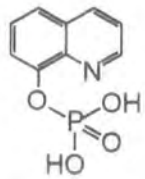	(**177**)[a]	-	2.61	-	5.11	-	4.87
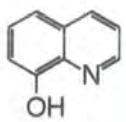	(**139**)[b]	9.27	-	12.5	10.5	8.52	7.28
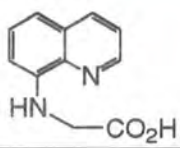	(**178**)[b]	3.8	7.7	4.0	8.1	3.6	7.2

a. reference 34 b. reference 3

Table 4.7 Comparison of similar ligands to (31)

The speciation diagram for ligand (31) shows only one ligand bound species, $(31)_2Zn_2(OH)_2$ which is present over the pH range 4 to 8.5 (figure 4.25).

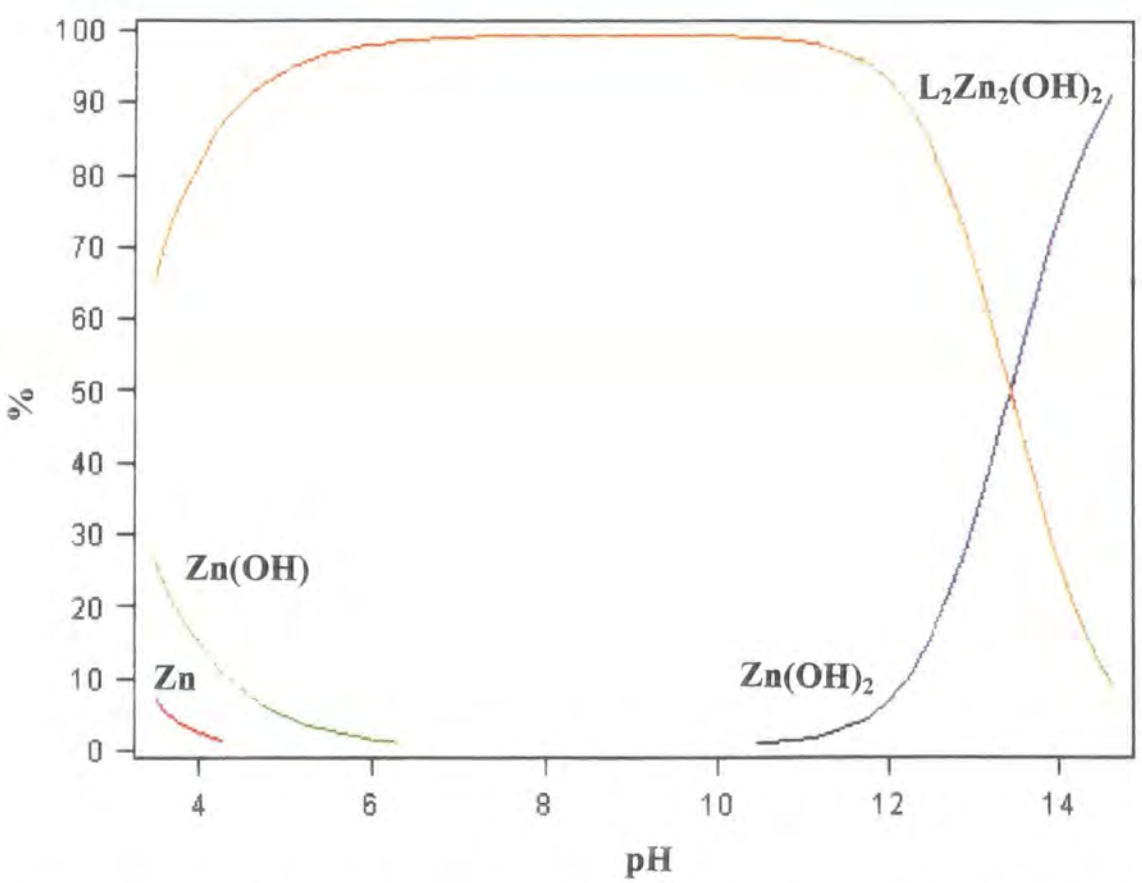

Figure 4.24 Speciation diagram for (31) plus zinc from pH 3.5 to 10 (298K, I = 0.1, H_2O)

4.6 Conclusions

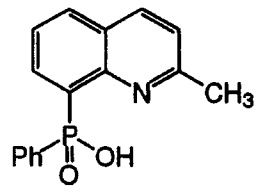

(31)

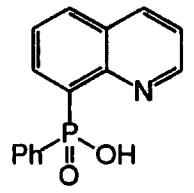

(30)

Figure 4.26 Structure of ligands (31) and (30)

Both of the target ligands defined in this chapter have been synthesised by versatile high yielding routes and the solution coordination chemistry assessed using NMR, fluorescence and UV spectroscopy, ESMS and potentiometric techniques.

There was a stark contrast observed between the solution coordination behaviour of the two ligand systems examined in this chapter, related to the presence of the methyl substituent in the C-2 position of ligand (31). For the methyl substituted ligand (31) both ^{31}P and fluorescence studies imply that the ligand forms ML_2 species when in excess over the metal, involving phosphinate ligation (figure 4.18). At higher metal concentrations ML species predominate in solution, consistent with ^{31}P NMR analysis. In contrast, the unsubstituted ligand (30) binds zinc in solution to form a weakly bound ML complex, as as shown by both NMR and fluorometric analysis.

Analysis of the UV spectra for the free ligand and the metal complexes substantiated the fact that (31) does not bind through the quinolinyl nitrogen, whereas the unsubstituted ligand (30) experiences significant changes in its absorption spectra when in the presence of zinc ions.

The data obtained from the ESMS revealed that only ML_2 species were detected for zinc, nickel and copper for 8-(2-methylquinolinyl)phenylphosphinic acid (31). No signals corresponding to a metal bound ligand species was observed with iron. In contrast, the unsubstituted ligand (30) forms ML and ML_2 species for nickel and copper but solely an ML_2 complex with zinc. For iron, species corresponding to ML, ML_2 and ML_3 were detected, implying that this ligand is incapable of imposing any geometric constraints on complex formation for this metal.

pH-Metric studies on 8-(2-methylquinolinyl)phenylphosphinic acid (31) implies that the ligand forms 2:1 complex species with nickel and copper with formation constants of $\log\beta_{ML_2}$=10.3 and 8.2 respectively. Attempts to fit the data for the zinc titration for either 1:1 or 2:1 stoichiometries failed. The only species which gave a satisfactory fit to the data was $L_2Zn_2(OH)_2$ with a formation constant of $\log K_{L_2Zn_2(OH)_2}$=9.8.

Synthesis of lipophilic analogous of this ligand series was not pursued because of the unsatisfactory performance of these ligands in the solution coordination chemistry experiments. The methyl substituted ligand (31) does not appear to bind through nitrogen and the unsubstituted ligand (30) is unable to discriminate against coordination to the ferric ion.

4.7 References

1. F. F. Runge; *Ann. Physik*, 1834, **31**, 68
2. E. Kimura and T. Koike; *Chem. Soc. Revs.*, 1998, 179
3. R. M. Smith and A. E. Martell, '*Critical Stabilty Constants Vol. 1 to 6*', Plenum Press, London
4. J. Kido and J. Endo; *Chem. Lett.*, 1997, 633
5. P. D. Zalewski, I. J. Forbes, R. F. Seamark, R. Borlinghaus, W. H. Betts, S. F. Lincoln and A. D. Ward; *Chem. Biol.*, 1994, **3**, 153
6. I. B. Mahadevan, M. C. Kimbar, S. F. Lincoln, E. R . T. Tiekirk, A. D. Ward, W. H. Betts, I. J. Forbes and P. D. Zalewski; *Aust. J. Chem.*, 1996, **49**, 561
7. D. Elbaum, S. K. Nair, M. W. Patchan, R. B. Thompson and D. W. Christianson; *J. Am. Chem. Soc.*, 1996, **118**, 8381
8. T. Koike, S. Kajitari, I. Nakamura, E. Kimura and M. Shiro; *J. Am. Chem. Soc.*, 1995, **117**, 1210
9. R. D. Hancock and A. E. Martell; *Chem. Rev.*, 1989, **89**, 1875
10. A. Escande and J. L. Galingné; *Acta Crystallogr.*, 1974, **B30**, 1647
11. J. Bjerrum and C. K. Jorgensen; *Rev. Trav. Chim.*, 1956, **75**, 658
12. Z. H. Skraup; *Monatsh.*, 1881, **2**, 139
13. O. Doebner and W. von Miller; *Ber.*, 1881, **14**, 2812
14. A. Combes; *Compt. Rend.*, 1888, **106**, 142
15. J. J. Eisch and T. Dluzniewski; *J. Org. Chem.*, 1989, **54**, 1269
16. C. M. Leir; *J. Org. Chem.*, 1977, **5**, 911
17. Y. Xu, Z. Li, J. Xia, H. Guo and Y. Huang; *Synthesis*, 1983, 377
18. J. A. Miles, R. C. Grabiak and M. T. Beeny; *J. Org. Chem.*, 1981, **47**, 3486
19. J. A. Miles, R. C. Grabiak and M. T. Beeny; *J. Org. Chem.*, 1981, **46**, 1677
20. J. I. G. Cadogan, D. J. Sears and D. M. Smith; *J. Chem. Soc. (C)*, 1969, 1314
21. E. P. Kyba and C. N. Chubb; *Inorg. Chem.*, 1984, **23**, 4766
22. Tidwell; *Org. React.*, 1990, **30**, 297
23. Y. S. Cheng, W. Liu and S. H. Chen; *Synthesis*, 1980, 223
24. C. M. O'Donnell, G. A. Knesel, T. S. Spencer and F. R. Stermitz; *J. Phys. Chem.*, 1970, **74**, 3555

25. A. P. de Silva, H. Q. N. Gunaratne, T. Gunnlaugsson, A. J. M. Huxley, C. P. McCoy, J. T. Rademacher and T. E. Rice; *Chem. Rev.*, 1997, **97**, 1515
26. T. Gunnlaugsson and D. Parker; *Chem. Commun.*, 1998, 511
27. M. H. Hutson, K. W. Haider and A. W. Czarnik, *J. Am. Chem. Soc.*, 1988, **110**, 4460
28. C. I. Sainzdiaz, H. Klocker, R. Marr and H. J. Bart; *Hydrometallurgy*, 1996, **42**, pp 1-11
29. N. Miralles, A. M. Sastre, M. Aguillar and M. Cox; *Solvent Extrac. Ion Exch.*, 1992, **10**, 51
30. N. N. Greenwood and A. Earnshaw; '*Chemistry of the Elements*', 1990, Pergamon, Oxford, 1411
31. W. Kuchen and H. Hertel; *Angew. Chem., Int. Ed. Engl.*, 1969, **2**, 89
32. R. M. Silverstein, G. C. Bassler and T. C. Morrill, '*Spectrometric Identification of Organic Compounds*', Wiley, New York, 1991, 311
33. E. Leise, A. Jaffrezic and A. Van Dorsselaer; *J. Mass. Spectrom.*, 1996, **31**, 537
34. A. Saha, N. Saha, L. Ji, J. Zhao, F. Gregán, S. A. Sajadi, B. Song and H. Sigel; *J. Biol. Inorg. Chem.*, 1996, **1**, 231
35. H. Irving and R. J. P. Williams; *J. Chem. Soc.*, 1953, 3192

Chapter Five

Pyridyl Derived Ligand Systems

5 Pyridyl Derived Ligand Systems

A new class of ligand which combine the pyridyl ring system with phosphinic or thiophosphinic acid donor groups is presented. Important examples of existing ligand systems based on pyridine for zinc coordination are highlighted (5.2). The design of the new ligands is discussed (5.3) and synthetic routes to the target compounds detailed (5.4). Complexation with various first row transition metals is assessed by techniques such as NMR, fluorescence and uv/visible spectrophotometry, ESMS and liquid-liquid extraction methods (5.5) and finally general conclusions are summarised (5.6).

5.1 Pyridines

Pyridine (179) and several of its methyl derivatives are obtained from coal tar, which contains about a 0.2% mixture of pyridine bases. Several large scale synthetic routes to pyridines are in common use: for example the vapour phase reaction between acetaldehyde, formaldehyde and ammonia over a silica-alumina catalyst gives mixtures of pyridine and the methylpyridines which are easily separable.[1]

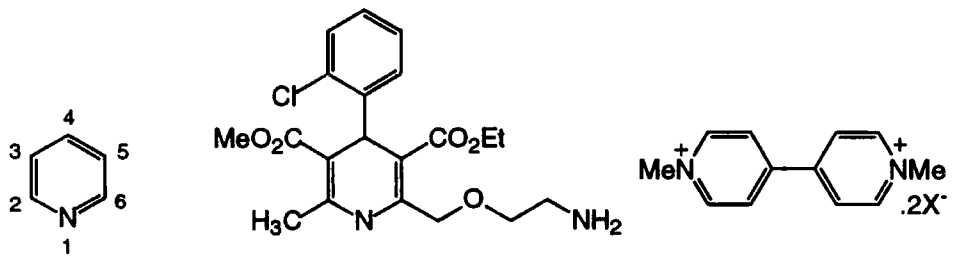

(179) **(180)** **(181)**

Figure 5.1 Pyridine (179) and two examples of industrial applications of the ring system (180) and (181)

Many pharmaceuticals and agrochemicals have been developed which incorporate the pyridine ring. Amlodipine (180) is an effective treatment for angina which is marketed by Pfizer, and paraquat (181) a potent herbicide produced by ICI (figure 5.1). Pyridines are ubiquitous in nature: in particular nicotinamide (182) constitutes a key component of a number of important coenzymes (figure 5.2).

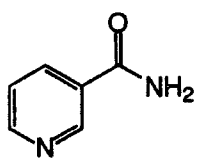

Nicotinamide

(182)

Figure 5.2 Structure of nicotinamide (182)

Nicotinamide adenine dinucleotide (NAD^+) (183) and its phosphate ($NADP^+$) (184) occur in the red blood corpuscles and mediates many biochemical redox reactions (figure 5.3).[2]

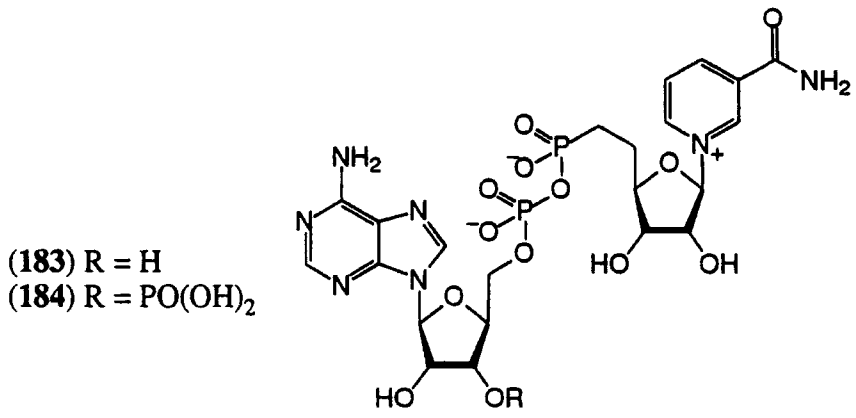

Figure 5.3 Structure of NAD^+ (183) and $NADP^+$ (184)

5.2 Previous Examples of Pyridyl Based Ligands for Zinc Coordination

Many of the pyridyl based ligand systems for zinc described to date have been applied to the production of biomimetic zinc complexes or used for the asymmetric addition of dialkylzinc reagents to carbonyls.

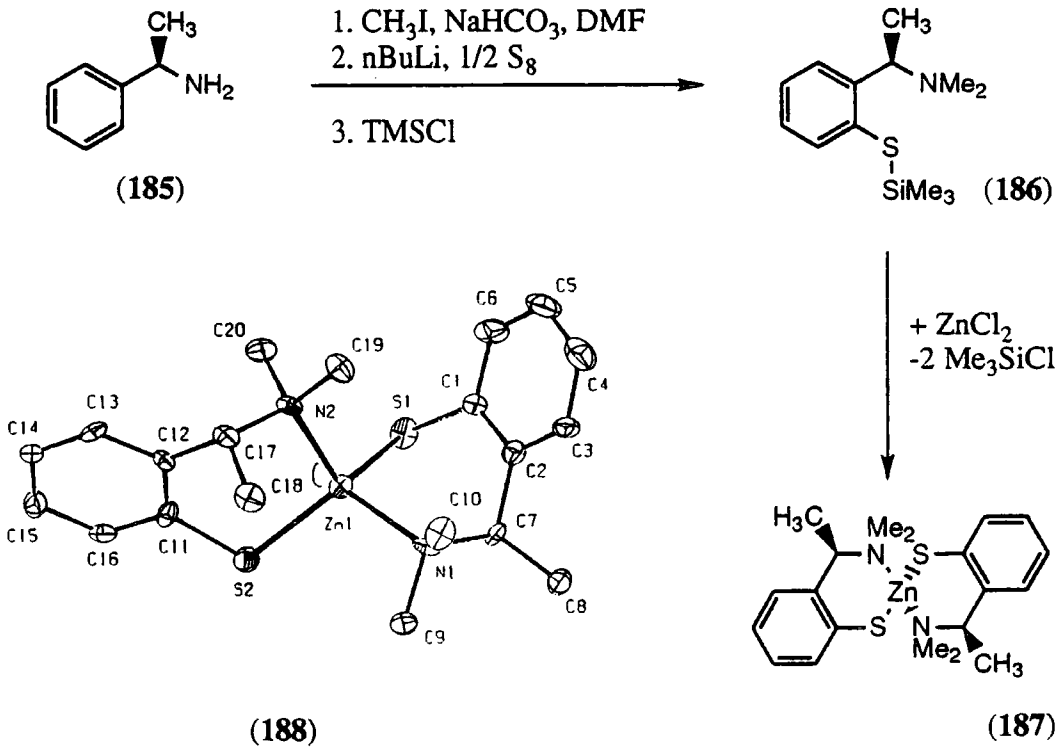

Scheme 5.1 Synthesis and crystal structure of zinc complex (188)

Van Koten and co-workers have investigated the use of S,N-chelating chiral zinc bis(amino-arenethiolates) as precursor catalysts for the enantioselective addition of dialkylzincs to aldehydes. The ligand was prepared by N-alkylation of commercially available chiral benzylamine (185), followed by *ortho* lithiation and quenching with sulfur. The resultant lithium amino-arenethiolate was quenched *in situ* with trimethylsilyl chloride to produce the precursor (186). Reaction of (186) with zinc dichloride produced the air-stable zinc complex (187) with loss of two molar equivalents of trimethylsilyl chloride. Examination of the solid state crystal structure (188) of the dimeric complex shows the zinc atom in a distorted tetrahedral environment with S-Zn-N bond angles of 100, 101, 120 and 118° (scheme 5.1).[3] Reaction of the catalyst (186) with diethylzinc followed by the addition of various aldehydes produced a significant rate enhancement and gave the resultant secondary alcohols in high enantiomeric excess (generally >90%).

In an attempt to study the mechanism of phosphate ester hydrolysis in *Escherischia coli* alkaline phosphatase, Fenton *et al.* have prepared and studied low molecular weight zinc complexes derived from tripodal ligands with a single phenolate donor (189).[4] The chosen set of donor atoms mimics that found in the natural system where zinc is coordinated by two histidines and an aspartate residue. Preparation of the zinc complex with ligand (189) (figure 5.4) and zinc(II) perchlorate produced a solid state dimeric structure (190) with two coordinated zinc atoms. The structure illustrates that two pyridyl nitrogens, an amine nitrogen and a phenoxy oxygen from the ligand make up the coordination sphere of zinc(II). Five coordination is achieved through bridging of the phenolate oxygen linking the two halves of the dimer, which provides both zinc atoms with a distorted square pyramidal coordination geometry (figure 5.4).

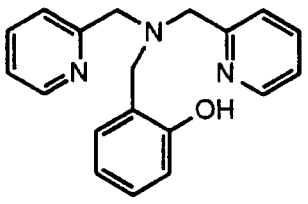

(189)

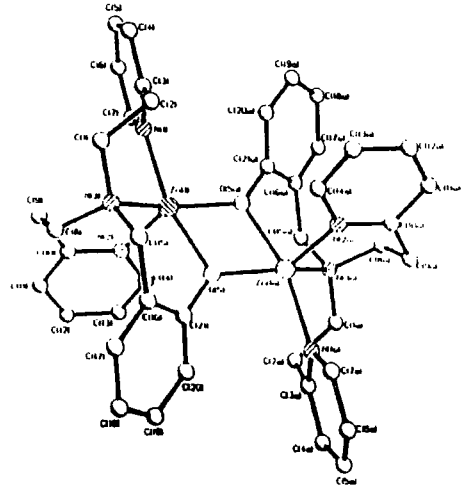

(190)

Figure 5.4 Ligand (189) and solid state structure $[(190)_2Zn_2][ClO_4]_2$

The hydrolysis of tris(4-nitrophenyl)phosphate with complex (190) in aqueous ethanol proceeded to give $^{-}O_2P[OC_6H_4(4\text{-}NO_2)]_2$ at 25°C and $^{2-}O_3P[OC_6H_4(4\text{-}NO_2)]$ at 35°C, with second order rate constants of 0.45 and 0.36$dm^3mol^{-1}s^{-1}$ at physiological pH.

Yashiro and co-workers have studied zinc complexes containing two or three zinc ions with a view to achieving phosphoester hydrolysis in diribonucleotides.[5] The di- and trinuclear zinc complexes of the ligands (191) and (192) were prepared under aqueous conditions by the addition of two and three molar equivalents of $Zn(NO_3)_2$ respectively, and their stoichiometry confirmed by ^1H NMR spectroscopy (figure 5.5).

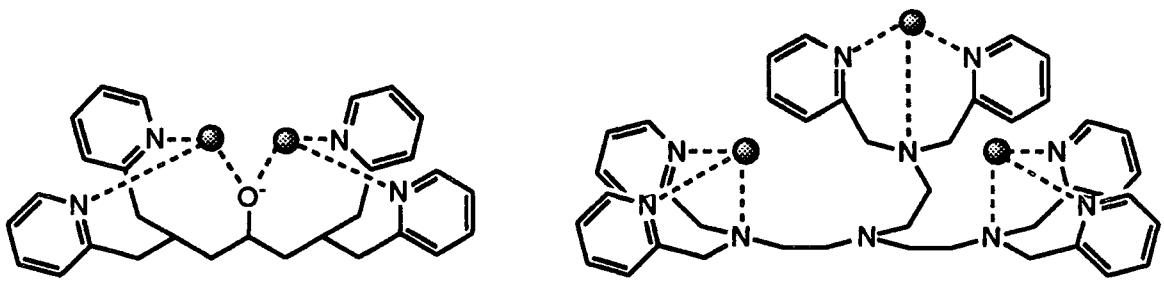

(191) ● = Zn^{2+} **(192)**

Figure 5.5 Structures of zinc complexes (191) and (192)

Hydrolysis of ribonucleotide dimers with both (191) and (192) was conducted at 50°C and pH 6.9, for all of the reactions examined good pseudo first order kinetics were observed. The trinuclear complex was shown to catalyse diribonucleotide hydrolysis efficiently, but showed a considerable dependence on the metal to ligand ratio. Optimal catalysis was observed at a metal to ligand ratio of 3:1, with the rate of hydrolysis decreasing at higher or lower ratios.

In zinc finger proteins, for example in alcohol dehydrogenase or spinach carbonic anhydrase, the metal ion is nearly always coordinated to at least one sulfur atom of cysteine. Vahrenkamp and co-workers have investigated ligands which present a N_2S donor set, which should mimic the coordination environment of zinc in many enzymes and finger proteins.[6] The ligand system examined was designed to encapsulate the metal ion, but still leave room for a labile ligand which may be replaced by a reactive substrate. N-(2-mercaptoethyl)picolylamine (195) was the ligand of choice, which was synthesised by reaction between picolylamine (193) and methylene sulfide (194), and the zinc complex (196) produced by reaction with half a molar equivalent of zinc perchlorate (scheme 5.2).

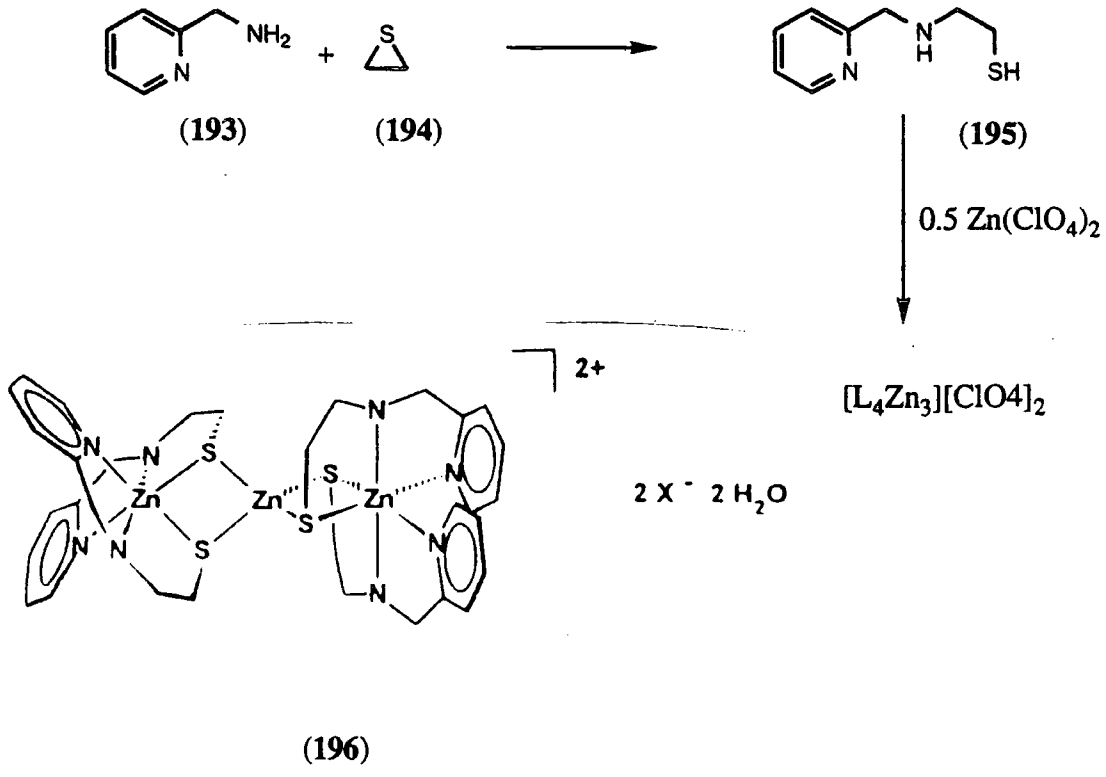

(196)

Figure 5.2 Synthesis of ligand (195) and the crystal structure $[(195)_4Zn_3]^{2+}$

The solid state structure reveals zinc in two distinct coordination environments, a central tetrahedral ion is flanked on both sides by octahedral $Zn(195)_2$ units. The 4:3 ratio of ligand to zinc was obtained irrespective of the stoichiometric ratio of the reactants.

5.3 Ligand Design

Using the previously outlined design criteria (Ch 1.4) a bidentate ligand system was considered based on the pyridine ring system. The ligand is appended with either phosphinic or thiophosphinic acid functionalities, and therefore presents either a NO or NS donor set which can bind to zinc in a [2+2] coordination mode (figure 5.6)

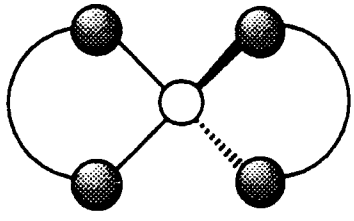

[2+2]

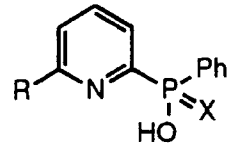

R = H, X = O (**32**)
R = Me, X = O (**33**)
R = Me, X = S (**34**)

Figure 5.6 Diagrammatic representation of [2+2] geometry and the target ligands (32), (33) and (34)

The ligand forms a five-ring chelate with metal ions, in contrast to the the previous systems described in this thesis, which form six-ring chelates. The advantages of using phosphinic acids has been highlighted elsewhere and a general method for their introduction has been described in detail (*vide supra* Ch. 3 and 4). The use of thiophosphinic acid donor groups with pyridine containing ligands will also be described. These are more acidic than the corresponding phosphinic acids and may extract zinc at lower pH.[7] The donor set in the putative ML_2 complex will be N_2O_2 or N_2S_2, which mimics many zinc containing enzymes, for example carboxypeptidase (N_2O_2) or alcohol dehydrogenase (N_2S_2).[8] In addition, the use of borderline Lewis bases should discriminate against coordination to harder ions, and the strong Lewis basicity of nitrogen may shorten the Zn-N bond and promote tetrahedral geometry by minimising steric interactions.[9, 10]

Modification of the lipophilicity of the pyridyl derived system is conceptually analogous to that described for the quinolinyl systems. The potential sites for modification are on the pyridine ring, or at the phosphorus atom.

Molecular modelling

Molecular modelling of the zinc complex was performed as described earlier (Ch. 3.3). The model shows tetrahedral zinc (green central ion) with two chelating 6-(2-methylpyridyl)phenylphosphinic acid ligands at their minimum energy structure (figure 5.7). The methyl substituent in the C-2 position inhibits formation of other coordination geometries, particularly square planar and octahedral. The two phenyl substituents on the phosphinic acid are oriented in and out the plane of the page, indicating that substitution in the *ortho* position of the phenyl ring should have no effect on the binding.

5.4 Synthesis

The general synthetic route to the pyridyl based ligands systems involves reaction between a suitably functionalised 2-bromopyridine (197) or (198) and ethylphenylphosphonite (94) to give the corresponding phosphinate ester (199) or (200) (scheme 5.3), which can be hydrolysed. Further functionalisation yields the corresponding thiophosphinic acid (34).

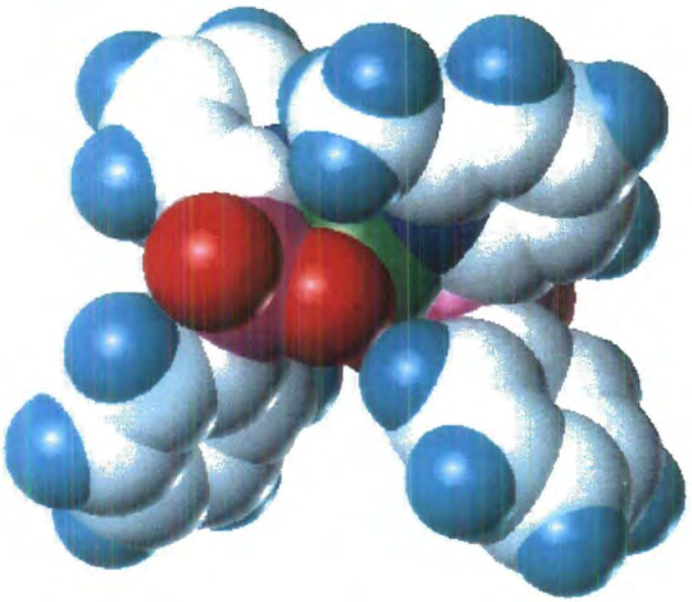

$Zn(\mathbf{33})_2$

$Zn(\mathbf{33})_2$

Figure 5.7 Molecular model showing the tetrahedral zinc complex of ligand (33), space filling (left) and line drawing (right)

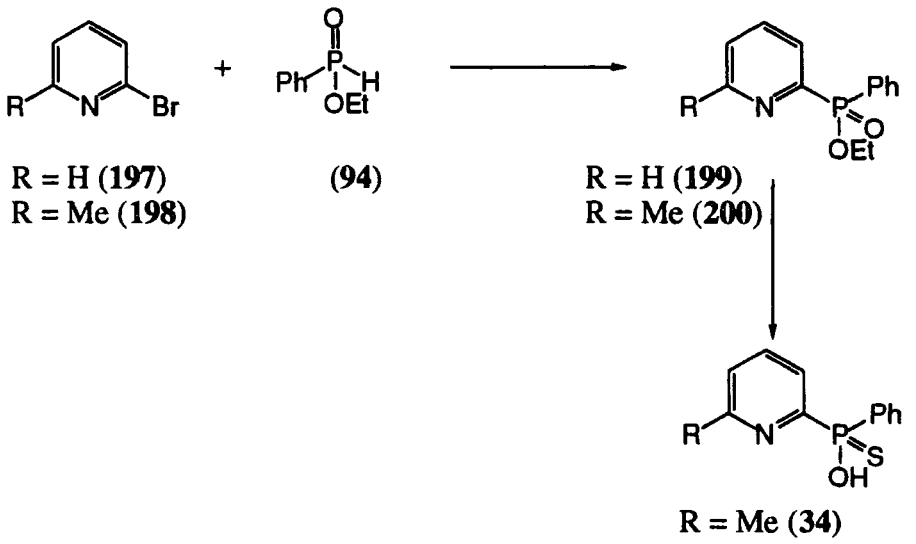

Scheme XX Proposed synthetic route to phosphinic and thiophosphinic acid substituted pyridines

The first pyridyl based ligand systems to be examined were the picoline and the unsubstituted derivatives. If good selectivity in binding was not achieved with these substituents, then more sterically demanding groups could be incorporated into the C-2 position of the ring.

2-Bromopicoline (198) was synthesised, following a procedure adapted from Case and Kasper.[11] To a solution of 2-aminopicoline (201) in hydrobromic acid was added bromine, followed by an aqueous solution of sodium nitrite maintaining a temperature less than 5°C. Immediately after the addition of sodium nitrite was complete a solution of aqueous sodium hydroxide was added maintaining a temperature less than 10°C (scheme 5.4). If the temperature was allowed to rise above any of the above limits or the sodium hydroxide solution was not added immediately then there was a tendency for dibromination to occur. For these reasons, all solutions were prepared beforehand and chilled, and the reaction vessel chosen had a large surface area to ensure efficient cooling.

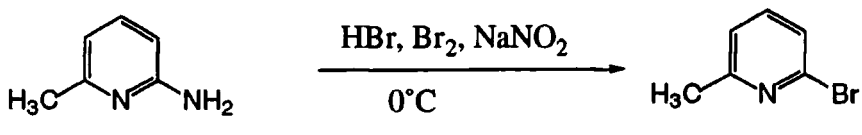

(201) (198)

Scheme 5.4 Preparation of 2-bromopicoline (198)

To synthesise the ethyl phenylphosphinate derivatives of the 2-bromo substituted pyridines an analogous procedure to that employed in the previous two chapters (*vide*

supra Ch.3 and 4) was used, namely palladium catalysed coupling of (197) and (198) with ethylphenylphosphonite (94) in the presence of $Pd(PPh_3)_4$ and triethylamine.[12] Following aqueous acidic work-up the products (199) and (200) were isolated as low melting solids which were purified by distillation under reduced pressure, without any observed degradation of the product. This indicates that these phosphinate appended pyridyl compounds are indeed robust, making then suitable for repeated use in the hydrometallurgic recovery of metals. Subsequent ester hydrolysis of (199) and (200) in hydrochloric acid (6M) proceeded to completion after 16 h under reflux. Lyophilisation gave the target compounds (32) and (33) (both with 57% overall yield) as their hydrochloride salts (scheme 5.5).

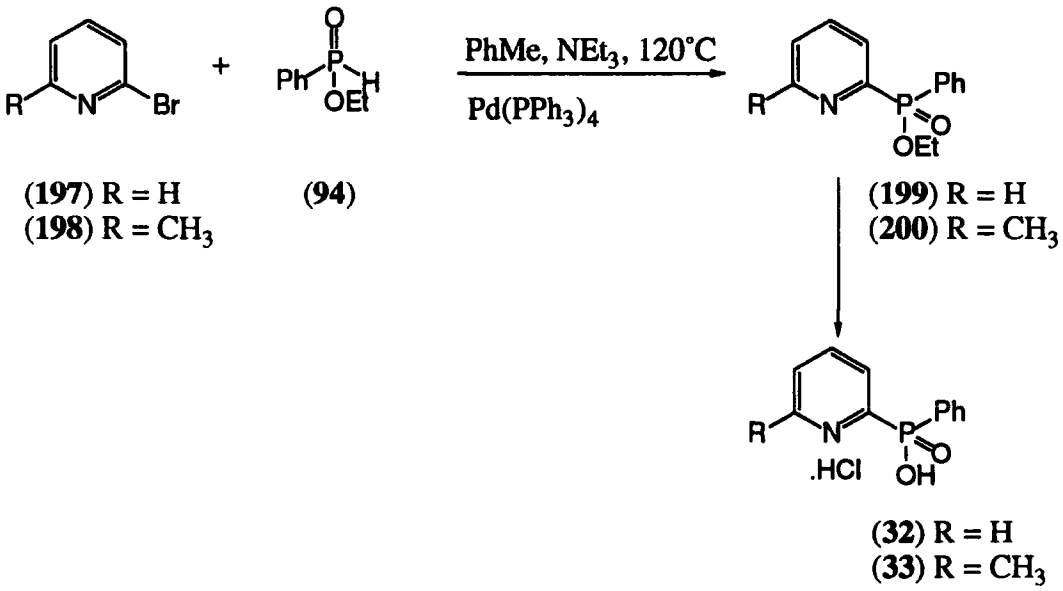

Scheme 5.5 Synthesis of 6-(2-methylpyridyl)phenylphosphinic acid (32) and 2-(pyridyl)phenylphosphinic acid (33)

All isomers of pyridine carboxylic acids are decarboxylated readily in acidic media, in the order 2>4>3 which takes place via the zwitterionic (202) tautomeric form (scheme 5.6).[13] In contrast, the pyridine phosphinic acids seem to be extremely stable towards cleavage of the C-P bond.

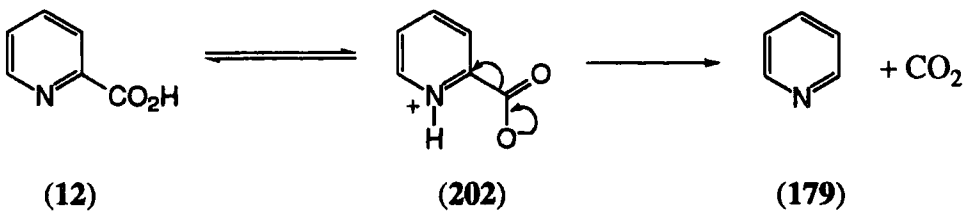

Scheme 5.6 Decarboxylation of picolinic acid (12)

Synthesis of thiophosphinic acid derivative

Several methods for the introduction of the thiophosphinic acid functionality were described in chapter 2. However, many of these approaches required the intermediacy of a thiophosphinate ester. Such esters are known to be extremely difficult to hydrolyse unless they possess an activated ester. Hydrolysis conditions often require enzymatic hydrolysis,[17, 18] or high pH (Ch.2 2.3).[19] Earlier work has shown that direct formation of a thiophosphinate ester is possible by reaction of a phosphinate ester with Lawesson's reagent (54),[20] P_4S_{10}[21] or $PSCl_3$[22] though this procedure produces esters which are difficult to hydrolyse to the corresponding acids. Attempts at direct sulfur transfer of phosphinates was attempted also by Cole where competing reactions hindered the effective formation of thiophosphinates.[23] The formation of thiophosphinic acid derivatives should ideally involve a direct conversion from the corresponding phosphinic acid by a sulfur transfer reaction. This would be advantageous as good methodology is now in place for the introduction of the phosphinates.

Work on similar aza-phosphinate ligands has addressed these problems.[24] The successful procedure used a method originally developed by Harger, involving activation of the phosphinic acid by formation of the phosphinic chloride and subsequent sulfur transfer using thiophosphoryl chloride and a catalytic quantity of DMF.[25, 26]

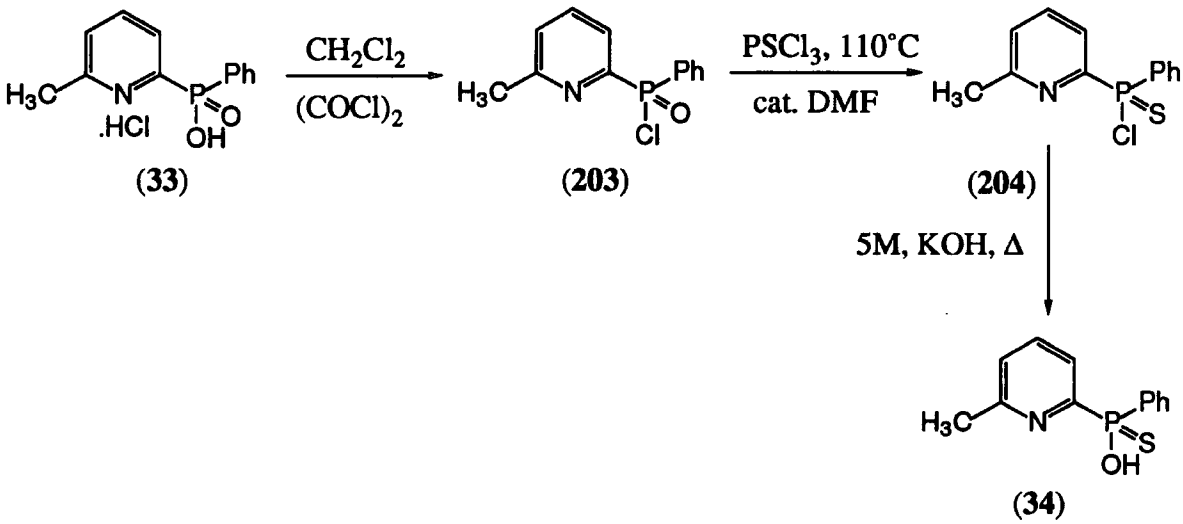

Scheme 5.7 Synthesis of 6-(2-methylpyridyl)phenylthiophosphinic acid (34)

Reaction of rigorously dried 6-(2-methylpyridyl)phenylphosphinic acid hydrochloride (33) as a suspension in dichloromethane with an excess of oxalyl chloride gave a clear solution. The reaction was followed by ^{31}P NMR. Conversion of the free acid (33, δ_P = 16.6ppm) to the phosphinic chloride (203, δ_P = 30.4) was found to be complete after 1 h. The solvent and excess oxalyl chloride were removed under reduced pressure and the

product dried for 2 hours to ensure all traces of oxalyl chloride was removed. Sulfur transfer was then accomplished by heating in thiophosphoryl chloride ($PSCl_3$) with a catalytic amount of DMF to give the corresponding thiophosphinic chloride (204) (δ_P = 63.3ppm). The P-Cl bond was surprisingly resistant to hydrolysis and complete hydrolysis to the thiophosphinic acid (34) was achieved only by heating in KOH (5M) for sixteen hours (scheme 5.7).

This synthetic route has several drawbacks, formation of the intermediate phosphinic chloride (203) produces a moisture sensitive intermediate which has to handled. It would be advantageous if the phosphinic chloride could be formed *in situ* followed by transfer of a sulfur atom. The viability of a route to the thiophosphinic chloride by conversion of the phosphinic acid (33) to the phosphinic chloride (203) and subsequent *in situ* sulfur transfer was investigated. The hydrochloride salt of the acid was added to thiophosphoryl chloride and heating resulted in a clear solution. Two drops of DMF were added to the solution and the mixture heated under reflux for 16 hours. Removal of the thiophosphoryl chloride under reduced pressure gave the thiophosphinic chloride (204) in 87% yield compared with 70% by the previous method (scheme 5.8).

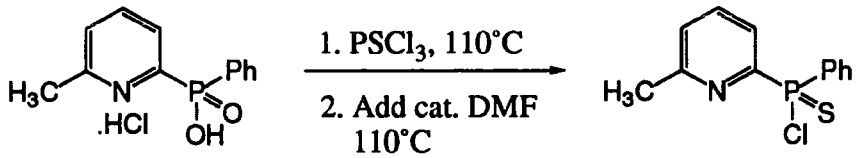

(33) **(204)**

Scheme 5.8 Modified synthesis of (34)

5.5 Solution Coordination Chemistry

The solution coordination chemistry of 2-(pyridyl)phenylphosphinic acid (32), 6-(2-methylpyridyl)phenylphosphinic acid (33) and 6-(2-methylpyridyl)phenylthio-phosphinic acid (34) was assessed by a combination of NMR, fluorescence and uv spectroscopy, ESMS and liquid-liquid extraction. In most cases speciation studies were carried out in methanol solution. When this was not possible, a stated percentage of another solvent was added to facilitate complete solution.

1.5.1 ^{31}P NMR Titrations

2-(Pyridyl)phenylphosphinic acid (32) and 6-(2-methylpyridyl)phenylphosphinic acid (33)

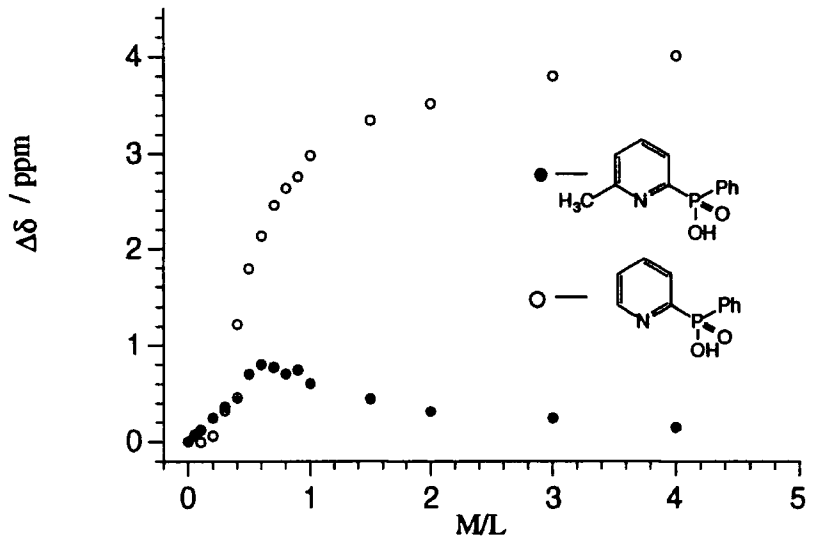

Figure 5.8 ^{31}P NMR titration of 2-(pyridyl)phenylphosphinic acid (32) and 6-(2-methylpyridyl)phenylphosphinic acid (33) plus $ZnTf_2$ (25% CD_3OD, 75% $CDCl_3$, 293K)

With the addition of zinc(II) triflate to 2-(pyridyl)phenylphosphinic acid (32), a shift to lower frequency in the ^{31}P NMR spectrum was observed (figure 5.8). Only one exchange broadened peak was observed for all M/L ratios examined, indicating that the ligand and metal are in fast exchange on the NMR timescale. A plot of the change in chemical shift against the metal to ligand ratio is shown (figure 5.8). It is evident from the form of the curve that there is a steady rise in $\Delta\delta$ for $0<M/L<1$ which becomes less pronounced in the region $1<M/L<5$. Since the slope of the curve appears to change gradient at M/L=1 this implies a 1:1 complex stoichiometry is favoured. The fact that $\Delta\delta$ still increases where $M/L>1$ indicates that further complexation is occurring.

$$M + L \overset{K_1}{\rightleftharpoons} ML \qquad K_1 = \frac{[ML]}{[M][L]} \qquad \text{eqn. 5.1}$$

Analysis of equation 5.1 provides an explanation for this; if the ML complex has a low stability constant then as more metal is added to the system then the position of the equilibrium must change in order to maintain a constant value for K_1. Therefore as more metal is added the equilibrium will be driven to the right.

A plot of the observed change in chemical shift against the metal to ligand ratio for 6-(2-methylpyridyl)phenylphosphinic acid (33) with addition of zinc is shown (figure 5.8). With the addition of zinc(II) triflate to the solution a shift of the ^{31}P signal to lower frequency was observed in the region 0<M/L<0.5 and a shift to higher frequency in the range 0.5<M/L<4. In all regions there was only a single exchange broadened signal, indicating fast exchange between the metal and ligand.

$$M + L \overset{K_1}{\rightleftharpoons} ML \qquad K_1 = \frac{[ML]}{[M][L]} \qquad \text{eqn. 5.1}$$

$$ML + L \overset{K_2}{\rightleftharpoons} ML_2 \qquad K_2 = \frac{[ML_2]}{[ML][L]} \qquad \text{eqn. 5.2}$$

$$ML_2 + M \overset{K_1/K_2}{\rightleftharpoons} 2\,ML \qquad \frac{K_1}{K_2} = \frac{[ML]^2}{[ML_2][M]} \qquad \text{eqn. 5.3}$$

In the region 0<M/L<0.5 there is an increase in $\Delta\delta$, which reaches a maximum close to M/L=0.5, indicating that the ligand is initially forming a ML_2 complex. To form a ML_2 complex the system must initially form a ML complex and the relative proportions of these species will be determined by the size of K_1, K_2 and K_3 (eqns. 5.1 to 5.3). However as more metal is added (0.5<M/L<3) there is an observed decrease in $\Delta\delta$, which implies the complex is reacting further, to form two ML complex species at higher metal concentrations. If K_1 is small (eqn. 5.1), and more metal is added, the system must respond to consume the metal and produce more ML species, driven by a relatively large K_3 value (eqn. 5.3). There also exists the possibilty for a termolecular complexation event, however incorporation of the 2-methyl substituent seems to discriminate against this.

Although the curves obtained from NMR titrations are not easily analysed quantitatively to give an accurate stability constant, comparisons can be made between the two ligands to give a qualitative order of stability. The form of the binding isotherm for 2-(pyridyl)phenylphosphinic acid (32) is consistent with stronger binding compared to 6-(2-methylpyridyl)phenylphosphinic acid (33).

Job's Method of Continuous Variations

Using Job's method it is possible to determine the predominant complex stoichiometry in solution. Experimentally this involves preparing different combinations of the metal and the ligand, such that the total concentration is constant (see appendix B).

$$[M_m L_n] = \frac{[L](\delta_{obs} - \delta_L)}{(\delta_{M_m L_n} - \delta_L)} \qquad \text{eqn. (5.4)}$$

Plotting the complex concentration (eqaution 5.4) against the percentage of ligand provides a curve which gives the stoichiometric ratio at the turning point (figure 5.9).

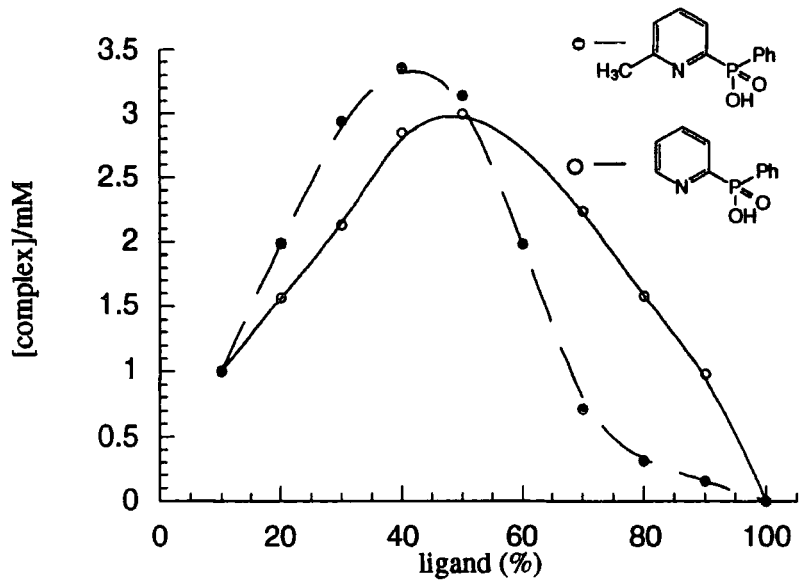

Figure 5.9 Job plot for (32) and (33) plus ZnTf2 (25% CH_3OH, 75% $CHCl_3$, 293K)

From the form of the curve it is evident that 2-(pyridyl)phenylphosphinic acid (32) has a turning point at 50% ligand concentration, indicating that the predominant stoichiometry in solution is 1:1. In contrast, 6-(2-methylpyridyl)phenylphosphinic acid (33) has a turning point at about 40% ligand concentration, indicating that a mixture of 1:1 and 2:1 complex stoichiometries may exist in solution.

6-(2-methylpyridyl)phenylthiophosphinic acid

With the addition of metal there was an observed shift to lower frequency of a single exchange broadened signal, indicating that the metal and ligand are in fast exchange on the NMR timescale (figure 5.10). In the range $0<M/L<0.5$ there is a sharp rise in $\Delta\delta$ which levels off at $M/L>0.5$. The shape of the curve indicates that the ML_2 complex is formed predominantly; that is K_2 (eqn. 5.2) is large in comparison to K_1 (eqn. 5.1).

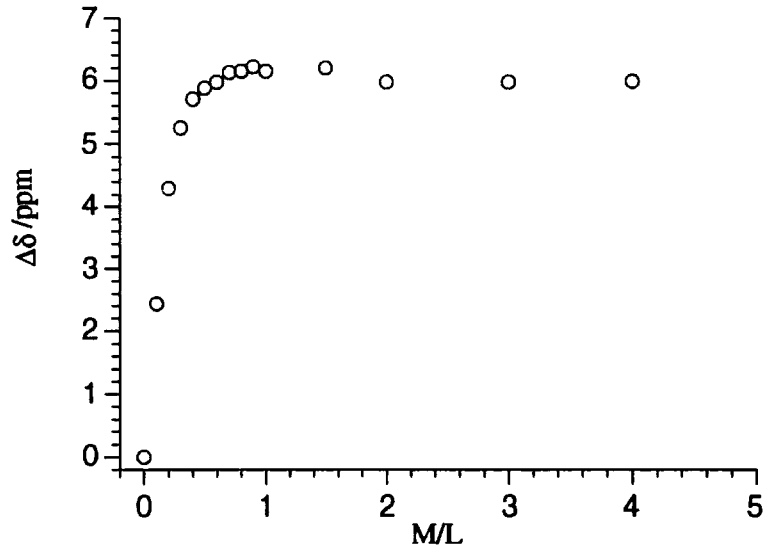

Figure 5.10 ^{31}P NMR titration of $ZnTf_2$ and 6-(2-methylpyridyl)phenylthiophosphinic acid (34) (25% CD_3OD, 75% $CDCl_3$, 293K)

Comparison of (33) and (34) ^{31}P NMR titrations

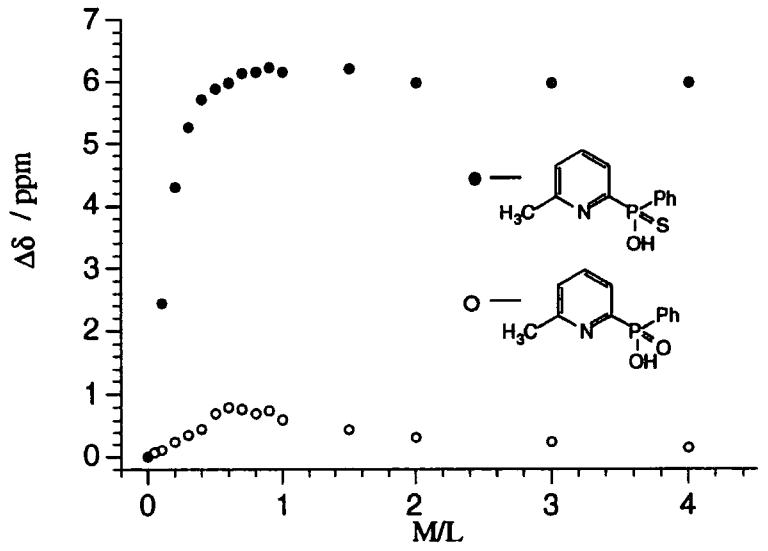

Figure 5.11 Comparison between (33) and (34) ^{31}P NMR titrations (293K, 25% CD_3OD, 75% $CDCl_3$)

Comparison of the NMR titration profiles for 6-(2-methylpyridyl)phenylphosphinic acid (33) and 6-(2-methylpyridyl)phenylthiophosphinic acid (34) reveals a similar curve profile for both species (figure 5.11). They both appear to form predominantly ML_2 complexes, and the former then more clearly tends to form a 1:1 complex upon addition

of excess zinc. Comparison of the form of the binding isotherm suggests that the stability constant for ML_2 formation (K_2 eqn. 5.2) is greater for the thiophosphinic acid derivative (34). This difference in stability may be attributed to several factors. Firstly, in five-ring chelate formation the longer P-S bond length (relative to the P-O) may impart a more favourable interaction with respect to the smaller zinc ion. Secondly, the greater polarisability of the thiophosphinic acid may favour zinc binding, as zinc is a borderline cation in the Pearson classification.

1.5.2 Fluorescence Studies

pH fluorescence titration

Variations in fluorescence intensity were monitored as a function of pH for 2-(pyridyl)phenylphosphinic acid (32), 6-(2-methylpyridyl)phenylphosphinic acid (33) and 6-(2-methylpyridyl)phenylthiophosphinic acid (34) starting at low pH by addition of trifluoroacetic acid and moving to high pH by incremental addition of sodium hydroxide solution. The variation in emission intensity was then monitored as a function of pH, between 1 and 10.

6-(2-Methylpyridyl)phenylphosphinic acid (33)

For ligand (33) a comparison of the fluorescence emission (λ_{ex}=270nm, λ_{ex}=280-550nm, slits = 8nm) spectra at pH 1.36, 4.03 and 9.03 is shown below (figure 5.12).

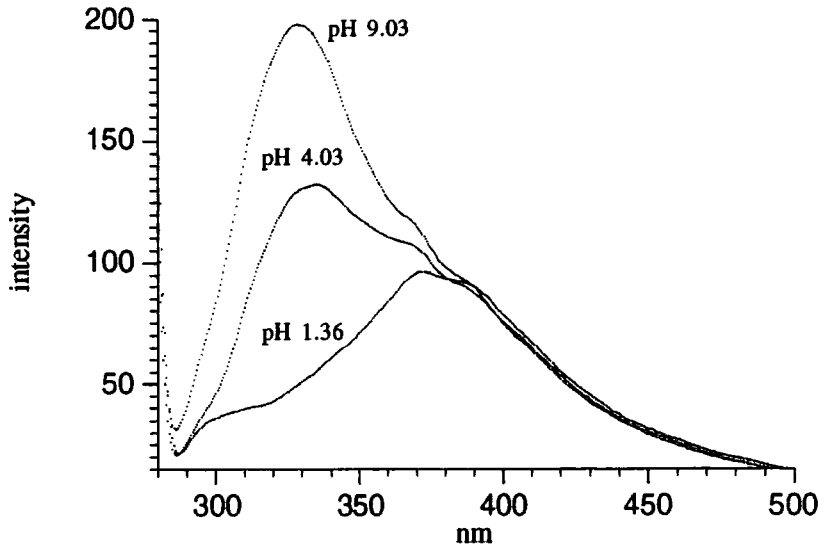

Figure 5.12 Comparison of emission spectra for ligand (33) at different pH (λ_{ex}=270nm, λ_{ex}=280-550nm, 90% H_2O, 10% MeOH)

This shows a large increase in the fluorescence intensity and a substantial hypsochromic shift of 45nm. A plot of the change in emission intensity at 328nm against pH is shown below (figure 5.13).

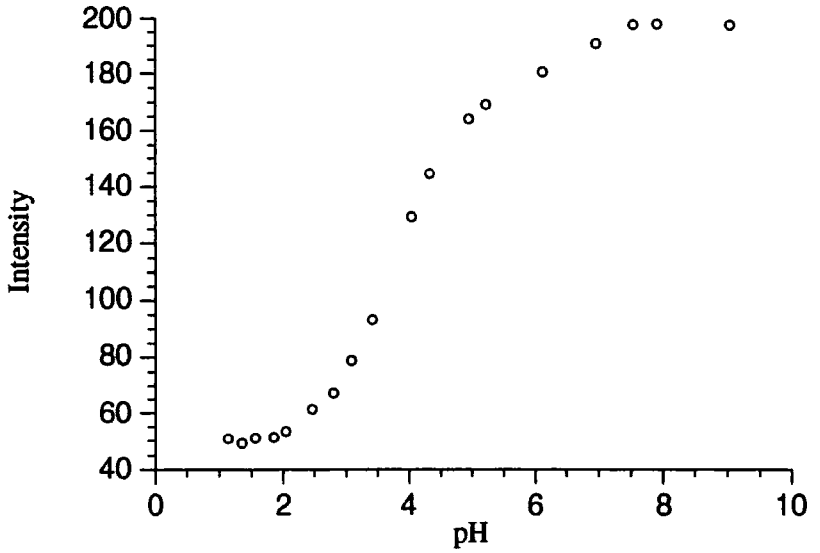

Figure 5.13 Variation in fluorescent intensity against pH at 328nm for (33) (λ_{ex}=270nm, λ_{ex}=280-550nm, 90% H_2O, 10% MeOH)

The profile obtained for the 6-(2-methylpyridyl)phenylphosphinic acid (33) is similar in form to that obtained for the corresponding methyl substituted quinoline ligand (31, Ch. 4.5.2). The pyridine chromophore is essentially similar to the quinoline chromophore and the same arguments can be applied to this system to explain the observed change in intensity as described previously (Ch. 4.5.2). Between pH 1 and 3 there is a slight increase in intensity, which rises rapidly between pH 3 and pH 5.5, and increases steadily from pH 5.5 to 9. A summary of the likely species present in solution is shown below (figure 5.14).

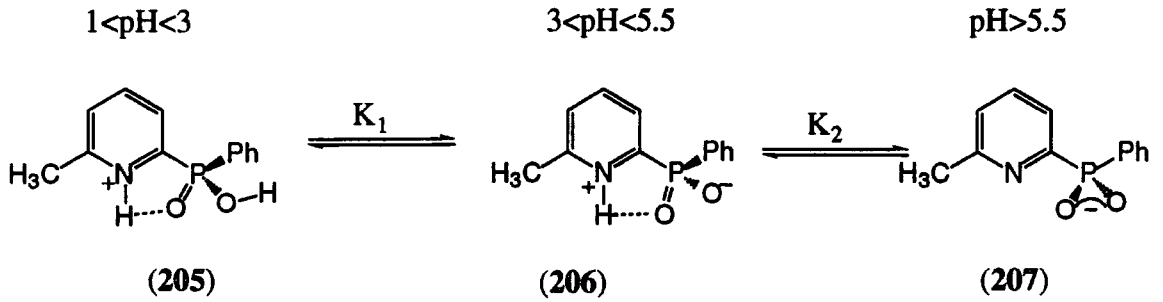

Figure 5.14 Possible species in solution at different pH for (33)

As with quinoline, the fluorescence intensity decreased when the nitrogen was protonated. The first rise in intensity (1<pH<3) is associated with deprotonation of the

phosphinic acid, and may be related to extended conjugation of the system and a resultant increase in intensity. In the pH range 3<pH<5.5 disappearance of the zwitterionic form allows formation of the anionic form (207) with a much larger increase in intensity. This rise is attributable to effect of protonation on the relative energy levels of the HOMO and LUMO of the system.* For the pyridinium cation both the HOMO and the LUMO are lowered in energy relative to the unprotonated species with a concomitant decrease in the energy gap of 0.43 eV. This decrease in the energy gap in the π–π^* transition results in the observed increase and shift in the emission intensity.

From observation of the change in fluorescence emission at 328nm (figure 5.13) the pKa values of the phosphinic acid and pyridyl nitrogen can be estimated. The first, slight rise in intensity is due to the phosphinic acid deprotonation and the pK_a can be estimated to be about 3, whereas the second large increase in intensity is due to the deprotonation of the pyridinium cation (pK_2), which is estimated to be 5.5. It must be rembered that these estimations correspond to excited state pK_as, which should be in close agreement to the ground state values.

2-(pyridyl)phenylphosphinic acid (32)

Performing the same experiment for 2-(pyridyl)phenylphosphinic acid (32) produced a similar variation in intensity and wavelength shift. In this case the pyridyl chromophore was excited at 260nm and the fluorescence emission monitored between 270 and 550nm. On moving from low to high pH a hypsochromic shift of 65nm with an associated increase in intensity was observed. The absorption maximum at low pH was at 389nm, whilst at high pH the absorption maxima shifted to 324nm. A plot of the change in intensity at 328nm against pH is shown below (figure 5.15).

The pH profile obtained for 2-(pyridyl)phenylphosphinic acid (32) is similar in form for that observed for 6-(2-methylpyridyl)phenylphosphinic acid (33, figure 5.14). As such the variations in fluorescence intensity will be due to same variations in structure with increasing pH. This comparison is valid as the only difference between the two ligands is the 2-methyl substituent, which will not affect the protonation processes but may influence the observed pK_a values.

The second, much more rapid rise in intensity is due to formation of the free base pyridine or anionic form of the ligand (207, figure 5.14). Analysis of this second portion

* The HOMO and LUMO energies of the pyridine and pyridinium cation were calculated using the Cache program with MOPAC and the AM1 force field. The HOMO and LUMO energies of pyridine were calculated to be -10.1 and -0.01 eV and for the pyridinium cation -15.78 and -6.10 eV respectively

of the curve gives an estimate of the pK_a for the excited ligand, which is estimated to be 5.2.

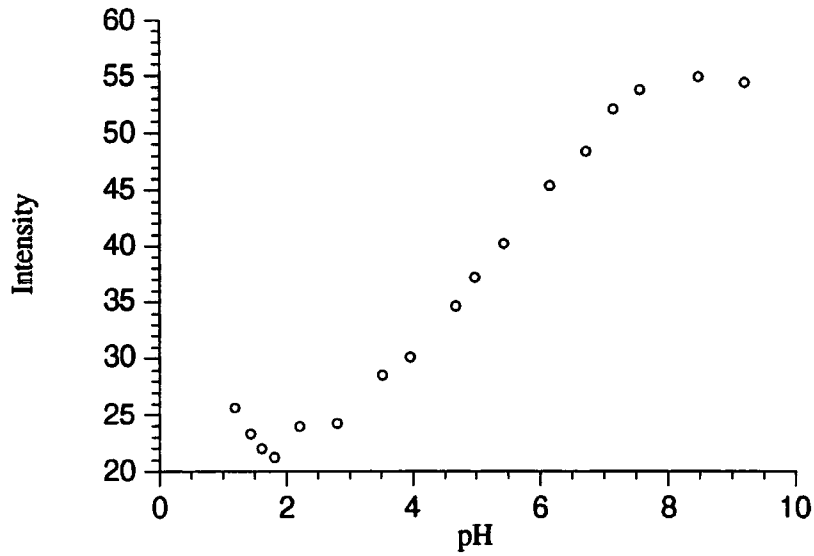

Figure 5.15 Variation of intensity at 328nm against pH for (32) (λ_{ex}=270nm, λ_{ex}=280-550nm, 90% H_2O, 10% MeOH)

Although the estimated pK_a values of the phosphinic acid groups are similar for both systems, the pK_a of the pyridyl nitrogen differs by 0.3 of a pK_a unit. The phosphinic acids are in a similar environment in both cases, and the acidity constants would be expected to be similar. The origins of the difference between the two pyridyl nitrogens may be associated to the 2-methyl substituent, which has a positive inductive effect on the pKa of the nitrogen atom. The increased induction from the methyl group has the effect of raising the pKa of the methyl substituted ligand (33) relative the unsubstituted derivative (32). This effect has been observed in similar systems; for instance when comparing 2-methyl picolinic acid and picolinic acid, the respective protonation constants for nitrogen are 5.95 and 5.21.[27]

6-(2-methylpyridyl)phenylthiophosphinic acid (34)

A similar experiment was performed for 6-(2-methylpyridyl)phenylthiophosphinic acid (34). In this case the pyridyl chromophore was excited at 270nm and the fluorescent emission monitored between 280 and 500nm, with emission and absorption slit widths of 8nm and a scan speed of 120nmmin^{-1}. Selected spectra (at pH 2.60, 3.84, 8.42 and 5.51) are shown below (figure 5.16).

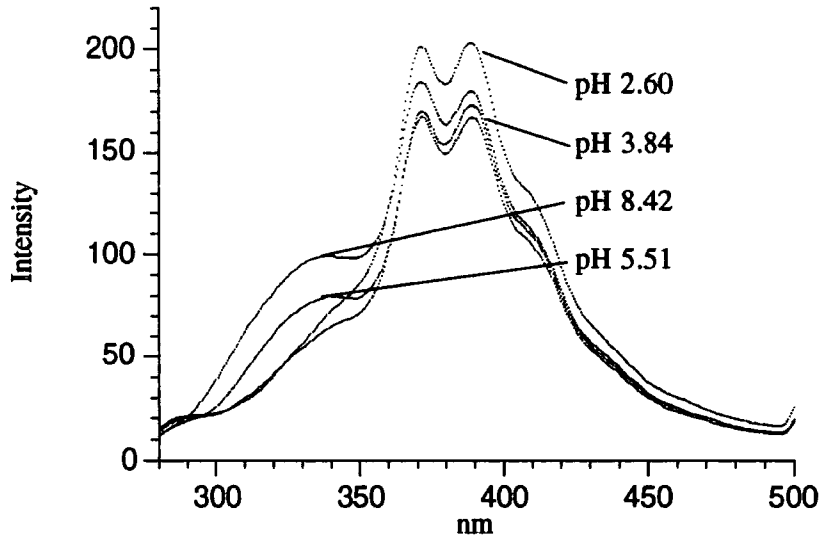

Figure 5.16 Spectra of (34) at various pH (λ_{ex}=270nm, λ_{ex}=280-500nm, 90% H_2O, 10% MeOH)

There is a marked difference between the emission spectra observed for the thiophosphinic acid derivative (34) and the previous two phosphinic acid appended ligands. The structure of the emission is different, possessing maxima at 327, 370 and 388nm, as opposed to the two maxima observed for the phosphinic acid ligands (32) and (33).

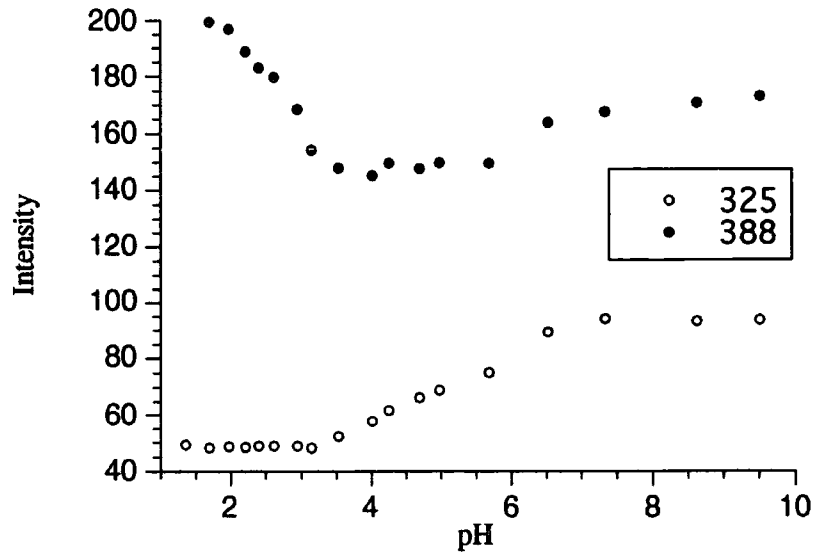

Figure 5.17 Change in intensity at 325 and 388nm for (34) as a function of pH (λ_{ex}=270nm, λ_{ex}=280-500nm, 90% H_2O, 10% MeOH)

In the pH range 0<pH<3.4 the only change in the emission spectra is a change of intensity of the maxima at 370 and 388nm, whereas above pH 3.4 a second peak appears at 327nm. A plot of the change in intensity against pH at 325 and 388nm is shown above (figure 5.17).

For this set of ligands there are two potential functionalities from which an electron can be formally excited (in a valence bond model), the pyridyl ring or the P=X (X = S or O) double bond. Both are π–π^* transitions, and the propensity for either of these transitions to occur depends on the oxidation potential of the ground state (or reduction potential of the excited state). For the phosphinic and thiophosphinic acid appended ligands in the pH range 1<pH<4 the pyridyl ring will be protonated. For the thiophosphinic acid ligand (34) in this pH range it seems a π–π^* transition originating from the P=S double bond is the lowest energy transition. This results in a decrease in the fluorescence intensity at 388nm, while the emission at 325nm (due to the pyridyl chromophore) is unaffected. However above pH 3.5 the intensity at 388nm is relatively unaffected compared to the intensity at 325nm, which increases. This implies that as the proportion of free pyridine ring in solution increases the aromatic π–π^* transition becomes the lowest energy transition. This allows for an easy estimate of the excited state pK_as of both the thiophosphinic acid and pyridyl nitrogen, which should be in close agreement with the ground state values. Analysis of the drop in fluorescence intensity at 388nm allows an estimation of the pK_a of the thiophosphinic acid, which is approximately 2.5. The increase in intensity at 325nm is associated with the pyridyl nitrogen , and gives an approximate value of 5.4 for the pK_a. The acidity constants for this ligand are in agreement with the nitrogen protonation constants for 6-(2-methylpyridyl)phenylphosphinic acid (33), and the value for the thiophosphinic acid is consistent with literature values for diaryl thiophosphinic acids.[28]

Zinc fluorescence titrations

Fluorescence titrations with the three ligands (32), (33) and (34) with added zinc will give information about how the pyridyl nitrogen is interacting with the metal in solution.

6-(2-methylpyridyl)phenylphosphinic acid (33)

For 6-(2-methylpyridyl)phenylphosphinic acid (33) the fluorescent emission spectra at all M/L ratios is shown below (figure 5.18). The pyridyl chromophore was excited at 270nm and the emission was monitored between 280 and 550nm with emission and absorption slit widths of 5nm and a scan speed of 120nm min^{-1}.

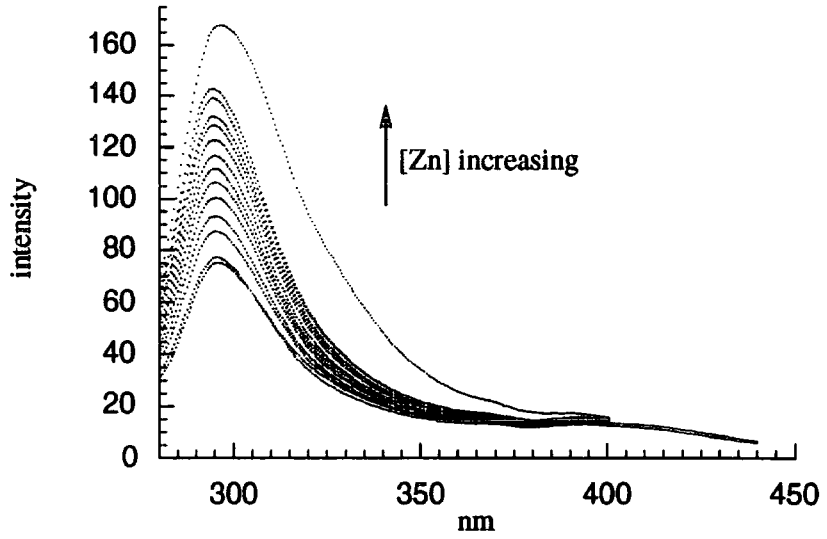

Figure 5.18 Variation of intensity for all M/L ratios for (33) plus added $Zn(ClO_4)_2$ (λ_{ex}=270nm, λ_{ex}=280-550nm, 90% MeOH, 10% H_2O)

With the addition of zinc to the ligand solution there is an increase in fluorescence intensity at 294nm, without any shift in the wavelength. The addition of zinc displaces the hydrogen bonded solvent and forms a chelate ring with the ligand, chelation effectively locks the conformation of the ligand and restricts internal rotation and vibration modes. This leads to a chelation enhanced fluorescence effect (CHEF) with a 2.3 fold increase in fluorescent intensity.[29, 30] Coordination of zinc to the nitrogen lone pair will have a similar effect on the frontier orbitals as described for the proton. This decreased energy gap will be more pronounced for the zinc atom because of its +2 charge, resulting in a greater fluorescence emission intensity. Plotting the change in intensity at 294nm against the M/L ratio should give an indication of the stoichiometry at this concentration (figure 5.19)

From the plot (figure 5.19) there is a rise in emission intensity until M/L=1 is reached, after this the curve is less steep. From NMR studies (*vide supra*) it appears that this ligand is forming a weak ML_2 complex with zinc, followed by ML complex formation at higher metal concentrations. The fluorescence titration seems to indicate that the system is forming a weak ML complex. As the concentration of the ligand in this titration is 1000 times less than in the NMR titration, and assuming that the equilibrium constant for ML_2 formation is small, then little of this complex species may be present.

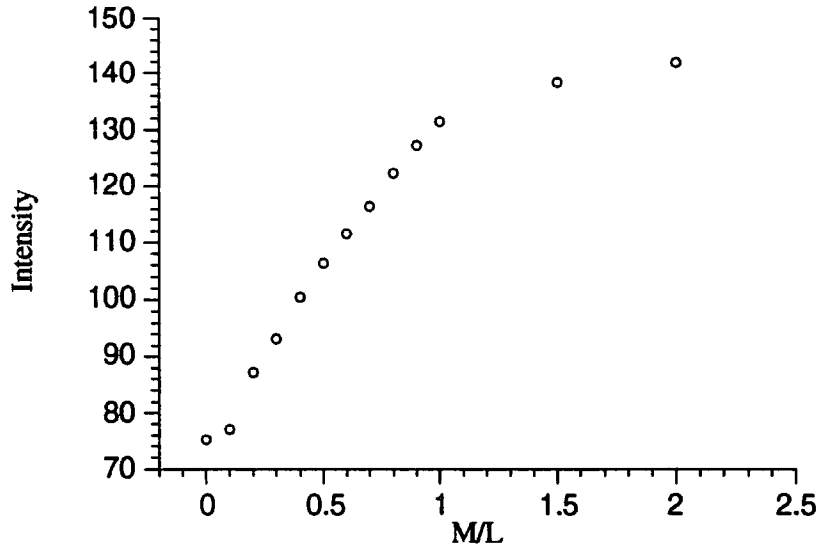

Figure 5.19 Variation in fluorescence intensity with added Zn for (33) at 294nm (λ_{ex}=270nm, λ_{ex}=280-550nm, 10% H_2O, 90% MeOH)

2-(pyridyl)phenylphosphinic acid (32)

An analogous titration for 2-(pyridyl)phenylphosphinic acid (32) was carried out. Excitation of the pyridyl chromophore at 260nm resulted in fluorescence emission which was monitored between 270 and 400nm.

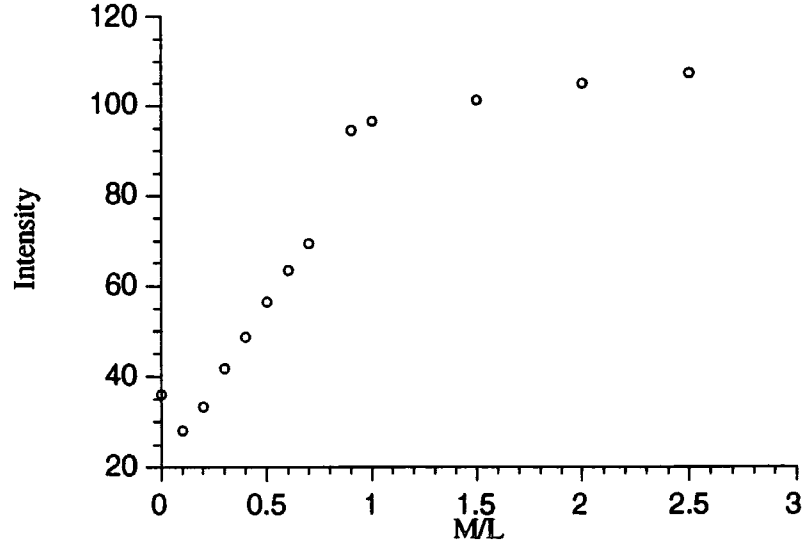

Figure 5.20 Variation of emission intensity at 294nm for (32) with addition of $Zn(ClO_4)_2$ (λ_{ex}=260nm, λ_{ex}=270-400nm, 10% H_2O, 90% MeOH)

Incremental addition of zinc(II)perchlorate produced a similar increase in the emission intensity as for the previous case. The emission maximum at 294nm increased between M/L=0 and M/L=1 with a slight rise between 1 and 3. Chelation of the zinc atom caused a CHEF effect,[29, 30] and a 4.1 fold increase in fluorescence intensity, with an associated contribution by the perturbation of the energy gap between the frontier orbitals. Plotting the change in emission intensity at 294nm against the metal to ligand ratio provides information regarding the stoichiometry of this ligand in solution (figure 5.20).
The form of the titration profile for 2-(pyridyl)phenylphosphinic acid (32) is similar to that for 6-(2-methylpyridyl)phenylphosphinic acid (33), and similar arguments can be applied to this system. From the NMR titration a relatively strong ML complex appears to form and this is mirrored in the fluorescence data. The profile increases until M/L=1 then only a slight after this, consistent with a 1:1 stoichiometry. The relative size of the 1:1 formation constant can be compared by contrasting the respective increase in fluorescence intensity. The unsubstituted ligand has a maximum 4.1 enhancement of intensity, whereas the methyl substituted ligand only creates a 2.3 fold increase.

6-(2-methylpyridyl)phenylthiophosphinic acid (34)

The same experimental procedure for 6-(2-methylpyridyl)phenylthiophosphinic acid (34) was carried out as for the previous two systems examined. The pyridyl chromophore was excited at 260nm and emission intensity monitored between 270 and 450nm.

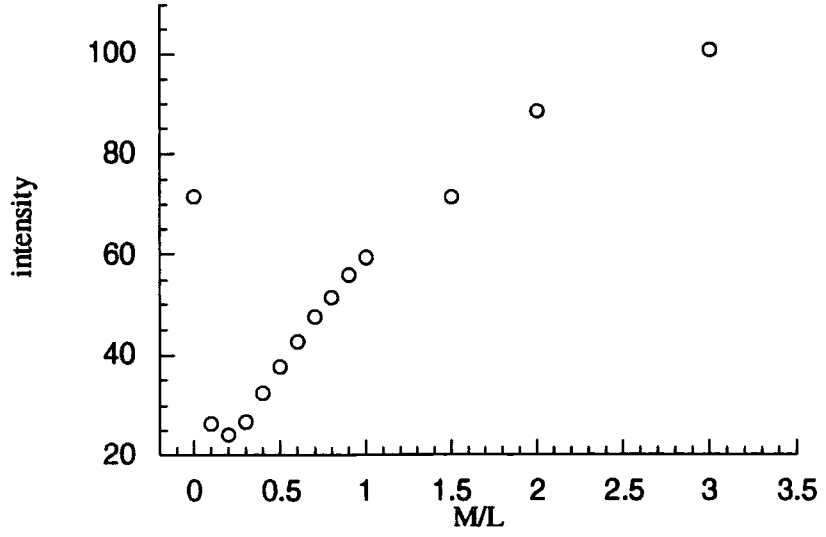

Figure 5.21 Variation in intensity for (34) with incremental addition of $Zn(ClO_4)_2$ at 309nm

Addition of zinc(II) perchlorate to the ligand solution caused an increase in the observed emission intensity at 309nm, which is the pyridyl emission band. A 4 fold increase in fluorescence intensity was observed again attributable to a combination CHEF effect and the perturbation of the energies of the frontier orbitals.[29, 30] A plot of emission intensity at 309nm against M/L ratio is shown below (figure 5.21).The shape of the curve is similar to the previous two examples. The stoichiometry at this concentration seems to be 1:1, which is in contrast to the NMR data (*vide supra*). In this example, the concentration of the ligand is 1000 times less than that for the NMR titration, and although ML_2 species may be in solution they are reacting further to form ML complex species with the addition of more metal.

1.5.3 UV and Visible Spectroscopy

Analysis of the free ligands, (32), (33) and (34) and their metal complexes by UV spectroscopy provides a further tool to probe the interaction of the pyridyl nitrogen with metals in the ground state. If the nitrogen atom binds the metal there will be a perturbation of the ground state molecular orbital, which will affect the absorption properties of the ligand. Fluorescence and UV spectroscopy were both carried out in Analar methanol and at the same concentration to allow consistent comparison of the two data sets.

2-(pyridyl)phenylphosphinic acid (32)

The UV absorption maxima for the free ligand (32) and the complexes with zinc, copper, nickel, cobalt and iron(III) perchlorates are summarised below, giving the absorption maxima and molar extinction coefficients (table 5.1)

In solution free pyridine has 2 major absorption bands, a B-band at 257nm and a weaker R-band which is often swamped by the B-band in solution.[31] The transitions responsible for these two transitions are π–π^* and n-π^* respectively. Comparison of the ligand (32) with free pyridine shows a large hypsochromic shift by approximately 50nm.

With the addition of a molar equivalent of zinc, nickel or cobalt to (32) there is only a slight change in the absorption maxima, there is a slight hyperchromic shift of the B-band while the R-band is relatively unaffected

For copper there is a large hyperchromic shift of the B-band, with the appearance of an intense shoulder at 220nm. The R-band experiences a slight hyperchromic shift, indicating that coordination of the nitrogen is occurring.

With the addition of a molar equivalent of iron (III) perchlorate a similar spectrum was recorded as for the previous examples, with both the B- and R-bands exhibiting minor hyperchromic shifts.

Ligand		Zinc(II)		Copper(II)	
λ_{max}/nm	ε/dm^{3}M^{-1}	λ_{max}/nm	ε/dm^{3}M^{-1}	λ_{max}/nm	ε/dm^{3}M^{-1}
208	14500	208	14500	207	17570
267	6860	271	6540	220 (s)	15600
320	1436	322	1196	264	7980
				327	1170

Nickel(II)		Cobalt(II)		Iron(III)	
λ_{max}/nm	ε/dm^{3}M^{-1}	λ_{max}/nm	ε/dm^{3}M^{-1}	λ_{max}/nm	ε/dm^{3}M^{-1}
207	17570	207	15400	208	15800
267	7150	268	7060	268	7830
308	1950	311	1950	323	1270

Table 5.1 UV absorption maxima for (32) as the free ligand and in the presence of metal ions (MeOH, 298K)

6-(2-methylpyridyl)phenylphosphinic acid (33)

The UV absorption maxima for the free ligand (33) and the complexes with zinc, copper, nickel, cobalt and iron(III) perchlorates are summarised below, giving the absorption maxima and molar extinction coefficients (table 5.2)

Comparison of the free ligand with pyridine shows a bathochromic shift of the R-band by approximately 10nm; this type of shift has been observed when comparing pyridine to 2-methylpyridine in solution.[31]

With the addition of a molar equivalent of zinc to the ligand solution the wavelength of the absorption maxima remain unchanged, whereas there is a marked hypochromic effect for both the B- and the R-band. The decrease in the extinction coefficient with the addition of zinc implies that coordination of the metal is perturbing the ground state molecular orbital, which affects the absorption characteristics of the system. A

comparison of the UV spectra of the free ligand (33) and the zinc complex is shown below (figure 5.22).

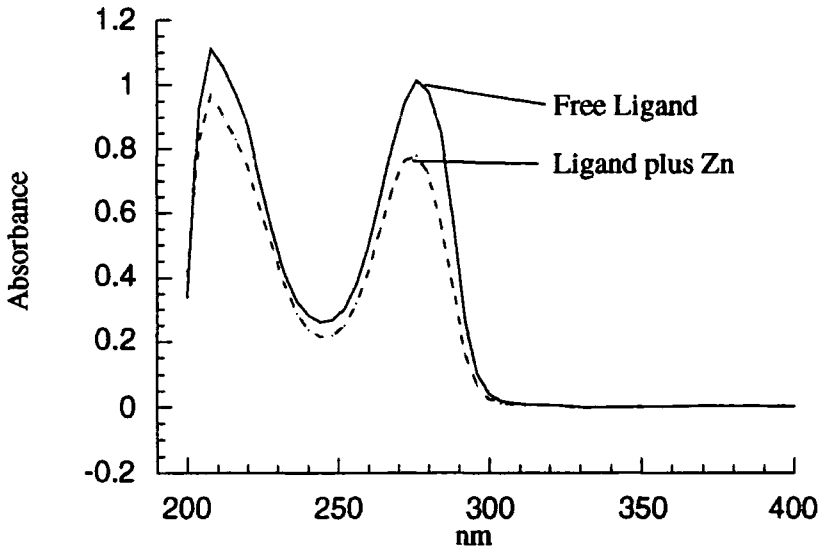

Figure 5.22 Comparison of UV spectra for (33) and (33) plus zinc (298K, CH_3OH)

Ligand		Zinc(II)		Copper(II)	
λ_{max}/nm	ε/dm^{3}M^{-1}	λ_{max}/nm	ε/dm^{3}M^{-1}	λ_{max}/nm	ε/dm^{3}M^{-1}
207	11000	207	9600	206	13400
275	10100	275	7700	270	9400
				300 (s)	970
Nickel(II)		**Cobalt(II)**		**Iron(III)**	
λ_{max}/nm	ε/dm^{3}M^{-1}	λ_{max}/nm	ε/dm^{3}M^{-1}	λ_{max}/nm	ε/dm^{3}M^{-1}
207	11500	207	11850	207	15600
275	9690	276	9200	220 (s)	13700
				270	9490

Table 5.2 UV absorption maxima for (33) as the free ligand and in the presence of metal ions (MeOH, 298K)

With the addition of nickel, cobalt and copper to the free ligand the absorption maxima for the B- and the R-band remain unchanged. In all three cases there is an observed hyperchromic effect for both bands which implies that the bound metal is affecting the ground state molecular orbital.

Addition of iron perchlorate to the ligand solution does not produce a substantially different spectrum. There is an increase in the molar extinction coefficient for the B-band, with appearance of a slight shoulder at 220nm and the R-band remains unaffected

6-(2-methylpyridyl)phenylthiophosphinic acid (34)

The UV absorption maxima for the free ligand (34) and the complexes with zinc, copper, nickel, cobalt and iron(III) perchlorates are summarised below, giving the absorption maxima and molar extinction coefficients (table 5.3).

Ligand		Zinc(II)		Copper(II)	
λ_{max}/nm	ε/dm^{3}M^{-1}	λ_{max}/nm	ε/dm^{3}M^{-1}	λ_{max}/nm	ε/dm^{3}M^{-1}
208	10000	208	11000	208	14680
220 (s)	7800	222 (s)	8100	224 (s)	11060
268	7100	263	7010	263	8290
		271 (s)	6200	271	6805

Nickel(II)		Cobalt(II)		Iron(III)	
λ_{max}/nm	ε/dm^{3}M^{-1}	λ_{max}/nm	ε/dm^{3}M^{-1}	λ_{max}/nm	ε/dm^{3}M^{-1}
208	12700	208	12550	209	17070
223 (s)	8800	223 (s)	8800	222 (s)	13500
264	6500	264	6500	257	9600
				338 (br)	2040

Table 5.3 UV absorption maxima for (34) as the free ligand and in the presence of metal ions (MeOH, 298K)

Comparison of the free ligand (34) to pyridine shows an unchanged B-band with a shoulder at 220nm, which is presumably attributable to the thiophosphinic acid functionality and a red shifted (by 10nm) R-band.[31]

With the addition of a molar equivalent of nickel, copper and cobalt there is an increase in the molar extinction coefficient for the B-band, whilst the R-band remains unaffected. This implies that coordination of the pyridyl nitrogen is perturbing the ground state, which gives rise to this change in extinction coefficient. A comparison of

the UV spectra for the free ligand and the copper complexes is shown below (figure 5.23).

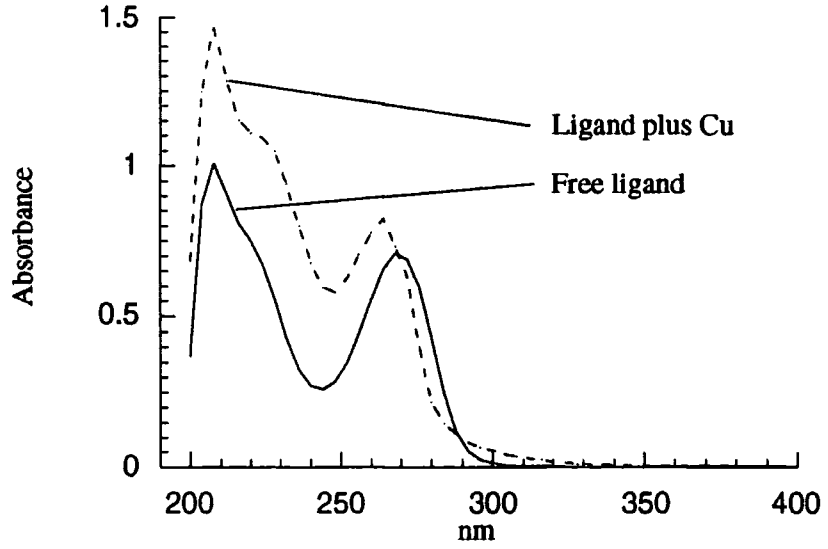

Figure 5.23 Comparison of (34) and (34) plus Cu (298K, CH_3OH)

With the addition of zinc the wavelength of the absorption maxima remains unchanged relative to the free ligand. However there is an observed hypochromic effect for both the B- and the R-bands. The spectrum for the iron complex is similar to that observed for the copper complex, with a large increase in the extinction coefficient for the B-band and a relatively unchanged R-band.

1.5.4 Electrospray Mass Spectroscopy

Complexation and electrospray analysis was carried out with (32) and (33) using zinc, copper, nickel and ferric perchlorate. Stock solutions of the ligands and metal salts were prepared with concentrations of the order 1mM. One to one stoichiometries of the metal complexes were prepared and the solutions diluted to make a final concentration of 0.01mM. Mass spectra were recorded in both the positive and negative ionisation modes. In this case, the negative ionisation spectra provided the best results.

2-(pyridyl)phenylphosphinic acid (32)

Zinc

With zinc the major species observed was the ML complex which was associated with two chloride ions occurring at 88% intensity. The ML_2 complex was also observed, (73%), associated with a single chloride ion. The deprotonated ligand was also observed

at a low intensity (14%). Good agreement between observed and theoretical isotope pattern (figure 5.24) was obtained.

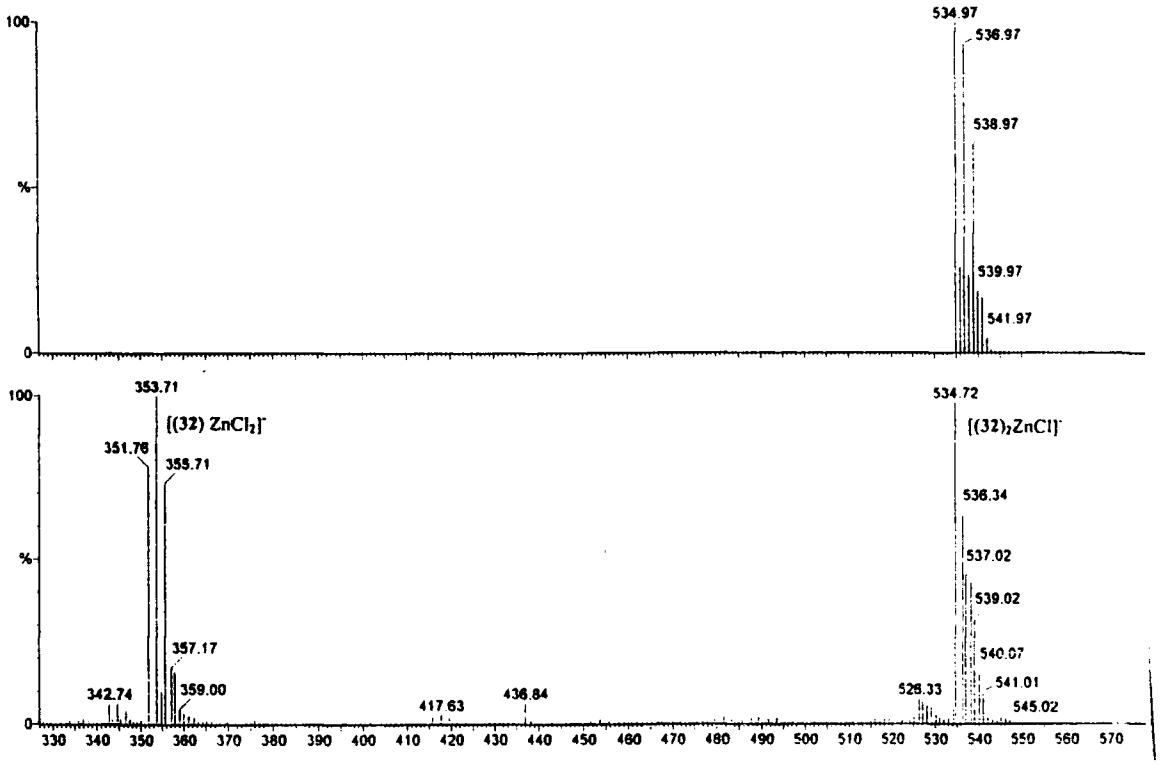

Figure 5.24 Observed $[(32)ZnCl_2]^-$ and $[(32)_2ZnCl]^-$ (lower) and calculated isotope patterns (above)

Copper and nickel

For copper and nickel the major species observed was the deprotonated ligand at 100% intensity. In both cases, no signal due to $[LMCl_2]^-$ was detected. However, $[L_2MCl]^-$ signals were observed in both cases. The observed relative intensities for these two species was 59 and 53% respectively for copper and nickel.

Iron

For iron a variety of species were observed in the mass spectrum. Signals corresponding to $[LFeCl_3]^-$, $[L_2FeCl_2]^-$, $[L_3FeCl]^-$ and $[L_4Fe]^-$ with intensities of 4, 8, 7 and 3% respectively. The major species observed was the free, anionic ligand. The range of species observed with iron and (32) implies that the absence of the methyl substituent does not impose any geometric constraints on the ligand.

A summary of all the major species observed in ESMS with 2-(pyridyl)phenyl-phosphinic acid (32) is tabulated below (table 5.4).

Metal	Species	Obs. Mass	Calc. Mass	Rel. Intensity
Zn	$[L]^-$	217.94	217.83	14%
	$[LZnCl_2]^-$	353.71	353.71	88%
	$[L_2ZnCl]^-$	534.72	534.97	73%
Cu	$[L]^-$	217.89	217.83	100%
	$[L_2CuCl]^-$	533.71	533.97	59%
Ni	$[L]^-$	217.91	217.83	100%
	$[L_2NiCl]^-$	528.71	528.98	53%
Fe	$[L]^-$	217.97	217.83	100%
	$[LFeCl_3]^-$	378.77	378.88	4%
	$[L_2FeCl_2]^-$	561.67	561.95	8%
	$[L_3FeCl]^-$	744.62	745.01	7%
	$[L_4Fe]^-$	928.13	928.01	3%

$ESMS^-$ cone voltage 30V, source temperature 60°C

Table 5.4 Summary of species observed in $ESMS^+$ for (32)

6-(2-methylpyridyl)phenylphosphinate (33)

Copper and nickel

For both copper and nickel the major species detected corresponds to the free ligand, $[L]^-$, which appears at 100% intensity. For nickel signals were detected for $[LNiCl_2]^-$ and $[L_2NiCl]^-$ at 8 and 6% intensity respectively. Copper only had signals corresponding to the free ligand and $[L_2CuCl]^-$ at 100% and 76% respectively.

Iron

With iron only two signals were detected, $[L]^-$ and $[L_2FeCl]^-$ at 100 and 3% respectively. There were no signals at higher mass. The incorporation of the 2-methyl substituent seems to be preventing formation of coordination numbers higher than four.

Zinc

With added zinc the major species detected was the deprotonated ligand, which has a relative intensity of 100%. Signals corresponding to $[LZnCl_2]^-$ and $[L_2ZnCl]^-$ were also observed with relative intensities of 27 and 18% respectively. There is excellent agreement between the observed isotope distribution and the calculated theoretical isotope pattern (figure 5.25).

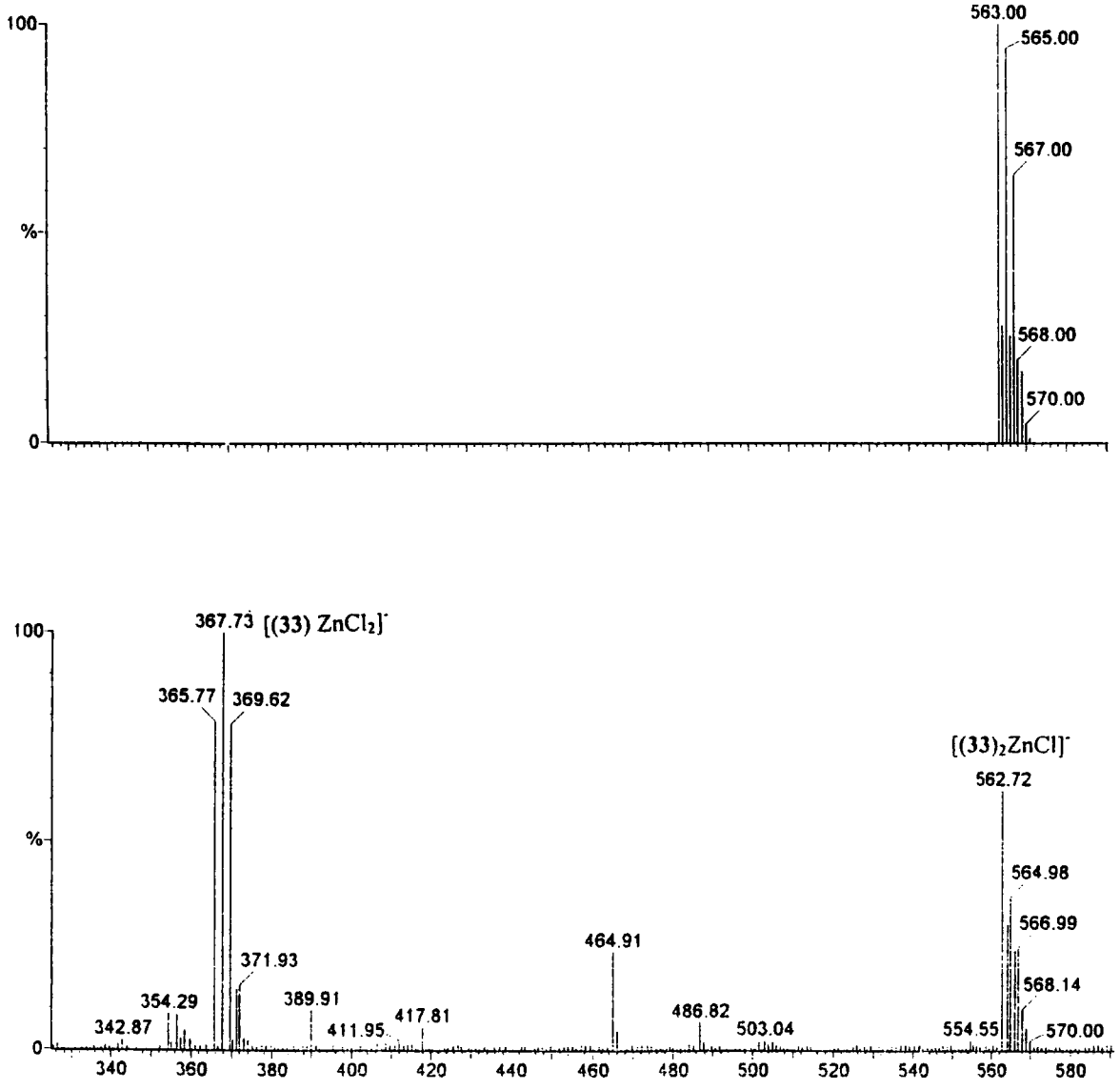

Figure 5.25 Observed $[(33)ZnCl_2]^-$ and $[(33)_2ZnCl]^-$ (lower) and isotope pattern (above)

A summary of the major species observed in ESMS$^-$ for 6-(2-methylpyridyl)phenyl-phosphinic acid (33) are tabulated below (table 5.5).

Metal	Species	Obs. Mass	Calc. Mass	Rel. Intensity
Zn	$[L]^-$	231.93	231.92	100%
	$[LZnCl_2]^-$	367.73	367.93	27%
	$[L_2ZnCl]^-$	562.72	563.00	18%
Cu	$[L]^-$	231.96	231.92	100%
	$[L_2CuCl]^-$	561.77	562.00	76%
Ni	$[L]^-$	231.96	231.92	100%
	$[LNiCl_2]^-$	361.75	361.92	8%
	$[L_2NiCl]^-$	556.48	557.01	6%
Fe	$[L]^-$	231.94	231.92	100%
	$[L_2FeCl]^-$	554.71	555.01	3%
	No higher species			

ESMS$^-$ cone voltage 30V, source temperature 60°C

Table 5.5 Summary of species observed in ESMS$^-$ for (33)

5.5.5 Liquid-Liquid Extraction

In order to assess the ligand's ability to transport metals across a liquid-liquid interface lipophilic analogues need to be synthesised which will allow good solubility in organic solvents. The lipophilicity of the pyridyl derived ligands (32) and (33) must be modified in such a way that the binding site is unaffected. It was envisaged that modification of the phosphinic acid functionality would be the most desirable position for manipulation of the lipophilicity.

There are a number of reported procedures for the synthesis of substituted ethyl phosphinous esters, with the final step in the synthetic sequence being reaction between a substituted phosphorus dichloride derivative and ethanol (Ch. 2.3). A more attractive approach involves formation of an intermediate aryl-diethyl phosphonite, followed by acid hydrolysis to give the desired lipophilic phosphinous ester.

The preparation of 4-dodecoxybromobenzene was accomplished using the procedure of Bates,[32] deprotonation of *para*-bromophenol (211) with sodium ethoxide in ethanol

followed by quenching with the commercially available dodecylbromide (212), gave 4-dodecoxybromobenzene (213) in high yield following recrystallisation from 40-60 petroleum ether. Grignard formation was achieved by reaction of (213) and magnesium turnings at reflux temperature, cannulated addition of the Grignard solution to diethyl chlorophosphonite gave the intermediate phosphine (214), which was characterised by ^{31}P NMR spectroscopy (δp=160.2ppm). Treatment of the P(III) intermediate with dilute hydrochloric acid (1M) at room temperature gave the desired lipophilic phosphinous ester (215) in 58% overall yield, following recrystallisation from 40-60 petroleum ether at -18°C (scheme 5.9).

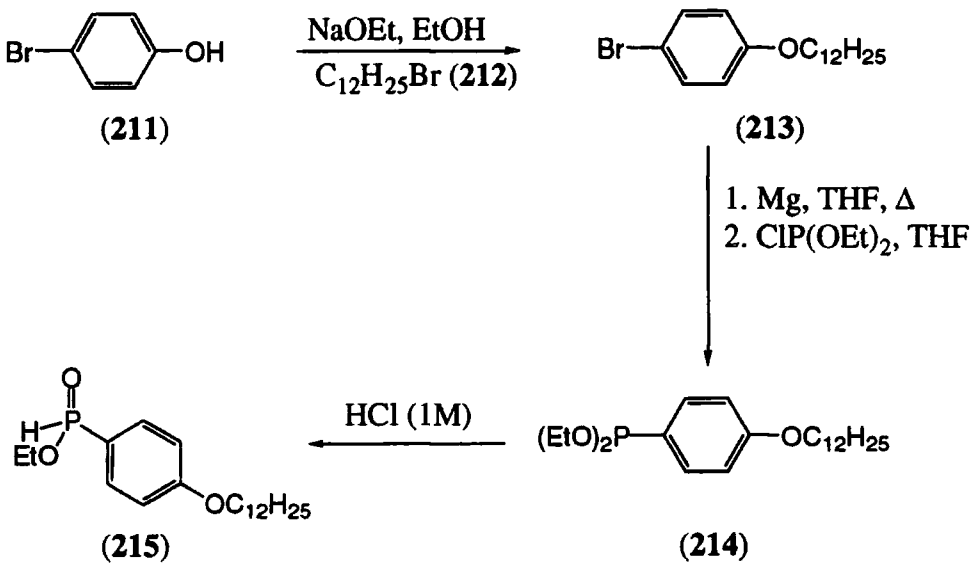

Scheme 5.9 Preparation of ethyl 4-(dodecoxybenzene)phenylphosphonite (215)

Synthesis of the lipophilic phosphinate esters was accomplished as previously described (*vide supra*), by palladium catalysed coupling with (215) and 6-bromo-2-methylpyridine (198) and 2-bromopyridine (197) in the presence of $Pd(PPh_3)_4$ and triethylamine.[12] Purification of the products by flash chromatography gave the phosphinate esters (216) and (217) in 25 and 23% yield respectively (scheme 5.10).

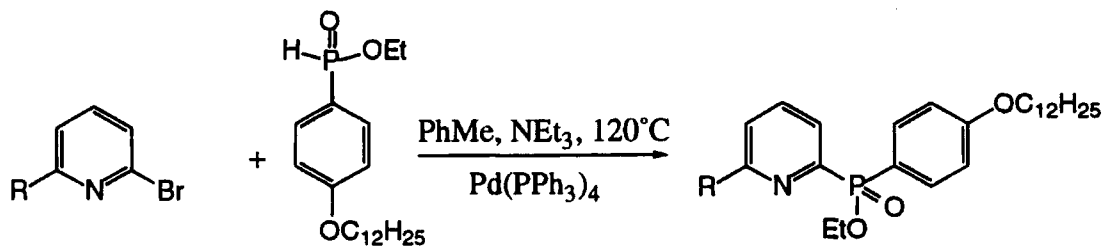

(**197**) R = H
(**198**) R = CH_3

(**215**)

(**216**) R = H
(**217**) R = CH_3

Scheme 5.10 Synthesis of lipophilic pyridyl ligands (216) and (217)

Subsequent ester hydrolysis using a 3:2 (v/v) mixture of 1,4 dioxane and hydrochloric acid (10M), gave the target compounds (218) and (219) in near quantitative yield as their hydrochloride salts, following removal of the solvent (scheme 5.11).

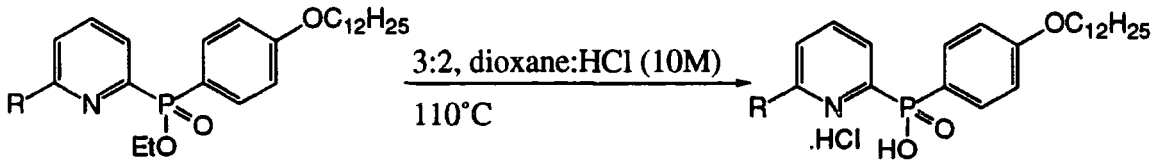

(**216**) R = H
(**217**) R = CH_3

(**218**) R = H
(**219**) R = CH_3

Scheme 5.11 Acid hydrolysis of (216) and (217) to produce the target ligands (218) and (219)

Unfortunately when extraction tests were performed with both of these ligands in either hexane, dichloromethane or toluene an inseparable emulsion was obtained at all pH values examined. In order to try and overcome this problem of aggregation, a derivative with a branched side chain was synthesised.

Reaction of 2-ethylhexylbromide (220) with magnesium turnings in diethylether produced the corresponding Grignard species. Cannulated addition of the Grignard reagent to a solution of diethyl chlorophosphonite, gave the intermediate P(III) species. Acid hydrolysis (1M, HCl) produced ethyl (2-ethylhexl)phosphonite (222) in 81% yield (scheme 5.12).

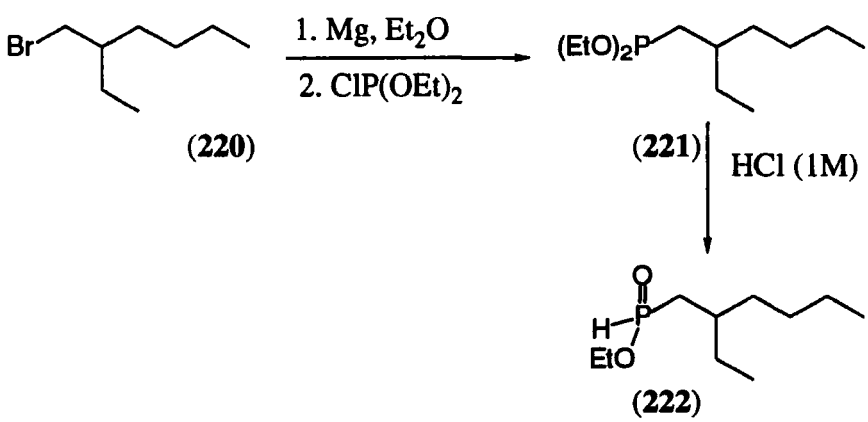

(**220**)

(**221**)

(**222**)

Scheme 5.12 Preparation of ethyl (2-ethylhexyl)phosphonite (222)

Synthesis of the lipophilic phosphinate ester was effected as previously described (*vide supra*), by palladium catalysed coupling between ethyl (2-ethylhexyl)phosphonite (222) and 2-bromopyridine (197) in the presence of $Pd(PPh_3)_4$ and triethylamine. Purification of the product by flash chromatography gave the phosphinate ester in 23% yield. This was hydrolysed in a 3:2 (v/v) mixture of 1,4-dioxane and hydrochloric acid (10M) to

give the target compound (224) in near quantitative yield as the hydrochloride salt. (scheme 5.13)

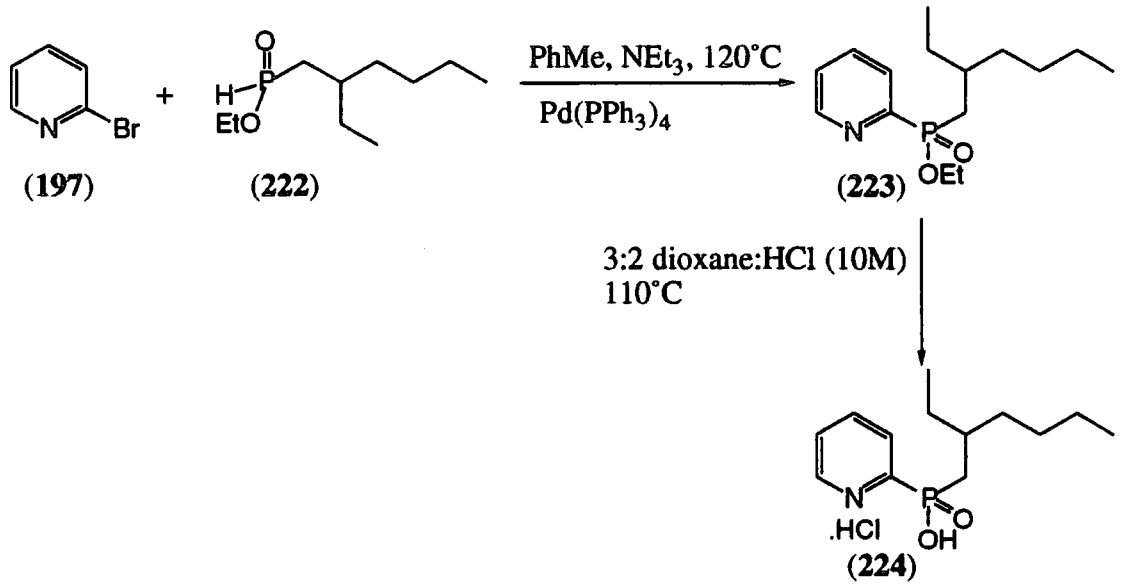

(197) (222) (223) (224)

Scheme 5.13 Acid hydrolysis of (223) to produce the target (224).

In order to assess the ligand's ability to transport zinc across an organic-aqueous interface the ligand was dissolved in toluene to produce a final concentration of 0.1M, and partioned into ten Eppendorf tubes. An equal volume of zinc chloride solution (0.5M) was added to each tube with an increase in the pH of zinc solution between each addition, measurements were taken over the pH range 0.96 to 3.90. For all of the samples examined there was a third milky layer between the organic and aqueous phase. Ion determination of the organic phase revealed zinc concentrations ranging between 40 and 100ppm. Saturation of the organic layer with zinc, assuming 1:1 complex formation, would produce a zinc concentration in the order 10^4ppm. Clearly, the nature of these lipophilic analogous does not auger well for the efficient extraction of zinc into an organic phase.

5.6 Conclusions

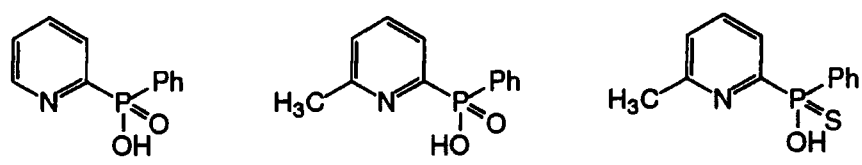

(32) (33) (34)

Figure 5.26 Structures of ligands (32), (33) and (34)

An efficient, high yielding route to pyridyl derived phosphinic acid ligands, (32) and (33), has been developed utilising a versatile palladium catalysed procedure. An

improved method for the conversion of the phosphinic acid into the thiophosphinic acid functionality by *in situ* generation of the phosphinic acid and subsequent sulfur transfer has been successfully investigated. A simple method for producing lipophilic derivatives, by manipulation of the phosphorus substituents has also been developed.

The solution coordination chemistry of the three ligands differs markedly. Analysis of the ligands by ^{31}P NMR spectroscopy indicates that both the methyl substituted ligands, (33) and (34), form predominantly ML_2 complexes in solution, whereas the unsubstituted ligand (32) forms mainly ML species at all metal concentrations. Fluorescence titrations with zinc indicated ML complex formation in all cases. Taking this information together with data obtained from NMR gave a clearer picture. If each ligand forms an ML_2 complex at low metal concentrations, which then goes on to form an ML complex as more metal is added, there will be a shallow increase in the observed emission intensity, which will achieve a turning point when the concentration of the ligand equals the concentration of the metal. If the ligand forms a strong ML complex at all metal concentrations then a steep increase in the curve will be observed, which will reach a maximum at equimolar concentrations of the metal and ligand. It is clear for both of the methyl substituted ligands that ML_2 complex formation is occurring, followed by ML formation. For the unsubstituted ligand (32) ML formation appears to predominate in solution.

The effect of the methyl substituent on complex stoichiometries is highlighted in the ESMS data. For copper, nickel and zinc only ML or ML_2 species were observed in both cases. With iron the unsubstituted ligand (32) forms ML, ML_2, ML_3 and ML_4 species. Incorporation of the methyl substituent inhibits higher ligand:metal stoichiometries, and only signals corresponding to ML_2 species were detected.

The synthesis of two lipophilic analogues of the pyridyl derived ligands using the dodecyl and 2-ethylhexyl solubalising groups was accomplished. However, extraction tests using both of these systems proved difficult with emulsion formation hampering efficient extraction. Unless some modification to these systems is performed, for example by the addition of some lipophilic cations, then their application as extractants will be limited.

5.7 References

1. R. A. Abramovitch; '*Pyridine and its derivatives*', 1974, Wiley-Interscience, New York
2. G. M. Cooper; '*The Cell, A Molecular Approach*', ASM Press, Washington, D.C., 1997, Ch. 10

3. E. Rijnberg, N. J. Neldes, A. W. Kleij, J. T. B. H. Jastrzebski, J. Boersma, M. D. Janssen, A. L. Spek and G. Van Koten; *Organometallics*, 1997, **16**, 2847
4. H. Adams, N. A. Bailey, D. E. Fenton and Q. Y. He; *J. Chem. Soc., Dalton Trans.*, 1996, **13**, 2857
5. M. Yashiro, A. Ishikubo and M. Komiyama; *Chem. Commun.*, 1997, 83
6. U. Brand and H. Vahrenkamp; *Inorg. Chem.*, 1995, **34**, 3285
7. (i) N. B. Devi, K. C. Nathsarma and V. Chakravortty, *Hydrometallurgy*, 1997, **4 5**,169 (ii) S. Amer and A. Luis; *Revista De Metalurgia*, 1995, **31**, 351
8. (i) H. Eklund, B. Nordström, E. Zepperzauer, G. Soderlund, I. Ohlsson, T. Bowie, B. O. Soderberg, O. Tapia and C. I. Brändén; *J. Mol. Biol.*, 1976, **102**, 27 (ii) M. H. Bracey, J. Christiansen, P. Tovar, S. P. Cramer and S. G. Cramer; *Biochemistry*, 1994, **33**, 13126 (iii) D. E. Fenton; '*Biocoordination Chemistry*', 1997, Oxford University Press, Oxford, 60-64
9. J. Bjerrum and C. K. Jorgensen; *Rev. Trav. Chim.*, 1956, **75**, 658
10. H. Siegel and R. B. Martin; *Chem. Soc. Rev.*, 1994, 83
11. F. H. Case and T. J. Kasper; *J. Am. Chem. Soc.*, 1956, **78**, 5842
12. Y. Xu, Z. Li, J. Xia, H. Guo, and Y. Huang; *Synthesis*, 1983, 377
13. T. L. Gilchrist; '*Heterocyclic Chemistry*' 1992, John-Wiley and Sons, New York, 152
14. H. Vorbrüggen; *Adv. Heterocycl. Chem.*, 1990, **49**, 117
15. D. Redmore; *J. Org. Chem.*, 1975, **12**, 1976
16. A. R. Katritzky and B. Lunt; *Tetrahedron*, 1969, **25**, 4291
17. P. K. Danikhel and Purnanand; *Indian J. Chem., Sect A.*, 1990, 29 (A) (9) 256
18. R. Honeycult, L. Ballantine, H. Le Baron, D. Paulson, V. Sein, C. Ganz and G. Milad, *ACS Symp Ser*, 1984, **259**, 343; *Chem .Abs.* 101 : 224809n
19. W. Steurbaut, W. Dejonckheere and R. H. Kips, *Meded. Fac. Landbouwnet Rijksuniv. Gent*, 1980, **45** (4) 943; *Chem. Abs.* 94 : 78413x
20. L. Horner and H. Lindel; *Chem. Ber.*, 1985, **118**, 676
21. J. P. Chupp and P. E. Newallis; *J. Am. Chem. Soc.*, 1962, **27**, 3832
22. K. A. Petrov. A. A. Basyuk, V. P. Evdakov, L. I. Mizrakh; *Zhurnal Obshcei Khimii*, 1964, 2226
23. E. Cole; '*Complexation Behaviour of Aza-Phosphinic Acids*', Ph.D. Thesis, University of Durham, 1993
24. M. A. M. Easson; '*Synthesis of Tailored Ligands for Radiopharmaceutical Applications*' Ph.D. Thesis, University of Durham, 1997
25. A. Chaudhry, M. Harger, P.Shuff and A. Thompson; *Chem . Commun.*, 1995, 83
26. M. P. Coogan and M. Harger; *J. Chem. Soc., Perkin Trans. 2*, 1994, 2101
27. R. M. Smith and A. E. Martell; '*Critical Stability Constants*' Vol 1 to 6, Plenum Press, London

28. D. E. C. Corbridge, '*Phosphorus: An Outline of its Chemistry, Biochemistry and Technology*'. 4th Ed., Elsevier (1990), Ch. 4 & 7

29. M. H. Hutson, K. W. Haider and A. W. Czarnik; *J. Am. Chem. Soc.*, 1988, **110**, 4460

30. A. P. de Silva, H. Q. N. Gunaratne, T. Gunnlaugsson, A. J. M. Huxley, C. P. McCoy, J. T. Rademacher and T. E. Rice; *Chem. Rev.*, 1997, **97**, 1515

31. R. M. Silverstein, G. C. Bassler and T. C. Morrill, '*Spectrometric Identification of Organic Compounds*', Wiley, New York, 1991, 311

32. G. B. Bates; '*Tetrahedrally Coordinating Ligands*', Ph.D. Thesis, University of Durham, 1995

Chapter Six

Experimental Methods

6 Experimental Methods

6.1 Methods

For all reactions performed, temperatures are quoted in degrees Celsius. All reactions were carried out under argon in apparatus which had been oven dried.

Basic alumina refers to Merck Alumina activity II-III, alumina refers to Merck alumina pre-soaked in ethyl acetate for at least 24 h prior to use and silica refers to Merck Kieselgel 230-400 mesh.

Analytical and preparative HPLC were performed on a Varian Vista 5500 or a Varian Star 5065 instrument fitted with a Hypersil ODS-C_{18} reverse phase column.

^{1}H, ^{13}C and ^{31}P NMR spectra were obtained with a Bruker AC 250 operating at 250.13, 62.9 and 101.26MHz respectively, Varian Gemini 200 operating at 200 and 50MHz respectively, Varian VXR operating at 200MHz, Mercury 200 operating at 200, 63 and 81MHz respectively, Unity 300 operating at 300 and 75MHz respectively or a Varian VXR 400s operating at 399.96 and 100.58MHz respectively. Spectra are described in ppm to higher frequency of TMS and are reported consecutively as position (δ_H, δ_C and δ_P), relative integral, multiplicity (abbreviated as singlet (s), doublet (d), triplet (t), quartet (q), quintet (p), multiplet (m) or a combination) and coupling constants (J Hz) if applicable. Infrared spectra were recorded on a Perkin-Elmer 1600 FT-IR spectrometer as KBr discs, neat films or using a golden gate apparatus. Absorbance maxima are quoted in wavenumbers. Ultraviolet spectra were recorded on a UVIKON 930 or a Unicam 2 spectrometer. Fluorescence emission spectra were recorded on a LS50B spectrofluorimeter using FLwinlab as the data collection program. Mass spectra were recorded on a VG 7070E, operating in FAB, EI^+ or DCI ionisation modes as stated. Electrospray ionisation mass spectra were obtained on a VG platform (Fisons Instruments), where major fragments are quoted as a percentage of the base peak intensity. Accurate mass spectroscopy was performed by the EPSRC Mass Spectroscopy service using FAB, EI^+ or DCI ionisation modes.

Combustion analysis was performed using an Exeter Analytical Inc CE440 elemental analyser. Metal concentration was determined by atomic absorption spectroscopy using a Perkin Elmer 5000 atomic absorption spectrophotometer.

Melting points were determined on a Kofler block melting point apparatus and are uncorrected.

All solvents were dried by distillation from the appropriate drying agent and water was purified by the PURITE system.

NMR Titrations

NMR titrations were carried out in a single 5mm oven dried tube. A solution of the ligand was prepared (typically 0.04M) in the deuterated solvent (25% CD_3OD, 75% $CDCl_3$) and 0.75ml of the solution transfered to the tube by Gilson pipette. A solution of the metal triflate was also prepared in the deuterated solvent (typically 0.4M). The metal solution was then added in increments of known volume to the ligand solution and the shift of a given proton or phosphorous resonance monitored as a function of the M/L ratio. Typically the M/L ratios examined were 0.1, 0.2, 0.3, 0.4, 0.5, 0.6, 0.7, 0.8, 0.9, 1.0, 1.5, 2.0, 2.5, 3.0, 4.0, 5.0. The change in shift of the given resonance is then plotted against the M/L ratio and the curve analysed using a least squares procedure[1, 2] to estimate the stability constant, K.

Fluorescence pH and Zinc Titrations

Fluorescence titrations were carried out in a quartz cell, stock solutions of the ligand (typically 1mM) and zinc perchlorate (10mM) were prepared. For the pH titrations 25ml of a 0.01mmol solution of the ligand was prepared in a 9 : 1 mixture of methanol and water. The pH was adjusted to approximately 1 with trifluoracetic acid and sodium hydroxide solution was added to raise the pH. The pH of the solution was measured with a standard pH electrode.

For the zinc titrations a 25ml solution of the ligand (0.01mM) was prepared in methanol. To this was added incremental amounts of zinc perchlorate solution (1mM), typically M/L ratios of 0.1, 0.2, 0.3, 0.4, 0.5, 0.6, 0.7, 0.8, 0.9, 1.0, 1.5, 2.0, 2.5, 3.0, 4.0, 5.0 were examined.

Speciation Analysis by Electrospray Mass Spectrometry

Stock solutions of the ligand and metal salts (triflate or perchlorate) were prepared (typically 1mmol) in freshly distilled methanol. To a sample of the ligand solution (1ml) and methanol (1ml) was added the appropriate volume of metal triflate solution to make a 1:1 or 1:2 metal to ligand ratio. Using 10µl of the test solution mass spectra were obtained on a VG Platform (II) electrospray mass spectrometer, with positive or negative ionisation modes. With a typical source temperature of 60°C and cone voltage of 30V.

Metal pH Extraction Isotherms

A stock solution of the ligand was prepared (0.1M, 8ml) in Analar dichloromethane (8ml). A zinc chloride solution was prepared in aqueous sulphuric acid (25ml, 0.5M, pH 0.14). To the ligand solution (750µl) was added an equal volume of the zinc chloride solution, and the mixture thoroughly agitated (Fisons 'Whirlimixer') for 5 min. The pH of the zinc chloride solution was raised with aqueous sodium hydroxide (4M, between 0.1 to 0.3ml) and an addition made to fresh ligand solution (the pH of the zinc chloride solution was monitored using a Russell CMAWL 3.7/180mm microelectrode). This procedure was repeated between the pH range 0.14 and 4.10.

The organic layers were separated and diluted with dichloromethane (5ml) and extracted with aqueous hydrochloric acid (1.5M, 2x5ml). The aqueous layer was carefully separated and the metal content determined by atomic absorption spectroscopy.

Liquid-Liquid Extraction

Liquid-liquid extraction studies were carried out by C. Chartroux at the Technical University of Dresden. The extraction studies were performed at 25±1°C in 2ml microcentrifuge tubes by mechanical shaking. Unless stated the shaking time was 30min; the phase ratio $V_{(org)}$:$V_{(aq)}$ was 1:1 (0.5ml each). All samples were centrifuged after extraction. The determination of metal concentrations in both phases was carried out radiometrically using γ-radiation measurement of $^{65}ZnCl_2$ and $^{203}HgCl_2$ in a NaI(Tl) scintillation counter (Cobra II; Canberra-Packard), and β-radiation of $^{63}Ni(NO_3)_2$ and $^{60}Co(NO_3)_2$ in a liquid scintillation counter (Tricarb 2500, Canberra-Packard). Aqueous solutions of metal salts were prepared of 0.1mM and the pH adjusted to 2 with NaOAc/HCl buffer. Chloroform solutions of the ligands were prepared of 1mM.

6.2 Chapter Two Experimental

Diphenylphosphorous acid via acid hydrolysis (50)[3]

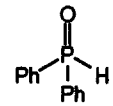

To a sodium ethoxide solution prepared from dry ethanol (5ml) and sodium (120mg, 5.2mmol) under argon at 0°C was added chlorodiphenylphosphine (0.93ml, 5.2mmol) and the mixture stirred at 0°C for 1h. Concentrated hydrochloric acid (10M, 2.5ml) was added and the temperature raised to 60°C for 12 h, the solvent was removed under vacuum to give a colourless viscous oil (1.04g, 100%).
δ_H ($CDCl_3$) 7.0-7.4 (10H, m, Ph), 7.71 (1H, d, $^1J_{PH}$=481Hz, PH); δ_P ($CDCl_3$) 18.7.

Diphenylphosphorous acid via trimethylsilyl bromide hydrolysis (50)[4]

To a sodium ethoxide solution prepared from dry ethanol (5ml) and sodium (100mg, 4.33mmol) under argon at 0°C was added chlorodiphenylphosphine (0.77ml, 4.33mmol) and the mixture stirred at 0°C for 1 h. The excess ethanol was removed under vacuum and trimethylsilyl bromide (1.65g, 10.8mmol) added and the reaction heated at 60°C for 3h. The mixture was cooled then taken up in diethyl ether (20ml) and shaken with water (3x20ml), the organic layer was dried ($MgSO_4$) and the solvent removed to give a colourless viscous oil (744mg, 86%).

NMR data was consistent with a sample prepared as described above.

Diphenylthiophosphinic acid (52)[5]

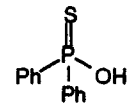

To diphenylphosphorous acid (1.04g, 5.2mmol) in chloroform (5ml) was added dry, crushed sulphur powder (166mg, 5.2mmol) and the temperature raised to 40°C for 2 h. The solvent was removed under vacuum and THF (5ml) added.The mixture was stirred for 1 h, filtered to remove the insoluble material and the THF removed under vacuum to give a white solid (1.21g, 100%).
δ_H ($CDCl_3$) 6.82 (1H, bs, POH), 7.3-7.5 (5H, m, Ph), 7.75-7.8 (5H, m, Ph); δ_C ($CDCl_3$) 128.7, 129.0, 131.2, 131.4, 132.2, 132.3; δ_P ($CDCl_3$) 75.7.

Diphenylethoxyphosphine sulfide (53)[6]

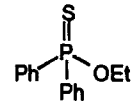

To diphenylethoxyphosphine (1g, 4.3mmol, prepared as for diphenylphosphorus acid) in chloroform (5ml) was added crushed sulfur powder (153mg, 4.8mmol) and the mixture heated at 40°C for 18h. The mixture was filtered through a 0.5μm syringe filter, and the chloroform removed under vacuum to give a pale yellow solid (1.13g, 100%).

δ_H ($CDCl_3$) 1.45 (3H, t, ^3J=7.0Hz, $OCH_2\underline{CH_3}$), 4.24 (2H, qd, $^3J_{HH}$=7.0Hz, $^3J_{HP}$=1.6 Hz, OCH_2CH_3), 7.51-7.56 (5H, m, Ph), 7.94-8.03 (5H, m, Ph); δ_P ($CDCl_3$) 80.7.

(4-methoxyphenyl)-methyldithiophosphinic acid (55)

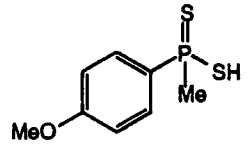

To a suspension of Lawesson's reagent (610mg, 1.51mmol) in dichloromethane (10ml) at room temperature was added a solution of methylmagnesium bromide (1.05ml, 3.02mmol, 3M soln.in diethylether) and the mixture was stirred for 10mins. Water (15ml) was added, and the organic layer further washed with water (2x20ml). The organic layer was separated, dried ($MgSO_4$) and the solvent removed to give a pale yellow crystalline product (644mg, 98%).

δ_H ($CDCl_3$) 2.39 (3H, d, $^2J_{PCH3}$=13.3Hz, $PC\underline{H_3}$), 3.69 (3H, s, $OC\underline{H_3}$), 7.04 (2H, dd, $^3J_{H3H2}$=8.7Hz, $^4J_{HP}$=2.5Hz, H3), 7.98 (2H, dd, $^3J_{H2H3}$=8.7Hz, $^3J_{HP}$=14.1Hz, H2) ; δ_C ($CDCl_3$) 30.1 (d, $^1J_{CP}$=59 Hz, $P\underline{C}H_3$), 56.0 (s, $O\underline{C}H_3$), 114.5 (d, $^2J_{CP}$=14 Hz, C2), 127.0 (d, $^1J_{CP}$=87 Hz, C1), 132.6 (d, $^3J_{CP}$=13 Hz, C3), 163.0 (s, C4); δ_P($CDCl_3$) 52.2; ESMS$^-$ 217 (100%, L^-).

(4-Methoxyphenyl)-phenyldithiophosphinic acid (56)

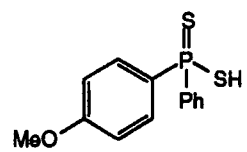

To a suspension of Lawesson's reagent (490mg, 1.2mmol) in dry THF (10ml) at 0°C was added phenylmagnesium bromide (3mls, 3mmol, 1M soln, in diethylether) and the mixture was stirred for 10mins. The THF was removed under vacuum and the remaining residue was treated with HCl (1.0M soln, 10ml), and extracted into dichloromethane (3x30ml). The organic phase was dried ($MgSO_4$) and the solvent removed under reduced pressure to give a white crystalline solid (570mg, 85%).

δ_H ($CDCl_3$) 3.95 (3H, s, $OC\underline{H_3}$), 7.10 (2H, dd, $^3J_{H3H2}$=8.7Hz, $^4J_{HP}$=2.9Hz, H3), 7.61(2H, dd, $^3J_{H2H3}$=8.7Hz, $^3J_{HP}$=14.5Hz, H2), 8.1 (5H, m, Ph); δ_P ($CDCl_3$) 55.6.

(N-Phenyl)amino-ethoxyphenylphosphine (62)

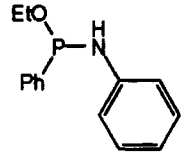

Ethoxyphenylchlorophosphine (663mg, 3.52mmol) was freshly prepared from dichlorophenylphosphine (1.71mmol) and diethoxyphenylphosphine (1.81mmol) at 0°C in the absence of solvent. Aniline (0.32ml, 3.52mmol) was added at 0°C followed by triethylamine (0.48ml, 3.52mmol) and the mixture left to warm to room temperature. Diethyl ether (10ml) was added and the salts removed by filtration. The filtrate was dried (K_2CO_3) and the solvent removed under reduced pressure to yield a viscous colourless oil (827mg, 96%).

δ_H ($CDCl_3$) 1.32 (3H, t, $OCH_2C\underline{H}_3$), 4.51 (2H, m, $OC\underline{H}_2CH_3$), 5.62 (1H, d, $^2J_{HP}$=8Hz, NH), 6.8 (5H, m, Ph), 7.81 (5H, m, N-Ph); δ_P ($CDCl_3$) 106.1.

(N-Phenyl)amino-ethoxyphenylphosphinesulfide (64)[7]

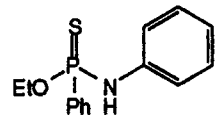

To (N-phenyl)amino-ethoxyphenylphosphine (750mg, 3.06mmol), prepared as described above, was added chloroform (5ml) and dry crushed sulfur powder (98mg, 3.06mmol) and the mixture heated at 40°C overnight. The reaction mixture was filtered to remove the insoluble material, and the solvent removed under reduced pressure to yield an opaque gum (967mg, 97%).

δ_H ($CDCl_3$) 1.38 (3H, t, $OCH_2C\underline{H}_3$), 4.15 (2H, m, $OC\underline{H}_2CH_3$), 5.88 (1H, d, $^2J_{HP}$=10Hz, NH), 7.12 (5H, m, Ph), 7.45 (5H, m, N-Ph); δ_P ($CDCl_3$) 67.3.

6.3 Chapter Three Experimental

2-Bromo-N-acetylaniline (89)

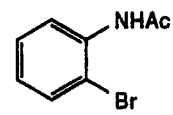

2-Bromoaniline (25g, 145mmol) was dissolved in acetic anhydride (30.6g, 300mmol) and sulfuric acid (2.5g) was added carefully. After the exothermic reaction had cooled the mixture was poured into warm water (100ml) with continuous stirring. The white solid was collected by filtration, washed with water (500ml) and vacuum dried to give the product (31g, 100%), mp 98°C (lit. 98-99°C).[8]

δ_H ($CDCl_3$) 2.72 (3H, s, $C\underline{H}_3$), 6.97 (1H, ddd, $^3J_{H5H6}$=7.9Hz, $^3J_{H5H4}$=7.1Hz, $^4J_{H5H3}$=1.3Hz, H5), 7.29 (1H, ddd, $^3J_{H4H3}$=7.9Hz, $^3J_{H4H5}$=7.1Hz, $^4J_{H4H6}$=1.5Hz,

H4), 7.52 (1H, dd, $^3J_{H3H4}$=7.9Hz, $^4J_{H3H5}$=1.3Hz, H3), 7.64 (1H, bs, NH), 8.29 (1H, dd, $^3J_{H6H5}$=7.9Hz, $^4J_{H4H6}$=1.5Hz, H6).

2-Bromo-6-nitro-N-acetylaniline (90)

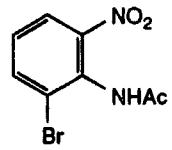

To a mixture of fuming nitric acid (6ml), trifluoroacetic acid (4.5ml) and water (2 drops) was added 2-bromo-6-nitro-N-acetylaniline (4g, 18.69mmol) with gentle heating over a period of 30 mins. The mixture was stirred at room temperature for 10 h and followed by TLC (silica 1% methanol : 99% dichloromethane R_f product = 0.2). The mixture was poured onto crushed ice (10ml) and the brown solid collected by filtration and washed with water (60ml). Recrystallisation from chloroform gave the required isomer (2-bromo-6-nitro-N-acetyl benzene) as white needle crystals (2.17g, 45%), mp 193-194°C (lit. 193°C).[9]
δ_H ($CDCl_3$) 2.24 (3H, s, CH_3), 7.26 (1H, dd, $^3J_{H4H3}$=8.7Hz, $^3J_{H4H5}$=7.6Hz, H4), 7.71 (1H, bs, NH), 7.86(1H, dd, $^3J_{H3H4}$=8.7Hz, $^4J_{H3H5}$=1.4Hz, H3), 7.91 (1H, dd, $^3J_{H5H4}$=7.6Hz, $^4J_{H5H3}$=1.4Hz, H5)

2-Bromo-6-nitroaniline (88)

A 33% ethanol / hydrochloric acid mixture was added to 2-bromo-6-nitro-N-acetyl aniline (4g, 15.4mmol) and the mixture heated under reflux for 3.5 h. The mixture was poured onto a basic ice solution (10ml) and the pH adjusted to 14 by addition of NaOH pellets. The resultant solid was collected by filtration and dried under vacuum to give a bright yellow crystalline solid (3.35g, 100%), mp 74-75°C (lit. 73-74°C).[10]
δ_H ($CDCl_3$) 5.72 (1H, bs, NH), 6.62 (1H, bs, NH), 6.61(1H, dd, $^3J_{H4H3}$=8.8Hz, $^3J_{H4H5}$=12.1Hz, H4), 7.69 (1H, dd, $^3J_{H4H5}$=12.1Hz, $^4J_{H5H3}$=1.1Hz, H5), 8.14 (1H, dd, $^3J_{H3H4}$=8.8, $^4J_{H3H5}$=1.1Hz, H3)

3-Bromo-1, 2-diaminobenzene (82)

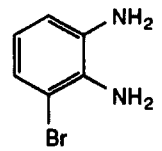

To a solution of tin(II) chloride dihydrate (8.36g) in concentrated hydrochloric acid (43ml) was added 2-bromo-6-nitroaniline (2.19g, 8.45mmol) and the mixture stirred at room temperature for 5 min. The mixture was heated under reflux for 30 mins, poured

onto crushed ice and the solution made basic (pH 14, NaOH pellets) and the aqueous layer extracted exhaustively with diethyl ether (5x100ml). The organic fractions were combined, dried (K_2CO_3) and the solvent removed under reduced pressure to give a pale yellow crystalline product (1.85g, 96%), mp 52-53°C (lit. 52-54°C).[11]
δ_H (CD_3OD) 6.38 (1H, dd, $^3J_{H5H4}$=9.2Hz, $^3J_{H5H6}$=7.9Hz, H5), 6.57 (1H, d, $^3J_{H6H5}$=7.9Hz, H6), 6.76 (1H, d, $^3J_{H4H5}$=9.2Hz, H4)

2-Methyl-4-bromobenzimidazole (81)

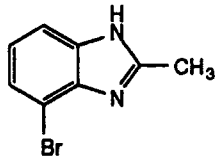

To 3-bromo-1, 2-diaminobenzene (2.5g, 13.37mmol) was added acetic anhydride (15ml) and the solution heated at 110°C for 2 h. The mixture was left to cool to room temperature and water (20ml) was added and the solution heated at 60°C for 1 h. Hydrochloric acid (3M, 20ml) was added and the mixture heated at 100°C for a further 2 h. Activated carbon (500mg) was added, and the solution filtered through a celite plug. The aqueous filtrate was made basic (ammonia 0.880 solution) and extracted with dichloromethane (4x100ml), dried (K_2CO_3) and the volatile organics removed under reduced pressure to give an off white-solid (2.82g, 89%), mp 136-138°C (lit. 137°C).[12]
δ_H ($CDCl_3$) 2.65 (3H, s, CH_3), 7.08 (1H, dd, $^3J_{H6H5}$=7.6Hz, $^3J_{H6H7}$=7.9Hz, H6), 7.38 (1H, d, $^3J_{H7H6}$=7.6Hz, H7), 7.46 (1H, d, $^3J_{H5H6}$=7.9Hz, H5)

1-(4-tert-Butylbenzyl)-2-methyl-4-bromobenzimidazole (92)

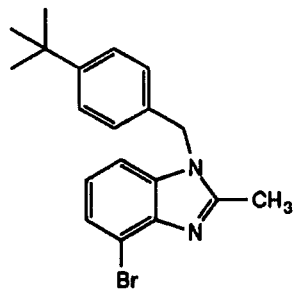

Dimethylformamide (15ml) was added to a mixture of 4-bromo-2-methylbenzimidazole (2.5g, 11.84mmol) and caesium carbonate (4.24g, 13.03 mmol) and the mixture stirred under argon for 2 h. 4-(tert-Butyl)benzyl bromide (2.93ml, d=1.236, 13.03mmol) was added and the mixture heated at 40°C for 12 h. After cooling, the DMF was removed by vacuum distillation, and the residue taken up in dichloromethane (15ml), washed with water (3x20ml), dried (K_2CO_3) and the dichloromethane reduced to minimal volume (1ml) followed by precipitation of the product with diethylether (10ml). This precipitate was filtered and dried to yield an off-white solid (4.01g, 95%), mp 134-135°C.

δ_H ($CDCl_3$) 1.25 (9H, s, ^tBu), 2.57 (3H, s, CH_3), 6.91 (2H, d, $^3J_{H10H11}$=2.6Hz, H10), 7.01 (1H, dd, $^3J_{H6H7}$=8.1Hz, $^3J_{H6H5}$=7.6Hz, H6), 7.14 (1H, d, $^3J_{H7H6}$=8.1Hz, H7), 7.28 (2H, d, $^3J_{H11H10}$=2.6Hz, H11), 7.38 (2H, d, $^3J_{H5H6}$=7.6Hz, H5).
δ_C ($CDCl_3$) 16.2 (CH_3), 33.3 (tBu), 36.56 (C2), 49.3 (CH_2), 110.8, 114.5, 125.2, 127.0, 127.9, 128.0, 134.3, 137.9, 153.2, 154.8.
EI$^+$ 356 (51%, M$^+$), 358 (49%, M$^+$); Found: M$^+$ 356.0888. $C_{19}H_{21}N_2Br$ requires M$^+$ 356.0888. Found: C, 63.62%: H, 5.98%: N, 7.58%. $C_{19}H_{21}N_2Br$ requires C, 63.87%: H, 5.92%: N, 7.58%.

Attempted preparation of 1-(4-tert-Butylbenzyl)-2-methylbenzimidazole-4-carboxylic acid

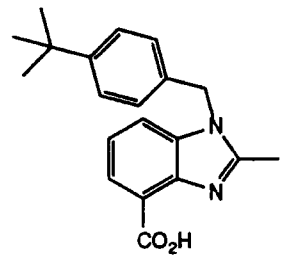

To a cold (-78°C) solution of 1-(4-tert-butyl)benzyl-4-bromo-benzimidazole (200mg, 0.53mmol) in dry degassed THF (10ml) was added a THF solution of n-butyl lithium (0.36ml, 0.57mmol, 1.6M) and the mixture left to stir for 1 h. Dry carbon dioxide was passed through the solution for 15 min and the soltuion allowed to warm to room temperature. Hydrochloric acid (3M, 8ml) was added and the solution stirred for 30 min, extracted with chloroform (3x40ml), dried (K_2CO_3) and the solvent removed under reduced pressure to give a brown solid.

^{1}H NMR analysis revealed a number of different species were present.

Attempted preparation of 1-(4-tert-Butylbenzyl)-2-methylbenzimidazole-4-(ethoxyphenyl phosphine)

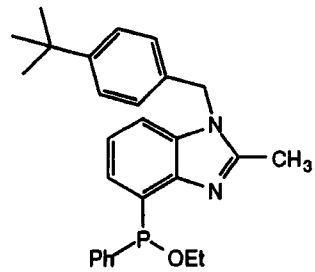

An analogous procedure to that described above was employed, however quenching of the supposed lithiate was performed with freshly prepared chloroethoxyphenyl-phosphine.

^{1}H and ^{31}P NMR analysis revealed a number of different species were present.

Attempted preparation of 1-(4-tert-Butylbenzyl)-2-methylbenzimidazole-4-[(4-methoxy)phenyl-dithiophosphinic acid)]

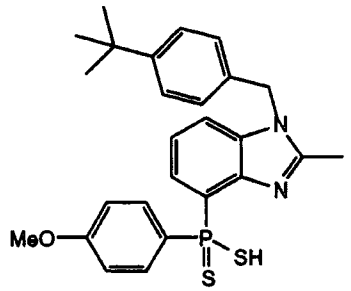

To magnesium turnings (190mg, 7.8mmol), activated by stirring vigorously under vacuum and sonication) was added dry degassed THF (5ml) and a single crystal of iodine. To this was added a solution of 1-(4-tert-butyl)benzyl-2-methyl-4-bromo benzimidazole (300mg, 0.79mmol) in THF (2ml), the mixture was then sonicated for 1 h, followed by boiling under reflux for 24 h. The mixture was then filtered under argon, and the filtrate added dropwise to a suspension of Lawesson's reagent (159mg, 0.39mmol) in THF (5ml) and stirred at room temperature for 16h. Hydrochloric acid (5ml, 3M) was added and the mixture stirred for 1 h, extracted with chloroform (3x50ml), dried (K_2CO_3) and the solvents removed under reduced pressure.

^1H and ^{31}P NMR analysis revealed that only starting material was present

Tetrakis(triphenylphosphine)palladium(0)[13]

$Pd[PPh_3]_4$

A mixture of palladium dichloride (856mg, 4.8mmol), triphenylphosphine (6.32g, 24mmol) and dry dimethyl sulfoxide (50ml) was heated to 140°C until complete solution had occured (ca. 2 h). The mixture was left to cool for 15 min and hydrazine hydrate (966mg, 19.3mmol) added. The solution was left to cool to room temperature and the yellow solid filtered off under argon. The bright yellow solid was washed with ethanol (2x10ml), diethyl ether (2x10ml) and dried under vacuum, to give the product (5.20g, 93%)

δ_P ($CDCl_3$) 16ppm.

Ethyl-1-(4-tert-butylbenzyl)-2-methylbenzimidazole-4-(phenylphosphonate) (95)

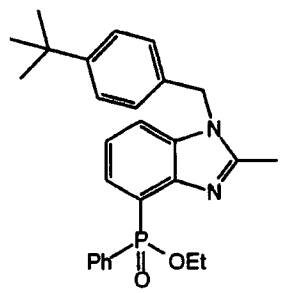

Using a procedure adapted from Huang[14] 1-(4-tert-butylbenzyl)-2-methyl-4-bromobenzimidazole (300mg, 0.84mmol), ethylphenylphosphonite (0.14ml, 0.924mmol) and triethylamine (0.39ml, 2.77mmol) were mixed in dry degassed toluene (5ml). Tetrakis(triphenylphosphine)palladium(0) (46mg, 0.04mmol) was added and the mixture degassed three times (freeze thaw cycle), then heated at 100°C for 96 h. The solution was diluted with dichloromethane (10ml), washed with 5% aqueous hydrochloric acid (2x10ml) and water (3x20ml), dried (K_2CO_3) and the solvent removed under reduced pressure to give an off white solid. Purification by column chromatography (alumina, eluant 2% MeOH/98% dichloromethane increasing to 8% MeOH/92% dichloromethane, R_f(product)=0.38 (8% MeOH/92% dichloromethane)) gave a white solid (233mg, 62%), mp 56-57°C.
δ_H ($CDCl_3$) 1.19 (9H, s, C($C\underline{H}_3$)$_3$), 1.32 (3H, t, ^3J=7.19Hz, $OCH_2C\underline{H}_3$), 2.52 (3H, s, 2-$C\underline{H}_3$), 4.09 (2H, qd, ^3J=7.19Hz, $^2J_{HP}$=2.2Hz, $OC\underline{H}_2CH_3$), 5.18 (2H, s, $NC\underline{H}_2Ar$), 6.91 (2H, d, $^3J_{H11H10}$=8.39Hz, H11), 7.01 (2H, ddd, $^3J_{HmPhHoPh}$=7.4Hz, $^3J_{HmPhHpPh}$=6.9Hz, $^4J_{HmPhP}$=3.6Hz, H*m*Ph), 7.12 (2H, d, $^3J_{H10H11}$=8.39Hz, H10), 7.25 (1H, dd, $^3J_{HpPhHmPh}$=6.9Hz, $^5J_{HpPhP}$=7.4Hz, H*p*Ph), 7.31 (1H, ddd, $^3J_{H6H7}$=8.2Hz, $^3J_{H6H5}$=7.4Hz, $^4J_{H6P}$=2Hz, H6), 7.47 (1H, d, $^3J_{H7H6}$=8.2Hz, H7), 7.79 (2H, dd, $^3J_{HoPhHmPh}$=7.4Hz, $^3J_{HoPhP}$=13.1Hz, H*o*Ph), 7.99 (1H, dd, $^3J_{H5H6}$=7.4Hz, $^3J_{H5P}$=12.9Hz, H5); δ_C ($CDCl_3$) 14.1 ($\underline{C}(CH_3)_3$), 16.5 (d, $^3J_{CP}$=7.6Hz, $OCH_2\underline{C}H_3$), 31.1 (C($\underline{C}H_3$)$_3$), 34.4 ($N\underline{C}H_2Ar$), 46.7 (2-$\underline{C}H_3$), 61.3 (d, $^2J_{CP}$=7.1Hz, $O\underline{C}H_2CH_3$), 113.7 (d, $^3J_{CP}$=3.5Hz, C6), 120.6 (d, $^1J_{CP}$=160.0Hz, C*i*Ph), 121.4 (d, $^2J_{CP}$=15.5Hz, C5), 125.8 (C11), 125.9 (C12), 127. 4 (d, $^4J_{CP}$=9.7Hz, C7), 127.9 (d, $^3J_{CP}$=16.1Hz, C*m*Ph), 131.6 (d, $^3J_{CP}$=3.4Hz, C8), 131.86 (d, $^2J_{CP}$=13.1Hz, C*o*Ph), 132.2 (d, $^3J_{CP}$=168.4Hz, C4), 135.6 (d, $^4J_{CP}$=15.3Hz, C*p*Ph), 143.2 (d, $^2J_{CP}$=12.7Hz, C9), 150.9, 153.1 (C2); δ_p ($CDCl_3$) 31.3; ESMS 447.15 (100%, LH^+); υmax (KBr disc)/cm^{-1} 3439, 2961, 1602, 1438, 1419, 1209, 1035; Found: M^+ 446.2123, $C_{27}H_{31}N_2PO_2$ requires M^+ 446.2123; Found: C, 72.83%: H, 7.16: N, 6.35. $C_{27}H_{31}N_2PO_2$ requires C, 72.62: H, 6.99: N, 6.27

1-(4-tert-Butylbenzyl)-2-methylbenzimidazole-4-(phenylphosphinic acid) hydrochloride (26)

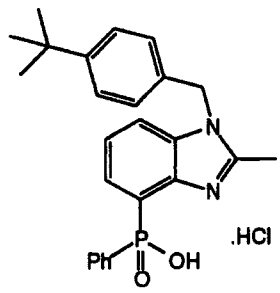

To ethyl-1-(4-tert-butylbenzyl)-2-methyl-4-(phenylphosphonate) benzimidazole (200mg, 0.45mmol) was added hydrochloric acid (6M, 10ml) and the mixture heated at 110°C for 16 h. After cooling, the acid was removed under reduced pressure to give a white solid (202mg, 99%), mp 172-174°C.

δ_H (CD_3OD) 1.25 (9H, s, ^tBu), 3.10 (3H, s, 2-$\underline{C}H_3$), 5.67 (2H, s, N$\underline{C}H_2$Ar), 7.02 (1H, dd, $^3J_{H6H7}$=8.4Hz, $^3J_{H6H5}$=8.4Hz, H6), 7.09 (2H, d, $^3J_{H10H11}$=8.3Hz, H10), 7.30 (1H, dd, $^3J_{HmPhHpPh}$=7.9Hz, $^4J_{HpPhP}$=7.8Hz, H*p*Ph), 7.32 (2H, d, $^3J_{H11H10}$=8.3Hz, H11), 7.50 (2H, ddd, $^3J_{HmPhHoPh}$=7.19Hz, $^3J_{HmPhHpPh}$=7.9Hz, $^4J_{HmPHP}$=3.2Hz, H*m*Ph), 7.59 (1H, d, $^3J_{H5H6}$=8.4Hz. H5), 7.17 (1H, d, $^3J_{H7H6}$=8.4Hz, H7), 8.07 (2H, dd, $^3J_{HpPhHmPh}$=7.2Hz, $^5J_{HpPhP}$=12.4Hz, H*p*Ph); δ_C (CD_3OD); 22.6 ($\underline{C}(CH_3)_3$), 31.2 (C($\underline{C}H_3)_3$), 34.6 (2-$\underline{C}H_3$), 48.5 (N$\underline{C}H_2$Ar), 114.6 (C2), 124.1 (C8'), 125.3 (d, $^2J_{CP}$=12.6Hz, C*o*Ph), 126.3 (C10), 126.6 (C11), 128.5 (d, J_{CP}=13.3Hz, C*m*Ph), 129.1, 129.8. 129.8 (d, $^1J_{CP}$=143.4Hz, C*i*Ph), 132.2, 132.3, 132.3 (d, $^1J_{CP}$=132.3Hz, C4), 152.1, 152.5; δ_p (CD_3OD) 28.0

ESMS 419.29 (100%, LH^+); υ_{max} (KBr disc)/cm^{-1} 3418, 2958, 2864, 1678, 1546, 1544, 1424, 1218, 1132 ; Found: MH^+ 419.1888, $C_{25}H_{28}N_2PO_2$ requires MH^+ 419.1888

1,2-Diamino-3-nitrobenzene (102)

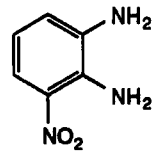

A solution of 2, 6-dinitroaniline (3g, 16.39mmol) in monoglyme (38ml) and chloroform (3.8ml) was hydrogenated over 10% palladium on carbon (152mg) at room temperature and a pressure of 3atm of hydrogen for 2 h. The catalyst was removed by filtration through a celite plug, and the filtrate concentrated by removal of the solvent under reduced pressure to give a red solid. Recrystallisation from water:ethanol 2:3 gave the product (2.28g, 91%) as a dark red crystalline solid mp 158-160°C (lit. 158-159°C).[15]

δ_H ($CDCl_3$) 3.42 (2H, bs, NH_2), 5.89 (2H, bs, NH_2), 6.55 (1H, dd, $^3J_{H4H5}$= 8.7Hz, $^3J_{H4H3}$=6.4Hz, H4), 6.86 (1H, d, $^3J_{H3H4}$=6.4Hz, H3), 7.65 (1H, d, $^3J_{H5H4}$=8.7Hz, H5).

2-Methyl-4-nitro-benzimidazole (103)

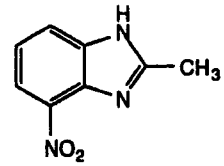

A solution of 1, 2-diamino-3-nitrobenzene (1.6g, 7.8mmol) in acetic anhydride (5ml) was heated at 100°C for 1h. The flask was then fitted with a condenser and water (5ml) was cautiously added to the cooled reaction mixture. The mixture was heated at 60°C for 1 h, after which hydrochloric acid (1M, 10ml) was added and the mixture heated at reflux for 2 h. Activated carbon (1g) was added and the mixture heated for a further 30 min. The solution was filtered through a celite plug and made basic (pH 14) by addition of NaOH. The aqueous layer was extracted exhaustively with dichloromethane

(6x25ml), the organic fractions combined, dried (K_2CO_3) and the dichloromethane removed under reduced pressure. Recrystallisation from dichloromethane gave 2-methyl-4-nitrobenzimidazole as a tan crystalline solid (1g, 58%) mp 216-217°C. δ_H ($CDCl_3$) 2.34 (1H, s, NH), 2.83 (3H, s, CH_3), 7.43 (1H, t, J = 8Hz, H6), 8.11 (1H, d, J = 8Hz, H5), 8.21 (1H, d, J = 8Hz, H7); δ_C ($CDCl_3$) 15.1, 118.7, 121.5, 126.5, 128.9, 132.7, 146.2, 153.7; ESMS 177.9 (100%, MH^+); υ_{max} (KBr disc)/cm^{-1} 2922, 1510 (NO_2), 1340 (NO_2), 1269, 1212, 1031, 819, 734. Found: MH^+ 178.0617. $C_8H_8N_3O_2$ requires MH^+ 178.0616.

1-(4-tert-Butylbenzyl)-2-methyl-4-nitrobenzimidazole (104)

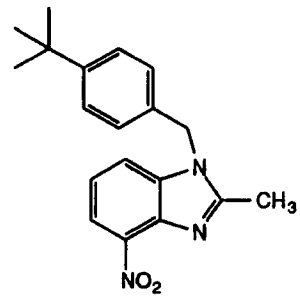

A mixture of 2-methyl-4-nitro-benzimidazole (1g, 5.64mmol) and caesium carbonate (2.03g, 6.2mmol) in dry dimethylformamide (5ml) was stirred at room temperature under argon for 30 min. 4-tert-Butylbenzyl bromide (0.91ml, 6.2mmol) was added and the solution stirred at 40°C for 12 h. After cooling the DMF was removed by distillation under reduced pressure, and the resulting gum dissolved in a minimal volume of dichloromethane (1ml). Trituration with diethylether (10ml) resulted in precipitation of the product. The solid was collected by filtration, washed with diethyl ether (30ml) and dried to give a brown solid (1.82g, 100%) mp 142-143°C. δ_H ($CDCl_3$) 1.27 (9H, s, tBu), 2.70 (3H, s, CH_3), 5.36 (2H, s, CH_2), 6.94 (2H, d, $^3J_{H10H11}$=8.6Hz, H10), 7.24 (2H, d, $^3J_{H11H10}$=8.6Hz, H11), 7.30 (1H, dd, $^3J_{H6H5}$=8.0Hz, $^3J_{H6H7}$=8.1Hz, H6), 7.53 (1H, d, $^3J_{H5H6}$=8.0Hz, $^4J_{H5H7}$=1.0Hz, H5), 8.09 (1H, d, $^3J_{H7H6}$=8.1Hz, $^4J_{H7H5}$=1.0Hz, H7); δ_C ($CDCl_3$) 14.9 (CH_3), 31.7 (tBu), 35.0 (C2), 47.8 (CH_2), 116.4, 119.5, 121.8, 126.3, 126.6, 126.7, 132.1, 137.0, 138.7, 138.9, 151.9, 156.9; ESMS 324.13 (MH^+, 100%), υ_{max} (KBr disc)/cm^{-1} 3065, 2964, 2866, 1432, 1527 (NO_2), 1342 (NO_2), 1209, 1070. Found: MH^+ 324.1712 . $C_{19}H_{21}N_3O_2$ requires MH^+ 324.1712.

1-(4-tert-Butylbenzyl)-2-methyl-4-aminobenzimidazole (105)

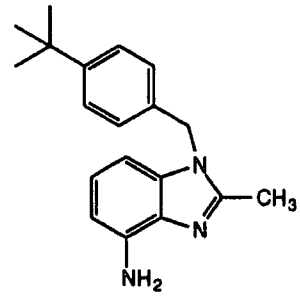

Tin(II) chloride dihydrate (3.01g, 13.37mmol) was added to 1-(4-tert-butylbenzyl)-4-nitrobenzimidazole (1.2g, 3.72mmol) in concentrated hydrochloric acid (20ml) and the mixture stirred at room temperature for 30min. The reaction mixture was then heated under reflux for 30 mins and the solution poured onto ice (30mls), made basic (pH 13) by careful addition of NaOH pellets and extracted with dichloromethane (4x100ml). The organic extracts were combined, dried (K_2CO_3) and the solvent removed under reduced pressure to give the product as a light orange solid. Recrystallisation from dichloromethane gave orange needle crystals (0.6g, 55%), mp 139-140°C.
δ_H ($CDCl_3$) 1.27 (9H, s, tBu), 2.51 (3H, s, CH_3), 4.47 (2H, bs, NH_2), 5.17 (2H, s, CH_2), 6.51 (1H, d, $^3J_{H5H6}$=7.7Hz, H5), 6.62 (1H, d, $^3J_{H7H6}$=7.9Hz, H7), 6.91 (1H, dd, $^3J_{H6H7}$=7.9Hz, $^3J_{H6H5}$=7.7Hz, H6), 6.92 (2H, d, $^3J_{H10H11}$=8.6Hz, H10), 7.32 (2H, d, $^3J_{H11H10}$=8.6Hz, H11); δ_C ($CDCl_3$) 14.4 (CH_3), 31.8 (tBu), 35.0 (C2), 47.4 (CH_2), 100.0, 106.7, 123.8, 126.3, 126.5, 131.0, 133.6, 136.8, 138.7, 150.0, 151.3; υ_{max} (KBr disc)/cm^{-1} 3065, 3025, 2964, 2866, 1890, 1251; Found: C, 77.53; H, 7.65; N, 14.07. $C_{19}H_{23}N_3$ requires C, 77.78; H, 7.90, N, 14.32

Tetramethyldiphosphine disulfide (107)

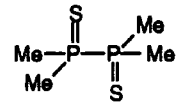

To a solution of methylmagnesium bromide (2M in diethyl ether, 120ml, 240mmol) cooled to -10°C was added a solution of trichlorophosphine sulfide (13.5g, 80mmol) in diethylether (100ml) maintaining the temperature between 0 and -10°C. The reaction was stirred for 30min then poured onto crushed ice. Sulphuric acid (10%, 90ml) was added with stirring, and the resultant white precipitate filtered off and washed with water to give a white solid. Recrystallisation from ethanol gave white needle crystals (4.16g, 56%); mp 225-227°C (lit. 225-229°C).[16]
δ_H ($CDCl_3$) 2.06 (12H, q, $^2J_{cp}$=5Hz, $C\underline{H}_3$); δ_P ($CDCl_3$) 35.5.

1-(4-tert-Butylbenzyl)-2-methyl-(4-aminodimethylphosphinesulfide)benzimidazole (27)

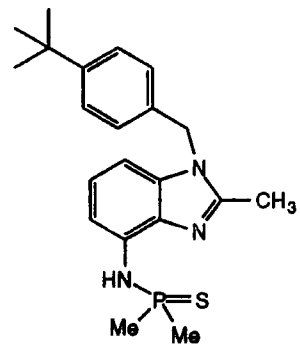

Tetramethyldiphosphinedisulfide (175mg, 0.93mmol) was suspended in tetrachloromethane (10ml) and bromine (150mg, 0.93mmol) added dropwise. The reaction was left to stir at room temperature for 1 h. To the resulting pale yellow solution was added 1-(4-tert-butylbenzyl)-4-aminobenzimidazole (500mg, 1.706mmol) and then triethylamine (0.268ml, 1.877mmol). The reaction was monitored by phosphorus NMR, δ_P dimer = 35.4ppm, δ_P bromo derivative = 62ppm. After 16 h , the reaction mixture was filtered and washed with water (20ml). Tetrachloromethane was removed under reduced pressure, and the resulting solid residue dissolved in a minimal volume of chloroform and the product precipitated with diethyl ether, filtered and dried to give the title compound (500mg, 76%) as a white solid, mp 168-70°C. δ_H ($CDCl_3$) 1.28 (9H, s, tBu), 2.13 (6H, d, PCH_3, $^2J_{CP}$=13.36Hz), 2.51 (3H, s, CH_3), 5.23 (2H, s, CH_2), 5.91 (1H, bd, NH, $^2J_{cp}$=9.24Hz), 6.87 (1H, d, $^3J_{H5H6}$=8.2Hz, H5), 6.98 (2H, d, $^3J_{H10H11}$=8.2Hz, H10), 7.11 (1H, dd, $^3J_{H6H5}$=8.2Hz, $^3J_{H6H7}$=7.0Hz, H6), 7.24 (1H, d, $^3J_{H7H6}$=7.0Hz, H7), 7.51 (2H, d, $^3J_{H11H10}$=8.2Hz, H11); δ_C ($CDCl_3$) 13.9 (2-$\underline{C}H_3$), 23.9 (d, $^1J_{cp}$=68.9, P$\underline{C}H_3$), 31.2 (tBu), 34.5 (C2), 47.0 (N$\underline{C}H_2$Ar), 102.9, 108.4, 123.0, 125.9, 125.9, 131.9, 132.6, 136.0, 150.3, 151.0; δ_P ($CDCl_3$) 54.7; ESMS 386.14 (100%, LH^+); υ_{max} (KBr disc)/cm^{-1} 3061, 2690, 2864, 1611, 1599, 1412, 1296, 1340, 1283, 1064. Found: MH^+ 386.1820. $C_{21}H_{29}N_3PS$ requires MH^+ 386.1836. Found: C, 65.3%: H, 7.18%: N, 10.7%. $C_{21}H_{29}N_3PS$ requires C, 65.4%: H, 7.3%: N, 10.8%.

4,4'-Dibromo-2,2'-bis-1-H-benzimidazole (115)[14]

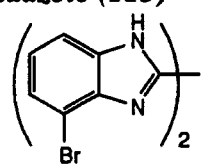

To a stirred solution of 1,2-diamino-3-bromobenzene (3.75g, 20.0mmol) in dry methanol (30ml) at room temperature was added methyl-2,2,2-trichloroacetimidate (1.2ml, 9.65mmol), followed by concentrated hydrochloric acid (10M, 3 drops). After 3 h, fine mesh potassium carbonate (0.63g) was added, followed by an additional portion (1.2g) 3 h later. The mixture was stirred for a further 18 h and water (100ml) added. The resultant yellow precipitate was collected by fitration and dried under

vacuum. The crude product was purified by refluxing in methanol to remove the solid impurities. After cooling to room temperature the mixture was filtered and the solid collected and dried under vacuum to give a yellow solid (2.91g, 75%), mp >350°C (lit >350°C). [17]

δ_H ($CDCl_3$, 0.5% TFA) 7.55 (2H, dd, $^3J_{H6H5}$=8.0Hz, $^3J_{H6H7}$=7.8Hz, H6), 7.83 (2H, d, $^3J_{H7H6}$=7.8Hz, H7), 7.89 (2H, d, $^3J_{H5H6}$=8.0Hz, H5); δ_C ($CDCl_3$, 0.5% TFA) 107.8 (CBr), 115.0, 131.0, 133.0, 133.2 (C-C), 133.8, 134.0.

1, 1'-Bis(4-tert-butylbenzyl)-4,4'-dibromo-2,2'-bisbenzimidazole (116)[15]

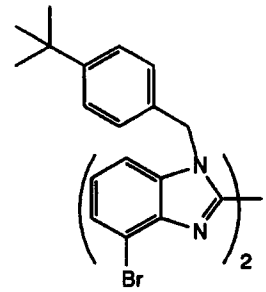

DMF (50ml) was added to a mixture of 4,4'-dibromo-2,2'-bis-1H-benzimidazole (2.97g, 7.58mmol) and caesium carbonate (5.43g, 16.7mmol) and the mixture stirred at room temperature under argon for 1 h. 4-(*tert*-Butyl)benzylbromide (3.78g, 16.7mmol) was added and the temperature raised to 80°C for 18 h. After cooling, methanol (70ml) was added and the precipitate collected by filtration, washed with water (40ml) and dried to give a white solid. Recrystallisation from methanol gave a white solid (4.7g, 90%); mp 316-317°C (lit 316-317°C).[18]

δ_H ($CDCl_3$, 0.5% TFA) 1.21 (18H, s, CH_3), 5.53 (4H, s, CH_2), 7.10 (4H, d, $^3J_{H10H11}$=8.4Hz, H10), 7.27 (4H, d, $^3J_{H11H10}$=8.4Hz, H11), 7.65 (2H, d, $^3J_{H7H6}$=7.9Hz, H7), 7.67 (2H, dd, $^3J_{H6H5}$=8.1Hz, $^3J_{H6H7}$=7.9Hz, H6), 7.96 (2H, dd, $^3J_{H5H6}$=8.1Hz, H5)

Attempted preparation of Diethyl-1,1'-di(4-tert-butylbenzyl)-2,2'-bisbenzimidazole-4,4'-bis(phenylthio -phosphinate) (118)

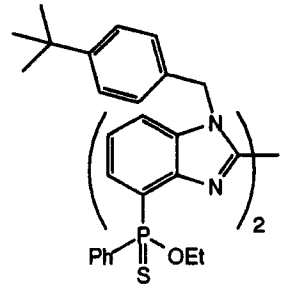

To a cold (-78°C) slurry of 1,1'-di(4-*tert*-butyl)benzyl-4,4'-dibromo-2,2'-bisbenzimidazole (300mg, 0.53mmol) in dry THF (10ml), was added a THF solution of n-butyl lithium (1.6M, 0.69ml, 1.31mmol) and the reaction stirred under argon until a deep red colour persisted (c. 1 h). Freshly made chloroethoxyphenylphosphine (241mg, 1.31mmol, made by the equimolar addition of dichlorophenylphosphine and

diethoxyphenylphosphine at 0°C under an argon atmosphere) was added and the mixture allowed to warm slowly to room temperature. Concentrated hydrochloric acid (10M 2.5ml) was added and the mixture stirred at room temperature for 16 h. The solvents were removed under reduced pressure, chloroform (10ml) and dry crushed sulphur powder (42mg, 1.31mmol) were added and the mixture heated at 40°C for 18 h. The reaction mixture was washed with water (3x15ml) the organic layer dried (K_2CO_3) and the solvents removed under reduced pressure, to yield a pale yellow gum.

ESMS (-) showed the presence of the desired product, however this could not be separated by gravity chromatography or HPLC.

Attempted preparation of 1,1'-Di(4-tert-butyl)benzyl-2,2'-bisbenzimidazole-4,4' bis[(4-methoxyphenyl)-dithiophosphinic acid)] (119)

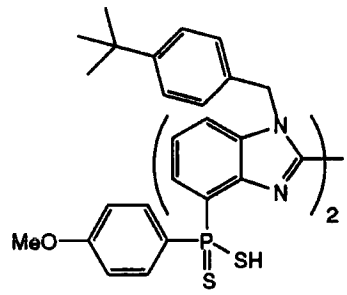

To a cold (-78°C) slurry of 1,1'- Di(4-*tert*-butylbenzyl)-4,4'-dibrom-2,2'-bisbenzimidazole (120mg, 0.21mmol) in dry THF (6ml) was added a THF solution of n-butyl lithium (1.6M, 0.23ml, 0.44mmol) and the reaction stirred under argon until a deep red colour persisted (c. 1h). Freshly prepared anhydrous magnesium bromide etherate[11] (2.62M, 2ml, 1.26mmol) was added and the reaction mixture allowed to warm to room temperature. The reaction mixture was frozen in liquid nitrogen, and dry Lawesson's reagent (140mg, 0.44mmol) added as a solid under argon, then the mixture allowed to slowly warm to room temperature. Concentrated hydrochloric acid (10M 3ml) was added and the mixture stirred for 12 h. Chloroform (15ml) was added and the solution washed with water (3x10ml), dried (K_2CO_3) and the solvent removed under reduced pressure.

ESMS (-) showed the presence of the desired product, however this could not be separated by gravity chromatography or HPLC.

Attempted preparation of 1,1'-Di(4-tert-butylbenzyl)-2,2'-bisbenzimidazole-4,4'-bis(thiocarboxylic acid)

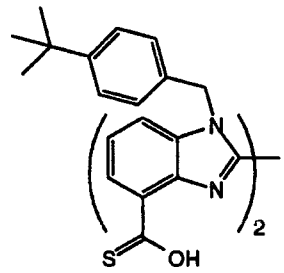

To a cold (-78°C) slurry of 1,1'-Di(4-*tert*-butyl)benzyl-4,4'-dibromo-2,2'-bisbenzimidazole (198mg, 0..35mmol) in dry THF (10ml) was added a THF solution of n-butyl lithium (1.6M, 0.38ml, 0.72mmol) and the reaction stirred under argon until a deep red colour persisted (1h). Dry carbonyl sulfide was bubbled through the mixture for 15 min which was then allowed to warm to room temperature. Water (15ml) was added and the solution made acidic (pH1) by addition of concentrated hydrochloric acid (10M). The mixture was extracted with chloroform (3x20ml), the organic layers were dried ($MgSO_4$) and the solvent removed under reduced pressure to give a yellow gum.

Neither ESMS (±) nor ^1H NMR showed the presence of the desired product

Diethyl-1,1'-Di(4-tert-butylbenzyl)-2,2'-bisbenzimidazole-4,4'-bis(phenylphosphinate) (120)

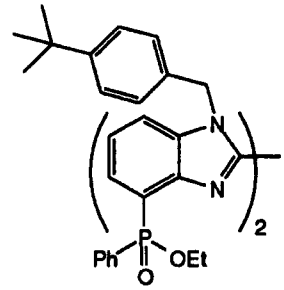

Using a procedure adapted from Huang,[14] 1,1'-bis(4-tertbutylbenzyl)-4,4'-dibromo-2,2'-bisbenzimidazole (1g, 1.46mmol), ethylphenylphosphonite (0.46ml, 3.07mmol) and triethylamine (1.5ml, 19.5mmol) were mixed in dry degassed toluene (5ml). Tetrakis(triphenylphosphine)palladium(0) (100mg) was added and the mixture was degassed three times (freeze thaw cycle), before being heated at 100°C for 96 h. The solution was diluted with dichloromethane (20ml), washed with aqueous hydrochloric acid (1M, 2x20ml) and water (3x20ml), dried (K_2CO_3)and the solvent removed under reduced pressure to give an off white solid. Purification by column chromatography (silica, eluant 1% MeOH/99% dichloromethane going to 10% MeOH/90% dichloromethane, R_f (product)=0.42 (10% MeOH/90% dichloromethane)) gave a white solid (655mg, 52%), mp 117-118°C.

δ_H ($CDCl_3$) 1.23 (6H, t, ^3J=8.0Hz, $OCH_2\underline{C}H_3$), 1.26 (18H, s, $C(\underline{C}H_3)_3$), 4.02 (4H, qd, ^3J=8.0Hz, $^2J_{HP}$=1.6Hz, $OC\underline{H}_2CH_3$), 6.22 (2H, d, ^2J=16Hz, $NC\underline{H}_2Ar$), 6.35 (2H, dd, ^2J=16Hz, ^2J= 8Hz, $NC\underline{H}_2Ar$), 7.01 (4H, d, ^3J=7.6Hz, H10), 7.15 (4H, ddd, $^3J_{HmPhHoPh}$=7.6Hz, $^3J_{HmPhHpPh}$=7.2Hz, $^4J_{HmPhP}$=3.99Hz, H*m*Ph), 7.24 (4H, d, ^3J=7.60Hz, H11), 7.31 (2H, dd, $^3J_{HpPhHmPh}$=7.6Hz, $^5J_{HoPhP}$=7.6Hz, H*p*Ph), 7.38 (2H, ddd, $^3J_{H6H7}$=8.0Hz, $^3J_{H6H5}$=7.6Hz, $^4J_{H6P}$=2.0Hz, H6), 7.56 (2H, d, $^3J_{H7H6}$=8.0Hz, H7), 7.97 (4H, dd, $^3J_{HoPhHmPh}$=7.6Hz, $^3J_{HoPhP}$=12.8Hz, H*o*Ph), 8.04 (2H, dd, $^3J_{H5H6}$=7.6, $^3J_{H5P}$=13.6Hz, H5); δ_C ($CDCl_3$) 16.7 (s, $OCH_2\underline{C}H_3$), 31.5 (s, $C(\underline{C}H_3)_3$), 34.7 (s, $\underline{C}(CH_3)_3$), 49.0 (s, $N\underline{C}H_2Ar$), 61.3 (d, $^3J_{CP}$=5.9Hz, $O\underline{C}H_2CH_3$), 122.9 (d, $^1J_{CP}$=134.3Hz, C*i*Ph), 124.0 (d, $^2J_{CP}$=12.8Hz, C5), 125.8 (C11), 126.9 (C10), 128.2 (d, $^3J_{CP}$=13.6Hz, C*m*Ph), 129.4 (C9), 129.4 (d, $^4J_{CP}$=12.0Hz, C7), 131.7 (d, $^3J_{CP}$=2.6Hz, C6), 132.0 (d, $^3J_{CP}$=10.6Hz, C*o*Ph), 133.6 (C12), 136.0 (d, $^4J_{CP}$=12.3Hz, C*p*Ph), 142.7 (d, $^3J_{CP}$=8.5Hz, C3'), 143.3 (C4'), 150.8 (C2); δ_P ($CDCl_3$) 32.1, 32.2 (RR/SS and RS diastereoisomers); vmax (KBr disc)/cm^{-1} 2961, 2866, 1438, 1220, 1035, 722; Found: MH^+ 863.3851; $C_{27}H_{31}N_2PO_2$ requires M^+ 863.3854

Methyl-5-hydroxypentanoate (125)[19]

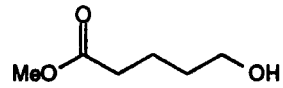

To a solution of sodium methoxide in methanol, prepared from sodium (0.25g, 0.01mol) and methanol (12.5ml), was added δ-valerolactone (5g, 0.05mol). The solution was heated under reflux for 3 h, poured into water (100ml) and the organic material extracted with diethylether (3x50ml) and chloroform (3x50ml). The organic extracts were combined, dried ($MgSO_4$) and the solvent removed under reduced pressure, to give a colourless oil (4.2g, 68%).

δ_H($CDCl_3$) 1.4-1.7 (4H, m, H3 and H4), 2.52 (2H, t, ^3J=7.2Hz, H5), 2.84 (1H, bs, OH), 3.51 (2H, t, ^3J=5.9Hz, H2), 3.6 (3H, s, $O\underline{C}H_3$). δ_C($CDCl_3$) 23.0 (C4), 33.8 (C3), 35.6 ($O\underline{C}H_3$), 53.4 (C5), 63.8 (C2), 176.0 ($\underline{C}$=O). υ_{max} (thin film/cm^{-1}; 3452 (br, OH), 2944, 2864, 1739 (C=O)

Methyl-5-(tert-butyldimethylsilyl)-pentanoate (128)

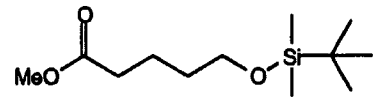

To a solution of methyl-5-hydroxypentanoate (4.5g, 0.034mol) in DMF (18ml) was added *tert*-butyldimethylsilylcholride (6.17g, 0.041mol) and imidazole (2.78g, 0.041mol) and the solution left to stir at ambient temperature for 16 h. The DMF was removed under reduced pressure and dichloromethane (50ml) was added to the residue, washed with water (3x50ml) and the water re-extracted with more dichloromethane (75ml). The organics were combined, dried ($MgSO_4$) and the solvent removed under

reduced pressure. The residue was purified by column chromotography on silica (eluant 3:1 hexane:dichloromethane, R_f product = 0.16) to give the product as a colourless oil (4.8g, 56%).

$\delta_H(CDCl_3)$ 0.01 (6H, s, C<u>H</u>$_3$), 0.86 (9H, s, tBu), 1.44-1.75 (4H, m, H3 and H4), 2.31 (2H, t, ^3J=7.5Hz, H5), 3.59 (2H, t, ^3J=6.0Hz, H2), 3.64 (3H, s, OC<u>H</u>$_3$); $\delta_C(CDCl_3)$ 5.4 (<u>C</u>H$_3$), 18.2 (tBu) 21.3, 25.8 (C3), 32.0 (C4), 33.7 (C5), 51.3 (C2), 62.5 (O<u>C</u>H$_3$), 173.9 (<u>C</u>=O); ESMS 246.95 (16%, MH^+), 268.95 (83%, MNa^+), 284.92 (100%, MK^+)

Ethyl-5-cyanobutyrate (132)

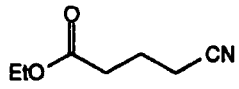

To a solution of potassium cyanude [caution!] (2g, 0.037mol) in DMF (15ml) was added ethyl-4-bromobutyrate (5g, 0.026mol) dropwise over a period of 30 min. The solution was then stirred for 2 h and heated at 80°C for 20 h. The mixture was diluted with chloroform (40ml) extracted with chloroform (2x40ml), washed with brine (80ml), dried (Na_2SO_4) and the solvents removed under reduced pressure. The residue was distilled under reduced pressure to give a colourless oil (3.45g, 66%), bp 100°C/5mmHg (lit. 100°C/5mmHg).[20]

$\delta_H(CDCl_3)$ 1.26 (3H, t, ^3J=7.1Hz, $OCH_2C\underline{H}_3$), 1.94-2.15 (2H, m, H3), 2.45(2H, t, ^3J=5.91Hz, H4), 3.46 (2H, t, ^3J=6.34Hz, H2), 4.10 (2H, q, ^3J=7.1Hz, OC<u>H</u>$_2$CH$_3$); $\delta_C(CDCl_3)$ 16.0 (C3), 18.2 (C4), 22.6 (C2), 22.6 ($OCH_2\underline{C}H_3$), 62.4 (O<u>C</u>H$_2$CH$_3$), 121.0 (<u>C</u>N), 173.8 (<u>C</u>=O); ESMS 163.77 (62%, MNa^+), 179.77 (100%, MK^+)

Attempted preparation of 1-(4-Bromo-1-H-benzimidazole)-3-cyanopropane[21]

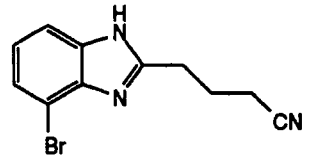

Using a procedure adapted from Leavitt,[21] 1, 2-diamino-3-bromobenzene (600mg, 3.2mmol) and ethyl-4-cyanobutyrate (416mg, 3.2mmol) were heated at 180°C for 16 h in polyphosphoric acid (6g). The dark solution was allowed to cool to 100°C and poured into water (100ml with rapid stirring. The solid was collected by filtration, suspended in concentrated ammonia (0.880) and extracted into chloroform (3x80ml). The organic fractions were combined, dried (K_2CO_3) and the solvent removed under reduced pressure to give a dark solid.

^1H and ESMS revealed none of the desired material, but implied the formation of the C-3 spaced bisbenzimidazole.

Bis(1, 3-propyl)-1 H-benzimidazole (133)

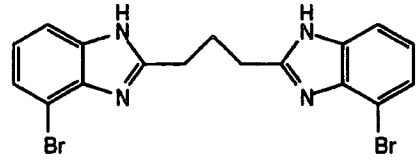

To a mixture of 1, 2-diamino-3-bromobenzene (730mg, 3.90mmol) and dimethyl glutarate (313mg, 1.95mmol) was added polyphosphoric acid (10ml) and the mixture heated at 180°C for 18 h. The black solution was allowed to cool to 100°C and poured in a thin stream into well stirred water (100ml), and stirring continued for 1 h. The mixture was filtered, the pH adjusted to 8 by addition of NaOH solution (3M) and the resultant dark solid collected by filtration and washed with water (2x10ml). The solid was dissolved in methanol (50ml) and treated with activated charcoal at 80°C for 30 min, filtered through celite and the solvent removed under reduced pressure to give an orange solid (500mg, 59%), mp 85-87°C

δ_H ($CDCl_3$) 2.34 (2H, t, ^3J=6.7Hz, 3-propyl $C\underline{H}_2$), 3.05 (4H, t, ^3J=6.7Hz, 2-propyl $C\underline{H}_2$), 7.13 (2H, dd, $^3J_{H6H7}$=7.87Hz, $^3J_{H6H5}$=7.89Hz, H6), 7.44 (2H, d, $^3J_{H7H6}$=7.87Hz, H7), 7.53 (2H, d, $^3J_{H5H6}$=7.89Hz, H5); δ_C ($CDCl_3$) 18.4 (CH_2), 36.2 (CH_2), 107.8 (C-Br), 115.0, 131.1, 133.5, 134.5, 141.6 (C2); ESMS 434.32 (45%, LH^+), 435.54 (100%, LH^+), 436.71 (51%, LH^+); υ_{max} (KBr disc)/cm^{-1} 3134, 2928, 2760, 1652, 1536, 1422, 1215, 1190, 1048, 932; Found: C, 47.36%; H, 3.62%; N, 12.45%. $C_{17}H_{14}N_2Br_2$ requires C, 47.03%; H, 3.25%; N, 12.90%.

4, 4'-Dibromo-1,1'-di(tert-butylbenzyl)-2,2'-bis(1,3- propyl)benzimidazole (134)

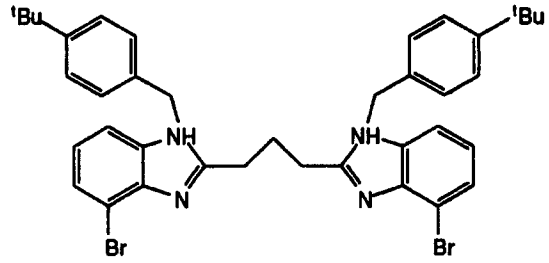

Dimethylformamide (15ml) was added to a mixture of bis(1,3-propyl)-1-H-benzimidazole (920mg, 2.12mmol) and caesium carbonate (1520mg, 4.66mmol, 2.2 equiv) and the mixture stirred under argon for 2 h. 4-(*tert*-Butyl) benzyl bromide (0.86ml, d=1.236, 4.66mmol, 2.2equiv) was added and the mixture heated at 80°C for 16 h. After cooling the DMF was removed by vacuum distillation, and the residue taken up into dichloromethane (40ml), washed with water (3x40ml), dried (K_2CO_3) and the dichloromethane reduced to a minimal volume (1ml) followed by precipitation of the product with diethyl ether (5ml). This yielded a pale orange solid (1477mg, 96%), mp 79-80°C.

δ_H ($CDCl_3$) 1.23 (18H, s, tBu), 2.44 (2H, t, ^3J=6.6Hz, 2-propyl $C\underline{H}_2$), 2.95 (4H, t, ^3J=6.6Hz, 1- and 3-propyl $C\underline{H}_2$), 5.38 (4H, s, CH_2), 7.21 (4H, d, $^3J_{H10H11}$=2.9Hz, H10), 7.33 (2H, dd, $^3J_{H6H7}$=8.1Hz, $^3J_{H6H5}$=7.6Hz, H6), 7.45 (2H, d, $^3J_{H7H6}$=8.1Hz,

H7), 7.61 (2H, d, $^3J_{H11H10}$=2.9Hz, H11), 7.69 (4H, d, $^3J_{H5H6}$=7.6Hz, H5); δ_C ($CDCl_3$) 16.1 (CH_3), 18.0, 33.2 (tBu), 36.5, 49.2 (CH_2), 110.8, 114.5, 125.1, 126.9, 127.9, 127.9, 134.3, 137.9, 153.1, 154.8; ESMS 724.51 (55%, LH^+), 726.33 (100%, LH^+), 727.27 (60%, LH^+); υ_{max} (KBr disc)/cm^{-1} 3388, 2954, 1894, 1732, 1628, 1532, 1426, 1274, 1182, 1604, 924, 738.

Ethyl-1,1'-bis(tert-butylbenzyl)-2,2'-bis(1,3-propyl)benzimidazole-4,4'-bis(phenylphosphinate) (135)

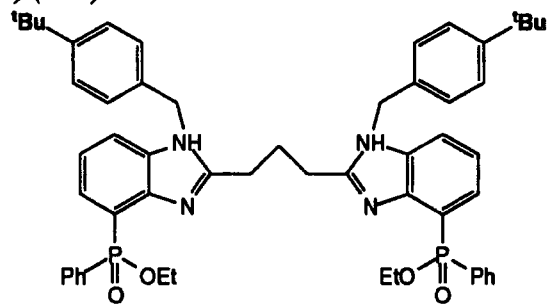

Using a procedure adapted from Huang[14] 4,4'-dibromo-1,1'-di(*tert*-butylbenzyl)-2,2'-bis(1,3-propyl)benzimidazole (300mg, 0.41mmol), ethylphenylphosphonite (0.14ml, 0.87mmol, 2.1 equiv.) and triethylamine (1ml) were mixed in dry degassed toluene (3ml). Tetrakis(triphenylphosphine)palladium(0) (10mg) was added and the mixture degassed three times (freeze thaw cycle), then heated at 125°C for 48 h. The solution was diluted with dichloromethane (20ml), washed with hydrochloric acid (1M, 2x20ml) and water (3x20ml), dried (K_2CO_3) and the solvent removed under reduced pressure to give an off white solid. Purification by column chromatography (silica gel, eluant 100% dichloromethane increasing to 8% MeOH/92% dichloromethane, R_f(product)=0.2 (8% MeOH/92% dichloromethane)) gave a light orange solid (230mg, 62%), mp 64-66°C δ_H ($CDCl_3$) 1.13 (18H, s, C($C\underline{H}_3$)$_3$), 1.29 (6H, t, ^3J=7.2Hz, OC$H_2C\underline{H}_3$), 2.41 (2H, t, ^3J=6.6Hz, 2-propyl C$\underline{H}_2$), 2.94 (4H, t, ^3J=6.6Hz, 3-propyl C$\underline{H}_2$), 4.09 (4H, qd, ^3J=7.2Hz, $^2J_{HP}$=2.0Hz, OC$\underline{H}_2CH_3$), 4.97 (4H, s, NC$\underline{H}_2$Ar), 6.61 (4H, d, ^3J=7.99Hz, H10), 6.90 (4H, d, ^3J=7.99Hz, H11), 7.22 (2H, ddd, $^3J_{H6H7}$=7.8Hz, $^3J_{H6H5}$=7.9Hz, $^4J_{H6P}$=2Hz, H6), 7.46 (4H, ddd, $^3J_{HmPhHoPh}$=8.0Hz, $^3J_{HmPhHpPh}$=7.5Hz, $^4J_{HmPhP}$=3.6Hz, H*m*Ph), 7.62 (2H, dd, $^3J_{HpPhHmPh}$=7.5Hz, $^5J_{HoPhP}$=8.0Hz, H*p*Ph), 7.56 (2H, d, $^3J_{H7H6}$=7.8Hz, H7), 7.83 (4H, dd, $^3J_{HoPhHmPh}$=8.0Hz, $^3J_{HoPhP}$=13.49Hz, H*o*Ph), 8.16 (2H, dd, $^3J_{H5H6}$=7.9Hz, $^3J_{H5P}$=13.6Hz, H5); δ_C ($CDCl_3$) 14.3 ($\underline{C}(CH_3)_3$), 16.7 (d, $^3J_{CP}$=7.6Hz, OC$H_2\underline{C}H_3$), 29.0, 31.2 (C($\underline{C}H_3$)$_3$), 34.6 (N$\underline{C}H_2$Ar), 46.7, 61.2 (d, $^2J_{CP}$=7.0Hz, O$\underline{C}H_2CH_3$), 114.0 (d, $^3J_{CP}$=3.1Hz, C6), 120.9 (d, $^1J_{CP}$=162.5Hz, C*i*Ph), 121.7 (d, $^2J_{CP}$=16.0Hz, C5), 126.1 (C11), 126.1 (C12), 127. 7 (d, $^4J_{CP}$=9.8Hz, C7), 128.2 (d, $^3J_{CP}$=16.5Hz, C*m*Ph), 131.9 (d, $^3J_{CP}$=3.8Hz, C8), 132.3 (d, $^2J_{CP}$=13.3Hz, C*o*Ph), 132.4 (d, $^3J_{CP}$=168.8Hz, C4), 135.8 (d, $^4J_{CP}$=15.5Hz, C*p*Ph), 143.5 (d, $^2J_{CP}$=12.8Hz, C9), 151.2, 153.3 (C2); δ_P ($CDCl_3$) 29.2; ESMS 905.31 (100%, LH^+); υ_{max} (KBr disc)/cm^{-1} 3420, 2962, 2868, 1725, 1709, 1690, 1483, 1270, 1112, 1044, 1012, 830, 746, 666; Found MH^+ 905.4325; $C_{55}H_{63}N_4P_2O_4$ requires MH^+ 905.4324

1,1'-Bis(tert-butylbenzyl)-bis(1,3-propyl)benzimidazole-4,4'-bis(phenylphosphinic acid) dihydrochloride (28)

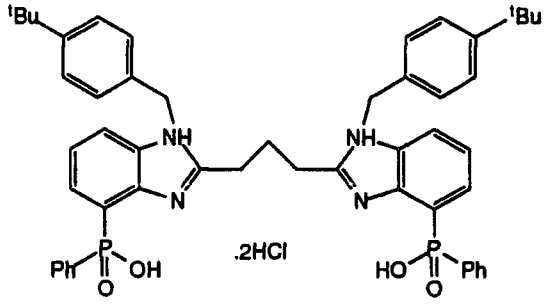

To a solution of ethyl-1,1'-bis(tert-butylbenzyl)-2,2'-bis(1,3-propyl)benzimidazole-4,4'-bis(phenylphosphinate) (100mg, 0.11mmol) in 1, 4 dioxane (6ml) was added concentrated hydrochloric acid (10M, 4ml). The solution was heated at 110°C and the reaction followed by ^{31}P NMR (δ_P (starting material) = 29.22, δ_P (product) = 16.44) until the reaction was complete (c. 20h). The solvent was removed under reduced pressure to give a pale orange solid (92mg, 99%). mp 173-175°C
δ_H (CD_3OD); 1.23 (18H, s, ^tBu), 2.01 (2H, t, ^3J=6.8Hz, 2-propyl $C\underline{H}_2$), 2.65 (4H, t, ^3J=6.8Hz, 1- and 3-propyl $C\underline{H}_2$), 5.52 (4H, s, $NC\underline{H}_2$), 7.35 (1H, dd, $^3J_{H6H7}$=8.5Hz, $^3J_{H6H5}$=8.3Hz, H6), 7.09 (2H, d, $^3J_{H10H11}$=8.3Hz, H10), 7.30 (1H, dd, $^3J_{HpPhHmPh}$=7.7Hz, $^5J_{HpPhP}$=7.2Hz, H*p*Ph), 7.32 (2H, d, $^3J_{H11H10}$=8.3, H11), 7.62 (2H, ddd, $^3J_{HmPhHoPh}$=7.1Hz, $^3J_{HmPhHpPh}$=7.7Hz, $^4J_{HmPHP}$=3.2Hz, H*m*Ph), 7.72 (1H, d, $^3J_{H5H6}$=8.3Hz, H5), 7.89 (1H, d, $^3J_{H7H6}$=8.5Hz, H7), 8.23 (2H, dd, $^3J_{HpPhHmPh}$=7.7Hz, $^5J_{HpPhP}$=12.0Hz, H*p*Ph); δ_C (CD_3OD); 22.6 ($\underline{C}(CH_3)_3$), 28.0, 31.1 ($C(\underline{C}H_3)_3$), 34.6, 48.8 ($N\underline{C}H_2Ar$), 114.9 (C2), 124.3 (C8'), 125.5 (d, $^2J_{CP}$=12.2Hz, C3'), 126.5 (C10), 126.9 (C11), 128.7 (d, J_{CP}=13.8Hz), 129.3, 130.0. 130.1 (d, $^1J_{CP}$=153.6Hz), 132.5, 132.6, 132.6 (d, $^1J_{CP}$=130.8Hz), 152.3, 152.8; δ_P (CD_3OD) 16.4; ESMS 847.23 (100%, L^-); υ_{max} (KBr disc)/cm^{-1} 3316, 2966, 2924, 2860, 1852, 1725, 1709, 1690, 1648, 1512, 1258, 1140, 1090, 830, 794; Found: MH^+ 848.3621; $C_{51}H_{55}N_4P_2O_4$ requires MH^+ 848.3620.

6.4 Chapter Four Experimental.

8-Bromo-2-methylquinoline (149)

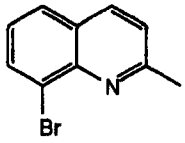

Using a procedure adapted from Leir,[22] crotonaldehyde (6.8g, 0.097mol) was added dropwise over a period of 30 min to a refluxing suspension of 2-bromoaniline (15.25g, 0.088mol) in hydrochloric acid (6M, 45ml). The dark mixture was heated at 120°C for 2 h then allowed to cool to room temperature and zinc(II)chloride (21.5g, 0.088mol) was added with stirring. The solution was left at 0°C for 16 h and the golden coloured

crystals collected by filtration, washed with hydrochloric acid (1M, 50ml), water (2x50ml), isopropyl alcohol (2x50ml) and diethylether (2x50ml). The solid was suspended in concentrated ammonia solution (150ml) and extracted exhaustively with diethyl ether. The organic extracts were combined, dried (K_2CO_3) and the solvent removed under reduced pressure to give a pale yellow solid (14.06g, 72%), mp 66-67°C (lit 67-68°C).[22]

$\delta_H(CDCl_3)$ 2.77 (3H, s, 2-C$\underline{H}_3$), 7.24 (1H, d, $^3J_{H3H4}$=8.4Hz, H3), 7.26 (1H, dd, $^3J_{H6H7}$=8.0Hz, $^3J_{H6H5}$ 7.6Hz, H6), 7.66 (1H, d, $^3J_{H7H6}$=8.0Hz, H7), 7.95 (1H, d, $^3J_{H4H3}$=8.4Hz, H4), 7.96 (1H, d, $^3J_{H5H6}$=7.6Hz, H5); ESMS 221.83 (49%, LH^+), 223.76 (51%, LH^+)

Ethyl 8-(2-methylquinolinyl)phenylphosphinate (161)

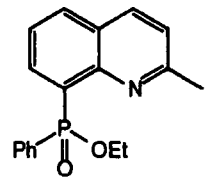

Using a procedure adapted from Huang,[14] 2-methyl-8-bromoquinoline (2.5g, 0.011mol), ethylphenylphosphonite (1.81ml, 0.012mol) and triethylamine (10ml, 0.071mol) were mixed in dry degassed toluene (30ml).

Tetrakis(triphenylphosphine)palladium(0) (210mg, 0.18mmol) was added and the mixture degassed three times (freeze thaw cycle), then heated at 100°C for 96 h. The solution was diluted with dichloromethane (50ml), washed with aqueous hydrochloric acid (1M, 2x60ml) and water (3x60ml), dried (K_2CO_3) and the solvent removed under reduced pressure to give an off white solid. Purification by column chromatography (alumina, eluant 2% MeOH/98% dichloromethane R_f(product)=0.3 (2% MeOH/98% dichloromethane)) gave a white solid (2.32g, 68%). mp 106-107°C

δ_H ($CDCl_3$) 1.36 (3H, t, ^3J=6.8Hz, $OCH_2C\underline{H}_3$), 2.63 (3H, s, 2-C$\underline{H}_3$), 4.13 (2H, qd, ^3J=6.8Hz, $^2J_{HP}$= 7.2Hz, $OC\underline{H}_2CH_3$), 7.19 (1H, d, $^3J_{H3H4}$=8.4Hz, H_3), 7.34-7.48 (3H, m, H*m*Ph & H*p*Ph), 7.53 (1H, ddd, $^3J_{H6H5}$=8.4Hz, $^3J_{H6H7}$=7.2Hz, $^4J_{H6P}$=2.8Hz, H6), 7.89 (1H, d, $^3J_{H5H6}$=8.4Hz, H5), 7.94 (1H, d, $^3J_{H4H3}$=8.4Hz, H4), 8.14 (1H, dd, $^3J_{HpPhHmPh}$=8.0Hz, $^5J_{HpPhP}$=12.8Hz, H*p*Ph), 8.49 (1H, dd, $^3J_{H7H6}$=7.2Hz, $^3J_{H7P}$=15.2Hz, H7); δ_C ($CDCl_3$) 16.4 (d, $^3J_{CP}$=6.8Hz, $OCH_2\underline{C}H_3$), 24.9 (2-$\underline{C}H_3$), 60.9 (d, $^2J_{CP}$=6.1Hz, $O\underline{C}H_2CH_3$), 122.2 (C3), 124.8 (d, $^3J_{CP}$=13.7Hz, C6), 126.1 (d, $^3J_{CP}$=9.2Hz, C4'), 127.5 (d, $^3J_{CP}$=13.7Hz, C*m*Ph), 128.4 (d, $^2J_{CP}$=12.8Hz, C8'), 129.7 (d, $^1J_{CP}$=134.3Hz, C*i*Ph), 131.3 (d, $^4J_{CP}$=3.1Hz, C*p*Ph), 131.9 (d, $^4J_{CP}$=10.0Hz, C2), 132.4 (d, $^4J_{CP}$=2.6Hz, C5), 132.7 (d, $^2J_{CP}$=10.7Hz, C*o*Ph), 133.2 (d, $^1J_{CP}$=111.4Hz, C8), 135.8 (C4), 136.1 (d, $^2J_{CP}$=8.9Hz, C2); δ_P ($CDCl_3$) 34.0; ESMS 386.14 (100%, LH^+); υ_{max} (KBr disc)/cm^{-1} 3530, 3056, 2973, 2361, 1823, 1607, 1224, 1119; Found: MH^+ 312.1153 $C_{18}H_{18}NPO_2$ requires 312.1153. Found: C, 66.46%; H, 5.9O%; N, 4.01%. $C_{18}H_{18}NPO_2.CH_3OH$ requires C, 66.46%; H, 6.35%; N, 4.08.

8-(2-methylquinoline)phenylphosphinic acid hydrochloride (31)

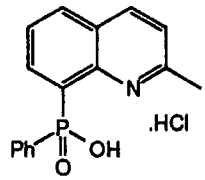

To Ethyl 8-(2-methylquinolinyl)phenylphosphinate (200mg, 0.65mmol) was added hydrochloric acid (6M, 50ml) and the mixture heated at 110°C for 16 h. After cooling the inorganic acid was removed under reduced pressure to give a white solid (206mg, 99%), mp 148-150°C.

δ_H (CD_3OD) 3.11 (3H, s, 2-$C\underline{H}_3$), 7.50 (3H, m, H*m*Ph, H*p*Ph), 7.92-8.01 (3H, m, H*o*Ph, H5), 8.02 (1H, d, $^3J_{H3H4}$=8.4Hz, H3), 8.36 (1H, dd, $^3J_{H7H6}$=8.0Hz, $^3J_{H7P}$=16.0Hz, H7), 8.41 (1H, d, $^3J_{H6H7}$=8.0Hz, H6), 9.06 (1H, d, $^3J_{H4H3}$=8.4Hz, H4); δ_C (CD_3OD) 22.0 (2-$\underline{C}H_3$), 123.9 (C3), 127.4 (d, $^3J_{CP}$=7.7Hz, C7), 128.6 (C6), 128.8 (C5), 129.0 (C4'), 130. 4 (d, $^1J_{CP}$=105.1Hz, C*i*Ph), 131.5 (d, $^3J_{CP}$=10.6Hz, C*m*Ph), 132.6 (d, $^2J_{CP}$=14.6Hz, C*o*Ph), 132.8 (d, $^2J_{CP}$=2.6Hz, C8'), 133.7 (d, $^1J_{CP}$=120.8Hz, C8), 139.8 (d, $^4J_{CP}$=7.3Hz, C8'), 146.8 (C4), 158.4 (C2); δ_P (CD_3OD) 26.7; ESMS 283.99 (L^-); υ_{max} (KBr disc)/cm^{-1} 3488, 3436, 3066, 3042, 2912, 2864, 2676, 2168, 2006, 1640, 1604, 1528, 1402, 1306, 1182, 1128, 1080, 908, 774, 698, 578; Found: MH^+ 284.0840 $C_{16}H_{15}NPO_2$ requires 284.0840.

8-Bromoquinoline (148)

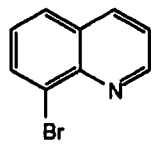

Using a procedure adapted from Leir,[22] acrolein (1.79g, 32.04mmol) was added dropwise over a period of 30 min to a refluxing suspension of 2-bromoaniline (5g, 29.07mmol) in hydrochloric acid (6M, 25ml). The dark mixture was heated at 120°C for 2 h then allowed to cool to room temperature. Zinc(II)chloride (7.1g, 29.07mmol) was added with stirring. The solution was left at 0°C for 16 h and the golden coloured crystals collected by filtration, washed with hydrochloric acid (1M, 10ml), water (2x15ml), isopropyl alcohol (2x20ml) and diethylether (2x20ml). The solid was suspended in concentrated ammonia solution (50ml) and extracted exhaustively with diethyl ether (5x50ml). The organic extracts were combined, dried (K_2CO_3) and the solvent removed under reduced pressure to give a dark oil which was further purified by short path distillation to give a pale yellow oil (3.73, 56%). bp (210°C/0.1mmHg) lit. (112-113°C/0.5mmHg).[23]

δ_H($CDCl_3$) 7.35 (1H, dd, $^3J_{H3H2}$=5.6Hz, $^3J_{H3H4}$=8.2Hz, H3), 7.42 (1H, $^3J_{H6H7}$=7.2Hz, $^3J_{H6H5}$=7.8Hz, H6), 7.71 (1H, d, $^3J_{H5H6}$=7.8Hz, H5), 8.05 (1H, d, $^3J_{H7H6}$=7.2Hz, H6), 8.10 (1H, $^3J_{H4H3}$=8.2Hz, H4), 9.01 (1H, $^3J_{H2H3}$=5.6Hz, H2); δ_C ($CDCl_3$) 121.7, 124.0 (C4'), 126.7, 127.6, 129.1 (C8'), 132.6, 136.3, 144.9 (C8), 150.9

Ethyl 8-(quinolinyl)phenylphosphinate (160)

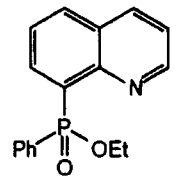

Using a procedure adapted from Huang,[14] 8-bromoquinoline (3.41g, 11.48mmol), ethyl-phenylphosphonite (2.16g, 12.63mmol) and triethylamine (8.8ml, 68.88mmol) were mixed in dry degassed toluene (10ml). Tetrakis(triphenylphosphine)palladium(0) (100mg) was added and the mixture degassed three times (freeze thaw cycle), then heated at 100°C for 96 h. The solution was diluted with dichloromethane (30ml), washed with hydrochloric acid (1M, 2x40ml) and water (3x40ml), dried (K_2CO_3) and the solvent removed under reduced pressure to give an off white solid. Purification by column chromatography (alumina, eluant 2% MeOH/98% dichloromethane R_f(product)=0.3 (2% MeOH/98% dichloromethane)) gave a white solid (2.32g, 68%), mp 100-102°C.

δ_H ($CDCl_3$) 1.36 (3H, t, ^3J=6.8Hz, $OCH_2\underline{C}H_3$), 4.16 (2H, qd, ^3J=6.8Hz, $^2J_{HP}$=7.2Hz, $OC\underline{H}_2CH_3$), 7.36-7.45 (4H, m, H*m*Ph, H*p*Ph, H3), 7.64 (1H, ddd, $^3J_{H6H5}$=8.0Hz, $^3J_{H6H7}$=7.6Hz, $^3J_{H6P}$=2.8Hz, H6), 7.99 (1H, d, $^3J_{H5H6}$=8.0Hz, H5), 8.04 (2H, dd, $^3J_{HoPhHmPh}$=6.8Hz, $^3J_{HoPhP}$=12.8Hz, H*o*Ph), 8.13 (1H, d, $^3J_{H4H3}$=8.4Hz, H4), 8.53 (1H, dd, $^3J_{H7H6}$=7.6Hz, $^3J_{H7P}$=16.0Hz, H7), 8.91 (1H, dd, $^3J_{H2H3}$=4.4Hz, $^5J_{H2P}$=1.6Hz, H2); δ_C ($CDCl_3$) 16.5 (d, $^3J_{CP}$=6.8Hz, $OCH_2\underline{C}H_3$), 61.0 (d, $^2J_{CP}$=6.0Hz, $O\underline{C}H_2CH_3$), 121.3 (C3), 125.6 (d, $^3J_{CP}$=13.8Hz), 127.7 (d, $^3J_{CP}$=13.7Hz, C*m*Ph), 128.0 (d, $^3J_{CP}$=8.8Hz, C4'), 130.3 (d, $^1J_{CP}$=133.6Hz, C*i*Ph), 131.4 (C5), 132.1 (d, $^2J_{CP}$=10.8Hz, C*o*Ph), 132.7 (d, $^1J_{CP}$=142.2Hz, C8), 135.9 (C4), 136.6 (d, $^2J_{CP}$=7.2Hz, C7), 147.9 (d, $^3J_{CP}$=7.3Hz, C8'), 150.3 (C2); δ_P ($CDCl_3$) 32.1 ; ESMS 386.14 (100%, LH^+); υ_{max} (KBr disc)/cm^{-1} 3447, 3062, 2981, 2932, 2900, 1593, 1562, 1492, 1438, 1389, 1306, 1224, 1199, 1119, 1034, 152, 840, 795, 750, 573 Found: MH^+ 298.0997. $C_{17}H_{17}NPO_2$ requires MH^+ 298.0996. Found: C, 68.03; H, 5.38; N, 4.66. $C_{17}H_{16}NPO_2$ requires C, 68.68%; H, 5.42%; N, 4.71.

(8-Quinolinyl)phenylphosphinic acid hydrochloride (30)

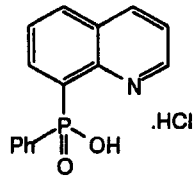

To ethyl (8-quinolinyl)phenylphosphinate (500mg, 1.67mmol) was added hydrochloric acid (6M, 20ml) and the mixture heated at 110°C for 16 h. After cooling the acid was removed under reduced pressure to give a white solid (447mg, 100%), mp 130-133°C δ_H (D_2O) 7.22-7.43 (3H, m, H*m*Ph, H3), 7.63 (2H, dd, $^3J_{HoPhHmPh}$=7.0Hz, $^3J_{HoPhP}$=12.4Hz, H*o*Ph),7.76 (1H, dd, $^3J_{H6H5}$=7.8Hz, $^3J_{H6H7}$=7.6Hz, H6), 7.94 (1H, dd, $^3J_{HpPhHmPh}$=7.8Hz, $^3J_{HpPhP}$=6.0Hz, H*o*Ph), 8.16 (1H, d, $^3J_{H5H6}$=7.8Hz, H5), 8.16 (1H, d, $^3J_{H4H3}$=7.2Hz, H4), 8.99 (1H, dd, $^3J_{H7H6}$=7.6Hz, $^3J_{H7P}$=8.4Hz, H7), 9.11 (1H, d, $^3J_{H2H3}$=5.4Hz, H2); δ_C (D_2O) 124.5 (C3), 131.4 (d, $^3J_{CP}$=12.8Hz, C*m*Ph), 131.5, 132.1, 132.2 (d, $^4J_{CP}$=5.5Hz, C5), 133.2 (d, $^2J_{CP}$=10.3Hz, C8'), 134.5 (d, $^2J_{CP}$=2.6Hz, C4'), 135.0 (C6), 136.3 (d, $^1J_{CP}$=136.7Hz, C*i*Ph), 137.9 (d, $^1J_{CP}$=143.9Hz, C8), 142.9 (d, $^2J_{CP}$=7.7Hz, C7), 147.1 (C8), 150.9 (C2); δ_P (D_2O) 23.2; ESMS 269.95 (100%, LH^+); υ_{max} (KBr disk)/cm^{-1} 3502, 3094, 3070, 3066, 2655, 2143, 2000, 1670, 1595, 1500, 1143, 1078; Found: C, 55.67; H, 4.70; N, 4.23%. $C_{15}H_{12}NPO_2.HCl.H_2O$ requires C, 55.65%; H, 4.87%; N, 4.32%.

6.5 Chapter Five Experimental

6-Bromo-2-methylpyridine (198)

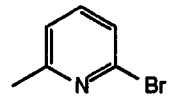

To a solution of 2-aminopicoline (5g, 46.2mmol) in hydrobromic acid (48%, 26ml) was added bromine (6.5ml). To this a solution of sodium nitrite (8g, 0.12mol) in water (12ml) was added dropwise keeping the temperature less than 5°C. After the addition was complete the mixture was stirred at 0°C for 15 min and sodium hydroxide (18g) in water (50ml) was added. The resulting solution was extracted exhaustively with diethyl ether (5x100ml), the organic extracts combined, dried (K_2CO_3) and the diethylether removed under reduced pressure to give a deep red oil. The oil was purified by short path distillation to give a colourless oil (6.5g, 82%). bp 91°C 15mm/Hg (lit. 102-103°C 15mm/Hg).[24]

δ_H($CDCl_3$) 2.46 (3H, s, C<u>H</u>$_3$), 7.04 (1H, d, $^3J_{H5H4}$=7.4Hz, H5), 7.21 (1H, d, $^3J_{H3H4}$=7.9Hz, H3), 7.37 (1H, dd, $^3J_{H4H5}$=7.4Hz, $^3J_{=H4H3}$=7.9Hz, H4).

Ethyl 2-(6-methylpyridyl)phenylphosphinate (200)

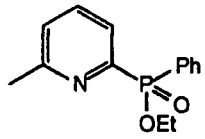

Using a procedure adapted from Huang,[14] 2-bromo-methylpyridine (3g, 17.4mmol), ethylphenylphosphonite (3.16ml, 20.95mmol) and triethylamine (10ml, 71mmol) were mixed in dry degassed toluene (30ml). Tetrakis(triphenylphosphine)palladium(0) (320mg, 0.27mmol) was added and the mixture degassed three times (freeze thaw cycle), then heated at 125°C for 16 h. The solution was diluted with dichloromethane (50ml), washed with hydrochloric acid (1M, 2x60ml) and water (3x60ml), dried (K_2CO_3) and the solvent removed under reduced pressure to give a dark solid. The residue was distilled under reduced pressure to give give a low melting point solid (3.2g, 70%), mp 32-33°C, bp 170°C/0.3mmHg.

δ_H ($CDCl_3$) 1.28 (3H, t, ^3J=7.2Hz, $OCH_2C\underline{H}_3$), 2.49 (3H, s, $C\underline{H}_3$), 4.05 (2H, qd, ^3J=7.2Hz, $^2J_{HP}$=2.0Hz, $OC\underline{H}_2CH_3$), 7.12 (1H, d, $^3J_{H5H4}$=7.6Hz, H5), 7.36 (2H, ddd, $^3J_{HmPhHpPh}$=7.6Hz, $^3J_{HmPhHoPh}$=7.2,Hz $^4J_{HmPhP}$=3.6Hz, H*m*Ph), 7.42 (1H, dd, $^3J_{HpPhHmPh}$=7.6Hz, $^5J_{HpPhP}$=7.2Hz, H*p*Ph), 7.57 (1H, ddd, $^3J_{H4H3}$=6.8Hz, $^3J_{H4H5}$=7.6Hz, $^4J_{H4P}$=4.8Hz, H4), 7.80 (1H, dd, $^3J_{H3H4}$=6.8Hz, $^3J_{H3P}$=6.4Hz, H3), 7.91 (2H, dd, $^3J_{HoPhHmPh}$=7.2Hz, $^3J_{HoPhP}$=12.0Hz, H*o*Ph); δ_C ($CDCl_3$) 15.4 (d, $^3J_{CP}$=6.1Hz, $OCH_2\underline{C}H_3$), 23.6 ($\underline{C}H_3$), 60.5 (d, $^2J_{CP}$=6.4Hz, $O\underline{C}H_2CH_3$), 124.2 (d, $^4J_{CP}$=22.8Hz, *p*Ph), 124.4 (d, $^3J_{CP}$=3.4Hz, C4), 127.2 (d, ^{3}JCP=13.0Hz, *m*Ph), 129.3 (d, $^1J_{CP}$=137.7Hz, *i*Ph), 131.2 (d, $^4J_{CP}$=2.6Hz, C5), 131.3 (d, $^2J_{CP}$=9.6Hz, *o*Ph), 134.9 (d, $^2J_{CP}$=10.7Hz, C3), 152.7 (d, $^1J_{CP}$=168.7Hz, C2), 158.5 (d, $^3J_{CP}$=20.2Hz, C1); δ_P ($CDCl_3$) 28.8; ESMS 545.12 (100%, L_2Na^+), 283.92 (24%, LNa^+), 261.95 (12%, LH^+); υ_{max} (KBr disc)/cm^{-1} 2982, 1636, 1225, 1121 (P=O), 1027 (P-O-C), 957.Found: MH^+ 262.0997. Found: C, 66.46%; H, 6.23%; N, 5.41%. $C_{14}H_{16}NPO_2$ requires C, 66.36%; H, 6.17%; N, 5.36.

2-(6-Methylpyridyl)phenylphosphinic acid hydrochloride (33)

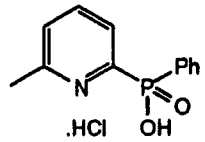

Ethyl 2-(6-methylpyridyl)phenylphosphinate (1g, 3.8mmol) was added to hydrochloric acid (6M, 30ml) and heated at 110°C for 16 h. The clear solution was left to cool to ambient temperature and the excess hydrochloric acid removed by lyophilization to give a white solid (880mg, 99%), mp 128-130°C

δ_H(CD_3OD) 2.87 (3H, s, $C\underline{H}_3$), 7.55 (2H, ddd, $^3J_{HmPhHpPh}$=7.6Hz, $^3J_{HmPhHoPh}$=7.0Hz, $^4J_{HmPhP}$=3.6Hz, H*m*Ph), 7.64 (1H, dd, $^3J_{HpPhHmPh}$=7.6Hz, $^4J_{HpPhP}$=7.2Hz, H*p*Ph,), 7.96 (2H, dd, $^3J_{HoPhP}$=12.8Hz, $^3J_{HoPhHmPh}$=7.0Hz, H*o*Ph), 8.10 (1H, d, $^3J_{H5H4}$=8.0Hz, H5), 8.22 (1H, dd, $^3J_{H4H5}$=8.0Hz, $^3J_{H4H3}$=7.6Hz, H4), 8.52 (1H, ddd, $^3J_{H3H4}$=7.6Hz,

$^3J_{H3P}$=8.0Hz, $^4J_{H3H5}$=2.8Hz, H3) ;δ_C(CD_3OD) 20.1 ($\underline{C}H_3$), 129.3 (d, $^3J_{CP}$=11.1Hz, C4), 130.1 (d, $^3J_{CP}$=14.1Hz, C*m*Ph) 131.5 (d, $^4J_{CP}$=7.2Hz, C5), 132.2 (d, $^1J_{CP}$=148.1Hz, C*i*Ph), 133.1 (d, $^2J_{CP}$=11.1Hz, C*o*Ph), 134.5 (d, $^4J_{CP}$=2.7Hz, C*p*Ph), 147.3 (d, $^2J_{CP}$=8.4Hz, C3), 151.6 (d, $^1J_{CP}$=130.9Hz, C1), 158.4 (d, $^3J_{CP}$=6.9Hz, C6); δ_P(CD_3OD); 16.6. ESMS 233.92 (100%, LH^+), 467.13 (61%, L_2H^+); υ_{max} (KBr disc)/cm^{-1} 3422, 2342, 1684, 1636, 1498, 1438; Found: C, 47.35%: H, 5.71%: N, 4.81%. $C_{12}H_{12}NPO_2.HCl.2(H_2O)$ requires C, 47.15%: H, 5.61%: N, 4.58%.

2-(6-Methylpyridyl)phenylthiophosphinic chloride (204)

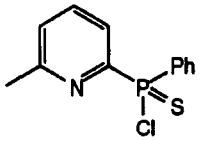

2-(6-Methylpyridyl)phenylphosphinic acid hydrochloride (780mg, 2.90mmol) was suspended thiophosphoryl chloride (25ml) and heated at 110°C until a clear solution was obtained (c. 30 min). A catalytic amount of DMF (1 drop) was added and the solution stirred at 110°C for 16 h. The thiophosphoryl chloride was removed under vacuum, and the residual oil was dissolved in diethyl ether (10ml) filtered and the ether removed under reduced pressure to give a yellow solid (676mg, 87%), mp 35-37°C δ_H ($CDCl_3$) 3.14 (3H, s, CH_3), 7.37-7.59 (3H, m, H3 and H*m*Ph), 7.97 (1H, d, ^{3}J=7.4Hz, H5), 8.04 (2H, dd, ^{3}J=6.0Hz ^{2}JHP=15.5Hz, H*o*Ph), 8.10 (1H, ddd, $^3J_{H4H5}$=7.4Hz, $^3J_{H4H3}$=8.2Hz. $^4J_{H5P}$=3.2Hz, H4), 8.31 (1H, dd, $^3J_{HpPhHmPh}$=7.8Hz, $^5J_{HpPhP}$=7.6Hz, H*p*Ph); δ_C ($CDCl_3$) 16.1 (CH_3), 128.5 (s, C3), 128.7 (d, $^3J_{CP}$=12.5Hz, *m*Ph), 129.1 (d, $^4J_{CP}$=16.2Hz, *p*Ph), 131.0 (d, $^1J_{CP}$=122.2Hz, *i*Ph), 131.7 (d, $^3J_{CP}$=3.1Hz, C4), 132.3 (d, $^2J_{CP}$=12.1Hz, C5), 132.6 (d, $^2J_{CP}$=10.7Hz, *o*Ph), 141.2 (d, $^1J_{CP}$=141.3Hz, C6), 146.4 (d, $^3J_{CP}$=8.1Hz, C2); δ_P ($CDCl_3$) 63.2; ESMS 264.54 (100%, [L - Cl + MeOH]$^+$); υ_{max} (KBr disc)/cm^{-1} 1601, 1508, 1437, 1284, 1132, 1108, 934, 878, 713, 689, 645.

2-(6-Methylpyridyl)phenyl thiophosphinic acid (34)

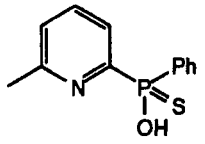

2-(6-methylpyridyl)phenylthiophosphinic chloride (200mg, 0.75mmol) was suspended in water (20ml) and the pH adjusted to 14 by addition of KOH pellets. The suspension was heated at 120°C for 18 h resulting in a clear solution. The solution was allowed to cool to room temperature and the pH adjusted to 6 by addition of dilute hydrochloric acid (1M) and extracted with dichloromethane (3x50ml). The organic extracts were combined, dried (Na_2SO_4) and the dichloromethane removed under reduced pressure to give a pale yellow solid (162mg, 87%), mp 84-85°C

δ_H ($CDCl_3$) 2.87 (3H, s, $C\underline{H}_3$), 7.30-7.43 (3H, m, H2, H3, H4), 7.64 (1H, dd, $^3J_{HpPhHmPh}$=10.8Hz, $^5J_{HpPhP}$=4.5Hz, H*p*Ph), 7.90 (2H, dd, $^3J_{HoPhHmPh}$=7.8Hz, $^3J_{HoPhP}$=6.9Hz, H*o*Ph), 8.23(2H, ddd, $^3J_{HmPhHpPh}$=10.8Hz, $^3J_{HmPhHoPh}$=7.8Hz, $^4J_{HmPhP}$=4.1Hz, H*m*Ph); δ_C ($CDCl_3$) 19.6 ($\underline{C}H_3$), 126.3 (d, $^4J_{CP}$=13.9Hz, C*p*Ph), 127.1 (d, $^3J_{CP}$=13.0Hz, C*m*Ph), 130.0 (d, $^4J_{CP}$=3.0Hz, C5), 130.4 (d, $^3J_{CP}$=2.9Hz, C4) 130.7 (d, $^1J_{CP}$=130.8Hz, C*i*Ph), 131.0 (d, $^2J_{CP}$=11.2Hz, C*o*Ph), 131.1 (d, $^2J_{CP}$=10.6Hz, C3), 151.7 (d, $^1J_{CP}$=168.6Hz, C2), 159.5 (d, $^3J_{CP}$=85.5Hz, C6); δ_P ($CDCl_3$) 52.9; ESMS 250.06 (100%, LH^+); υ_{max} (KBr disc)/cm^{-1} 3424, 3050, 2958, 2920, 2852, 2050, 1624, 1588, 1512, 1438, 1378, 1270, 1128, 1100, 1032, 984, 912, 868, 734, 682, 637, 518; Found C, 57.74%; H, 4.91%; N, 5.38%, $C_{12}H_{12}POSN$ requires: C, 57.82%; H, 4.85%; N, 5.62%.

Ethyl (2-pyridyl)phenylphosphinate (199)

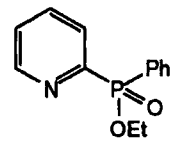

Using a procedure adapted from Huang,[14] 6-bromopyridine (8.16g, 0.0517mol), ethyl-phenylphosphonite (9.35ml, 0.062mol) and triethylamine (25ml, 0.18mol) were mixed in dry degassed toluene (50ml). Tetrakis(triphenylphosphine)palladium(0) (500mg, 0.42mmol) was added and the mixture degassed three times (freeze thaw cycle), then heated at 115°C for 16 h. The solution was diluted with dichloromethane (100ml), washed with hydrochloric acid (1M, 2x100ml) and water (3x100ml), dried (K_2CO_3) and the solvent removed under reduced pressure to give a dark solid. The residue was distilled under reduced pressure to give give a low melting point solid (7.42g, 58%), mp 26°C, bp 165°C/15mmHg.

δ_H ($CDCl_3$) 1.20 (3H, t, ^3J=7.2Hz, $OCH_2C\underline{H}_3$), 4.05 (2H, qd, ^3J=7.2Hz, $^2J_{HP}$=3.2Hz, $OC\underline{H}_2CH_3$), 7.17 (1H, m, H5), 7.24-7.36 (3H, m, H*m*Ph, H*p*Ph), 7.61 (1H, ddd, $^3J_{H4H3}$=6.4Hz, $^3J_{H4H5}$=7.9Hz, $^4J_{H4P}$=4.4Hz, H4), 7.83 (2H, dd, $^3J_{HoPhHmPh}$=6.7Hz, $^3J_{HoPhP}$=11.9Hz, H*o*Ph), 7.95 (1H, dd, $^3J_{H3H4}$=6.4Hz, $^3J_{H3P}$=6.8Hz, H3), 8.58 (1H, dd, $^3J_{H6H5}$=4.8Hz, $^4J_{H6P}$=2.4Hz, H6); δ_C ($CDCl_3$) 16.0 (d, $^3J_{CP}$=6.5Hz, $OCH_2\underline{C}H_3$), 61.2 (d, $^2J_{CP}$=6.0Hz $O\underline{C}H_2CH_3$), 125.2 (d, $^4J_{CP}$=3.4Hz, C5), 127.6 (d, $^2J_{CP}$=22.9Hz, C3), 127.9 (d, $^3J_{CP}$=13.0Hz, *m*Ph), 129.7 (d, $^1J_{CP}$=138.1Hz, *i*Ph), 131.7 (d, $^2J_{CP}$=9.9Hz, C4), 131.9 (d, $^3J_{CP}$=2.7Hz, C3), 135.6 (d, $^4J_{CP}$=10.3Hz, *o*Ph), 150.0 (d, $^3J_{CP}$=20.6Hz, C6), 154.2 (d, $^1J_{CP}$=168.3Hz, C2); δ_P ($CDCl_3$) 28.8; ESMS 247.93 (96%, LH^+), 269.95 (100%, LNa^+); υ_{max} (KBr disc)/cm^{-1} 1510, 1498, 1217, 118, 1021, 950; Found: MH^+ 248.0840, $C_{13}H_{15}NPO_2$ requires MH^+ 248.0840.

(2-Pyridyl)phenylphosphinic acid hydrochloride (32)

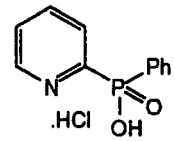

Ethyl (2-pyridyl)phenylphosphinate (2g, 8.09mmol) was added to hydrochloric acid (6M, 25ml) and heated at 110°C for 16 h. The clear solution was left to cool to ambient temperature and the excess hydrochloric acid removed by lyophilization to give a white solid (2.05g, 99%), mp 116-118°C.

δ_H (CD_3OD) 7.51-7.59 (3H, m, H*p*Ph, H*m*Ph), 7.94 (2H, dd, $^3J_{HoPhHmPh}$=6.8Hz, $^3J_{HoPhP}$=12.4Hz, H*o*Ph), 8.12 (1H, dd, $^3J_{H3H4}$=5.6Hz, $^3J_{H3H2}$=10.4Hz, H3), 8.35 (1H, $^3J_{H5H4}$=10.8Hz, $^3J_{H5P}$=12.0Hz, H5), 8.62 (1H, dd, $^3J_{H4H3}$=5.6Hz, $^3J_{H4H5}$=10.8Hz, H4), 8.86 (1H, d, $^3J_{H2H3}$=10.4Hz, H2); δ_C (CD_3OD) 129.7, 130.0 (d, $^4J_{CP}$=13.3Hz, C*m*Ph), 131.5 (d, $^2J_{CP}$=11.1Hz, C4), 133.1 (d, $^3J_{CP}$=10.7Hz, C*o*Ph), 133.7 (d, $^1J_{CP}$=130.7Hz, C*i*Ph), 134.0, 134.2, 144.3 (C2), 144.5 (d, $^1J_{CP}$=166.5Hz, C6); δ_P (CD_3OD) 12.4; ESMS 217.83 (100%, L^-); υ_{max} (KBr disc)/cm^{-1} 3432, 3090, 3042, 2936, 2864, 2664, 2124, 1640, 1580, 1511, 1425, 1282, 1218, 1148, 1048, 992, 770; ESMS 217.89 (100%, L^-)

4-Dodecoxybromobenzene (211)

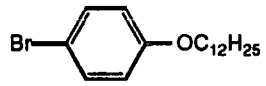

To a sodium ethoxide solution prepared from dry ethanol (150ml) and sodium (2.76g, 0.12mol) was added 4-bromophenol under an argon atmosphere. After 30 min dodecyl bromide (23.05g, 0.1mol) was added and then the solution heated at 90°C for 48 h. Water (100ml) was added and the pH adjusted to 14 with sodium hydroxide solution (1M) and the organics extracted with diethyl ether (3x150ml). The combined organics were washed with sodium hydroxide solution (1M, 2x200ml), dried (K_2CO_3) and concentrated to give a low melting solid. Recrystallisation from 40-60 petroleum ether gave colourless crystals (32.4g, 79%), mp 26-27°C (lit. 27°C).[25]

δ_H ($CDCl_3$) 0.89 (3H, t, ^3J=6.9Hz, C$\underline{H}_3$), 1.27-1.47 (18H, m, C$\underline{H}_2$'s), 1.77 (2H, p, ^3J=8.1Hz, ^3J=6.8Hz, OCH$_2$C$\underline{H}_2$), 3.91 (2H, t, ^3J=6.8Hz, OC$\underline{H}_2$CH$_2$), 6.77 (2H, d, $^3J_{H3H2}$=9.0Hz, H3), 7.36 (2H, d, $^3J_{H2H3}$=9.0Hz, H2); δ_C ($CDCl_3$) 14.4 (C$\underline{H}_3$), 22.9, 26.2, 29.4, 29.6, 29.6, 29.8, 29.8, 29.9, 29.9, 32.1 (OCH$_2$C$\underline{H}_2$), 68.4 (OC$\underline{H}_2$CH$_2$), 112.7 (C4), 116.5 (C3), 132.4 (C2), 158.4 (C1).

Ethyl 4-(dodecoxyphenyl)phosphonite (215)

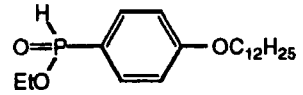

To magnesium turnings (4.5g, 188mmol), activated by heating under vacuum at 80°C for 16h, in THF (50ml) was added a solution of 4-dodecoxybromobenzene (16g,

46.9mmol) in THF (100ml) over a period of 1 h maintaining a reaction temperature of 70°C, and heating continued for 1 h after the addition was complete. After allowing the mixture to cool to room temperature the resultant dark brown solution was transferred by cannula to a solution of diethylchlorophosphonite (8mls, 56.3mmol) in THF (50ml) maintaing a reaction temperature between -5 and 0°C. After the addition was complete the THF was removed under vacuum and dry benzene added (100ml) and the salts removed by filtration. An aliquot of the mixture was removed and analysed by ^{31}P NMR giving a chemical shift of 160.24ppm, consistent with the proposed intemediate. Hydrochloric acid (1M, 100ml) was added and the solution stirred at room temperature for 30min under argon, the organic layer was seperated, dried ($MgSO_4$) and the volatile organics removed under reduced pressure to give a pale oil, which was recrystallised from 40-60 petroleum ether to give a low melting solid (11.5g, 73%), mp -2 to 0°C $\delta_H(CDCl_3)$ 0.80 (3H, t, ^3J=6.9Hz, $C\underline{H}_3$), 1.14-1.38 (18H, m, $C\underline{H}_2$'s), 1.29 (3H, t, ^3J=6.9Hz, $OCH_2C\underline{H}_3$), 1.72 (2H, p, ^3J=6.6Hz, ^3J=7.2Hz, $OCH_2C\underline{H}_2CH_2$-), 3.92 (2H, t, ^3J=6.6Hz, $OC\underline{H}_2CH_2CH_2$-), 4.04 (2H, qd, ^3J=6.9Hz, $^3J_{HP}$=2.0Hz, $OC\underline{H}_2CH_3$), 6.91 (2H, dd, $^3J_{H3H2}$=8.7Hz, $^4J_{H3P}$=2.4Hz, H3), 7.47 (1H, d, $^1J_{HP}$=561.4Hz, P-$\underline{H}$), 7.69 (2H, dd, $^3J_{H2H3}$=8.7Hz, $^3J_{H2P}$=13.2Hz, H2); $\delta_C(CDCl_3)$ 14.3 (CH_3). 16.5 (d, $^3J_{CP}$=6.4Hz, $OCH_2\underline{C}H_3$), 22.8, 26.1, 29.2, 29.5, 29.7, 29.7, 29.8, 29.8, 32.1 (OCH2CH2CH2-), 61.7 (d, $^2J_{CP}$=6.3Hz, O$\underline{C}$H2CH3), 68.3 ($O\underline{C}H_2CH_2CH_2$-), 114.8 (d, $^2J_{C2P}$=14.7Hz, C2), 120.9 (d, $^1J_{C1P}$=138.8Hz, C1), 133.0 (d, $^3J_{C3P}$=13.34, C3), 163.1 (d, $^4J_{C4P}$=2.9Hz, C4); $\delta_P(CDCl_3)$ 24.8; ESMS 355.12 (100%, LH^+), 731.93 (24%, L_2Na^+); υ_{max} (thin film)/cm^{-1} 3464, 2940, 2860, 1658, 1648, 1600, 1508, 1472, 1310, 1254, 1484, 950, 798, 700; Found: C, 67.69%; H, 9.61%. $C_{20}H_{35}PO_3$ requires C, 67.77%; H, 9.95%.

Ethyl 2-(6-methylpyridyl)-4-(dodecoxy)phenylphosphinate (217)

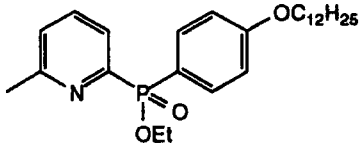

Using a procedure adapted from Huang,[14] 2-bromo-6-methylpyridine (1.86g, 0.011mol), Ethyl 4-(dodecoxyphenyl)phosphonite (3.56g, 0.01mol) and triethylamine (5ml, 0.035mol) were mixed in dry degassed toluene (5ml). Tetrakis(triphenylphosphine)palladium(0) (46mg, 0.04mmol) was added and the mixture degassed three times (freeze thaw cycle), then heated at 120°C for 48 h. The solution was diluted with diethylether (100ml), washed with 5% aqueous hydrochloric acid (2x50ml) and water (3x50ml), dried (K_2CO_3)and the solvent removed under reduced pressure to give an off white solid. Purification by flash chromatography (silica, eluant 100% dichloromethane increasing to 2% MeOH/98% dichloromethane, R_f(product)=0.24 (2.5% MeOH/97.5% dichloromethane)) gave an orange oil (1.14g, 23%).

δ_H ($CDCl_3$) 0.83 (3H, t, ^3J=6.9Hz, $C\underline{H}_3$), 1.14-1.40 (18H, m, $C\underline{H}_2$'s), 1.31 (3H, t, ^3J=7.2Hz, $OCH_2C\underline{H}_3$), 1.72 (2H, p, ^3J=6.6Hz, ^3J=7.5Hz, $OCH_2C\underline{H}_2CH_2$-), 2.53 (3H, s, $C\underline{H}_3$), 3.93 (2H, t, ^3J=6.6Hz, $OC\underline{H}_2CH_2CH_2$-), 4.09 (2H, qd, ^3J=7.2Hz, $^3J_{HP}$=3.3Hz, $OC\underline{H}_2CH_3$), 6.90 (2H, dd, $^3J_{HoPhHmPh}$=9.0Hz, $^2J_{HoPhP}$=3.0Hz, H*o*Ph), 7.15 (1H, d, $^3J_{H5H4}$=8.1Hz, H5), 7.59 (1H, ddd, $^3J_{H4H5}$=8.1Hz, $^3J_{H4H3}$=7.8Hz, ^{4}JH4P=4.8Hz, H4), 7.82 (1H, dd, $^3J_{H3H4}$=7.8Hz, $^3J_{H3P}$=6.6Hz, H3), 7.88 (2H, dd, $^3J_{HmPhHoPh}$=9.0Hz, $^3J_{HmPhP}$=11.4Hz, H*m*Ph); δ_C ($CDCl_3$) 14.0 (CH_3), 16.3 (d, $^3J_{CP}$=6.4Hz, $OCH_2\underline{C}H_3$), 22.5, 24.5 (2-$\underline{C}H_3$), 25.8, 28.9, 29.2, 29.4, 29.4, 29.4, 29.5, 31.7 ($OCH_2\underline{C}H_2CH_2$-), 61.1 (d, $^2J_{CP}$=6.1Hz, $O\underline{C}H_2CH_3$), 67.9 ($O\underline{C}H_2CH_2CH_2$-), 114.0 (d, $^2J_{CP}$=14.2Hz, C*o*Ph), 121.0 (d, $^1J_{CP}$=144.7Hz, C*i*Ph), 125.1 (d, $^2J_{CP}$=3.5Hz, C5), 128.3 (d, $^4J_{CP}$=12.3Hz, C3), 134.1 (d, $^3J_{CP}$=11.16, C*m*Ph), 134.1 (d, $^3J_{CP}$=10.9Hz, C4), 154.2 (d, $^1J_{CP}$=169.5Hz, C2), 159.3 (d, $^3J_{CP}$=20.3Hz, C6), 162.2 (d, $^4J_{CP}$=2.9Hz, C*p*Ph); δ_P ($CDCl_3$) 29.8; υ_{max} (golden gate)/cm^{-1} 3455, 2921, 2851, 2557, 2359, 2025, 1880, 1597, 1503, 1446, 1389, 1293, 1255, 1220, 1122, 1030, 951, 830, 775; *m/z* (CI) 446 (22%, MH^+); Found: M^+ 445.2745; $C_{26}H_{40}PO_3N$ requires M+ 445.2746

Ethyl 2-(pyridyl)-4-(dodecoxy)phenylphosphinate (216)

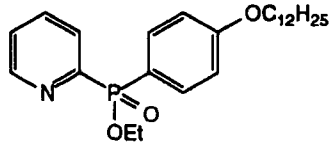

Using a procedure adapted from Huang,[14] 2-bromopyridine (1.58g, 0.01mol), Ethyl 4-(dodecoxyphenyl)phosphonite (3.56g, 0.01mol) and triethylamine (5ml, 0.035mol) were mixed in dry degassed toluene (5ml). Tetrakis(triphenylphosphine)palladium(0) (46mg, 0.04mmol) was added and the mixture degassed three times (freeze thaw cycle), then heated at 120°C for 96 h. The solution was diluted with diethylether (50ml), washed with 5% aqueous hydrochloric acid (2x10ml) and water (3x20ml), dried (K_2CO_3) and the solvent removed under reduced pressure to give a pale yellow oil. Purification by flash chromatography (silica, eluant 1% MeOH/99% dichloromethane increasing to 2% MeOH/98% dichloromethane, R_f(product)=0.19 (2.5% MeOH/97.5% dichloromethane)) gave a clear oil (1.1g, 25%).

δ_H ($CDCl_3$) 0.80 (3H, t, ^3J=6.9Hz, $C\underline{H}_3$), 1.14-1.38 (18H, m, $C\underline{H}_2$'s), 1.29 (3H, t, ^3J=7.2Hz, $OCH_2C\underline{H}_3$), 1.72 (2H, p, ^3J=6.6Hz, ^3J=8.1Hz, $OCH_2C\underline{H}_2CH_2$-), 3.9 (2H, t, ^3J=6.6Hz, $OC\underline{H}_2CH_2CH_2$-), 4.04 (2H, qd, ^3J=7.2Hz, $^3J_{HP}$=3.3Hz, $OC\underline{H}_2CH_3$), 6.93 (2H, dd, $^3J_{HoPhHmPh}$=8.7Hz, $^3J_{HoPhP}$=2.7Hz, H*o*Ph), 7.28 (1H, dd, $^3J_{H3H4}$=6.6Hz, $^3J_{H3P}$=2.4Hz, H3), 7.71 (1H, ddd, $^3J_{H4H3}$=6.6Hz, $^3J_{H4H5}$=6.0Hz, $^4J_{H4P}$=10.7Hz, H4), 7.89 (2H, dd, $^3J_{HmPhHoPh}$=8.7Hz, $^3J_{HmPhP}$=11.7Hz, H*m*Ph), 8.08 (1H, dd, $^3J_{H5H4}$=6.0Hz, $^3J_{H5H6}$=4.5Hz, H5), 8.75 (1H, d, $^3J_{H6H5}$=4.5Hz, H6); δ_C($CDCl_3$) 14.0 (CH_3), 16.4 (d, $^3J_{CP}$=6.4Hz, $OCH_2\underline{C}H_3$), 22.6, 25.9, 29.0, 29.3, 29.5, 29.5, 29.5, 29.6, 31.8 ($OCH_2\underline{C}H_2CH_2$-), 61.3 (d, $^2J_{CP}$=5.9Hz, $O\underline{C}H_2CH_3$), 68.0 ($O\underline{C}H_2CH_2CH_2$-), 114.3 (d, $^2J_{CP}$=14.2Hz, C*o*Ph), 120.8 (d, $^1J_{CP}$=145.8Hz, C*i*Ph), 125.3 (d, $^2J_{CP}$=3.4Hz, C5),

127.7 (d, $^4J_{CP}$=22.7Hz, C3), 134.1 (d, $^3J_{CP}$=11.1Hz, C*m*Ph), 135.8 (d, $^3J_{CP}$=10.4Hz, C4), 150.3 (d, $^3J_{CP}$=19.9Hz, C6), 155.1 (d, $^1J_{CP}$=154.2Hz, C2), 162.4 (d, $^4J_{CP}$=3.2Hz, C*p*Ph); δ_P ($CDCl_3$) 27.1; υ_{max} (golden gate)/cm^{-1} 2922, 2851, 2743 (br), 2364, (2158 (s), 2030 (s), 1972 (s), 1594, 1395, 1254, 1222, 1119, 1029; *m/z* (EI) 431 (14%, M^+), 402 (22%, $[M-Et]^+$), 387 (35%, $[M-OEt]^+$), 262 (29%, $[M-C_{12}H_{25}]^+$); Found: M^+ 431.2616; $C_{25}H_{38}PO_3N$ requires M+ 431.2589

2-(6-Methylpyridyl)-4-(dodecoxy)phenylphosphinic acid (219)

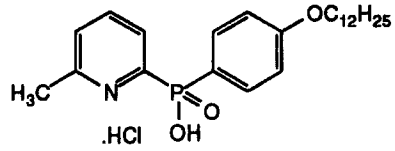

A solution of Ethyl 2-(6-methylpyridyl)-4-(dodecoxy)phenylphosphinate (1.14g, 2.56mmol) was heated in a mixture of 1,4-dioxane and hydrochloric acid (10M, 2:3, 30ml) at 120°C for 48 h. The solvent was removed under reduced pressure to give a pale orange solid (1.15g, 99%), mp 58-60°C

δ_H (CD_3OD) 0.46 (3H, t, ^3J=6.6Hz, C$\underline{H}_3$), 0.79-1.09 (18H, m, C$\underline{H}_2$'s), 1.35 (2H, p, ^3J=6.6Hz, ^3J=7.5Hz, $OCH_2C\underline{H}_2CH_2$-), 2.45 (3H, s, C$\underline{H}_3$), 3.61 (2H, t, ^3J=6.6Hz, $OC\underline{H}_2CH_2CH_2$-), 6.65 (2H, dd, $^3J_{HoPhHmPh}$=8.7Hz, $^2J_{HoPhP}$=2.4Hz, H*o*Ph), 7.46 (2H, dd, $^3J_{HmPhHoPh}$=8.7Hz, $^3J_{HmPhP}$=12.6Hz, H*m*Ph), 7.59 (1H, d, $^3J_{H5H4}$=8.1Hz, H5), 7.77 (1H, dd, $^3J_{H3H4}$=7.5Hz, $^3J_{H3P}$=7.2Hz, H3), 8.09 (1H, ddd, $^3J_{H4H5}$=8.1Hz, $^3J_{H4H3}$=7.5Hz, ^{4}JH4P=2.4Hz, H4); δ_C (CD_3OD) 14.4 (CH_3), 20.2, 23.7 (2-$\underline{C}H_3$), 27.0, 30.1, 30.4, 30.6, 30.7, 30.8, 30.8, 33.0 ($OCH_2\underline{C}H_2CH_2$-), 62.1 ($O\underline{C}H_2CH_2CH_2$-), 116.0 (d, $^2J_{CP}$=14.1Hz, C*o*Ph), 121.9 (d, $^1J_{CP}$=156.7Hz, C*i*Ph), 129.1 (d, $^2J_{CP}$=10.Hz, C4), 129.8 (d, $^4J_{CP}$=12.8Hz, C3), 132.9 (d, $^3J_{CP}$=8.3Hz, C5), 135.2 (d, $^3J_{CP}$=11.4Hz, C*m*Ph), 147.4 (d, $^3J_{CP}$=8.1Hz, C6), 151.4 (d, $^1J_{CP}$=131.9Hz, C2), 164.7 (C*p*Ph); δ_P (CD_3OD) 13.8; υ_{max} (golden gate)/cm^{-1} 3254, 2923, 2531, 2484, 2156, 1596, 1408, 1288, 1255, 1125, 1046, 963, 869, 963; *m/z* (EI), 417 (9%, M^+), 249 (15%, $[M-C_{12}H_{25}]^+$); Found: M^+ 417.2422, $C_{24}H_{36}PO_3N$ requires 417.2432

2-(Pyridyl)-4-(dodecoxy)phenylphosphinic acid (218)

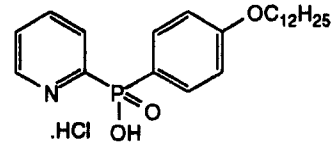

A solution of 2-(pyridyl)-4-(dodecoxy)phenylphosphinate (1.1g, 2.55mmol) was heated in a mixture of 1,4-dioxane and hydrochloric acid (10M, 2:3, 30ml) at 120°C for 60 h. The solvent was removed under reduced pressure to give a pale orange solid (1.11g, 99%), mp 54-56°C

δ_H(CD_3OD) 0.0 (3H, t, ^3J=6.6Hz, C$\underline{H}_3$), 0.3-0.6 (18H, m, C$\underline{H}_2$'s), 0.9 (2H, p, ^3J=7.1Hz, ^3J=6.3Hz, $OCH_2C\underline{H}_2CH_2$-), 3.1 (2H, t, ^3J=6.3Hz, $OC\underline{H}_2CH_2CH_2$-), 6.1 (2H, d,

$^{3}J_{HoPhHmPh}$=7.2Hz, H*o*Ph), 7.0 (2H, dd, $^{3}J_{HmPhHoPh}$=7.2Hz, $^{3}J_{HmPhP}$=10.2Hz, H*m*Ph), 7.3 (1H, dd, $^{3}J_{H3H4}$=6.3Hz, $^{3}J_{H3P}$=3.2Hz, H3), 7.5 (1H, dd, $^{3}J_{H4H3}$=6.3Hz, $^{3}J_{H4H5}$=6.9Hz, H4), 7.81 (1H, dd, $^{3}J_{H5H4}$=6.9Hz, $^{3}J_{H5H6}$=5.2Hz, H5), 8.15 (1H, d, $^{3}J_{H6H5}$=5.2Hz, H6); $\delta_C(CD_3OD)$ 14.5 (CH_3), 23.6, 26.9, 30.0, 30.3, 30.3, 30.6, 30.6 30.6, 32.9 ($OCH_2\underline{C}H_2CH_2$-), 69.1 ($O\underline{C}H_2CH_2CH_2$-), 115.8 (d, $^{2}J_{CP}$=14.7Hz, C*o*Ph), 123.6 (d, $^{1}J_{CP}$=155.7Hz, C*i*Ph), 129.6 (d, $^{2}J_{CP}$=5.6Hz, C5), 130.0 (d, $^{4}J_{CP}$=24.1Hz, C3), 132.7 (d, $^{3}J_{CP}$=10.1Hz, C4), 135.1 (d, $^{3}J_{CP}$=11.6, C*m*Ph), 147.6 (d, $^{3}J_{CP}$=7.2Hz, C6), 153.6 (d, $^{1}J_{CP}$=126.5Hz, C2), 164.1 (d, $^{4}J_{CP}$=2.7Hz, C*p*Ph); $\delta_P(CD_3OD)$ 9.9; υ_{max} (golden gate)/cm^{-1} 3334, 2925, 2851, 2358, 2332, 2182, 1966, 1888, 1596, 1505, 1449, 1357, 1291, 1252, 1197, 1128, 1042, 882; *m/z* (EI) 403 (8%, M+), 235 (34%, [M-$C_{12}H_{25}$]$^+$); Found: M$^+$ 403.2253, $C_{23}H_{34}PO_3N$ requires 403.2276

Ethyl (2-ethylhexyl)phosphonite (222)

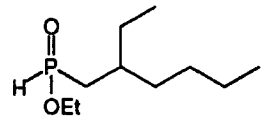

To magnesium turnings (2g, 83.5mmol), activated by heating under vacuum at 80°C for 16h, in diethylether (50ml) with a single crystal of iodine was added a solution of 2-ethylhexylbromide (8g, 41.4mmol) in diethylether (100ml) over a period of 1 h, and then heated at 70°C for 1 h. After allowing the mixture to cool to room temperature the resultant dark brown solution was transfered by canula to a solution of diethylchlororphosphonite (6.5mls, 45.5mmol) in diethylether (50ml) maintaing a reaction temperature between -5 and 0°C. After the addition was complete the salts were removed by filtration. Hydrochloric acid (1M, 100ml) was added and the solution stirred at room temperature for 30min under argon, the organic layer was seperated, dried ($MgSO_4$) and the volatile organics removed under reduced pressure to give a pale oil, (6.9g, 81%), which was used without further purification.
$\delta_H(CDCl_3)$ 0.78 (3H, t, ^{3}J=7.2Hz, CH_3), 0.85 (3H, t, ^{3}J=6.9Hz, $C\underline{H}_3$), 1.2-1.4 (8H, m, $C\underline{H}_2$'s), 1.31 (3H, t, ^{3}J=6.9Hz, $OCH_2C\underline{H}_3$), 1.71 (1H, m), 2.21 (2H, s, $PC\underline{H}_2$-), 4.13 (2H, dq, ^{3}J=6.9Hz, $^{2}J_{HP}$=3.4Hz, $OC\underline{H}_2CH_3$), 7.11 (1H, d, $^{1}J_{HP}$=528.1Hz, P$\underline{H}$); $\delta_C(CDCl_3)$ 10.3 ($\underline{C}H_3$), 13.9 ($\underline{C}H_3$), 16.1 (d, $^{3}J_{CP}$=6.1Hz, $OCH_2\underline{C}H_3$), 22.6, 26.8 (d, $^{3}J_{CP}$=9.7Hz, C3), 28.3 (d, $^{3}J_{CP}$=1.9Hz, C7), 28.9 (C5), 31.0 (d, $^{1}J_{CP}$=178.3Hz, C1), 33.6 (d, $^{2}J_{CP}$=13.6Hz, C3), 61.7 (d, $^{2}J_{CP}$=5.5Hz, $O\underline{C}H_2CH_3$); $\delta_P(CDCl_3)$ 39.7; ESMS 206.88 (100%, MH$^+$), 228.86 (28%, MNa$^+$); υ_{max} (golden gate)/cm^{-1} 2959, 2927, 2864, 2156, 2042, 1640, 1461, 1238, 1043, 973, 790

Ethyl 2-(pyridyl)-(2-ethylhexyl)phosphinate (223)

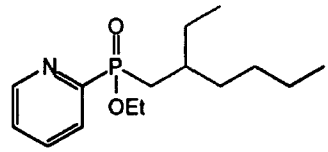

Using a procedure adapted from Huang[14] 2-bromopyridine (1.91g, 0.012mol), Ethyl (2-ethylhexyl)phosphonite (2.27g, 0.011mol) and triethylamine (5ml, 0.035mol) were mixed in dry degassed toluene (5ml). Tetrakis(triphenylphosphine)palladium(0) (46mg, 0.04mmol) was added and the mixture degassed three times (freeze thaw cycle), then heated at 120°C for 96 h. The solution was diluted with diethylether (50ml), washed with 5% aqueous hydrochloric acid (2x10ml) and water (3x20ml), dried (K_2CO_3) and the solvent removed under reduced pressure to give a pale yellow oil. Purification by flash chromatography (silica, eluant 1% MeOH/99% dichloromethane increasing to 3% MeOH/93% dichloromethane, R_f(product)=0.21 (3% MeOH/97.5% dichloromethane)) gave a clear oil (0.72g, 23%).

δ_H ($CDCl_3$) 0.71 (3H, t, ^3J=6.6Hz, C$\underline{H}_3$), 0.83 (3H, t, ^3J=6.9Hz, C$\underline{H}_3$), 1.01-1.55 (8H, m, C$\underline{H}_2$'s), 1.22 (3H, t, $^3J_{HP}$=7.2Hz, OCH$_2$C$\underline{H}_3$), 1.78 (1H, m), 2.01 (2H, dd, $^2J_{HP}$=16.1Hz, $^2J_{HH}$=6.3Hz, PC$\underline{H}_2$-), 4.05 (2H, dq, ^3J=7.2Hz, $^2J_{HP}$=8.3Hz, OC$\underline{H}_2$CH$_3$), 7.38 (1H, dd, $^3J_{H3H4}$=6.3Hz, $^3J_{H3P}$=14.3Hz, H3), 7.79 (1H, ddd, $^3J_{H4H3}$=6.3Hz, $^3J_{H4H5}$=6.5Hz, $^4J_{H4P}$=7.2Hz, H4), 8.09 (1H, dd, $^3J_{H5H4}$=6.5Hz, $^3J_{H5H6}$=6.6Hz, H5), 8.74 (1H, $^3J_{H6H5}$=6.6Hz, H6); δ_C ($CDCl_3$) 10.2 (C$\underline{H}_3$), 14.1 (C$\underline{H}_3$), 16.4 (d, $^3J_{CP}$=6.4Hz, OCH$_2$C$\underline{H}_3$), 22.8, 27.0 (d, $^3J_{CP}$=8.6Hz, C3), 28.1 (d, $^3J_{CP}$=1.6Hz, C7), 28.4 (C5), 31.1 (d, $^1J_{CP}$=100.1Hz, C1), 33.3 (d, $^2J_{CP}$=8.6Hz, C3), 60.7 (d, $^2J_{CP}$=6.9Hz, OCH2CH3), 125.7 (d, $^3J_{CP}$=3.3Hz, C4), 132.0 (d, $^2J_{CP}$=9.87, C3), 136.0 (d, $^4J_{CP}$=9.2Hz, C5), 150.4 (d, $^3J_{CP}$=19.2Hz, C6), 155.0 (d, $^1J_{CP}$=149.9Hz, C2); δ_P ($CDCl_3$) 42.6; ESMS 567.07 (12%, LH$^+$), 589.07 (100%, LNa$^+$); υ_{max} (golden gate)/cm^{-1} 2957, 2926, 2872, 1960, 1573, 1461, 1425, 1218, 1144, 1032, 951, 770, 555

2-(Pyridyl)-(2-ethylhexyl)phosphinic acid (224)

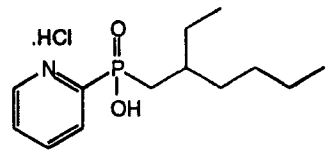

A solution of ethyl-2-(pyridyl)-(2-ethylhexyl)phenylphosphinate (500mg, 1.71mmol) was heated in a mixture of 1,4-dioxane and hydrochloric acid (10M, 2:3, 20ml) at 120°C for 48 h. The solvent was removed under reduced pressure to give a pale orange oil (495mg, 99%)

δ_H ($CDCl_3$) 0.74 (3H, t, ^3J=6.7Hz, C$\underline{H}_3$), 0.79 (3H, t, ^3J=7.0Hz, C$\underline{H}_3$), 1.09-1.42 (8H, m, C$\underline{H}_2$'s), 1.73 (1H, m), 1.96 (2H, dd, $^2J_{HP}$=15.3Hz, $^2J_{HH}$=6.6Hz, PC$\underline{H}_2$-), 7.33 (1H, dd, $^3J_{H3H4}$=6.7Hz, $^3J_{H3P}$=15.4Hz, H3), 7.43 (1H, ddd, $^3J_{H4H3}$=6.7Hz, $^3J_{H4H5}$=7.8Hz, $^4J_{H4P}$=7.6Hz, H4), 7.62 (1H, dd, $^3J_{H5H4}$=7.8Hz, $^3J_{H5H6}$=6.9Hz, H5), 8.25 (1H, $^3J_{H6H5}$=6.9Hz, $^3J_{H6P}$=3.6Hz, H6); δ_C ($CDCl_3$) 9.7 (C$\underline{H}_3$), 13.6 (C$\underline{H}_3$), 22.3 26.3 (d,

$^3J_{CP}$=8.5Hz, C3), 27.7 (d, $^3J_{CP}$=1.9Hz, C7), 33.2 (C5), 33.7 (d, $^1J_{CP}$=107.6Hz, C1), 34.6 (d, $^2J_{CP}$=8.5Hz, C3), 126.4 (C4), 128.1 (d, $^2J_{CP}$=12.2, C3), 131.5 (d, $^4J_{CP}$=10.1Hz, C5), 144.2 (d, $^3J_{CP}$=9.3Hz, C6), 153.3 (d, $^1J_{CP}$=120.1Hz, C2); δ_P ($CDCl_3$) 30.7; ESMS 255.94 (100%, LH^+), 278.82 (24%, LNa^+), 511.05 (22%, L_2H^+); υ_{max} (golden gate)/cm^{-1} 3396, 2934, 2810, 2865, 1961, 1676, 1658, 1609, 1450, 1121, 1050, 886, 750, 661

Preparation of Metal Triflates

Cadmium Trifluoromethanesulfonate

To a solution of cadmium chloride (1.16g, 6.3mmol) in dry methanol (10ml) was added a solution of silver trifluromethanesulphonate (2.48g, 9.6mmol) and the mixture heated under reflux for 3 h. The solution was allowed to cool to room temperature and filtered under argon. The methanol was removed under reduced pressure to give a white solid which was dried under vacuum. Recrystallisation from acetonitrile gave a white solid (1.9g, 64%)
Found: Cd: 23.74%, $CdO_6S_2F_6.2CH_3OH$ requires Cd; 23.60%

Lead Trifluoromethanesulfonate

Trifluoromethanesulfonic acid (3ml) was carefully added to lead(II) chloride (1.0g, 3.6mmol) in a two necked flask fitted with a nitrogen bubbler. A steady stream of nitrogen was passed through the suspension and the mixture was warmed to 60°C for 30 min. Anhydrous diethyl ether (10ml) was added and the white solid removed by filtration and washed with ether (4x20ml). The solid was extracted into acetonitrile (3x25ml), the solution filtered and the solvent removed under reduced pressure to give a white solid (1.42g, 79%).
Found: Pb; 39.61%. $PbO_6C_2F_6S_2.H_2O$ requires Pb; 39.58%

6.6 References

1. L. Collie, J. E. Denness, D. Parker, F. O'Carroll and C. Tachon *J. Chem. Soc., Perkin Trans. 2*, 1993, 1747; using a routine in 'Kaleidagraph'
2. K. A. Connors; '*Binding Constants, The Measurement of Molecular Complex Stability*', John Wiley and Sons, New York, 1987
3. D. Camp, P. C. Healey, I. D. Jenkins, B. W. Skelton and A. H. White; *J. Chem. Soc., Perkin Trans. 1*, 1991, 448
4. C. E. McKenna, M. T. Higa, N. H. Cheung and M. C. McKenna; *Tetrahedron Lett.*, 1977, **2**, 1977

5. C. Yuan, H. Feng and Q. Ling; *Synthesis*, 1989, **1**, 48
6. J. R. Lloyd, N. Lowther, G. Zsabo, C. Hall and J. Dennis; *J. Chem. Soc., Perkin Trans. 2*, 1985, 1813
7. L. Ramaswami and I. Kirch; *J. Am. Chem. Soc.*, 1953, **75**, 1763
8. J. D. Parrack; *J.Chem. Soc*, 1962, 924.
9. J. Gibson and B. Johnson; *J. Chem. Soc*, 1928, 3093.
10. F. H. Jackson and A. T. Peters; *J. Chem. Soc. C.*, 1929, 268.
11. S. Sanders and N. P. Peet; *J. Heterocyclic. Chem.*, 1979, **16**, 33.
12. S. H. Dandegaonker and I. Recakar. *J. Karnatak. Univ*, 1961, **6**, 25.
13. D. R. Coulson; *Inorg. Synth.*, **13**, 1972, 121.
14. Y. Xu, Z. Li, J. Xia, H. Guo, and Y. Huang; *Synthesis*, 1983, 377.
15. I. D. Entwistle; *J. Chem. Soc., Perkin Trans. 1*. 1975, 1300.
16. G. W.Parshall; *Org. Synth.*, 1965, **45**, 102.
17. G. B. Bates, *Synthesis of Tetrahedrally Coordinating Ligands*, Ph. D. Thesis, University of Durham, 1995, p 166
18. *ibid*, p 167
19. H. Ohta, H. Tetsukawa and N. Noto; *J. Org. Chem.*, 1982, **47**, 2400
20. E. Leete and J. A. McDonell; *J. Am. Chem. Soc.*, 1981, **103**, 654
21. D. W. Hein, R. J. Alheim and J. J. Leavitt; *J. Am. Chem. Soc.*, 1957, **79**, 427
22. C. M. Leir; *J. Org. Chem.*, 1977, 35, 911
23. L. Eisch; *J. Org. Chem.*, 1962, **27**, 1318
24. F. H. Case and T. J. Casper; *J. Am. Chem. Soc.*, 1956, **78**, 5842
25. G. B. Bates, *Synthesis of Tetrahedrally Coordinating Ligands*, Ph. D. Thesis, University of Durham, 1995, p 173

Appendices

Appendix A

Derivation of a 1:1 binding model, assuming the metal and ligand are in fast exchange*
:

$$L + M \underset{}{\overset{K_1}{\rightleftharpoons}} ML \qquad K_1 = \frac{[ML]_{eqm}}{[M]_{eqm}[L]_{eqm}}$$

$$\delta_P = \frac{\delta_0[ML]_{eqm} + \delta_1[ML]_{eqm}}{[L]_{eqm} + [ML]_{eqm}} \qquad \text{at equilibrium}$$

Where δ_0 = ^{31}P NMR chemical shift in the absence of added metal and δ_1 = ^{31}P NMR chemical shift of the 1:1 complex in fast exchange. The mass balance at equilibrium is $[L]_{int} = [L]_{eqm} + [ML]_{eqm}$, where $[L]_{int}$ is the initial concentration of the ligand and $[ML]_{eqm}$ and $[L]_{eqm}$ the equilibrium concentration of the complex and the ligand respectively. Therefore the observed chemical shift at equilibrium is the weighted average of the species in solution:

$$\delta_P = \frac{\delta_0[L]_{eqm} + \delta_1[ML]_{eqm}}{[L]_{eqm} + [ML]_{eqm}}$$

$$= \frac{\delta_0([L]_{int} - [ML]_{int}) + \delta_1[ML]_{eqm}}{[L]_{int}}$$

$$= \frac{[ML](\delta_1 - \delta_0) + \delta_0[L]_{int}}{[L]_{int}}$$

$$= \frac{[ML]_{eqm}(\delta_1 - \delta_0)}{[L]_{int}} + \delta_0$$

$$\delta_P - \delta_0 = \frac{[ML]_{eqm}(\delta_1 - \delta_0)}{[L]_{int}} = \Delta\delta_P$$

Initially		At eqm.	
	$[L] = [L]_{int}$		$[L]_{eqm} = [L]_{int} - [ML]_{eqm}$
	$[M] = [M]_{int}$		$[M]_{eqm} = X[L]_{int} - [ML]_{eqm}$
	$[ML] = 0$		$[ML]_{eqm} = [ML]_{eqm}$

* Adapted from; K. A. Connors; *'Binding Constants, The Measurement of Molecular Complex Stability'*, John Wiley and Sons, New York, 1987

Where $X = [M]_{int}/[L]_{int}$

Substituting the equilibrium concentrations into the equilibrium constant gives:

$$K_1 = \frac{[ML]_{eqm}}{\left([L]_{int} - [ML]_{eqm}\right)\left(X[L]_{int} - [ML]_{eqm}\right)}$$

$$[ML]_{eqm} = K_1\left\{X[L]_{int}^2 - [L]_{int}[ML]_{eqm} - X[L]_{int}[ML]_{eqm} + [ML]_{eqm}^2\right\}$$

$$0 = K_1[ML]_{eqm}^2 - K_1[ML]_{eqm}\left\{1 + X[L]_{int} + [L]_{int}\right\} + K_1X[L]_{int}^2$$

Solving the quadratic for $[ML]_{eqm}$ gives:

$$[ML]_{eqm} = \frac{K_1\left\{1 + X[L]_{int} + [L]_{int}\right\}}{2K_1} \pm \sqrt{\frac{\left(K_1\left\{1 + X[L]_{int} + [L]_{int}\right\}\right)^2 - 4K_1^2X[L]_{int}^2}{2K_1}}$$

and as,

$$\Delta\delta_P = \frac{[ML]_{eqm}(\delta_1 - \delta_0)}{[L]_{int}} \therefore [ML]_{eqm} = \frac{\Delta\delta_P[L]_{int}}{(\delta_1 - \delta_0)}$$

substituting for $[ML]_{eqm}$ gives:

$$\Delta\delta_P = \frac{(\delta_1 - \delta_0)}{2K_1[L]_{int}}\left[K_1\left\{1 + X[L]_{int} + [L]_{int}\right\} \pm \sqrt{\left(K_1\left\{1 + X[L]_{int} + [L]_{int}\right\}\right)^2 - 4K_1^2X[L]_{int}^2}\right]$$

Points on the graph are experimental values ($\Delta\delta$P versus X) and the theoretical curves are those calculated by a general curve fitting procedure to the above equation, giving the equilibrium constant, K_1 and the ^{31}P chemical shift of the 1:1 complex

Appendix B

Method of continuous variation, or Job's method.*

Define the overall binding constant as:

$$m\mathrm{M} + n\mathrm{L} \rightleftharpoons \mathrm{M_mL_n} \qquad \beta_{mn} = \frac{[M_mL_n]}{[M]^m[L]^n} \qquad (1)$$

* Adapted from; K. A. Connors; *'Binding Constants, The Measurement of Molecular Complex Stability'*, John Wiley and Sons, New York, 1987

A set of solutions of ligand and metal were prepared, such that the sum of the total ligand and metal concentration was constant. Suppose separate solutions of L and M, each of concentration c mol/L, are mixed by taking v_M ml of metal and v_L ml of ligand solution, therefore $v_M + v_L = v$, where v is constant. The total ligand concentration is $L_t = v_L c$ and the total metal concentration $M_t = v_M c$, it follows that $M_t + L_t = vc$ and define the dimensionless quantity x (the mole fraction of ligand):

$$x = \frac{L_t}{M_t + L_t} = \frac{L_t}{vc} \qquad (2)$$

The mass balance equations for this system are:

$$M_t = [M] + m[M_m L_n] \qquad (3)$$

$$L_t = [L] + n[M_m L_n] \qquad (4)$$

Combining (3) and (4) with (2) gives (5) and (6), where $c_f = vc$

$$c_f(1-x) = [M] + m[M_m L_n] \qquad (5)$$

$$c_f x = [M]^m [L]^n \qquad (6)$$

$$\beta_{mn}[M]^m [L]^n = [M_m L_n]$$

Combining these with (1) gives:

$$\beta_{mn}\left\{c_f(1-x) - m[M_m L_n]\right\}^m \left\{c_f x - n[M_m L_n]\right\}^n = [M_m L_n] \qquad (7)$$

Taking logarithms and differentiating with respect to x, and set $d[M_mL_n]/dx = 0$

$$\log\beta_{mn} + m\log\left\{c_f(1-x) - m[M_m L_n]\right\} + n\log\left\{c_f x - n[M_m L_n]\right\} = \log[M_m L_n] \qquad (9)$$

$$\frac{d(\log[M_m L_n])}{dx} = \frac{m}{c_f(1-x)} - \frac{n}{c_f x} = 0 \qquad (10)$$

$$\frac{n}{m} = \frac{x}{(1-x)} \qquad (11)$$

Gives the stoichiometric ratio (11). Plotting the complex concentration in solution, which is given by equation (12) against the mole fraction of the ligand, x, gives the stoichiometric ratio at the turning point (i.e. when $d[M_mL_n]/dx = 0$).

$$[M_mL_n] = \frac{[L](\delta_{obs} - \delta_L)}{(\delta_{M_mL_n} - \delta_L)} \qquad (12)$$

Where δ_{obs} = observed ^{31}P NMR chemical shift of the system, δ_L = ^{31}P NMR chemical shift of the free ligand and δ_{MmLn}= limiting ^{31}P NMR chemical shift of the complex, determined from the NMR titration.

Appendix C Publications

C. D. Edlin, S. Faulkner, D. Parker and M. P. Wilkinson; "An efficient metal-templated route to C-functionalised derivatives of [12]aneN$_4$". *J. Chem. Soc., Chem. Commun.*, 1995, 1877

C. D. Edlin and D. Parker; "Synthesis of Heterocyclic Aza-Phosphinate Ligands Based on the Benzimidazole Skeleton". *Tetrahedron Lett.*, 1998, **39**, 2797

C. D. Edlin, S. Faulkner, E. Larsi, J. Lin, F. Neth, D. Parker, M. Port, M. P. Wilkinson and M. Woods; "Ligands Derived from C-Aryl Substituted Derivatives of Cyclen Form Kinetically Unstable Complexes with Lanthanide (III) ions". *New. J. Chem.*, 1998, Accepted

Appendix D Conferences, Lectures, Research Colloquia and Lectures

The author attended the following meetings:

Stereochemistry at Sheffield, University of Sheffield, December 1995

RSC UK Macrocycles Group Meeting, University of Sheffield, January 1996

RSC Dalton Regional Meeting, University of Edinburgh, April 1997

Zeneca Case symposium,* Grassmere, May 1997
"Synthesis of Tailored Ligands for Zinc Complexation".

21st Century Heterocyclic Chemistry, University of Sunderland, May 1997

RSC National Congress, Young Chemists Symposium,* University of Aberdeen, September 1997
"Getting the Right Fit; Synthesis of Tailored Ligands"

SCI Medicinal Chemistry Symposium, Churchill College, University of Cambridge, September 1997

ICI Poster Presentation, University of Durham,† December 1997 (1st prize winner)

SCI Ion Exchange and Solvent Extraction in the Processing of Non Ferrous Metals, Belgrave Square, London, March 1998

RSC National Congress, Young Chemists Symposium,* University of Durham, April 1988
"Getting the Right Fit; Synthesis of Tailored Ligands"

Zeneca Case symposium,* Grassmere, May 1997
"Tailored Ligands for Zinc Complexation".

XXIII International Symposium on Macrocyclic Chemistry,† Turtle Bay, Hawaii, USA, June 1998

* Indicates an oral presentation
† Indicates a poster presentation

The author attended the following lecture courses:

NMR Spectroscopy, by Dr. A. M. Kenwright and Dr. D. O'Hagan
Organometallic Chemistry, by Prof. D. Parker
Mass Spectroscopy, by Dr. M. Jones

The author attended the following colloquia between October 1995 and September 1998

1995

October 13 Prof. R. Schmutzler, Univ Braunschweig, FRG.
Calixarene-Phosphorus Chemistry: A New Dimension in Phosphorus Chemistry

October 18 Prof. A. Alexakis, Univ. Pierre et Marie Curie, Paris,
Synthetic and Analytical Uses of Chiral Diamines

October 25 Dr.D.Martin Davies, University of Northumbria
Chemical reactions in organised systems.

November 1 Prof. W. Motherwell, UCL London
New Reactions for Organic Synthesis

November 3 Dr B. Langlois, University Claude Bernard-Lyon
Radical Anionic and Psuedo Cationic Trifluoromethylation

November 8 Dr. D. Craig, Imperial College, London
New Stategies for the Assembly of Heterocyclic Systems

November 15 Dr Andrea Sella, UCL, London
Chemistry of Lanthanides with Polypyrazoylborate Ligands

December 8 Professor M.T. Reetz, Max Planck Institut, Mulheim
Perkin Regional Meeting

1996

January 24 Dr Alan Armstrong, Nottingham Univesity
Alkene Oxidation and Natural Product Synthesis

February 7 Dr R.B. Moody, Exeter University
Nitrosations, Nitrations and Oxidations with Nitrous Acid

February 14 Dr J. Rohr, Univ Gottingen, FRG
Goals and Aspects of Biosynthetic Studies on Low Molecular Weight Natural Products

February 28 Prof. E. W. Randall, Queen Mary & Westfield College
New Perspectives in NMR Imaging

March 6 Dr Richard Whitby, Univ of Southampton
New approaches to chiral catalysts: Induction of planar and metal centred asymmetry

March 7 Dr D.S. Wright, University of Cambridge
Synthetic Applications of Me_2N-p-Block Metal Reagents

March 12 RSC Endowed Lecture - Prof. V. Balzani, Univ of Bologna
Supramolecular Photochemistry

October 14 Professor A. R. Katritzky, University of Gainesville,University of Florida, USA
Recent Advances in Benzotriazole Mediated Synthetic Methodology

October 16 Professor I. Ojima, Guggenheim Fellow, State University of New York at Stony Brook
Silylformylation and Silylcarbocyclisations in Organic Synthesis

October 23 Professor H. Ringsdorf (Perkin Centenary Lecture), Johannes Gutenberg-Universitat, Mainz, Germany
Function Based on Organisation

November 13 Dr G. Resnati, Milan
Perfluorinated Oxaziridines: Mild Yet Powerful Oxidising Agents

November 18 Professor G. A. Olah, University of Southern California, USA
Crossing Conventional Lines in my Chemistry of the Elements

November 19 Professor R. E. Grigg, University of Leeds
Assembly of Complex Molecules by Palladium-Catalysed Queueing Processes

1997

January 15 Dr V. K. Aggarwal, University of Sheffield
Sulfur Mediated Asymmetric Synthesis

February 4 Dr A. J. Banister, University of Durham
From Runways to Non-metallic Metals - A New Chemistry Based on Sulphur

February 12 Dr Geert-Jan Boons, University of Birmingham
New Developments in Carbohydrate Chemistry

February 18 Professor Sir James Black, Foundation/King's College London
My Dialogues with Medicinal Chemists

February 25 Professor A. G. Sykes, University of Newcastle
The Synthesis, Structures and Properties of Blue Copper Proteins

March 4 Professor C. W. Rees, Imperial College
Some Very Heterocyclic Chemistry

March 5 Dr J. Staunton FRS, Cambridge University
Tinkering with biosynthesis: towards a new generation of antibiotics

October 22 Prof. R.J. Puddephatt (RSC Endowed Lecture), University of Western Ontario
Organoplatinum chemistry and catalysis

October 23 Prof. M.R. Bryce, University of Durham, Inaugural Lecture
New Tetrathiafulvalene Derivatives in Molecular, Supramolecular and Macromolecular
Chemistry: controlling the electronic properties of organic solids

October 29 Prof. Bob Peacock, University of Glasgow
Probing chirality with circular dichroism

October 28 Prof. A P de Silva, The Queen's University, Belfast
Luminescent signalling systems

November 5 Dr Mimi Hii, Oxford University
Studies of the Heck reaction

November 11 Prof. V Gibson, Imperial College, London
Metallocene polymerisation

November 19 Dr Gareth Morris, Department of Chemistry, Manchester Univ.
Pulsed field gradient NMR techniques: Good news for the Lazy and DOSY

November 26 Prof. R.W. Richards, University of Durham, Inaugural Lecture
A random walk in polymer science

December 2 Dr C.J. Ludman, University of Durham
Explosions

December 3 Prof. A.P. Davis, Department. of Chemistry, Trinity College Dublin.
Steroid-based frameworks for supramolecular chemistry

December 10 Prof. Mike Page, Department of Chemistry, University of Huddersfield
The mechanism and inhibition of beta-lactamases

1998

January 20 Prof. J. Brooke, University of Lancaster
What's in a formula? Some chemical controversies of the 19th century

January 27 Prof. Richard Jordan, Dept. of Chemistry, Univ. of Iowa, USA.
Cationic transition metal and main group metal alkyl complexes in olefin polymerisation

February 3 Dr J. Beacham, ICI Technology
The chemical industry in the 21st century

February 4 Prof. P. Fowler, Department of Chemistry, Exeter University
Classical and non-classical fullerenes

February 24 Prof. R. Ramage, University of Edinburgh
The synthesis and folding of proteins

February 25 Dr C. Jones, Swansea University
Low coordination arsenic and antimony chemistry

March 11 Prof. M.J. Cook, Dept of Chemistry, UEA
How to make phthalocyanine films and what to do with them.

March 18 Dr John Evans, Oxford University
Materials which contract on heating (from shrinking ceramics to bullet proof vests)